ASSESSMENT OF DNA STRUCTURE AND INTEGRITY IN THE HUMAN SPERMATOZOON

by

Claudia Román Montañana

A thesis submitted to
The University of Birmingham

For the Degree of
DOCTOR OF PHILOSOPHY

College of Medical and Dental Sciences
School of Clinical and Experimental Medicine
Institute of Metabolism and Science Research
University of Birmingham
September 2019

Abstract

Male fertility is routinely assessed by basic semen analysis, but this is poorly predictive of fertility outcome. One promising advanced diagnostic is assessing sperm DNA damage, but there is a lack of method standardisation, clinical thresholds and comparison data for different assays. The objective of this study was to validate standardised methods for the assessment of sperm DNA quality using TUNEL, Acridine orange (AO) and Chromomycin A_3 (CMA_3) in slide-based assays; and assess prognostic value for fertility and miscarriage.

The data obtained reveals that using differing optimal mounting solution for different assays is key to reliable results. The use of DNA fragmentation inductors such as DNase and hydrogen peroxide in donor samples confirmed and validated the use of AO and TUNEL for detecting DNA damaged cells.

A novel semi-automated computer-based scoring system for fluorescence microscopy images was devised and compared with visual operator results for intra-assay variability of AO and TUNEL assays. This system allowed objective and consistent results free of operator subjectivity.

The assessment of TUNEL, AO and CMA_3 values in a subset of patients from the HABSelect trial showed no correlation between the assays corroborating that different assays measure different aspects of DNA quality. The number of patient samples assessed were insufficiently powered to draw firm conclusions related to clinical outcome, but we believe they are useful in making a case for further investigations in the field.

Dedication

To my family who always believed in me

To my grandad who passed away and to who I could not say goodbye.

Acknowledgements

First and foremost, I would like to thank to Dr Jackson Kirkman-Brown for all his support and encouragement. Thanks for believing in me 4 years ago when I applied for this PhD. Things were not always easy, but you always tried to give me some peace of mind and kept me going. I realise now about all the patience you had. For this I am very thankful.

I would like to thank to Dr Sarah Conner for all her kind input, time, and expert and critical advice.

I cannot forget all the help I got in regard to microscopy from Dr João Correia which was key for my thesis. Thanks for your remote assistance every time my Metamorph journals were not working or crashing!

I am deeply grateful to Dr Clare Ray, my mentor during all this journey. You were always open to listen my worries and gave me advice not only as a professional, but also friend. Your encouragement and words always helped me to overcome difficult moments. Thank you with all my heart because without you I am not sure I could have made it!

I would also like to thank to the tech team, and especially to Matt Sutton and Dean Gentle, for your selfless teaching on molecular biology and cell culture which helped me to grow my technical skills.

Thank you to all the staff at the Birmingham Woman's Hospital Fertility Centre and also Birmingham Medical School. Thanks to all my colleagues in the reproductive biology and genetics (RBG) research group, to the maths team and to Dr Lorraine

Frew, Dr Jevan Medlock and Sofia Tsagdi for all the donor recruitment and work you do for us in the lab.

Thanks to Dr David Miller and all the personnel involved in the HABSelect clinical trial including all the patients who consented to the use of their samples for research, without which my research could not have been done.

I am also indeed very grateful to the NHIR who funded my research.

I wish to thank my dear friends Dr Gary Woodward and Daniel Tomás Crespo Belenguer for all your help you gave me during my PhD; your discussions and suggestions really helped me to question myself and my research and encouraged me to learn new skills such as coding and bioinformatics. I am indebted with you two.

I owe my deepest gratitude to my family who always encouraged me to pursue my career and to do my best. You gave me the push to start this crazy journey that has been the PhD, even though that entailed to move to another country and be far from you. You have always been very supportive and kind.

And last, but not least, I cannot find words to express my gratitude to my partner Simon D'Arcy, you were one of my best discoveries during my PhD. Thanks for all the emotional support, kindness and love. Thanks for listening all my talk rehearsals about sperm, English proof-reading, and uncalculated help at home. You made England my home and my time through my thesis easier and full of memories.

Table of content

Table of figures

Table of tables

List of Abbreviations

AC	Adenylate Cyclase
AO	Acridine Orange
AOT	Acridine Orange Test
AP	Apyrimidinic
APE1	apurinic/apyrimidinic endonuclease
ART	Assisted Reproductive Techniques
ATM	Ataxia Telangiectasia Mutated
BER	Base Excision Repair
BP	Biochemical Pregnancy
CP	Clinical Pregnancy
CV	Coeffecient of Variation
DAPI	4′,6-Diamidine-2′-phenylindole dihydrochloride
DBD-FISH	DNA Breakage Detection-Fluorescence *In Situ* Hybridization
DC	Distal Centriole
DDR	DNA Damage Response
DFI	DNA Fragmentation Index
DGC	Density Gradients Centrifugation
DNA	Deoxyribonucleic Acid
DSB	Double Strand Breaks
DSBR	DNA Double Strand Break Repair
dsDNA	Double Stranded DNA
DTT	Dithiotreitol
dUTP	2'-deoxyuridine 5'-triphosphate
FISH	Fluorescent *In Situ* Hybridisation
FITC	Fluorescein isothiocyanate
FR	Fertilisation Rates
GFP	Green fluorescent protein
GG-NER	Global Genome NER
HA	Hyaluronic Acid
HDS	High DNA Stainability
HR	Homologous Recombination
ICSI	Intracytoplasmic Sperm Injection
ISNT	*In Situ* Nick Translation
IUI	Intrauterine insemination
IVF	*In Vitro* Fertilisation
LB	Live Birth
MAR	Matrix Attachment Regions
MMR	Mismatch Repair

MSOME	Motile Sperm Organellar Morphology Examination
MZT	Maternal to Zygotic Transition
NER	Nucleotide Excision Repair
NHEJ	Non-Homologous End-Joining
NO	Nitric Oxide
OGG1	Oxoguanine Glyscosylase 1
OR	Odds Ratio
PBS	Phosphate-buffered saline
PC	Proximal Centriole
PCM	Pericentriolar Material
PFA	Paraformaldehyde
PGD	Preimplantation Genetic Diagnosis
PI	Propidium Iodide
PICSI	Physiological Intracytoplasmic Sperm Injection
PKA	Protein Kinase A
PRR	Post Replication Repair
PUFA	Polyunsaturated Fatty Acids
RNA	Ribonucleic Acid
ROI	Regions of Interest
ROS	Reactive Oxygen Species
RPA	Replication Protein-A
RPL	Recurrent Pregnancy Loss
RR	Relative Risk
RT	Room Temperature
SB	Subtraction of Blank Method
SCD	Sperm Chromatin Dispersion
SCGE	Single-Cell Gel Electrophoresis
SCSA	Sperm Chromatin Structure Assay
SDD	Sperm DNA Damage
SDF	Sperm DNA Fragmentation
SSB	Single Strand Breaks
ssDNA	Single Stranded DNA
TC-NER	Transcription-Coupled NER
TdT	Terminal Deoxynucleotidyl Transferase
TK	Tyrosine Kinase
TP	Tyrosine Phosphatase
TS	Threshold Setting
TUNEL	Transferase dUTP Nick End Labelling
UNG	Uracil DNA Glycosylase

CHAPTER 1. Introduction

1.1 Male infertility and miscarriage - definition and prevalence

Infertility

Infertility is defined as the failure to achieve a clinical pregnancy after 12 months or more of regular unprotected sexual intercourse (Zegers-Hochschild et al. 2009). According to WHO, infertility affects 13% to 15% of couples worldwide (World Health Organization (WHO 1984)). This figure has been suggested to be an underestimate due to the difficulty of reporting these cases (Mehta et al. 2016). The prevalence of infertility has been suggested to be lower in developed countries and higher in developing countries (Cates et al. 1985). In the UK it is estimated that one in seven couples suffer from infertility problems (NHS, 2020).

Fertility problems are suggested to be solely due to male problems in 30% of cases, female problems in 35%, and a combination of both male and female problems in 20%. In addition, 15 % of cases are reported as unexplained or "idiopathic" infertility (Forti and Krausz 1998, Poppe and Velkeniers 2002). These figures suggest that the male factor is involved in up to half of infertility cases or that one in twenty men in the general population are infertile (McLachlan and de Kretser 2001).

Miscarriage

Miscarriage is defined as the loss of a pregnancy before 24 weeks of gestation (Royal College of Obstetricians and Gynaecologists, 2011). According to Tommy’s National

Centre for Miscarriage Research, miscarriage is the most common complication of pregnancy with 1 in 4 women experiencing at least 1 miscarriage during their reproductive lifetime. This is translated into approximately 250,000 miscarriages per year in the United Kingdom (Tommy's National Centre for Miscarriage Research, 2020). Miscarriage most often occurs during the first trimester and it is usually, but not necessarily, accompanied with vaginal bleeding, cramping and pain in the lower abdomen (NHS, 2018).

It is important to differentiate between miscarriage and recurrent miscarriage, which is the loss of three or more pregnancies in a row. Recurrent miscarriage is also known as recurrent pregnancy loss (RPL). RPL has much lower prevalence than sporadic miscarriage affecting approximately 1 in 100 women. While sporadic miscarriages are most often caused by abnormal embryos that are unable to develop and implant, recurrent miscarriage is a multifactorial condition that may involve genetic, anatomic, endocrine, antiphospholipid antibody syndrome, immunologic, and environmental factors (Pillarisetty and Gupta, 2020).

1.2 Sperm production and transport in the male tract

Sperm cells are produced in the seminiferous tubules of the testes in a complex process called spermatogenesis that takes approximately 74 days (Heller and Clermont, 1964, Henkel *et al.*, 2003). The parenchyma of the testis is organised into hundreds of conical lobules that are formed by the seminiferous tubules and the intertubular tissue described below (**Figure 1.1A)**.

The seminiferous tubules are formed by multi-layered germinal epithelium and very thin peritubular tissue (lamina propia). The germinal epithelium contains spermatogenic cells in their different developmental stages embedded in Sertoli cells. The Sertoli cells, interconnected with each other by tight unions, provide support and nutrients to the developing sperm cells which are stratified according to developmental stage with the most immature closer to the lamina propia and the most mature closer to the lumen (Holstein *et al.*, 2003) (**Figure 1.1B**). The intertubular space contains connective tissue cells, microvessels, nerve fibres, macrophages, fibroblast and the Leydig cells. The Leydig cells have endo and paracrine roles, alongside the Sertoli cells, to regulate testicular function and sperm production (Lejeune *et al.*, 1992) .

Close to the membrane of the tubules there is a population of stem cells denominated spermatogonia. Based on their nuclear appearance there are two types of spermatogonia; A dark and A pale. The A dark spermatogonia form the stem cell pool allowing the male to produce sperm cells during their whole life (Clermont, 1966). The pattern of division of the A pale spermatogonia remains uncertain, however it has been suggested that A pale spermatogonia proliferate by mitosis to renew the A pale cells and to produce a third type of spermatogonia known as type B. The B spermatogonia look like the A pale cells but they divide by mitosis to form the first precursor of the sperm cells, the primary spermatocytes. The primary spermatocytes undergo the first meiotic division to originate a pair of secondary spermatocytes that complete the second meiosis division forming four haploid cells called spermatids (**Figure 1.1C**). The spermatids go under a differentiation process called spermiogenesis characterised by dramatic morphological changes such as the formation of flagellum,

the acrosome structure, cellular polarisation, and compaction of the DNA and nucleus due to the exchange of histones by protamines (O'Donnell, 2015).

The cell clones produced after each division remain linked to each other by cytoplasmic bridges to transfer metabolites and nutrients and to communicate to each other, so they can develop and divide synchronously (Fawcett *et al.*, 1959) (**Figure 1.1C**). The spermatogenic cells move from the basement membrane towards the lumen of the seminiferous tubules as they divide and differentiate. Individual sperm cells are released into the lumen by a process called spermiation (**Figure 1.1C**).

The sperm cells released into the lumen of the seminiferous tubes are conducted to the rete testis and efferent ducts that lead into the epididymis (Roosen-Runge and Holstein, 1978) (**Figure 1.1**). During the journey through the epididymis, local secretions trigger maturation of the sperm cells including the acquisition of progressive motility (Hoskins *et al.*, 1978) and fertilisation capability (Gervasi and Visconti, 2017). This maturation process is completed in the female reproductive tract post-ejaculation by the capacitation process that allows them to fertilise the oocyte. Epididymal transit takes between two to four days in humans (Bedford, 1994), and the sperm are mainly stored in the proximal ductus (vas) deferens until ejaculation (Turner, 1995). During ejaculation, the sperm are propelled through the vas deferens by peristaltic action passing through the ampulla and reaching the ejaculatory duct. The seminal vesicles and the prostate gland secret fluids, known as seminal plasma, into the ejaculatory duct that mixes with the sperm cells forming the semen. Finally, the semen is released via the urethra (**Figure 1.2**) (Puppo and Puppo, 2016).

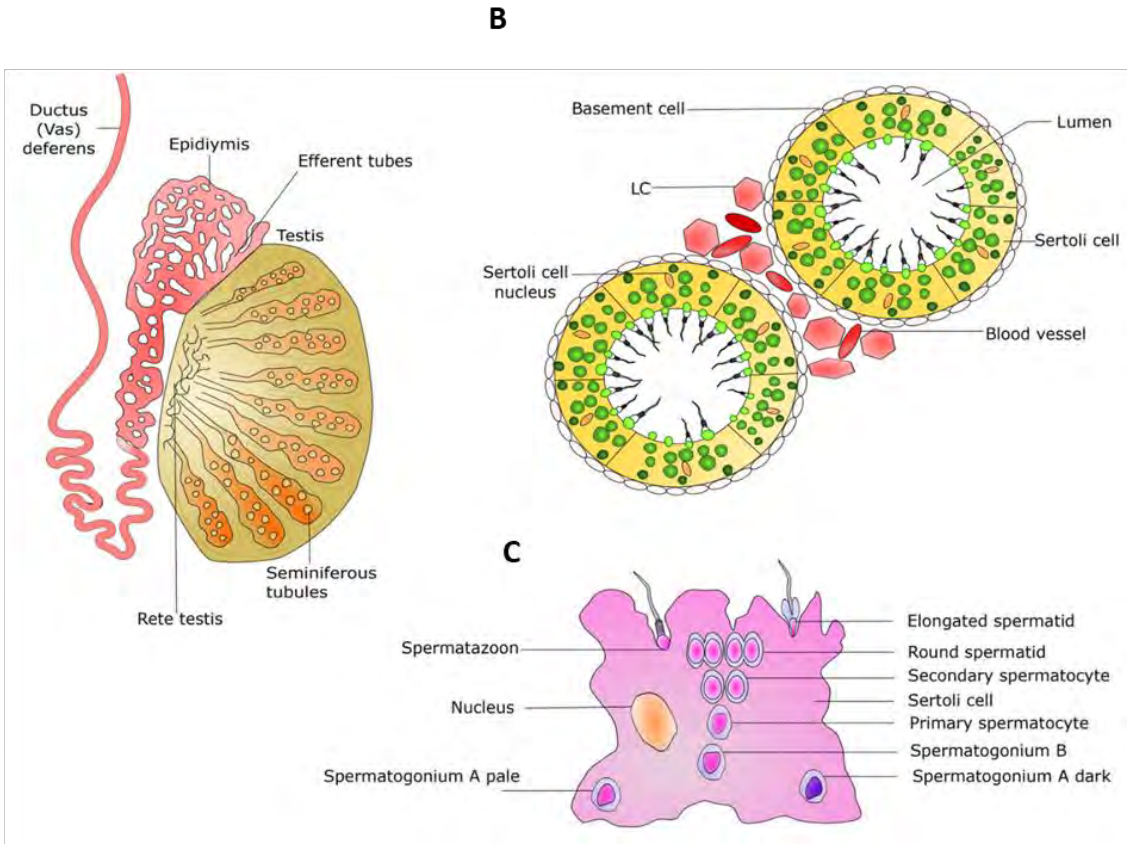

Figure 1.1 Organisation of the testis and the Sertoli cells.

A. Representation of the testis, seminiferous tubules, epididymis and ductus (vas) deferens. **B.** Cross-section of two seminiferous tubules showing the interconnection between Sertoli cells (yellow). Leydig cells (LC) (pale red) are located within the interstitium of the testis between the seminiferous tubules. C. The spermatogonia go through different stages of the spermatogenesis and the sperm cells are eventually released in the lumen of the seminiferous tubules. During the different divisions, the clonal cells remained attached to each other by cytoplasmic bridges. Adapted from Spermatogenesis Online (Zhang, Y. *et al.*, 2013)

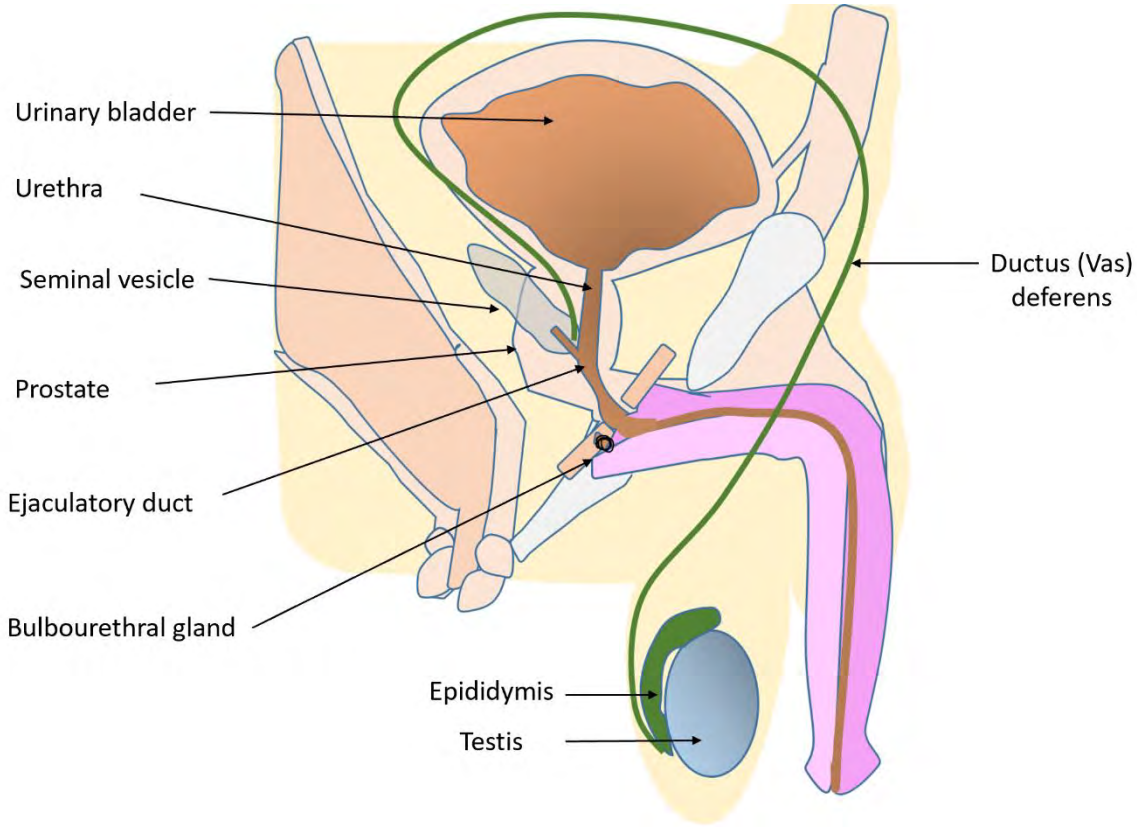

Figure 1.2 Path of sperm through the male reproductive tract

After the sperm are produced in the seminiferous tubules, they are led to the epididymis and stored in the cauda epididymis until ejaculation. During ejaculation, the sperm are driven into the ductus (vas) deferens and the ejaculatory duct. The sperm, mixed with the secretions from the prostatic gland and seminal vesicles, forming semen which is released to the exterior via urethra. Adapted from (Encyclopaedia Britannica, 2012).

1.3 Sperm structure

Human sperm cells measure approximately 55 µm and are divided into head, neck, mid-piece and tail (Fawcett, 1975). The head is a flat oval structure that contains a highly compact nucleus and acrosome responsible for the release of enzymes involved in the penetration of the oocyte vestments (Fawcett, 1975, Yang *et al.*, 2018). The neck of the sperm contains the structures denominated capitulum, striated columns, and the

proximal and distal centrioles (Manandhar *et al.*, 2000) (**Figure 1.3A**). The proximal centriole (PC) is transferred to the oocyte during the fertilisation. The distal centriole (DC) was believed to degenerate during the spermiogenesis together with the surrounding pericentriolar material (PCM) (Fawcett and Phillips, 1969). However, recent investigations showed that the DC remains attached to the base of the axoneme (**Figure 1.3A**) forming a new and atypical structure which has been proved to be able to recruit the PCM and microtubule forming proteins such as ϒ-tubulin. Moreover, in bovine fertilisation, the DC recruits PCM to form an aster and a new daughter centriole suggesting that the DC and the remodelling process could play an important role during fertility and embryo development alongside the PC (Fishman *et al.*, 2018). The mid-piece contains the axoneme structure formed by two central microtubules surrounded by nine double microtubules and extends until the end piece. In bovine and human sperm, nine dense outer fibres surround the microtubules enclosed by the mitochondrial sheath at the mid-piece. The dense outer fibres extend from the mid-piece to the principal piece but decrease in number from nine to seven with the microtubules protruding at the end piece (Linck *et al.*, 2016) **(Figure 1.3B**). The tail or flagellum allows the sperm to move through the female tract towards the Fallopian tubes to meet and penetrate the outer layers of the oocyte.

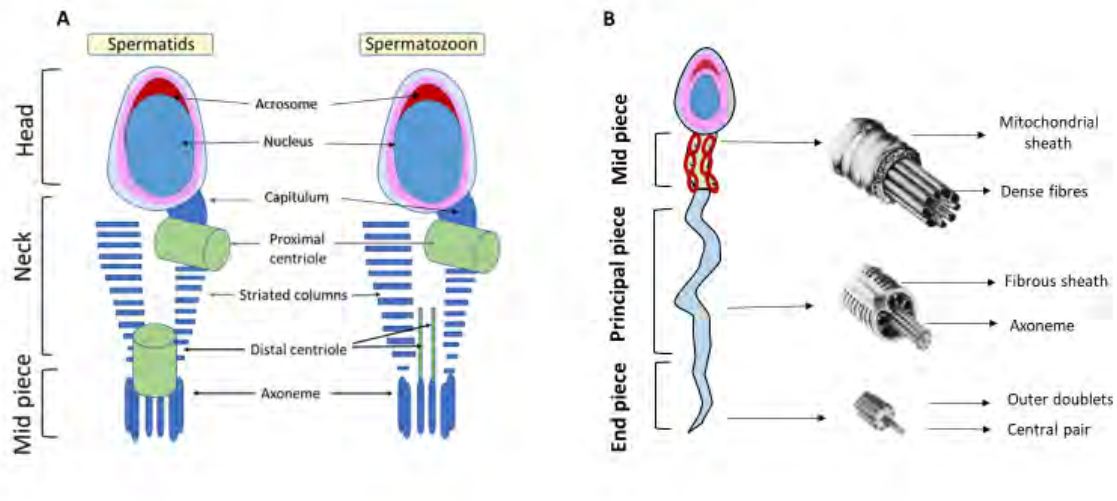

Figure 1.3 Typical structure of human sperm cells. A. Representation of the head, neck and mid piece of human spermatids and sperm cells. The distal centriole forms an atypical structure that remains attached to the base of the axoneme after spermiogenesis. **B.** Cytoskeletal organization of the sperm tail and axoneme in transverse sections at different levels: middle, principal and end piece. Adapted from (Fawcett, 1975, Fishman *et al.*, 2018)

1.4 Sperm DNA organisation

In somatic cells, nuclear chromatin is composed of DNA packed by octamers of histones forming nucleosome structures (Pienta and Coffey, 1984) that are coiled into helices called solenoids (Finch and Klug, 1976). In contrast, sperm cells replace their histones with protamines during the spermiogenesis (Tanphaichitr *et al.*, 1978) to form highly compacted structures called toroids (**Figure 1.4**). Toroids pack the DNA more efficiently by forming loop domains attached to the sperm nuclear matrix by Matrix Attachment Regions (MAR) (Martins and Krawetz, 2007, Nadel *et al.*, 1995) (**Figure**

1.4). Each loop is formed by one toroid structure (Sotolongo *et al.*, 2003) which contains approximately 50 Kb of DNA (Hud *et al.*, 1993). The toroids are linked by short segments of uncoiled DNA called toroid linkers which are particularly sensitive to DNA-damaging factors, like DNase. The high sensitivity to nuclease of the toroid linkers suggests they are bound by histones (Ward, 2010). Histone-protamine exchange perturbations might involve an increase susceptibility to DNA damage (De Iuliis, Thomson *et al.*, 2009).

In human sperm, approximately 2-15 % of histones remain after spermiogenesis bound to the sperm DNA (Ward, 2010). These remaining histones are highly acetylated which is mark of transcriptionally active genes spermiogenesis (Govin *et al.*, 2006, Rousseaux *et al.*, 2008). Because of mature spermatozoa are transcriptionally inactive It has been proposed that the remaining histones act as epigenetic marks that play a key role in the regulation of the gene expression in the zygote during early embryogenesis (Gatewood *et al.*, 1990, Steger *et al.*, 2011).

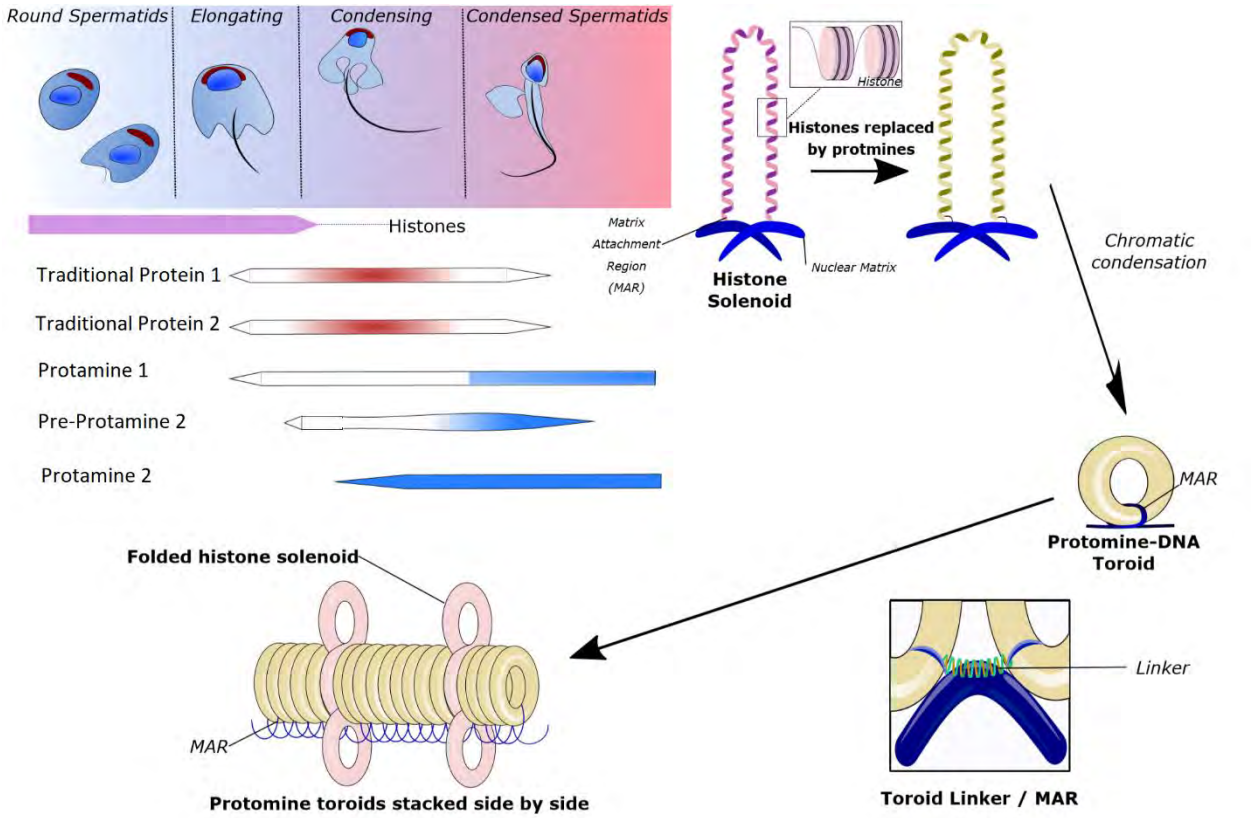

Figure 1.4 Representation of histone replacement during spermiogenesis by transitional proteins and later by protamines. Histones are present in round and elongated spermatids and they are replaced by transitional proteins before being exchanged for protamines to allow a more efficient compaction of the DNA in the condensed spermatids. The protamine and DNA form the toroid structures which are attached to the by Matrix Attachment Regions (MAR). Some of the histones remain after the spermiogenesis forming folded histone solenoids imbibed into the DNA toroids. The toroid linkers are more exposed and susceptible to sperm DNA damage. Adapted from (Ward, 2010) and Cleveland Clinical Center for Medical Art & Photography © 2010 (Agarwal and Sharma, 2011)

1.5 Sperm DNA damage

The terms Sperm DNA Fragmentation (SDF) and Sperm DNA Damage (SDD) are often used interchangeably; however, they can be regarded as slightly different concepts. SDF comprises single strand breaks (SSB) or double strand breaks (DSB). SDD covers any alteration of the integrity and structure of the DNA including abasic sites, base modifications (most commonly oxidation of guanosine forming 8-OHdG), and DNA-DNA or DNA-protein crosslinks (**Figure 1.5**) (Aitken *et al.*, 2009).

Nuclear and mitochondrial DNA damage can be induced by many different factors including cigarette smoking, irradiation, chemotherapy and pathophysiologic conditions such as leukocytospermia and varicocele. Most authors summarise all these factors under four main mechanisms which are described below; apoptotic processes; deficiencies in the chromatin packaging; the presence of Reactive Oxygen Species (ROS); and other external environmental factors.

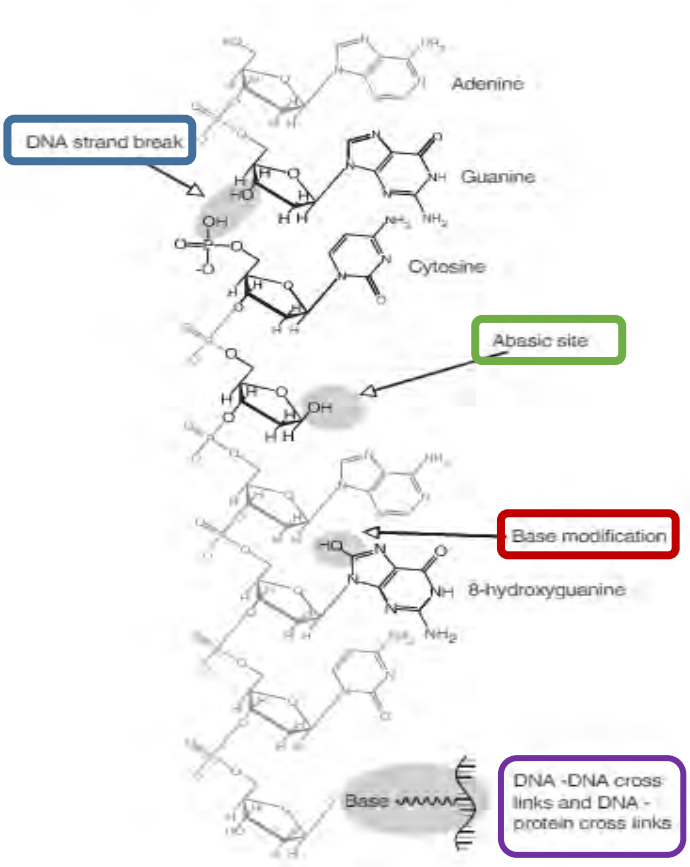

Figure 1.5 Possible types of DNA damage in human sperm. The four main sperm DNA damage types are shown: strand breaks that can be single or double (single in the figure), abasic site when the nitrogenous base is missing, base modification mainly by oxidization (8-OHdG adducts formation), and cross-links between DNA and proteins. Adapted from (Aitken *et al.*, 2009).

1.5.1 Apoptosis

Apoptosis is the physiological process that eliminates excess or damaged cells. In somatic cells different processes take place during the apoptosis, for example alterations of the plasma membrane, mitochondrial permeabilisation, caspase

activation, and eventually the condensation and fragmentation of the DNA. However, apoptosis in spermatozoa is not triggered at cell cycle checkpoints, as in somatic cells, but rather represents a form of programmed senescence (Aitken and Baker, 2013).

During spermatogenesis, many spermatocytes, predominantly in the pachytene stage, are eliminated by apoptosis to achieve the optimal germ:Sertoli cell ratio (Aitken and Baker, 2013) . The Fas/FasL system seems to be a major mediator of this process (Lin et al., 2010). A maladjustment of apoptosis can lead to an imbalance between germ and Sertoli cells and to the appearance of defective spermatozoa with apoptotic markers (Aitken and Curry, 2011, Almeida *et al.*, 2009). These spermatozoa may have gone through 'abortive apoptosis' which implies the start but not completion of the apoptotic process. Spermatozoa with apoptotic markers are more likely to experience DNA fragmentation and cause male infertility (Rodriguez *et al.*, 1997). A high number of apoptotic germ cells have been observed in the testes of infertile patients, aside from in cases of obstructive infertility (Lin, W. W. *et al.*, 1997).

1.5.2 Deficient chromatin packing

During spermiogenesis, one of the most important changes is the condensation of the DNA which occurs in two steps, one in the testis and the other in the epididymis. First, in the testis, the histones are exchanged for transition proteins and eventually for protamines (Poccia, 1986). Secondly, in the epididymis, the DNA is highly compacted by the formation of inter and intramolecular disulphide bonds between cysteine residues present in protamines (Corzett *et al.*, 2002, Kosower *et al.*, 1992, McKay *et al.*, 1986). There are two types of human protamines, P1 and P2. P2 have a lower

cysteine content and so form fewer inter and intramolecular cross-links compared with P1 (Corzett *et al.*, 2002). During this DNA rearrangement, nucleases create nicks to release torsional energy and allow the exchange of histones for protamines. Topoisomerase II has been proposed to cleave and ligate these nicks (Manicardi *et al.*, 1995, McPherson and Longo, 1992, Virant-Klun *et al.*, 2002). If incomplete maturation and/or Topoisomerase II defects occur, mature sperm cells with DNA breaks not ligated might appear in the ejaculate as showed in rat (McPherson and Longo, 1993). Also, a general protamine deficiency has been described in the sperm of infertile men compared to control (Silvestroni *et al.*, 1976, Zhang, X. *et al.*, 2006).

According to a recent systematic review of data for 1086 individuals, infertile men commonly have downregulated P2 expression which leads to P1:P2 ratio perturbation (Ni *et al.*, 2016). Although the protamine ratio is normally altered by the under-expression of P2, P1 over-expression has also been described in a small group of sub-fertile men (Aoki *et al.*, 2005). The meta-analysis revealed that sperm DNA damage evaluated by TUNEL, SCD, SCSA and Comet correlates with CMA_3 (R^2 = 0.71) and protamine deficiency (R^2 = 0.53) but not with the P1:P2 ratio (Ni *et al.*, 2016).

1.5.3 Oxidative stress

1.5.3.1 Forms of oxidative stress

Reactive Oxygen Species (ROS) are chemically reactive molecules containing oxygen which are by-products of normal cell metabolism. ROS include radicals such as the hydroxyl radical ($OH^{\cdot}$) and non-radical species such as the superoxide anion ($O_2^{\cdot-}$) and

hydrogen peroxide (H_2O_2). The superoxide anion radical ($O_2^{\cdot-}$) is firstly formed by the addition of an extra electron to O_2 (de Lamirande and O'Flaherty, 2008) and consequently it can turn into other ROS, including hydrogen peroxide (H_2O_2), hydroxyl ($OH^{\cdot}$), and peroxyl ($HO_2^{\cdot}$) radicals (Kothari *et al.*, 2010, Sharma and Agarwal, 1996) (**Figure 1.6)**.

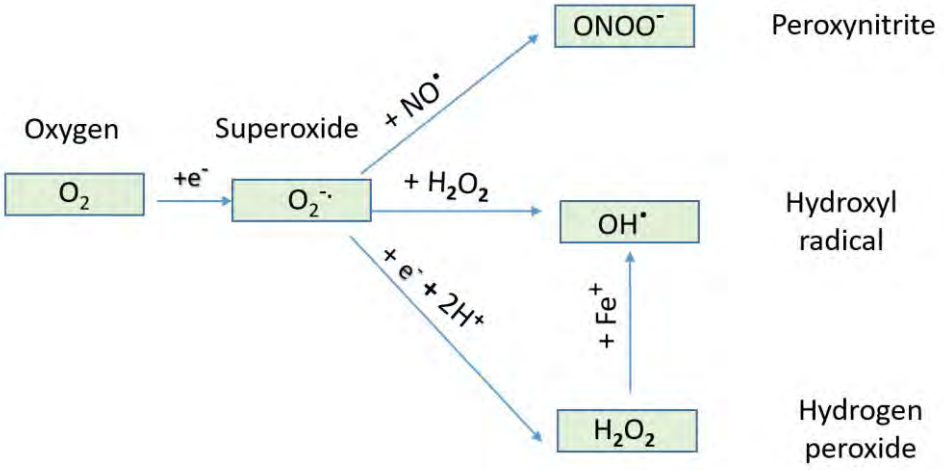

Figure 1.6 ROS formation. The addition of an electron to the oxygen molecule forms a superoxide radical which can produce peroxynitrite, hydroxyl radical or hydrogen peroxide by different reactions. e^-: electron. (Source: personal collection)

Low concentrations of ROS are needed for specific sperm functions, such as capacitation and the acrosome reaction (Aitken *et al.*, 1995). If the balance between ROS and antioxidants is perturbed and ROS production prevails, an oxidative status is reached which can damage cell structures like plasma membranes, proteins and DNA (Agarwal *et al.*, 2003, Gharagozloo and Aitken, 2011).

Antioxidants, scavenger enzymes and zinc play an important role in the regulation of ROS concentrations. Enzymatic scavengers include superoxide dismutase, catalase, glutathione peroxidase, and glutathione transferase and ceruloplasmine. Non-

enzymatic antioxidants include albumin, β-carotenes, l-carnitine, glutathione, pyruvate, taurine, hypotaurine, ubiquinol, ascorbic acid, α-tocopherol and zinc (Agarwal and Sekhon, 2011, Tavilani *et al.*, 2008).

The main sources of ROS in semen are leukocytes and immature or abnormal spermatozoa (Fisher and Aitken, 1997, Sakkas *et al.*, 2003). Leukocytes in semen, under physiological conditions, produce up to 1,000 times more ROS than spermatozoa. Men with normal, abnormal and leukocytospermic semen exhibited ROS levels of 19.75 ± 8.12 RLU/sec/10^6 sperm, 95.03 ± 33.63 RLU/sec/10^6 sperm and 890.17 ± 310.23 RLU/sec/10^6 sperm respectively (Homa *et al.*, 2015). In cases of genitourinary infection, the number of leukocytes is increased, and large amounts of ROS are released to eliminate the pathogenic agent (Plante *et al.*, 1994) but potentially also affecting sperm cells.

Mature sperm cells can also be a source of ROS produced in the plasma membrane and the mitochondria. In the plasma membrane, ROS are produced by the nicotinamide adenine dinucleotide phosphate (NADPH)-oxidase system, while in the mitochondria they are produced by the NADH-dependent oxido-reductase (diphorase) system (Aitken *et al.*, 1997, Walczak-Jedrzejowska *et al.*, 2013). The mitochondria of abnormal sperm cells have been suggested, in most cases, as the most important source of ROS (Aitken and De Iuliis, 2010, Koppers *et al.*, 2008).

The nicotine and the cadmium (Cd^{2+}) contained in the cigarettes have been related to an increase in DNA strands breaks (Hengstler *et al.*, 2003). Other external sources of ROS include xenobiotics, such as herbicides and pesticides like Paraquat (Hossain *et al.*, 2010, Whorton *et al.*, 1979), heat and electromagnetic radiation (De Iuliis, Newey

et al., 2009, Hourcade *et al.*, 2010), and radio and chemotherapies such as cyclophosphamide (Das *et al.*, 2002, Ghosh *et al.*, 2002). However, high levels of sperm DNA damage were observed in cancer patients before the treatment suggesting that cancer itself might be related to sperm DNA damage (O'Flaherty *et al.*, 2008).

1.5.3.2 ROS mechanisms of DNA damage induction, lipid peroxidation and motility impairment of human sperm cells

Sperm cells are particularly sensitive to oxidative damage as they lack apurinic/apyrimidinic endonuclease (APE1) (Smith *et al.*, 2013), an enzyme part of the base excision repair (BER) process (explained with more detail in 1.5.1.2). In this pathway, a specific glycosylase (OGG1) removes the oxidized base and creates an abasic site. Consequently, the APE1 cleaves the abasic site and creates a 3'-OH residue where DNA polymerase β inserts a guanine before the nicks are ligated by ligase II/XRCC1. As sperm cells lack APE1, they cannot repair the DNA damage, and it remains until the spermatozoa fertilizes the oocyte which will then have to commence with the DNA repair (Gawecka *et al.*, 2013, Shimura *et al.*, 2002).

Aitken *et al*. proposed a two-step model where a poorly-protaminated defective spermatozoon is more susceptible to ROS damage (Aitken *et al.*, 2009). In Step 1, vulnerable or poorly-protaminated DNA forms during the spermiogenesis. In Step 2, ROS preferentially oxidizes the poorly protaminated sperm and triggers the oxidative DNA damage or apoptosis causing strand breaks. Although the ROS can come from many sources as explained above, the hydrogen peroxide released from the sperm cell's own mitochondria is proposed to be the main source.

Interestingly, during the capacitation process, sperm mitochondria (Koppers *et al.*, 2008) and/or plasma membrane NADPH oxidase (Boerke *et al.*, 2013, Musset *et al.*, 2012) release superoxide that in combination with nitric oxide generates peroxynitrite which is a very toxic and selective oxidant. Peroxynitrite and hydrogen peroxide facilitate tyrosine phosphorylation by tyrosine phosphatase inhibition. Superoxide, hydrogen carbonate and calcium activate soluble adenylyl cyclase stimulating the cAMP production. cAMP activates protein kinase A which triggers the tyrosine phosphorylation cascade through tyrosine phosphatase suppression and tyrosine kinase activation (Lewis, B. and Aitken, 2001). The cholesterol of the plasma membrane is oxidised to oxysterol and the fluidity of the membrane decreases facilitating Ca^{2+} entry (Boerke *et al.*, 2013) (**Figure 1.7**).

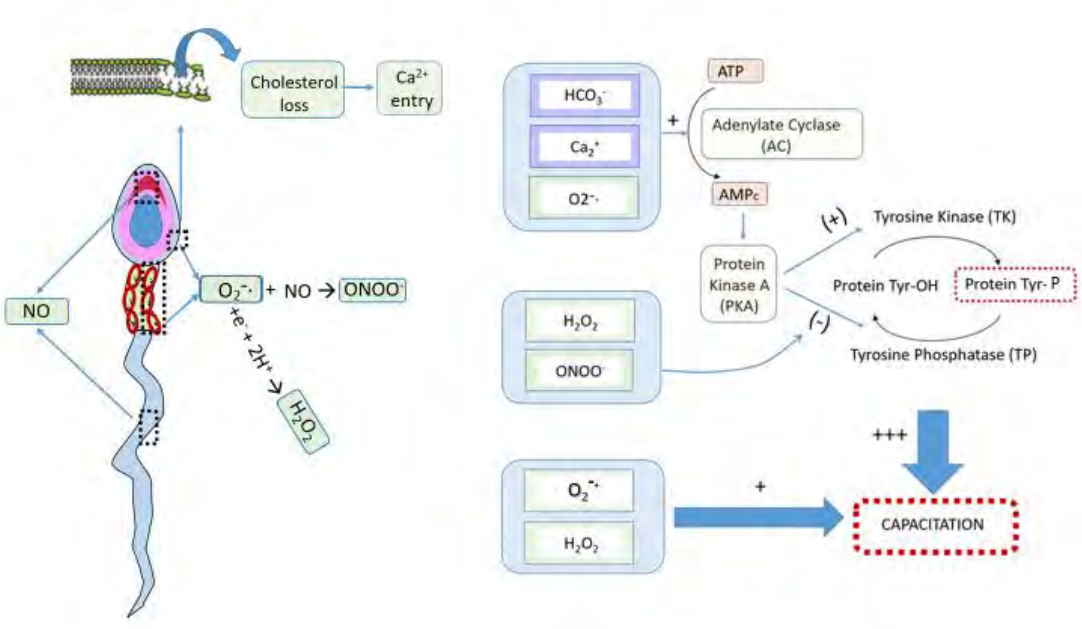

Figure 1.7 ROS mechanisms leading to capacitation in mammalian sperm.

During capacitation, superoxide is released by the NADPH-oxidase in the plasma membrane and the NADH-dependent oxidase-reductase in mitochondria of the sperm cells. Nitric oxide (NO) is produced by nitric oxid synthase localised in the tail and acrosome of the sperm. Superoxide, in combination with nitric oxide, form peroxynitrite. Superoxide activates

Adenylate Cyclase (AC) increasing the levels of cAMP and activating Protein Kinase A (PKA) which promotes Tyrosine Kinase (TK) activity and inhibits Tyrosine Phosphatase (TP). H_2O_2 and $ONOO^-$ contribute to the tyrosine phosphorylation by inhibiting Tyrosine Phosphatase (TP). The increase in tyrosine phosphorylation is the major driving force for capacitation (vertical largest arrow) but other redox-sensitive pathways (horizontal blue arrow) may also contribute. During capacitation there is cholesterol loss which increases the permeability and fluidity of the plasma membrane facilitating the Ca^{2+} entry necessary for the acrosome reaction. Adapted from (Ford, 2004).

The plasma membrane of the spermatozoa is particularly vulnerable to lipid peroxidation due to the high proportion of polyunsaturated fatty acids (PUFA) (Jones *et al.*, 1978, Jones *et al.*, 1979). Lipid peroxidation is a self-propagating reaction and it has been associated with an impairment of the fusion between spermatozoa and oocyte due to alterations in membrane fluidity and inactivation of membrane-bound receptors (Aitken *et al.*, 2014, Christova *et al.*, 2004, Sanocka and Kurpisz, 2004). Radicals formed during the lipid peroxidation can induce superoxide release by the mitochondria (Aitken *et al.*, 2014).

A relationship between lipid peroxides and sperm motility has been reported before (Aitken *et al.*, 2012, Jones *et al.*, 1979). H_2O_2 is considered the most cytotoxic reactive oxygen species and it can majorly impair the sperm motility. Low concentrations of H_2O_2 can significantly decrease the beat frequency of spermatozoa (Aitken *et al.*, 1993).

A sustained ROS production eventually overwhelms the sperm cell's defensive capabilities and the oxidative status triggers the intrinsic apoptotic cascade (**Figure 1.8**) (Aitken, 2011). However, the secretions of the female reproductive tract contain pro-survival factors such as prolactin or insulin (Pujianto *et al.*, 2010) which are

suggested to activate phosphatidylinositide 3-kinase (PI3 kinase) and generate inositol triphosphate (PIP3) to phosphorylate the serine/threonine kinase AKT. AKT prevents spermatozoa undergoing apoptosis by different mechanisms; one is the maintenance of the pro-apoptotic factor phosphorylated-BAD (Aitken and Baker, 2013).

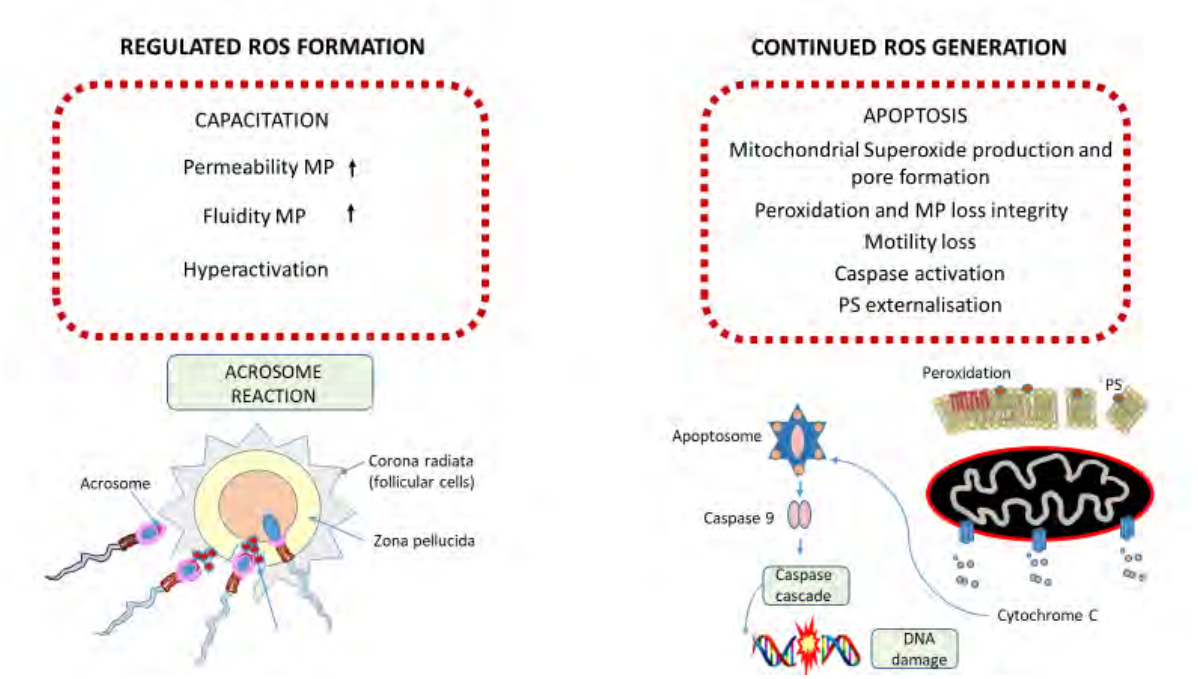

Figure 1.8 The role of ROS during capacitation and apoptosis.

ROS are necessary for the capacitation process, but if there is a continued ROS production the apoptosis cascade characterized is induced by the mitochondrial superoxide production, lipid peroxidation, cytochrome C release, caspase activation, phosphatidylserine exposure, oxidative DNA damage and death. (Source: personal collection)

1.6 Repair of sperm DNA damage

Sperm DNA damage can be repaired during spermatogenesis before transcription and translation stop post-spermiogenesis. If damage occurs during storage in the

epididymis, transit through the male reproductive tract, or ejaculation, it can be repaired by the oocyte post-fertilisation (Men *et al.*, 2016), and zygote or embryo (Derijck *et al.*, 2008). Below I describe the repair processes that occur during each stage.

1.6.1 DNA repair during spermatogenesis

DNA damage is not a rare event in mammalian cells; 10^5 errors have been estimated to occur per cell per day (Lindahl, 1993). A cell with DNA damage can either activate the apoptotic pathway and eliminate the cell or repair the lesion. Before completing meiosis, spermatogenic cells can repair DNA damage by different pathways depending on the type of damage. This repair capability decreases through spermatogenesis (Olsen *et al.*, 2005, Sotomayor and Sega, 2000), becoming restricted in elongating spermatids due to the inaccessibility of the DNA repair machinery to the condensed chromatin as a result of the exchange of histones by protamines (Wouters-Tyrou *et al.*, 1998). The different mechanisms or pathways for DNA repair are collectively called the DNA Damage Response (DDR). In the mammalian germline, the DDR includes the mechanisms of: Nucleotide Excision Repair (NER), Base Excision Repair (BER), Mismatch Repair (MMR), DNA double strand break repair (DSBR) and Post Replication Repair (PRR) (Gonzalez-Marin *et al.*, 2012, Gunes *et al.*, 2015). The main DDR mechanisms that operate during spermatogenesis are summarized below.

1.6.1.1 Nucleotide excision repair

This pathway repairs lesions that cause the distortion of the DNA helix structure such as oxidative damage, pyrimidine dimers caused by ultraviolet radiation, DNA intra-strand cross-links, and mismatched bases or bulky adducts. There are two possible mechanisms: Global Genome nucleotide excision repair (GG-NER) and Transcription-Coupled NER (TC-NER). The GC-NER detects and repairs errors in the whole genome

(Fagbemi *et al.*, 2011), while TC-NER is specific to errors in the transcribed strand (Iyama and Wilson, 2013). During damage recognition, the two mechanisms use different proteins, but after recognition, the same protein machinery is used in both GC-NER and TC-NER (Gunes *et al.*, 2015). The proteins XPC/RAD23B used in GC-NER are highly expressed in oocyte (O'Donovan *et al.*, 1994).

1.6.1.2 Base excision repair

Base excision repair (BER) is the pathway responsible for the removal of bases damaged by oxidation or adduction that do not disturb the DNA helix structure. Specific base substitutions are recognized by DNA glycosylases, for example uracil DNA glycosylase (UNG) and 8-Oxoguanina glyscosylase 1 (OGG1) which cleave the N-glycosidic bond producing an abasic site. The abasic sites are cleaved by apurinic or apyrimidinic (AP) endonucleases and the Single Strand Breaks (SSB) produced can be sealed by either DNA ligase III (short-patch) or by ligase I (long-patch) (Said *et al.*, 2004). UNG is highly expressed in germinal vesicles, while OGG1 is present at moderate levels in the oocyte but higher levels in the spermatogenic cells, and APE1 is present in oocyte but absent in spermatogenic cells. DNA repair starts in spermatogenic cells with the creation of abasic sites by OGG1, but due to the lack of APE1, the repair has to continue in the oocyte during the S-phase of the first division of the zygote (Gunes *et al.*, 2015).

1.6.1.3 Mismatch repair

Mismatch repair (MMR) is responsible for the recognition of insertions, deletions and mis-incorporation of bases on the non-template DNA strand that occur during the replication (Jiricny, 2006). These errors are typically due to tautomerization of the DNA

(Gunes *et al.*, 2015). The change in the structure of the DNA produced by the DNA-base pair mismatch and the insertion-deletion loop mismatch are recognized by the homologous heterodimers MutSα and MutSβ in eukaryotes (Jun *et al.*, 2006). MutS heterodimers recruit MutL to activate MutH and create nicks in the new synthetized DNA strand. MutH recruits DNA helicase II which separates the DNA strands. Exonuclease 1 (EXO1) then digests the single DNA strand and DNA Polymerase δ (DNA Pol δ) fills the gap with the correct nucleotides and finally the DNA ligase seals the gap (Gunes *et al.*, 2015). The mismatched base is removed alongside some of the adjacent bases. Up to 1000 adjacent bases may be removed in this process (Brown *et al.*, 2001).

The MMR machinery needs to differentiate the template (parental) strand from the newly synthesized strand with the erroneous base. In eukaryotes, in the case of the leading strand synthesis, the differentiation is due to the PCNA-DNA bound which determines the orientation of MutLα incision while enhancing its exonuclease activity (Pluciennik *et al.*, 2010). For the lagging strand synthesis, the MMR machinery identifies the new-synthesized strand due to the transient nicks of the Okazaki fragments (Nick McElhinny *et al.*, 2010).

1.6.1.4 Double strand breaks

Double Strand Breaks (DSBs) can be repaired in the mammalian cells by two different pathways: The Non-Homologous End-Joining (NHEJ) and Homologous Recombination (HR) mechanisms (Iyama and Wilson, 2013).

HR is an error-free mechanism which takes place during S phase of interphase and G2 phase as it needs an homologous sister chromatid for execution (Gunes *et al.*,

2015). Ataxia Telangiectasia Mutated (ATM) and MRE11-RAD50-NBS1 complex are activated by DNA double strand breaks and resect the DNA ends in 3'-ssDNA that are later covered by Replication Protein-A (RPA) to remove structural disruptions. Then RPA is replaced by RAD51 homologous sequence on the sister chromatid. RAD51C-BRCA2 complex perform the homologous pairing (Iyama and Wilson, 2013).

On the other hand, NHEJ directly ligates the DNA strand ends without the need for a template but deletions or insertions are generated during the process. Ku70 and Ku80 recruit DNA-PKCs which subsequently mediate the recruitment of XRCC4 and DNA ligase IV complex (Gonzalez-Marin *et al.*, 2012).

The relative contribution of both pathways depends on the cell type. For example, in mammalian germ cells the DSBs are mainly repaired by the NHEJ pathway (Gonzalez-Marin *et al.*, 2012). However, because the spermatogenic cells lack some of the repair proteins and also showed specific DSB repair kinetics, a new mechanism independent of DNA-PKcs has been suggested in the spermatogenic cells (Gonzalez-Marin *et al.*, 2012, Rube *et al.*, 2011). This new pathway known as Alternative NHEJ involves PARP-1 and the ligation by the XRCC1-DNA ligase III complex, proteins which are involved in the BER pathway and SSB repair (Audebert *et al.*, 2004). NHEJ has been suggested as a main DNA repair mechanism in round spermatids in mice.

1.6.2 DNA repair post-fertilisation

Sperm cells that fail to repair their DNA during spermatogenesis or that have DNA damage due to their storage in the cauda epididymis or transit through the male and

female tracts, can retain their fertilising ability but they might later cause negative consequences for the future embryo. (Zenzes *et al.*, 1999). These damaged cells can be repaired by the oocyte during fertilisation and by the embryo. Jaroudi *et al*. demonstrated the existence of repair genes involved in the HR and NHEJ pathways in human MII oocytes and blastocyst by microarray analysis (Jaroudi *et al.*, 2009). Both DDR pathways compete for the repair of DSB. The conditions or reasons that triggers each pathway on the cell are still unknown (Gonzalez-Marin *et al.*, 2012).

The ability of the oocyte to repair DNA damage depends on the level and type of damage. For example, Ahmadi et al. suggested that the oocyte can repair sperm DNA damage when this is less than 8% (Ahmadi and Ng, 1999). SSB are generally easier to repair than double strand breaks (DSB), although polymerases can also repair DSB (Gonzalez-Marin *et al.*, 2012). Moreover, the repair ability of the oocyte has been shown to decrease with the age of the female (Meseguer *et al.*, 2011).

In summary, depending the level and type of damage the oocyte can either fully repair the sperm DNA damage (compensable damage), fail to repair the damage (non-compensable damage), or partially repair the damage (partial compensable damage). When the damage cannot be fully repaired, the embryo may fail to implant or may arrest its development and end in miscarriage (Gonzalez-Marin *et al.*, 2012). The worst scenario occurs when the oocyte partially repairs the sperm DNA as new deletions and sequence errors may be introduced generating abnormal offspring (Gonzalez-Marin *et al.*, 2012).

After fertilisation, but before the maternal to zygotic transition (MZT) that occurs at the 4-8 cell stage in the human embryo, DNA damage repair relies on the maternal

genome and transcripts from the oocyte. Chromosome aberrations in the zygote can arise during the first metaphase due to paternal DNA damage (Matsuda *et al.*, 1989). However, DSB can also be repaired in the zygote; differentiated somatic cells can be repaired by the NHEJ, and embryonic cells by the HR pathways (Derijck *et al.*, 2008). NHEJ is active in G1 while HR is active during S/G2 when the sister chromatids are available to be used as a template for the homologous recombination (Rothkamm *et al.*, 2003). Matsuda *et al.* also suggested a role for poly (ADP-ribose) polymerase (PARP) in zygote DSB repair (Matsuda *et al.*, 1989).

The failure of embryo development during and after implantation of *in vivo* and *in vitro* generated embryos with normal karyotype could be explained due to the presence of unrepaired DNA (Tesarik *et al.*, 2004). This phenomenon is commonly known as the 'paternal late effect'. The paternal late effect has been correlated with low blastocyst formation rate and implantation failure that occurs with pre-implantation embryos between the post-embryonic genome activation and the blastocyst stage. HR has been proposed as the mainly DDR pathway during and after the implantation.

1.7. Measurement of the sperm DNA damage

The different techniques used for the study of the Sperm DNA Damage (SDD) are typically classified as direct or indirect tests. The direct assays assess the number of pre-existent SSB or DSB. In contrast, indirect assays measure the susceptibility of sperm DNA to damage. Understanding the parameters measured in each assay and the information that gives is very important (**Table 1.1**) (Muratori *et al.*, 2010). The

clinician or researcher should study carefully which test is more appropriate for their purpose as they have different basis, advantages and disadvantages (**Table 1.1**).

Direct assays include the Terminal Deoxynucleotidyl Transferase-Mediated dUTP Nick End-Labelling (TUNEL) test, the In-Situ Nick Translation test (ISNT), and the Single-Cell Gel Electrophoresis (SCGE) more commonly known as Comet assay, at neutral pH. While the indirect group is composed by the Sperm Chromatin Structure Assay (SCSA), the Sperm Chromatin Dispersion test (SCD), and the Comet assay at alkaline pH (Lewis, S. E. *et al.*, 2008).

The same sample may obtain different sperm "DNA damage" scores depending on which assay is used, and even when using same assay, it may score differently due to the lack of standardisation (Muratori *et al.*, 2010). Due to the wide variety of tests and technique variances, it is not currently possible for any test to claim independently verified thresholds or clinically relevant ranges.

1.7.1 TUNEL and *in situ* nick translation assays

This technique was first described by Gavrieli *et al*. (Gavrieli *et al.*, 1992) and modified later by Mitchell *et al*. specifically for sperm by inclusion of an additional preliminary step of decondensing the sperm nucleus using the reducing agent dithiothreitol (DTT) (Mitchell *et al.*, 2011). TUNEL can be performed using fluorescence microscopy or flow cytometry.

The TUNEL test is based on the 3'-OH groups of DNA fragments being marked by the Terminal Deoxynucleotidyl Transferase (TdT) enzyme which adds fluorophore-conjugated dUTPs (alternative markers to fluorophores such as haptens like biotin are also available). Flow cytometry analyses the fluorescence according to a threshold

channel value on a relative intensity scale, allowing the study of more cells in less time. On the other hand, fluorescence microscopy is cheaper and permits the simltaneous study of the morphology and fluorescence in single sperm cells. In either scenario the fluorescence is usually determined as a binary positive or negative for single cells; but actually, a quantitation of the fluorescence level is theoretically possible and should be an index of damage levels.

Another technique very similar to TUNEL is *In Situ* Nick Translation (ISNT) developed by Rigby and Berg (Rigby *et al.*, 1977), which instead of the TdT enzyme uses DNA polymerase I (Pol I). Despite the similarities between the two techniques, only TUNEL is in common use.

1.7.2 Comet assay

Comet was designed by Östling & Johansson in 1984 (Ostling and Johanson, 1984). It consists of ingle cell electrophoresis to quantify strand breaks using fluorescence microscopy.

In the Comet assay, the cells are mixed with melted agarose and placed on glass slides. Detergents and high salt concentrations are added to lyse the cell membranes and remove nucleoproteins, protamines and histones and to release the relaxed DNA in a supercoiled nucleoid structure (Lewis, S. E. *et al.*, 2013). Enzymatic treatment can be used to decondense and release the DNA (Aydos *et al.*, 2015, McAuliffe *et al.*, 2014, Trisini *et al.*, 2004). Nucleoids are exposed to an electrophoretic field and the broken strands migrate though the gel. Intact DNA forms the head of the Comet shape and does not migrate, while the tail is formed by broken DNA of different sizes (Lewis, S. E. *et al.*, 2013, Ostling and Johanson, 1984). Different DNA-specific fluorescent dyes

can be used for Comet pattern visualization under fluorescence microscopy, such as DAPI (4′,6-Diamidine-2′-phenylindole dihydrochloride) or SYBR Green I.

In this test the intensity ratio (head:tail) of the Comet represents the amount of DNA fragmented while the distance between the head and the tail is correlated with the relative sizes of the DNA fragments (Hughes *et al.*, 1996).

The Comet assay was later modified by Singh e*t al*. (Singh *et al.*, 1988) who used a very high pH buffer (pH=13), which denatures and unwinds the DNA strands (Afanas'eva *et al.*, 2009). This last variation is called alkaline Comet while the original assay is termed Comet or neutral Comet.

There is some controversy in the literature about the nature of the breaks that each variant of the Comet assay can detect. Some suggest both variants can detect single and double strand breaks whilst others are quite clear that Comet in neutral conditions can only detect DSB (Hughes *et al.*, 1996, Singh *et al.*, 1988, Tarozzi *et al.*, 2007). Alkaline Comet can detect DSB, SSB and alkali labile sites which are suspected to be abasic sites (Barratt *et al.*, 2010, Ross and Tang, 1985). Alkaline Comet is the preferred version as it is considered the most sensitive as it allows the detection of more types of DNA damage.

Comet software calculates the parameters of head DNA (%), tail DNA (%), tail length, and olive tail moment. The fluorescence emitted by the head is compared to the tail to determine the percentage of DNA present in the head and tail. Comet can be used to analyse the percentage of damage in a single cell from 0 to 100 %. It is suitable for testicular and oligozoospermic sperm samples, where the number of sperm is low, because as Hughes *et al*. demonstrated, analysis of 50 sperm is sufficient to provide

a measurement of DNA damage of the total sperm population with a coefficient of variance lower than 4% (Hughes *et al.*, 1997).

1.7.3 Sperm chromatin dispersion assay

The Sperm Chromatin Dispersion (SCD) assay consists of the measurement of the halo pattern created by denatured sperm DNA when it is exposed to an acid solution and later to a lysis solution to remove sperm proteins. This, relaxes the chromatin loops and creates peripheral halos. DNA strand breaks and nicks act as denaturation origins when DNA is exposed to the acid solution and prevent the extension of the nucleoids. Therefore, halos are absent from damaged sperm or are not as large as the halos from intact DNA sperm. These halos are visualized by either brightfield or fluorescence microscopy (Ankem *et al.*, 2002, Cook and Brazell, 1978).

The correlation between Halo dispersion size and DNA fragmentation has been shown by DNA Breakage Detection-Fluorescence *In Situ* Hybridization (DBD-FISH) analysis (Fernandez *et al.*, 2003). DBD-FISH is a technique to quantify DNA breakage. In DBD-FISH the cells are exposed to alkaline and protein removal solutions, so the DNA breaks turn into single-stranded DNA and whole genome probes can be hybridized and detected. More probe hybridizes when the DNA is fragmented and therefore the fluorescence intensity obtained is higher (Vazquez-Gundin *et al.*, 2000).

The SCD assay does not require a large number of sperm cells and only requires bright field microscopy or fluorescence microscopy. It is possible to simultaneously perform different tests on processed samples by SCD, for example FISH (Muriel *et al.*, 2007), and as previously has been suggested there is a possible association between aneuploidy and sperm fragmentation (Levron *et al.*, 2001, Ohashi *et al.*, 2001).

However, as mentioned above no data supported the use of the SCD test in the meta-analysis of Osman et al. (Osman *et al.*, 2015).

1.7.4 Acridine orange test and sperm chromatin structure assay

The Acridine Orange Test (AOT) and the Sperm Chromatin Structure Assay (SCSA) are both based on the susceptibility of sperm DNA to denaturation in acid conditions followed by staining with acridine orange (AO) fluorescent DNA-binding dye.

Nash and Plaut observed for first time, in Drosophila, that after staining DNA with AO in the presence of formaldehyde, different colour fluorescence was emitted depending on whether the DNA was previously denatured (Nash and Plaut, 1964). When the AO is conjugated to native DNA (double stranded DNA) it intercalates as a monomer, whereas when it is bound to single stranded DNA it precipitates as an aggregate. Monomer and aggregate exhibit same excitation profiles (475-500 nm) but they have different peak emission wavelengths ; for the monomer the peak is at 525 nm (green) while for the aggregate it occurs at 650 nm (red) (Ichimura *et al.*, 1971, Kapuscinski *et al.*, 1982).

The fluorescence can be measured by microscopy or by flow cytometry. The SCSA test uses flow cytometry and its protocol is very similar to the AO protocol. The SCSA software permits quick analyses of a large number of cells. This big data allows the creation of a scatter plot with the ratio between red and green sperm, and to calculate some important parameters: the DNA Fragmentation Index (DFI), the percentage of sperm cell with a medium-high denaturation in the sample (%DFI) and the High DNA Stainability (HDS).

DFI is calculated by dividing the red fluorescence by the total fluorescence of the sperm heads. It is proportional to the amount of DNA strand breaks or sperms with protamine defects.

DFI = [red fluorescence / (red +green) fluorescence]

% DFI refers to the number of sperm cells with a DFI score above a set-up threshold (different for each flow cytometry as it depends on the settings selected). These cells with DFI above the set threshold are considered damaged.

HDS is equivalent to the percentage of sperm with high green fluorescence. These green sperm are thought to be immature due to abnormal chromatin, DNA or protein (Bungum *et al.*, 2011a)

AO is particularly sensitive to pH changes as it is a weak base (pK_a = 10.5); at high pH the molecule is deprotonated while at low pH the molecule is protonated and can form aggregates which exhibit different fluorescence and give a false result **(Fig. 1.9)**. Moreover, the aggregate exhibits different lipophilic properties. The deprotonated form (monomer) can pass through membranes, for example the nucleus and cytosol, and emits green fluorescence. However, inside acidic organelles, the AO molecules are protonated [AOBH+] due to the low pH and form aggregates that are trapped and emit red fluorescence. Therefore, AO can be used to stain organelles with low pH such as lysosomes (Thome *et al.*, 2016). Special attention should therefore be paid to pH changes in AO protocols, including the AOT and SCSA assays.

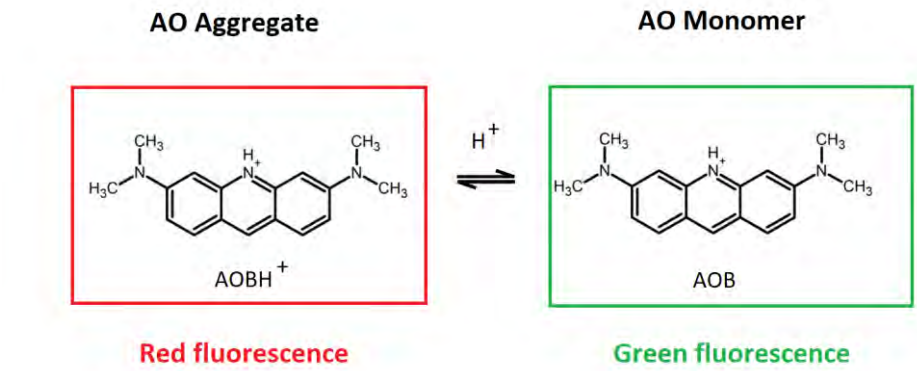

Figure 1.9 Acid- Base process on Acridine Orange (AO). On the right side the deprotonated form (monomer) is represented and on the left, the protonated form (aggregate) which exhibit different excitation and emission fluorescence. (Source: personal collection)

DNA DAMAGE ASSAYS					
		Basis of Assay	Parameters measured	Advantages	Disadvantages
Direct assays	TUNEL	TdT adds labelled nt to free 3-OH groups in the end fragments Fluorescent microscopy / cytometry	• % Cells with labelled DNA • Level of labelling	• Few sperm cells are needed (suitable for oligozoospermic cells) • Reliable • No expensive equipment is required	• Thresholds not standardized • Many assay protocols
	Neutral COMET	Electrophoresis of individual sperm cells. The DNA fragments forms the tail and the intact DNA the head. Fluorescent microscopy	It only measures DSB • % head DNA, % tail DNA • Tail lenght • Olive tail momento • % damage (0-100%) on single cell	• Few sperm cells are needed	• Thresholds not standardized • Not as sensitive as the alkaline version. It only detects dsb
Indirect assays	Alkaline COMET	Same as neutral comet except for the use of alkaline buffer which induces the DNA denaturation and undwinds the DNA strands Fluorescent microscopy	It measures SSB, and DSB • Same parameters as neutral comet	• Few sperm cells are needed • Sensitive	• Thresholds not standardized • It may identify clinically unimportant fragmentation
	SCD	Formation of halos due to the DNA relaxation after acidic DNA denaturation and lysis and chromatine protein removal Bright- field microscope	• % sperm cells with small or absent halo • Siza of the halo	• Simple. It uses bright-field microscopy	• Limited clinical data
	SCSA	Mild acid DNA denaturation. AO binds to DNA and due to its metachromatic properties if: - ds DNA (intact DNA) = AO emits in Green - ss DNA (denaturate DNA)= AO emits in red It uses fluoresecence microscopy or cytometry	• DFI, % DFI • % HDS	• Many cells rapidily examined • Most publised studies reproducible	• Expensive equipment required
	AO	Same as SCSA	• % DFI	• Simple • The AO assay, In contrast to TUNEL, allows the morphology and sperm damage determination at the same time	• Heterogenous staining • Difficult to distinguish colours, specially in the same cell when it emits in red and green at the same time

Table 1.1 Summary of the main assays for DNA damage determination. Basis of the assays, parameters measured, advantages and disadvantages are shown for each assay.

Abbreviations: nt (nucleotides), SSB (Single Strand Breaks), DSB (Double Strand Breaks), DFI (DNA Fragmentation Index), HDS (High DNA Stainability). (Source: personal collection).

1.8 Clinical relevance of sperm DNA damage

1.8.1 Sperm DNA damage related to male infertility and basic semen analysis

The primary test for assessing male fertility is basic semen analysis (ESHRE Capri Workshop Group 2004, Forti and Krausz 1998, Jose-Miller et al. 2007) performed according to World Health Organization (WHO) Guidelines (WHO, 2010b). The European Society of Human Reproduction and Embryology (ESHRE) recommend a slightly higher standard of testing (Barratt et al. 2011). In either form, basic semen analysis takes only simple visual measurements; as such, men who have abnormal sperm according to WHO criteria often still contribute to a spontaneous pregnancy and, conversely, men with values above the reference WHO ranges may still suffer from infertility (Guzick et al. 2001, van der Steeg et al. 2011).

Because basic semen analysis parameters do not provide an accurate prediction of fertility, many different 'advanced' tests of sperm have been developed and suggested to assess or diagnose other sperm abnormalities that are not revealed by standard analysis. These include: anti-sperm antibody tests (MacMillan and Baker 1987); acrosome integrity tests (Franken et al. 2000); sperm penetration assay (Barros et al. 1979, Rogers et al. 1979); oocyte binding assay (Liu et al. 1988); hemi-zona assay (Burkman et al. 1988); hyaluronic binding assay (Huszar et al. 2006, Prinosilova et al. 2009, Yogev et al. 2010), and reactive oxygen species (Erel 2005, Valavanidis et al. 2009)(ROS) test among others (Samplaski et al. 2010).

The quality of the genetic material being delivered by the sperm, to the conceptus, is a key factor neglected by all the above current tests. For this reason assessment of sperm DNA damage has gained clinical research impetus and different tests have been developed.

Many studies have reported an association between sperm DNA damage and male infertility using a range of assays such as SCSA (Evenson *et al.*, 1999, Giwercman *et al.*, 2010, Spano *et al.*, 2000) and TUNEL (Carrell *et al.*, 2003). Correlation of DNA damage levels and Assisted Reproductive Technique (ART) outcomes has been examined using SCSA (Evenson *et al.* 2002, Larson-Cook *et al.* 2003, Oleszczuk *et al.* 2016), Comet (Morris *et al.* 2002, Tomsu et al. 2002), TUNEL (Benchaib *et al.* 2003), and AO (Virant-Klun et al. 2002).

A clinical DNA damage threshold independent of sperm concentration, motility and morphology has been suggested for the SCSA assay. A %DFI ≥ 30 was found to be incompatible with fertility (live birth) (Evenson *et al.* 1999). Spano *et al*. found that fecundability, the probability of a pregnancy in a menstrual cycle, declines with the % DFI and becomes negligible when %DFI is ≥40 (Spano *et al.*, 2000). Evenson *et al.* classified male fertility potential according to the DFI measured by SCSA in: very low (% DFI > 30), low (% DFI = 25-30), high (% DFI = 15-24), very high (% DFI <15). Different clinical thresholds have been suggested for the TUNEL assay. According to Sergerie et al. a 20% cut-off for positive TUNEL cells can distinguish with a reasonable confidence (both positive and negative predicting values were above 90 %) between fertile men with offspring and infertile males (Sergerie *et al.* 2005).

The parameters measured by basic semen analysis generally correlate with SDD levels; oligoasthenoteratozoospermic samples usually show increased SDD (Huang *et al.* 2005, Irvine *et al.* 2000, Lopes *et al.* 1998, Zini *et al.* 2001). However, it is possible to have high SDD and normal semen parameters (Larson-Cook *et al.* 2003).

1.8.2 Sperm DNA damage and assisted reproductive technique outcomes

Assisted Reproductive Techniques (ART) include Artificial Insemination (AI), *In Vitro* Fertilisation (IVF), Intracytoplasmic Sperm Injection (ICSI), gamete and embryo cryopreservation, and Preimplantation Genetic Diagnosis (PGD). AI consists of the insertion of prepared sperm directly into the uterus with fertilisation occurring *in vivo* while in IVF and ICSI fertilisation takes place outside the body. In IVF, an oocyte is combined with prepared sperm in a dish, while in ICSI the oocyte is injected with a single sperm cell selected by the embryologist according to good morphology and motility. Both IVF and ICSI involve the hormonal treatment of the woman to increase the number of oocytes produced.

In the same way that DNA damage has been observed to have negative implications for natural conception, it has been reported that for couples where the male partner has high sperm DNA damage levels there is a lower chance of pregnancy after IVF treatment. Perhaps surprisingly no such association has been observed for ICSI(Bungum *et al.*, 2007, Collins *et al.*, 2008, Osman *et al.*, 2015, Practice Committee of the American Society for Reproductive Medicine, 2013, Zini *et al.*, 2011). For Intrauterine insemination (IUI), a lower *Odds Ratio* (OR) for men with % DFI > 30 to achieve pregnancy and delivery has been reported for the SCSA assay (Bungum *et*

al., 2007) while Muriel *et al.* found no statistically significant difference in SDD measured by the SCD assay in men achieving a pregnancy or not (Muriel *et al.*, 2006). The reason for the superior probability of pregnancy in men with higher SDD in the ICSI group is unknown. However, the female partner is less likely to have a fertility problem in the ICSI group and therefore their high quality oocytes are more likely to repair DNA damage in the male pronucleus as described in 1.5.2 (Bungum *et al.*, 2007, Osman *et al.*, 2015). In conclusion, men with SDD are more likely to achieve a pregnancy by using IVF and ICSI than natural conception. When SDD is greater than 30%, ICSI seems to offer higher probability of pregnancy. Again, the studies included are quite heterogeneous in terms of assay, protocol, threshold, inclusion and exclusion criteria used and outcome measured, and usually no power calculation is provided. Therefore, the case for routine sperm DNA testing for predicting the outcomes of ART has not been established (Collins *et al.*, 2008).

The long-term effects in the offspring conceived by ART with sperm DNA damage is uncertain. However, experimental animal studies have shown that the microinjection of sperm with fragmented DNA can lead to autosomal anomalies both inherited and *de novo* causing fertility problems in the offspring (Devroey and Van Steirteghem, 2004). Therefore, analyses of sperm DNA damage should be performed when ARTs are applied, especially ICSI as it neglects all the natural barriers of sperm selection. Applying protocols for selecting the sperm cells with intact DNA seems crucial to avoid deleterious effects in the offspring when using ARTs.

1.8.3 Sperm DNA damage and miscarriage

Traditionally, research to understand and prevent miscarriage has been focused on females with mininal investigation of the male side. However, SDD has gained popularity in miscarriage research in recent years as several systematic reviews have suggested SDD as a potential risk of pregnancy loss after natural, IVF or ICSI pregnancies (Deng *et al.*, 2019, Robinson *et al.*, 2012, Zini *et al.*, 2008, Zini, 2011). Moreover, recurrent pregnancy loss has also been associated with sperm DNA damage in a recent publication including 13 prospective studies (McQueen *et al.*, 2019). Although the study characteristics are heterogeneous and there is no routine assay or even standardised protocols for the different DNA damage assays used, a higher rate of spontaneous pregnancy loss in couples with sperm DNA damage has been observed with near consistency in all the available studies. The mechanism(s) responsible for the pregnancy loss are unknown. However, sperm DNA damage has been associated with abnormal embryo development and impaired implantation in animal studies (Ahmadi and Ng, 1999, Perez-Crespo *et al.*, 2008).

What is remarkable about these data is that, to date, no other sperm test has been linked to pregnancy loss and/or post-natal health. Most of studies that passed inclusion criteria were heterogeneous and used different DNA damage assays and thresholds for SCSA, TUNEL, and Comet. Most data only strongly supported the last two methods, this is in agreement with a further publication that ran all three assays in parallel (Simon *et al.*, 2014). No data supported the use of the SCD test (Osman *et al.*, 2015).

A more extended revision of studies regarding clinical outcomes such as pregnancy and miscarriage rates, and sperm DNA damage measured by the AO and TUNEL assays is offered in chapters 2 and 3, respectively. In Chapter 4 a study of the sperm DNA damage and the reproductive outcomes is performed with a subset of samples of the clinical trial HABSelect using the integrity tests of AO, TUNEL and CMA_3.

1.9 Hypothesis. Aims and objectives

Based on the literature and systematic reviews in the field, SDD has been shown to increase the risk of infertility and miscarriage. However, SDD testing has not been included in routine andrology laboratory testing as the evidence that links SDD and male infertility and miscarriage has been reported as insufficient (Practice Committee of the American Society for Reproductive Medicine, 2013). Another reason is the lack of knowledge about the best test for assessing SDD and the expensive instruments and reagents needed. SCSA was one of the first assays developed for SDD testing and it has been proved to accurately quantify SDD and to predict to some extent, clinical outcomes such as clinical pregnancy and miscarriage. However, an important downside of the SCSA assay is the cost of the flow cytometry instrumentation needed. The price of a flow cytometer can be variable; for example, the price of the the Accuri C6 in the lower-middle range of benchtop instruments is £42,000, but most instruments range from £64,000 to £85,000. The price of the antibodies can also be expensive. Commercial providers of the SCSA assay typically charge £42-50 if the sample is prepared in advance and no sorting is needed. In any case, the cost of SDD testing using flow cytometry seems too costly to be paid in addition to the expensive Assisted

Reproductive Techniques (ART) that our patients pay. Fluorescence microscopy coupled with methods to objectively quantify damaged cells may provide a good affordable alternative for SDD testing.

Hypothesis

This work is based on the following hypotheses:

- Different SDD assays detect different types of DNA damage.
- Decompaction of the chromatin is linked to higher SDD.
- Men with higher SDD values are more likely to have lower clinical pregnancy and higher miscarriage rates.

Aim and objectives

The work presented aimed to quantify, in a reliable, reproducible and cost-efficient manner, SDD by using fluorescence microscopy and semi-automatic objective scoring methods. The integrity assays selected for the study were AOT and TUNEL as they have been suggested to target different types of SDD and they have been supported by clinical data. Therefore, the different objectives of the study were:

- To optimise and validate the fluorescence integrity assays AOT, TUNEL and CMA_3. Different mounting solutions are assessed and positive controls using radical oxidative species such as H_2O_2 and nuclease enzymes such as DNase are used for this purpose.

- To develop semi-automatic scoring methods using clustering and graph gating methods for an objective and time-efficient scoring of the positive cells and SDD (%).
- To investigate the effect of the freezing-thawing procedure in SDD.
- To study the relationship between SDD and basic semen analysis (total count, concentration, motility) and abstinence.
- To study the evolution of SDD, if it is constant or changes across time.
- To analyse the relationship between the AOT, TUNEL and CMA_3 assays.
- To investigate the clinical relevance of the SDD by studying the correlations between SDD, pregnancy and miscarriage in surplus frozen semen samples from a subgroup of participants of the HABSelect trial. Due to the limited volume of the surplus semen, the number of integrity assays performed per sample varied, conferring the priority to the direct assay, TUNEL.
- To identify the integrity assay that correlates best with the clinical outcomes, pregnancy and miscarriage.

CHAPTER 2: Acridine Orange as an indicator of human sperm chromatin quality

2.1 INTRODUCTION

2.1.1 Acridine orange: a dual fluorescence nucleic acid stain

Acridine Orange (AO) is a cationic nucleic dye capable of differentiating between double-stranded DNA (dsDNA) and single-stranded DNA (ssDNA) by the formation of products with different physico-chemical properties, such as solubility and fluorescence (Kapuscinski *et al.*, 1982, Lerman, 1963). This molecule is used in the SCSA assay (reviewed in Chapter 1, 1.6.4) to differentiate between dsDNA and ssDNA in sperm and quantify the DNA Fragmentation Index (DFI (%)) of the sample.

AO at low concentration (< 100 mM), intercalates in-between the DNA base pairs of dsDNA as monomers, so hydrophobic forces are important. These monomers emit green fluorescence (522 nm). However, with Ribonucleic acid (RNA) the AO molecules can intercalate into the base pairs or bind through the phosphate group of the RNA due to differential charges (ionic binding) leading to the stacking of the dye (dye-dye stacking) and the condensation and precipitation of the complex, changing the emission spectra towards red (638 nm) (Plemel *et al.*, 2017). At high concentration, AO preferentially binds to the RNA by ionic interaction as more molecules of AO can be bound to the phosphate group of the nucleic acid in comparison with intercalation binding (1:1 *vs* 1:4).

AO at low concentration (50 µM), pH ≈ 7, and at room temperature (RT), dissolved in aqueous solution emits a single peak of fluorescence at ≈ 525 nm (green emission) (Ichimura *et al.*, 1971, Kapuscinski *et al.*, 1982, Plemel *et al.*, 2017). However, the addition of DNA to a low-concentration AO solution (50 µM) slightly shifts the emission spectra of the intercalated product towards a shorter wavelength still within the green emission range (≈ 515 nm). The addition of RNA leads to a double peak emission spectrum (≈ 515 nm and ≈ 650 nm, green and red) due to the formation of two products, the intercalated AO-RNA (green emission) and the precipitated AO-RNA (red emission) (Plemel *et al.*, 2017).

At concentrations > 200 µM (*i.e.,* 500 µM) AO emits a single peak at 650 nm (red) independently of the nucleic acid added and when dissolved as free AO molecules in water at pH ≈ 7 at RT.

2.1.1.1 Acridine orange for the analysis of DNA susceptibility to acid denaturation: base of the sperm chromatin structure assay

The effect of low pH alongside heat on DNA denaturation, was studied by assessing the fluorescence change, green to red, in AO-stained salivary glands of *Drosophila* (Nash and Plaut, 1964). Cells were fixed with 45 % acetic acid, treated with 0.3 - 1 N HCl and stained with AO showed red fluorescence, whilst the exact same treatment but using lower molality of HCl (0.1 N) showed yellow-green fluorescent cells. Because the concentrations of acid used were too low to cause appreciable purine removal, it was concluded that the red fluorescence emitted from the chromosomes after the AO staining was due to acid denaturation rather than depurination (Nash and Plaut, 1964).

The concept of a DNA denatured fraction (α_t) was proposed by Darzynkiewicz *et al.* to calculate the DNA susceptibility of single cells to heat denaturation by dividing the red intensity by the total intensity (red + green) of single cells (Darzynkiewicz *et al.*, 1975a). Five years later, Evenson in collaboration with Darzynkiewicz and Melamed found a similar cell denaturation pattern for acid-denatured and AO-stained semen samples of fertility patients (Evenson *et al.*, 1980). This assay was later commercialised as the Sperm Chromatin Structure Assay (SCSA) for which the result is expressed as the DNA Fragmentation Index (DFI) (%). The DFI (%) of the ejaculate or sample is calculated by scoring the percentage of cells outside the main sperm population according to their single-cell DFI parameter. The single-cell DFI parameter is calculated by the equation developed by Evenson (Evenson, 2016).

DFI = [red fluorescence / (red +green) fluorescence]

SCSA is usually classified as an indirect assay for DNA damage as it might appear to measure the susceptibility of DNA to be damaged under low pH conditions. However, the DNA susceptibility to low pH is linked to the quality of the chromatin, as DNA with previous fragmentation or other types of damage is more prone to acid denaturation (Evenson, 2016), the type of damage targeted by the assay is still debated (Bungum *et al.*, 2011b).

High DNA Stainability (HDS (%)) is a further parameter that can be assessed when performing the SCSA assay. HDS is thought to measure the percentage of immature sperm with abnormal nuclear proteins and chromatin structure (Evenson, 2017).

HDS (%) is calculated based on the percentage of cells with high green intensity. According to Evenson, who uses a 1024 x 1024 gradations (channels) for the green and red fluorescence intensities, high DNA stained cells correspond to those with gradation values above 750 in the green fluorescence channel (Evenson, 2018).

2.1.2 AO, laboratory outcomes and clinical utility

The majority of the studies in the literature use SCSA and it is difficult to find large studies that only use AOT. As SCSA and AOT follow the same principle, it seems appropriate to consider equally the clinical evidence from both tests. Moreover, SCSA is considered the most objective and accurate version of the AOT. For these reasons, the clinical evidence showed in this chapter has been based mostly on SCSA studies.

2.1.2.1 AO and basic semen parameters

Conflicting results have been obtained regarding the association and correlation between DFI and classical sperm parameters such as motility, morphology and concentration. The correlation often seems to be weak ($-0.22 < r < -0.46$) (Evenson *et al.*, 1999, Spano *et al.*, 1998) which is also in line with a recent meta-analysis (Cho and Agarwal, 2017). DFI being somewhat independent of classical basic semen analysis parameters, so having a potential separate, independent predictive ability is a motivator for its clinical use.

Interestingly, HDS has been correlated with abnormal head shape and acrosome (Boe-Hansen *et al.*, 2006).

2.1.2.2 AO and fecundability

Fecundability or in-vivo male fertility declines as a function of the percentage DFI (%) (Evenson *et al.*, 1999, Giwercman *et al.*, 2010, Spano *et al.*, 2000). A lower DFI value does not necessarily imply normal fertility, as the whole natural process involves other sperm traits such as adequate motility, morphology, acrosome integrity, etc. However, the presence of a DFI (%) of 30 - 40 % is related with fertility impairment (Evenson *et al.*, 1999, Spano *et al.*, 2000). In fact, according to the DFI measured by SCSA the in-vivo male fertility potential can be classified into: poor (DFI > 30%), fair (DFI = 25 - 30 %), good (DFI = 15 - 24 %), and excellent (DFI < 15 %) (Evenson *et al.*, 2002).

2.1.2.3 AO and assisted reproductive techniques IUI clinical data: biochemical and clinical pregnancies and IUI deliveries

One of the few studies that evaluates the implications of high DFI % in the IUI success in 387 cycles, showed that the *Odds Ratios* (OR) for biochemical pregnancy, Clinical Pregnancy (CP) and delivery were significantly lower for couples with DFI > 30 % as compared with those with DFI ≤ 30 % (Bungum *et al.*, 2007).

IVF and ICSI fertilisation rates

DFI (%) had no impact in the fertilisation rates in 178 couples undergoing IVF and 174 ICSI (Virro *et al.*, 2004). However, in a larger study with 1117 couples undergoing IVF and 516 ICSI, the fertilisation rate was significantly lower in IVF couples with DFI greater than 30 %, but no effect was observed in ICSI couples (Oleszczuk *et al.*, 2016).

Interestingly, lower fertilisation rates were related with higher HDS (HDS ≥ 15 %) in IVF but not ICSI couples (Virro *et al.*, 2004).

IVF and ICSI embryo development

The presence of denatured sperm cells (higher DFI (%)) in the ejaculate was associated with a decrease in the embryo quality in the IVF but not ICSI groups, although it was not statistically significant (Oleszczuk *et al.*, 2016).

Virro *et al*. showed that men with DFI greater than 30 % had a lower blastocyst rate than men with DFI lower than 30 % in the ICSI ($p = 0.07$) and IVF ($p = 0.03$) groups (Virro *et al.*, 2004). HDS (%) was not related to blastocyst rate, biochemical pregnancy (BP), ongoing pregnancies at 12 weeks, or miscarriage (Virro *et al.*, 2004).

IVF and ICSI biochemical pregnancies

No statistical difference was found between men with DFI < 30 % and men with DFI > 30 % stablishing a biochemical pregnancy in the IVF (n = 388) or ICSI (n = 223) groups in the study undertaken by Bungum *et al.* (Bungum *et al.*, 2007). However, when considering together the IVF and ICSI groups (n = 249), Virro *et al*. found a statistical difference between couples arising a biochemical pregnancy when the male partner had a DFI greater or lower value than 30 % ($p = 0.02$) and no correlation between HDS (%) and BP was observed (Virro *et al.*, 2004).

IVF and ICSI clinical pregnancies

The CP rate appears to be associated with the percentage of denatured cells in the ejaculate. The CP rate obtained in IVF (n = 139), ICSI (n = 47) and mixed IVF/ICSI (n = 24) patients was higher in patients with DFI < 27 %, however it was not statistically significant (Boe-Hansen *et al.*, 2006, Larson *et al.*, 2001, Larson-Cook *et al.*, 2003). However, none of the men with DFI > 27 % was able to achieve a clinical pregnancy (Larson *et al.*, 2001). By dividing the damaged cells according the number of channels in moderately damaged (250 to 649 channels) and highly damaged (650 to 1000 channels) the CP was found incompatible with percentages of both moderately and highly damaged cells greater than 15 % as well as with more than 27 % of total damaged cells (highly and moderately damaged) (Larson-Cook *et al.*, 2003).

When using a DFI cut-off of 30 %, no statistically significant difference was found in the number of pregnancies ongoing at 12 weeks of gestation in the group of high and low DFI (%) in 249 IVF and ICSI patients (Virro *et al.*, 2004). A recent study involving 1633 patients found no statistically significant difference between the OR for achieving CP when DFI is higher in IVF, ICSI or mixed IVF/ICSI groups were studied (Oleszczuk *et al.*, 2016). This lack of association was also observed by Bungum *et al*. in the IVF and ICSI groups, but not in the IUI when using a 30% threshold (Bungum *et al.*, 2007).

HDS (%) was not correlated with ongoing pregnancies at 12 weeks (Virro *et al.*, 2004).

IVF and ICSI live birth rates

The ORs for Live Births (LBs), computed as the number of deliveries per started cycle (%), were not statistically significant between the high and low DFI (%) groups in IVF

(n = 388) or ICSI (n = 223). However, this association as stated before was statistically significant in the IUI group (n = 387) (Bungum *et al.*, 2007).

In the study of Oleszczuk the OR for LB of couples who underwent *ovum* pick-up (1117 for IVF and 516 for ICSI couples) was significantly lower when DFI was greater than 20 % in the IVF but not tin the ICSI group (Oleszczuk *et al.*, 2016).

2.1.2.4 AO and miscarriage

Since many miscarriages have an unexplained cause, it has been hypothesised that sperm DNA quality may be one causative factor (Kirkman-Brown and De Jonge, 2017). There is disagreement about the correlation between DFI scored by SCSA and miscarriage, as some authors found a clear relationship while others find none (Robinson *et al.*, 2012).

An increase in the miscarriage rate was observed in couples with male partner with DFI > 30 % in the pooled IVF and ICSI groups but it was not statistically significant (Virro *et al.*, 2004). Bungum *et al*. found no difference for the miscarriage rate in men with > 30 % and < 30 % DFI in the IUI, IVF and ICSI individual groups. However, when pooling together all the patients an applying a cut-off of DFI > 60 % the OR for miscarriage increased to 2.4, although it was still no significant probably due to a low number of patients (Bungum *et al.*, 2007). The reason why the majority of the cited studies in this section did not find a statistically significant difference between groups of high and low DFI (%) might be due to a low number of patients as when increasing the number of men by pooling IVF and ICSI groups a significantly increased for the OR for miscarriage was obtained for men with DFI > 40 % (Oleszczuk *et al.*, 2016).

Moreover, some male partners of couples with history of recurrent miscarriage were found to have DFI ≥ 15 % according to several studies (Check *et al.*, 2005, Leach *et al.*, 2015)

Evenson studied the DFI (%) and HDS (%) in 165 presumably fertile couples wishing to achieve pregnancy over 12 menstrual cycles and found that couples with DFI > 30 % experienced a delay in the pregnancy or did not get pregnant. Out of 18 natural miscarriages, seven (39 %) were correctly predicted using the DFI and high green DNA stainability (HDS) parameters (six from high DFI and one from HDS) (Evenson *et al.*, 1999). The association with HDS and miscarriage in ART is not very clear, as different authors have shown different results; for example Lin *et al*. found that men with HDS > 15 % undergoing IVF but not ICSI had significantly higher miscarriage rates (Lin, M. H. *et al.*, 2008), while Jerre *et al.* found an association between HDS > 15 % and ICSI miscarriage, but not with IVF (Jerre *et al.*, 2019). Virro *et al.* did not find any correlation between HDS (%) and miscarriage rates in IVF and ICSI patients (Virro *et al.*, 2004)

Overall, all these results seem to indicate a relationship between sperm DNA damage and miscarriage. However, DNA-damaged sperm can fertilise the oocyte, and that explains that high levels of SDD are not always associated with a decrease in fertilisation rate as it has been observed with other DNA damage assays as comet (Morris *et al.*, 2002) and ISNT (Twigg *et al.*, 1998).

2.1.2.5 Clinical utility

High DFI values do not appear to affect the fertilisation rate but they decrease the blastocyst rate and according to some authors they might end in a pregnancy loss as

mentioned before. This chain of events seems to be more prevalent in natural conception and IUI. Although DNA damage has been shown to decrease the success of the fertility treatment, *in vitro* techniques as IVF and specially ICSI seem to be able in some cases to by-pass the DNA damage and lead to clinical pregnancy and live birth (Virro *et al.*, 2004).

Men with high sperm DNA damage should be advised in first place to try lifestyle changes like decreasing the abstinence before the natural or clinical intervention as some authors have proven a link between abstinence and DNA damage by other SDD assays like TUNEL and SCD (Comar *et al.*, 2017, Pons *et al.*, 2013, Sanchez-Martin *et al.*, 2013). ICSI seemed the optimal treatment for couples with high DFI (Bungum *et al.*, 2007, Chi *et al.*, 2017) even in those who had recurrent miscarriage history after IVF treatment (Check *et al.*, 2005).

Study	IVF-FR	ICSI-FR	IVF-ED	ICSI-ED	IVF-P	ICSI-P	IVF-M	ICSI-M	IVF-LB	ICSI-LB
Boe-Hansen 2006 139 IVF/ 47 ICSI cut-off = 27%	nd	nd	nd	nd	YES (-) (OP)	NO (OP)	nd	nd	nd	nd
Bungum 2000 388 IVF/ 223 ICSI cut-off = 30%	nd	nd	nd	nd	NO (BP, CP)	NO (BP, CP)	nd	nd	NO	NO
Larson 2000 24 IVF and ICSI cut-off = 27%	nd	nd	nd	nd	YES (CP)		nd	nd	nd	nd
Larson-Cook 2003 89 IVF and ICSI cut-off = 27%	nd	nd	nd	nd	YES (CP)		nd	nd	nd	nd
Oleszczuk 2016 1117 IVF/ 516 ICSI cut-off = 0-10%, 10-20%, 20-30%, >30%	YES (-) when DFI>30%	NO	NO	NO	NO (CP)	NO (CP)	YES (-) when DFI>40%		YES (-) when DFI>20%	NO
Virro 2004 178 IVF / 174 ICSI cut-off = 30%	NO	NO	NO	YES	YES (-) (BP) (OP)		NO		nd	nd

Table 2.1. Summary of the studies mentioned in the text that looked the association or correlation between DFI (%) levels and Fertilisation rate (FR, Embryo Development (ED), Pregnancy (P), Miscarriage (M) and Live Birth (LB).

Associations/correlation are shown in green whilst no association/correlation are shown in red. OP= Ongoing Pregnancy, BP= Biochemical Pregnancy, CP= Clinical Pregnancy, nd= no data available

2.1.3 Advantages and pitfalls of the traditional AOT and the SCSA

SCSA was one of the first SDD assays developed (1980) and it has been used in many studies with animal and human sperm predicting male infertility and the success of ART, and helping to decide the fertility treatment most appropriate for the couple (Evenson *et al.*, 2002). In cases of high DFI (%) the success of IUI is low so couple are generally encouraged to try other, more complex ART, especially ICSI (Evenson, 2011).

SCSA has a robust and well detailed protocol claimed as user-friendly and with very high repeatability; 132 frozen aliquots from human and animal samples were distributed between 7 different laboratory centres and the DFI (%) obtained for aliquots from same sample was almost exact (25 % *vs* 26 % of DFI) and the correlation obtained for the overall samples was 0.9871 (Evenson *et al.*, 2002). Other alleged advantages are the suitability for frozen samples as Evenson demonstrated in mouse and board semen cryopreserved in semen extender that DFI (%) was not affected after the thawing of the cryopreserved pellets (Evenson *et al.*, 1989, Evenson *et al.*, 1994). However, some damage can be induced by the cryopreservation method in human sperm (Liu *et al.*, 2016) probably due to different level of chromatin compaction when compared to Evenson animal studies.

The amount of data obtained in short time by SCSA (5000-10000 readings in less than five minutes) is another claimed advantage of the assay (Evenson *et al.*, 2002), although the benefit of assessing such a number of cells has not been corroborated with further publications. Typically, for the assessment of sperm, one or two counts of 200 cells are enough to accurately determine the concentration, motility and morphology (WHO, 2010a).

However, the major inconvenience of the assay is the very high price of the flow cytometry and the lack of vision to assess the morphology of the cells and discard possibly debris that influence the results. In this context, fluorescence microscopy could be the solution to these problems (Tejada *et al.*, 1984). However, the AO fluorescence microscopy assessment relies on the operator ability to differentiate between green and red stained cells which makes the assay very subjective and represents a big problem for any colour-blind operators. Moreover, the cells are not always clearly green or red which makes the assay even more subjective and complicated.

Fluorescence microscopy with coupled sensitive monochrome camera and filters for green and red channels could offer similar results to flow cytometry; single-cell DFI could be calculated based on the green and red intensities extracted from acquired images from AO-stained slides. Applying an appropriate threshold, damaged cells above a certain DFI would be identified as damaged and a percentage of damaged cells (DFI (%)) could be given for every ejaculate.

2.2 AIM OF THE STUDY

The principal aim of the study was to optimise and develop a method to quantify in a reliable and reproducible manner the DNA Fragmentation Index (DFI) as an indicator of the Sperm DNA Damage (SDD) by exposing semen samples to low-pH denaturation, staining them with AO and quantifying the red and green intensity fluorescence with fluorescence microscopy and a high resolution camera.

The study involved:

- The assessment of the use of commercial mountants on the AO fluorescence emission.
- The description of the parameters obtained with the semi-automatic equipment and its relation to the AO visual assessment. Calculation of the DFI in an equivalent manner as for the SCSA assay which is performed with flow cytometry
- The calibration of the semi-automatic equipment based on the AO visual assessment.
- The validity of the AO semi-automatic assay when compared to the AO traditional visual assessment.
- The analysis of the intra and inter-variability of the visual and semi-automatic assessment for AO.
- The investigation of possible DNA damage inductors to use as positive controls such as H_2O_2 and DNase.
- The investigation of the effects of the freezing-thawing procedure on DNA when storing samples for a later assessment.

- The comparison of DFI (%) between donors and patients of clinical trial HABSelect.

2.3 MATERIAL AND METHODS

Unless otherwise stated all reagents were purchased from Sigma-Aldrich

2.3.1 Sperm preparation

2.3.1.1 Fresh donor samples

Pre-cleaned snowcoat microscope slides (3800340, Leica Biosystems) were dipped for 5 min in working Poly-L-Lysine solution (1:10) prepared from Poly-L-lysine sol 0.01 % (Sigma-Aldrich), and dried overnight or at least for 1 hour at room temperature (RT) until they were dried.

Control semen samples were acquired from five volunteer donors of the Birmingham Women's Hospital (HFEA centre 0119, Ethics Committee Reference Number 13/EM/0272). The donors were anonymised as A, B, C, D, and E. The same donors were used in Chapter 3. All donors presented good concentration, motility and morphology results according to WHO criteria (WHO, 2010a). Ejaculates were obtained by masturbation after 1-5 days of sexual abstinence depending on the experiment and allowed to liquefy. The semen was washed in Phosphate-buffered saline (PBS) by centrifugation (2 min, 600 g, RT) and the pellet was re-suspended in PBS to achieve a final concentration of 10 x 10^6 cells / ml approximately.

10 µL of fresh-washed sperm (10 x 10^6 cells / ml) and frozen-thawed prepared sperm (2.3.1.2) were pipetted over the centre of pre-coated slides and spread manually by circular and gentle movements with the tip of the pipette in a small area of approximately 3 cm x 3 cm. The slides were allowed to dry for at least 60 min at RT before commencing the AO staining protocol.

The number of donors, samples and replicates used in each experiment is detailed in the captions below the figures and tables in the results section (2.4).

2.3.1.2 Frozen donor samples

An aliquot from the same three donors A, B and D used in 2.3.1.1 was prepared in three different dates by gradients (PureConception™, CooperSurgical) and frozen This aliquots were used for AO (Chapter 2) and TUNEL (Chapter 3) stainings.Briefly, a density gradient was prepared by under-layering 1 ml of 40 % (ART-2040, CooperSurgical) with 1 ml 80 % (ART-2080, CooperSurgical) and a top layer of 1 ml liquefied semen was added in a 15 ml polystyrene Falcon tube (05-527-90, Fisher Scientific). The samples were then centrifuged (12 min, 600 g, RT). The supernatant was discarded and 3 ml of Phosphate Buffered Saline (PBS) were added to the pellet and resuspended by 'flicking' the tube prior to the centrifugation (12 min, 600 g, RT). The supernatant was discarded, and the pellet re-suspended in 588 µl Gamete buffer (Sydney IVF Gamete Buffer, Cooper) and 412 µl of cryoprotectant (SpermFreeze™, FertiPro) gently added drop by drop. The samples were homogenised and split in cryovials containing 250 µl each and immersed in LN_2 after allowed 10 min at RT to equilibrate.

On the day of the AO assay, the cryovials were immersed in a water bath at 37 ºC to thaw. Thawed samples were transfer to a 15 ml Falcon tube (05-527-90, Fisher Scientific) and 1.75 ml of PBS was gently added to the samples. Samples were mixed gently by flicking the tube and then centrifuged (500 g for 10 min), supernatant removed, the pellet re-suspended in 2 ml of PBS and centrifuged a second time (500 g for 10 min). Finally, the pellet was diluted in PBS, adjusted to a final concentration of approximately 10 x 10^6 spermatozoa / ml and used to make smears following the same procedure as with fresh donor samples (2.3.1.1).

2.3.1.3 HABSelect patient samples

A subset of 134 male patient samples from the HABSelect trial were used in this chapter. 16 assisted conception units licensed by the Human Fertilisation and Embryology Authority (HFEA) in the UK took part in the trial. HABSelect was approved by the National Research Ethics Service (approval number 13/YH/0162) and by the doctors of the assisted conception units. Patients eligible for HABSelect trial gave consent for the donation of the residual semen samples for biomedical research to the Human Biomaterials Resource Centre (HBRC) Biobank, University of Birmingham.

All patients were indicated for ICSI treatment and their age was comprised between 18-55 years old. The sperm preparation and fertility treatment were performed outside the University of Birmingham by the participating clinics.

Briefly, the sperm were prepared according to the local protocol and used for the ICSI/PICSI treatment, the surplus of the sample was then collected, centrifuged (500 g 10min) and frozen following local protocol.

On the day of the AO assay, the samples were thawed following the same protocol as for the frozen donor samples (2.3.1.2), but the final concentration aimed for a minimum of 2.5 x 10^6 spermatozoa/ml, as HABSelect patients usually exhibited lower concentration than the donors. The smear procedure was the same as with fresh and frozen donor samples detailed above (2.3.1.1).

2.3.2 Acridine orange assay

The protocol followed was the one described by Tejada *et al.,* (Tejada *et al.*, 1984). Briefly, 0.1 M solutions of NaOH and HCl were prepared by diluting sodium hydroxide pellets (99 %) (BDH Laboratory Supplies) and hydrochloric acid (36.5% - 38 %) (Sigma-Aldrich), respectively, in 80 MΩ nanopure water. Carnoy's solution was prepared by mixing methanol 100 % (BDH-VWR) and acetic acid (100 %) (BDH Laboratory Supplies) in a proportion of 9:1 in a fume cupboard. AO working solution (12 µg/ml) was prepared by diluting AO ready-to use solution (A3568, Thermofisher) in 80 MΩ nanopure water. NaOH, HCl and Carnoy solution were stored at 4 ºC and used for 1 month before preparing new solutions. The AO working solution was wrapped with foil to protect it from light exposure, kept at 4 ºC and used for a total of 4 months.

The smears were firstly immersed in PBS for 5 min, and for 30 seconds in HCl (0.1 M) and then 30 seconds in NaOH (0.1 M). The sperm cells were then fixed in Carnoy's solution for 2 hours at RT and allowed to air dry for 60 min at RT before storing at 4º C for later processing. The AO staining was performed immersing the slides for 5 min in a Coplin jar with approximately 10 ml of AO working solution (12 µg/mL). The slides

were hold in a rack and immersed in approximately 350 ml of 80 MΩ nanopure water contained in a clean staining box. The wash was performed under gentle and manual agitation for 5 min. A total of three washes were performed to ensure the elimination of the AO excess. The samples were allowed to dry for 60 min at RT before mounted with DPX mountant (06522, Sigma-Aldrich) using a Pasteur pipette and 22 mm x 22 mm coverslips.

2.3.2.1 Study of the suitability of different commercial mounting solutions for use in combination of the AO staining assay

A preliminary study with donor samples PBS-washed and AO-stained mounted with a range of commercial mountants (**Table 2.2**) was performed to assess their suitability and select the most appropriate to use in combination with the AO assay. The mounted slides were let to dry overnight and kept at 4 ºC till visualization. Subsequent to this study all routine protocol samples stained with AO were mounted using DPX.

Mounting	*Company*	*Characteristics*
Permafluor™	**Thermo Fisher Scientific (TA-030-FM)**	**Aqueous Mounting Media**
Fluoromount™	**Sigma-Aldrich (F4680)**	**Aqueous Mounting Media**
Fluoroshield™	**Sigma-Aldrich (F6182)**	**Aqueous Mounting Media**
Clearium ®	**Leica Biosystems (3801102)**	**<60 % Toluene, <10 % dibutyl phthalate, <5 % butylated hydroxitoluene**
DPX	**Sigma-Aldrich (06522)**	**Destirene dissolved into Toluene-xylene**
Eukitt ® Hardening Solution	**Sigma-Aldrich (03989)**	**45 % acrylic resin and 55 % xylenes**

Table 2.2 Composition and AO appearance for sperm cells with six different commercial mounting solutions

.

2.3.2.2 AO assay validation with samples exposed to DNA-damage inductors (positive controls)

A series of damage inducers were employed to create DNA damage in the sperm samples in order to validate our system. Hydrogen peroxide in different concentrations (H_2O_2) (Sigma-Aldrich, H1009) and DNase (3 U/ml) (Thermo-Fisher, EN0521) was used before and after the fixation for different periods of time. The DNase solution (3 U / ml) was prepared on the experiment day by adding 3 µl DNase I, RNase free 1 U / µl, 100 µl 10x Reaction buffer containing Ca^{2+} and Mg^{2+} to activate the enzyme and 897 µl of Permeabilisation Solution. The permeabilisation solution was prepared by adding 0.1 g sodium citrate (Sigma-Aldrich) and 100 µl Triton X-100 (Sigma-Aldrich) to 100 ml of distilled water.

Exposure to the reducing agent dithiothreitol (DTT) (Sigma-Aldrich) was also studied. DTT reduces the di-sulphide bonds and therefore the HCl used in the AO assay should increase the denaturation of the DNA, so higher DFI (%) should be expected.

2.3.3 AO scoring

The stained slides were visualized on an Olympus fluorescence microscope (BX61) with a Xenon lamp using a 60x oil immersion objective, and a QUANTUM: 512SC camera (Photometrics) attached to a PC running Cairn Metamorph software (version 7.8.13.0). A monochromator was used to limit the excitation light from the Xenon lamp to 490 ± 7.5 nm and a long-pass emission filter for the direct visualization of the multiple colour-fluorescent cells. Two emission filters were set up in a filter wheel; 525 ± 18 nm and 630 ± 30 nm for the imaging and quantification of the individual wavelengths green and red, respectively.

2.3.3.1 AO visual scoring

200 sperm cells stained by AO were visualised by eye under the fluorescence microscope and classified in 3 categories: green-yellow, orange and orange-red. The % of damaged cells was calculated in accordance to WHO recommendations for binomial assays such as motility, vitality and acrosome reaction (WHO, 2010b). Briefly, orange and orange-red cells were counted in a total of 200 cells to calculate the percentage of damaged cells. A second count of orange and orange-red cells was performed in a total of 200 new cells in different fields of view from the first counting. If the difference between the two percentages was acceptable according to the Appendix 7.3 in the WHO manual (WHO, 2010b), the average was computed and given as the

DNA Fragmentation Index (DFI (%)) of the sample. Briefly, the acceptance of these binomial assays depends on the number of total cells accounted (**Figure 2.1**) and on the average percentage of positive cells between the 2 counts (**Table 2.3**); when counting 2 x 200 cells, a maximum of a 10 % (40 cells) difference between the 2 counts is acceptable (**Figure 2.1**). However, the maximum difference accepted due to a 5 % sampling error is different (from 0 % to 10 %) depending on the final average percentage of positive cells among the total population investigated (400) (**Table 2.3**). If the difference was not acceptable then two new counts were performed and averaged again. If the difference was found not to be acceptable at the second count, then the sample was not included in the analysis as the difference could not be justified by a reasonable sampling error (5 %) and the slide was suspected not to be homogenously stained. The difference between the two visual assessments was not acceptable in 6 out of 118 patients, and when repeated for two counts, they were found acceptable and therefore were all included in the analysis. Only one of the donor slides was rejected as the difference between the two counts was not acceptable after the second attempt. A further analysis of the slide showed a lack of the homogeneity of the staining. This same effect was observed in many of the slides from our collaborator laboratory in Leeds. They were informed about the issue and their slides were rejected and not included in our work.

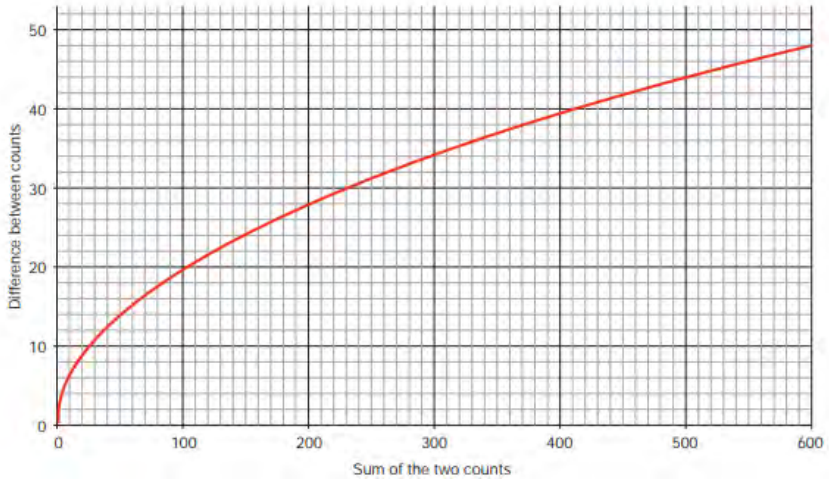

Figure 2.1 Acceptable difference between two replicate counts based on the total number of sperm cells assessed. Extracted from WHO laboratory manual for the Examination and processing of human semen (WHO, 2010b)

Average (%)	Acceptable Difference*
0	1
1	2
2	3
3–4	4
5–7	5
8–11	6
12–16	7
17–23	8
24–34	9
35–65	10

Average (%)	Acceptable Difference*
66–76	9
77–83	8
84–88	7
89–92	6
93–95	5
96–97	4
98	3
99	2
100	1

*Based on the rounded 95% confidence interval.

Table 2.3 Acceptable difference between the two percentages of cells accounted from a total of 400 cells (2x200) based on the percentage average. Extracted from WHO manual (WHO, 2010b).

2.3.3.2 Semi-automatic AO scoring method based on acquired grey-scale images using correspondent filters for the red and green emission, Quantafrag.

Images were acquired and analysed using MetaMorph® Microscopy Automation and Image Analysis Software. For practical purpose we named this AO scoring method

based on the semi-automatic quantification of individual emission wavelengths of acquired images Quantafrag.

Acquisition settings

A fixed exposure and gain for the two channels were employed (400 and 600ms exposure time for the green and red channels and gain = 1 for both). These exposure times were based on initial experiments which demonstrated the red channel needed higher exposure than the green in order to achieve the best resolution and dynamic range. This would be in accordance with the SCSA parameters set by Evenson where the red photomultiplier has a higher gain than the green (~125 / 1,000 and ~475 / 1,000 channels, respectively) (Evenson, 2013).

Different exposure times can be used, and the same results will be obtained as long as the ratio between the red and green channels (1.5) is maintained and no photon-saturation or photo-bleaching occurs.

Unlike other dyes and fluorophores, such as fluorescein in the TUNEL assay (*In Situ* Cell Death Detection Kit from Roche), the AO molecules at the exposure and gain used (data no included) showed no obvious photobleaching according to preliminary tests.

Image analysis process and data acquisition

Different fields of view were imaged till reaching a minimum number of 200 cells. Although a number between 500 - 1000 cells was usually reached.

For each field of view, two grey scale images were acquired, one corresponding to the red and one to the green channel. The images were superimposed in an additive manner and Regions of Interest (ROI) were created around the sperm heads by

thresholding the resultant image. The superimposition of both channels allowed the visualization of the total area of the sperm heads, so the ROIs were representative, and the average intensities were accurately computed. This process was repeated for every plane. The image analysis process is summarised in **Figure 2.2**

The inclusion of debris and cell clumps into the data analysis was minimised by applying filters for area (0 - 300 pixels), shape factor (0.8 - 1).

The information regarding intensity, shape and size of the ROIs was extracted into an excel spreadsheet. The process was repeated for every plane. The intensity was measured in several ways, as the average (intensity (arb.u) / area (pixels)) and also the total intensity (arb. u) for both green and red channel.

Afterwards, the DNA Fragmentation Index (DFI) was calculated as first described in 1975 (Darzynkiewicz *et al.*, 1975b) and currently used in the SCSA assay (Evenson *et al.*, 1980)

DFI= Red average intensity / (Green + Red) average intensity

**Average Intensities are measured in intensity (arb.u) / area (pixels)*

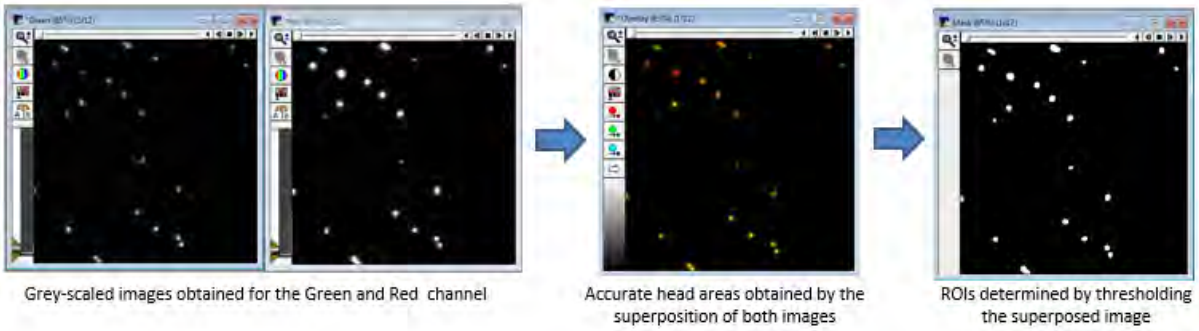

Grey-scaled images obtained for the Green and Red channel

Accurate head areas obtained by the superposition of both images

ROIs determined by thresholding the superposed image

Image Plane	Object #	R Average intensity	G Average intensity	R Total intensity	G Total intensity	Area head	Shape factor	DFI
1	1	7188.58	2379.59	2235647	740052	311	0.86	0.75
1	2	6398.04	2067	882929	285246	138	1	0.76
1	3	3520.03	3203.23	584325	531737	166	0.82	0.52
1	4	2782.47	3117.36	161383	180807	58	1	0.47
1	5	7715.17	1945.61	1218997	307407	158	1	0.80
1	6	3147.29	2720.65	195132	168680	62	1	0.54
1	7	9244.96	1571.35	2311240	392838	250	0.99	0.85
1	8	6369.47	2458.08	904465	349048	142	1	0.72
1	9	6716.22	2290.54	1101460	375649	164	0.98	0.75
1	10	5831.03	2703.37	828006	383878	142	1	0.68
1	11	6529.22	2095.81	985912	316467	151	0.98	0.76
1	12	2416.33	2818.98	123233	143768	51	1	0.46
1	13	2856.86	3065.08	202837	217621	71	1	0.48
1	14	6815.65	2286.78	1117767	375032	164	0.97	0.75
1	15	6259.51	2544.68	431906	175583	69	0.88	0.71
1	16	5686.11	2591.79	807427	368034	142	1	0.69
1	17	4522.45	3092.92	551739	377336	122	0.97	0.59
1	18	3909.47	3321.34	469136	398561	120	1	0.54
1	19	4173.14	2920.66	496604	347558	119	1	0.59
1	20	4015.98	3168.37	461838	364362	115	1	0.56
1	21	6876.08	2726.81	1980312	785320	288	0.8	0.72

Data extracted from the ROIs

Figure 2.2 Process for image acquisition and single-cell data extraction. Images are acquired in different areas of the slide. Grey-scale images for the green (left) and red (right) channel are automatically acquired for every field of view by using the filter cube with the specified filters in 2.3.4. Once the image acquisition of the slide is completed, the grey-scale images of both channels (green and red) are superimposed in an additive manner and Regions Of Interest (ROI) are drew around the sperm heads by using the thresholding tool. The final step consists in the extraction of the data of interest in an excel file, the average and total intensity for green and red, and the size and shape factor of the sperm heads. The DFI is calculated with the green and red average intensities:

DFI= Red average intensity/(Green+Red) average intensity

2.3.3.2.1 Calibration of the DFI threshold of Quantafrag based on the traditional visual method

Donor samples (three donors, 60 cells in total) were used to calibrate the semi-automatic system based on the visual colour exhibited by the stained cells. While the corresponding visual colours of individual cells were annotated (green, yellow, orange and red), single plane images were acquired using the correspondent filters as described before. Using Metamorph® we extracted single-cell information from the images regarding emission light alongside the sperm size and shape factor. The DFI was also calculated according to the formula described in 2.3.3.2. A comparison between the visual colour category and the green and red average intensity and DFI from the cells was done to find the best visual colour discriminator. The correlation between the DFIs (%) obtained with the visual and Quantafrag methods was studied in 118 patients whilst using different cut-offs for the Quantafrag system.

2.3.3.3 Consistency of the AO assay: inter an intra-variability for the AO visual and Quantafrag assessment

Patient sample smears previously prepared, frozen, stained with AO by a collaborator laboratory in Leeds were sent to Birmingham so we could compare the DFI (%) obtained with Quantafrag and their results and calculate the inter-assay variability.

Intra-assay variability was assessed by our laboratory via studying the correlation of % DFI assessed by Quantafrag and visually for two replicates of donor samples. The visual assessment result for each replicate was based on the average of two independent scorings in order to check the acceptance of the replicates and to give a

reliable percentage of damage as explained in 2.3.3.1. The CV (%) was calculated in six samples from three donors and in nine frozen-thawed samples from three donors.

2.3.4 DNA damage scoring for donors and HABSelect patients

In this chapter a total of seven different donors were used for the different experiments. To compare the DNA damage levels of a normal population and the patients, a total of nine frozen samples from three donors, and 15 fresh samples from seven donors were used to compare the DFI % values obtained by the visual method and also the semi-automatic system Quantafrag when using a specific cut-off (0.66). The correlation and the agreement between both methodologies was studied for the patient population which had a very wide range in DNA damage levels.

2.3.5 Statistics

The measurement error for the AO assay was calculated within sperm donor sample replicates using the coefficient of variance (CV (%)):

CV (%) = SD/Average

The agreement between the two methods was studied by the Bland-Altman test. The average of the measurement for both methods was plotted against the difference between the measurements for both methods. The bias computed by the SD was studied.

The correlation was calculated by the Pearson r and R square coefficients

To analyse if the difference between green and red emission intensities, and DFI were statistically different between the visual colour categories of the cells the Tukey test was employed assuming normal distribution.

To analyse if the difference of DFI between two groups was statistically significant the non-parametric test of Mann-Whitney was employed. When comparing more than two groups the Kruskal-Wallis alongside the post-hoc of Dunn's multiple comparison test were employed.

To analyse if the damage inductors increased significantly the percentage of positive cells (% DFI for the AO staining assay when applying a cut-off of DFI > 0.66 the Chi-squared two-sided test was performed. To compare if the % DFI between the donors and patients was significantly different, the Chi-squared two-sided test was performed.

2.4 RESULTS

2.4.1 Acridine orange assay

2.4.1.1 Mounting experiments

Use of the aqueous mountants Permafluor, Fluoromount and Fluoroshield had a dramatic effect upon assay results, with only green cells being observed and a very high green background, no red emission could be observed at all when exposing to the specified exaltation light for the AO molecule (**Figure 2.3 A, B, C**). The mountants Clearium, DPX and Eukitt allowed classification of sperm cells into different categories by eye with heads having differing tonalities from green to red (**Figure 2.3 D, E, F**).

The different intensity ranges obtained with the 6 mentioned commercial mounting solutions were compared to determine the most suitable for the AO assay in 3 donor samples. After subtracting the relevant background intensity from each fluorescent channel (Green and Red), dynamic ranges were calculated and plotted in a box and whiskers graph (**Figure 2.4**). Although Clearium showed the wider dynamic range for the green channel, DPX showed the best dynamic range for the red channel while also having a good range for the green channel. No photobleaching assay was perform as the dye showed good stability over the image acquisition.

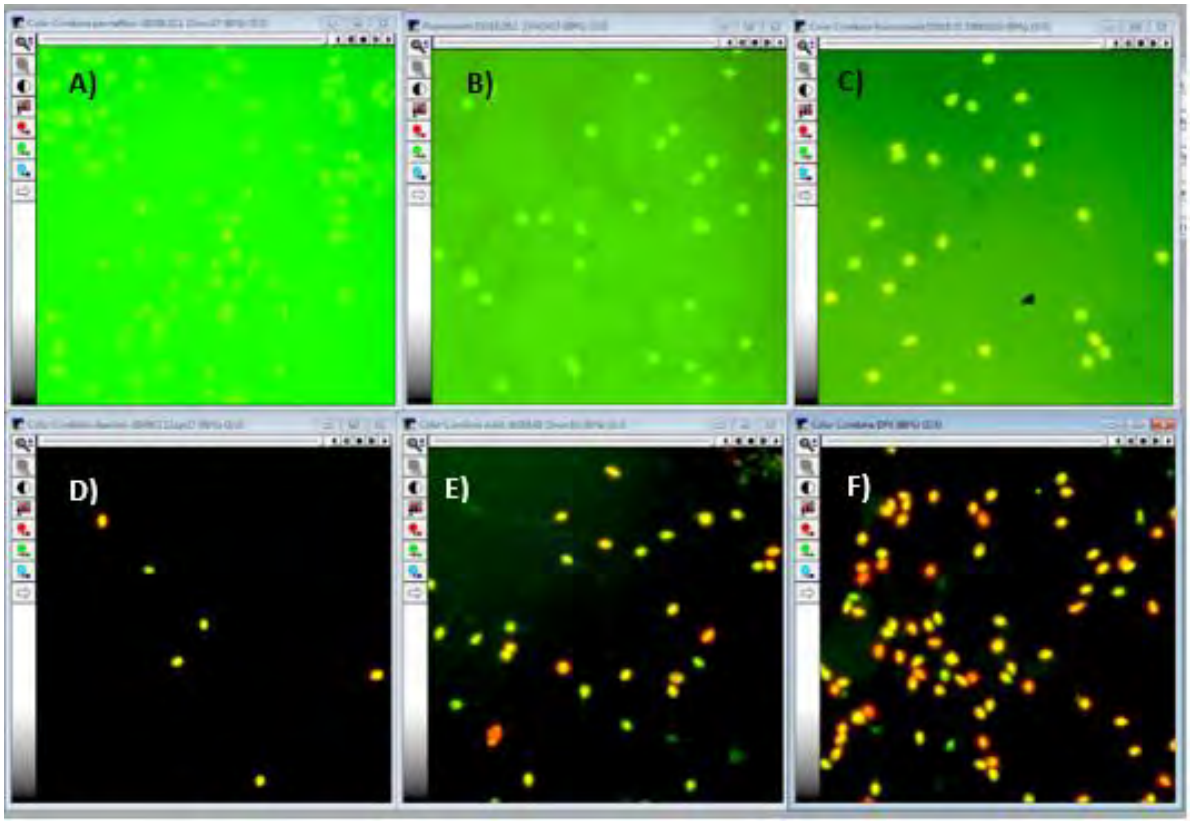

Figure 2.3 Visualization of AO stainings for the different mountants. The background and sperm cells when using **A)** Permafluor, **B)** Fluoromount, **C)** Fluoroshield were totally green. **D)** Clearium, **E)** Eukitt and **F)** DPX had much lower background, and sperm cells exhibited different colours; green, yellow, orange and red. The experiment was performed with three donors (A, B and C). Each donor sample was used to prepare 6 different smears; one for each mountant. The figure shows the images corresponding to donor A.

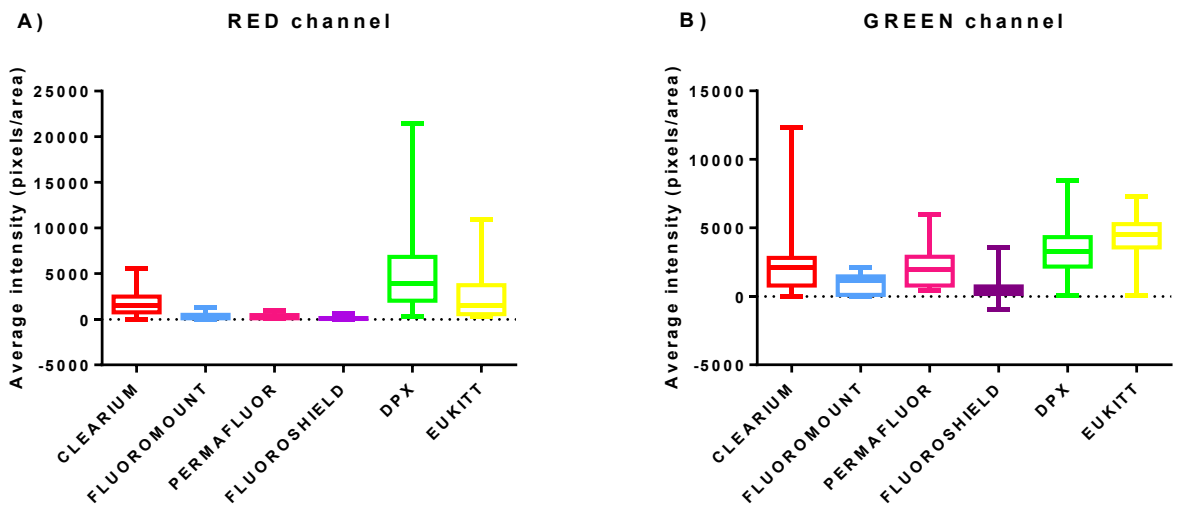

Figure 2.4 Red and Green intensities calculated by Quantafrag for positive control slides according to the different mountant. All intensities were calculated subtracting their correspondent average backgrounds for each channel. The experiment was performed with 2658 sperm cells from three donors (A, B, and C).

2.4.1.2 AO assay validation with samples exposed to DNA-damage inductors (positive controls)

The DFI ranges of a total of 6 ejaculates from different days of 2 donors were measured by the AO assay and our semi-automatic developed equipment at the baseline level and after exposed to the DNA damage agents, hydrogen peroxide (H_2O_2) and DNase. The effect of the reducing agent Dithiothreitol (DTT) on the DNA susceptibility to denaturation was also investigated.

a) DNA oxidative damage by hydrogen peroxide (H_2O_2)

After exposure the slides to HCl, NaOH and Carnoy´s solution the samples were split in two aliquots. One aliquot was directly stained with AO and the other aliquot was exposed to 1mM H_2O_2 treatment before staining with AO.

Exposing the fixed sperm cells to H_2O_2 (1mM) for 15 minutes produced a statistical significant increase in the DFI according to Kruskal-Wallis ($p<0.0001$) (**Figure 2.5 A**), a slight displacement to the right of the DFI distribution (**Figure 2.5 B**), and an increase on the number of positive cells (DFI>0.66) according to the Chi-squared 2 sided (% DFI) (**Figure 2.5 C**)

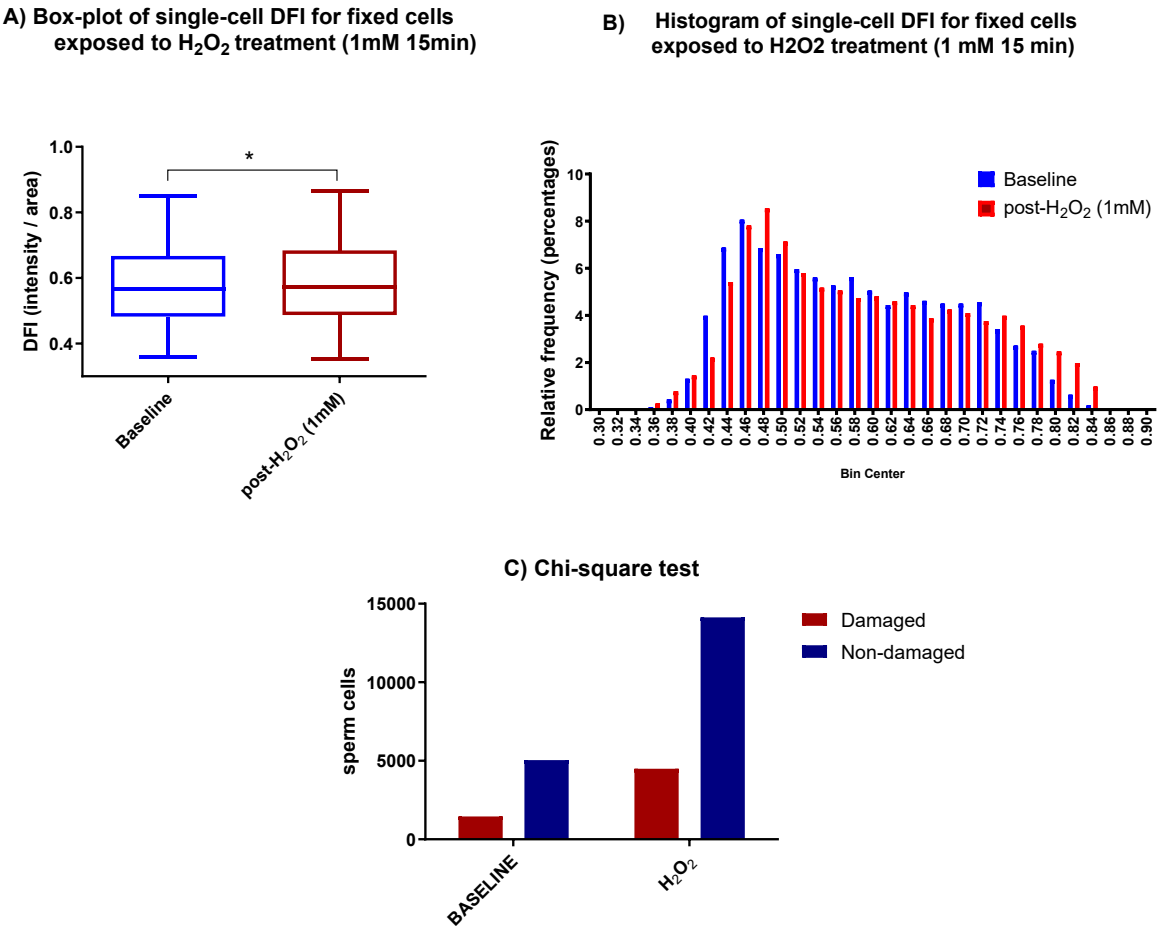

Figure 2.5 Effect of H_2O_2 exposure to the DFI and % DFI (>0.66) in fresh and fixed donor samples. A total of 19176 cells from three different ejaculates from two donors (A and B) (n = 6) were imaged for this experiment. The H_2O_2 treatment produced a significant increase in the DFI range according to the Mann-Whitney test ($p < 0.0001$) **(A)**, a slight displacement of the

DFI distribution **(B)**, and a statistically significant increase in the number of damaged cells % DFI (> 0.66) according to the Chi-square two-sided test (p = 0.005) **(C)**.

The effect of higher H_2O_2 concentrations and duration treatments (up to 9.8 M for 1 h) were also studied in more detail within 1 donor (donor A). There was a statistically significant difference of DFI between the groups according the Krukal-Wallis test. Dunnett's multiple comparison test concluded that only the 0.5 / 1mM 15min treatments decreased significantly the DFI mean values when comparing with the baseline values (**Figure 2.6**). The rest of combinations did not change the DFI mean value before (baseline group) and after the treatment.

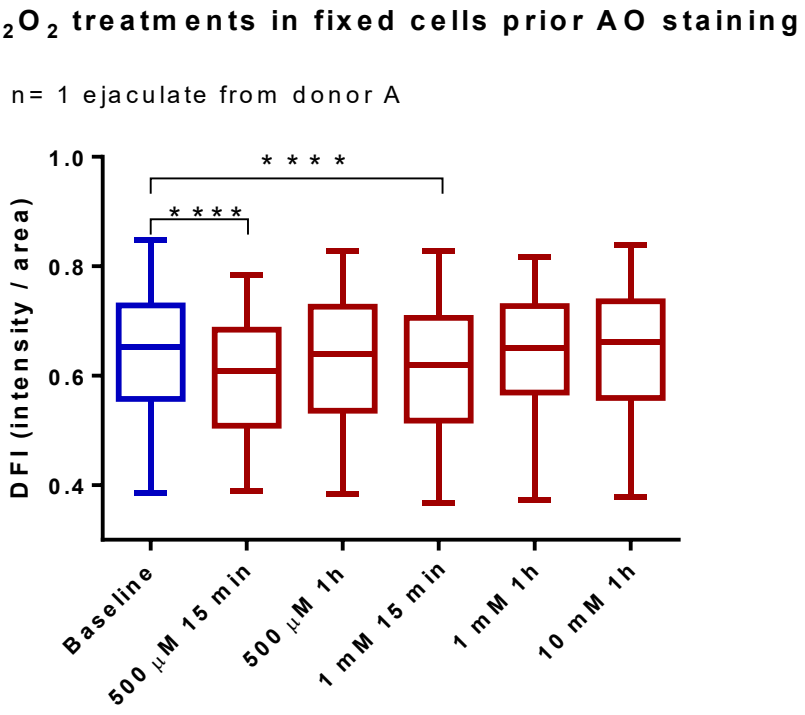

Figure 2.6 Effect of different H_2O_2 treatments (concentration and time) in wash and fixed sperm. A total of 6309 cells from 1 sample (donor A) were analysed in this experiment.

Dunnett's multiple comparison test showed statistically difference when comparing the DFI of the baseline and 500 µM or 1 mM 15 min H_2O_2 treatments.

The detailed observation of the images obtained when using H_2O_2 showed an increase in the background fluorescence, especially on the green wavelength (**Figure 2.7**). This increase was proportional to the concentration and time of H_2O_2.

A)

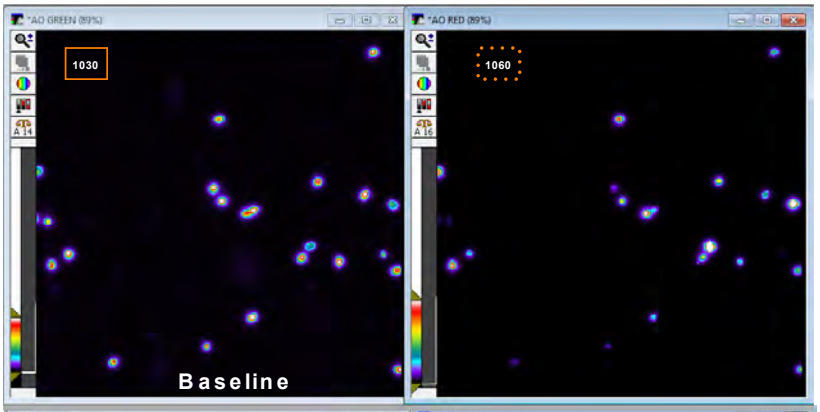
1030
1060
Baseline

B)

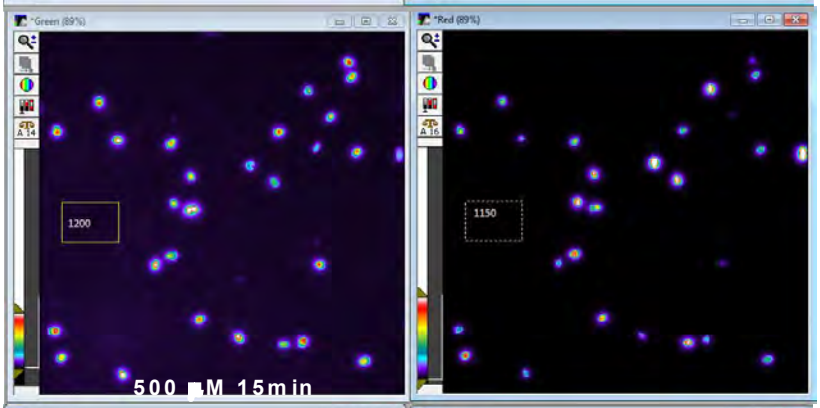
1200
1150
500 mM 15min

C)

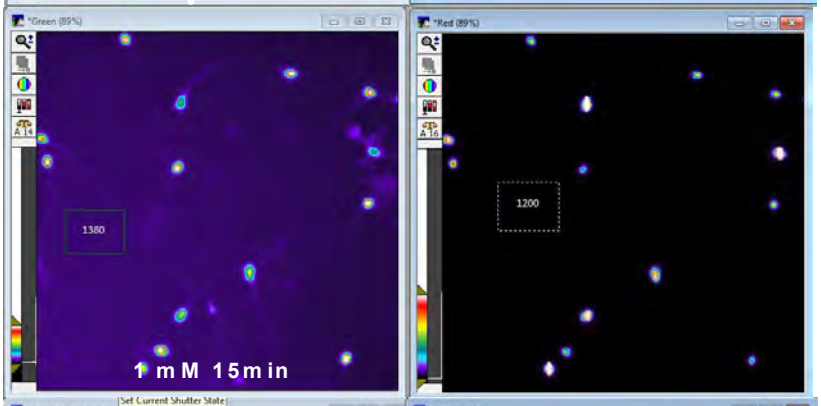
1380
1200
1 mM 15min

D)

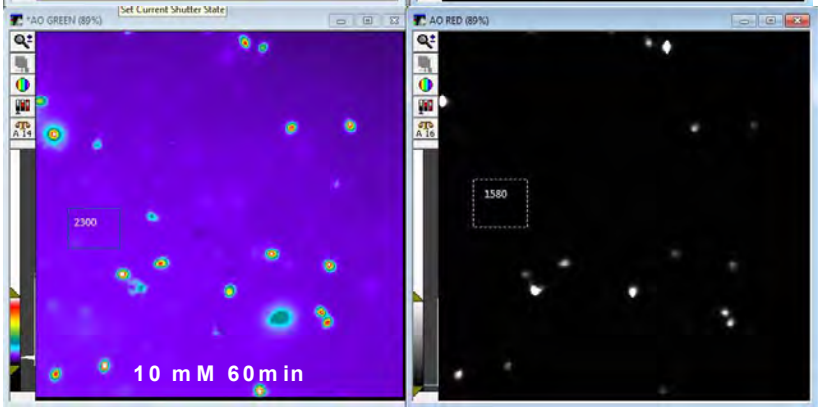
2300
1580
10 mM 60min

Figure 2.7 Fluorescent background and H_2O_2 concentrations. The figure shows the images obtained from slides treated with different H_2O_2 concentrations from donor A used in Figure 2.6 after applying the pseudo-colour view display on Metamorph to facilitate the observation of the different intensity between images. The AO protocol followed was the same for all the slides and also the microscopy acquisition setting. The background fluorescence on the green channel was 1030, 1200, 1380, and 2300 for the baseline, 500 µM and 15 min, 1 mM and 15 min, 1mM and 15 min, and 10 mM and 60 min respectively.

The effect of exposing the cells to H_2O_2 (1 mM) just after removing the semen, but before performing the denaturation step of the AO protocol was also investigated (**Figure 2.8**). After one-hour treatment there was some increase on the DFI values; however, after three hours of exposure to H_2O_2 (2 mM) the DFI values of the distribution decreased. Interestingly, leaving the samples for three hours in PBS increased the DFI values similarly to adding 1 mM H_2O_2 for one-hour treatment.

Exposing the cells to 9.6 M H_2O_2 concentration led to total cell loss from the smear (so no score could be taken and hence there is no data in the graph).

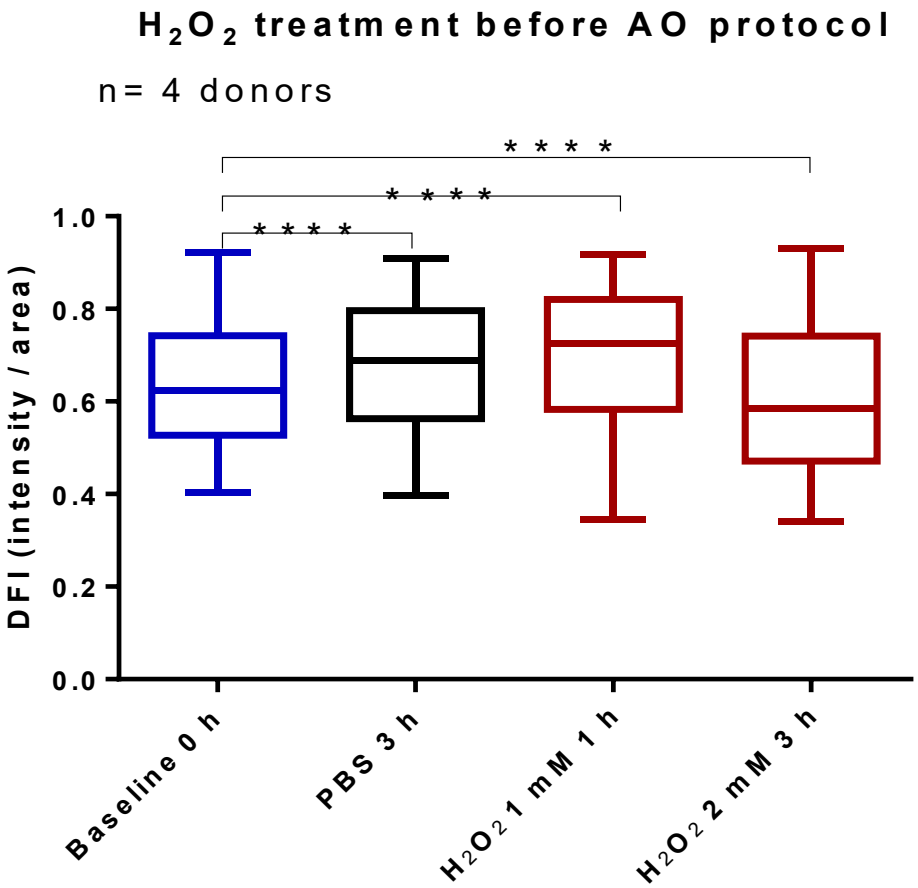

Figure 2.8 Effect of one and three-hour treatments with H_2O_2 (1mM) upon the DNA denaturation (DFI). The one-hour treatment with H_2O_2 led to an increase in the DFI values similar as leaving the samples in PBS for three hours. The H_2O_2 three-hour treatment led to a decrease in the DFI values and the 9.6 M one-hour treatment with H_2O_2 led to the complete cell loss in the smear. The experiment was performed with 4 donors (A, B, C and E) and different slides for each treatment (baseline, PBS 3h, H_2O_2 1mM 1h, and H_2O_2 2 mM 3 h)

b) DNA damage by the nuclease DNase

We investigated the effect of exposing the DNA to DNase (3U/ml) diluted in permeabilisation solution as explained in 2.2.2.2 for one hour. DNase was combined with permeabilisation solution to allow the enzyme to reach the nucleus before applying

the AO protocol and after the semen was washed with PBS. The distribution for the DFI values increased significantly ($p < 0.0001$) (**Figure 2.9**). A more detailed analysis showed inter-variability on the treatment response (**Figure 2.10**); two of the three donors (A and B) responded to the DNase treatment. Donor E did not experience an increase in the DFI values.

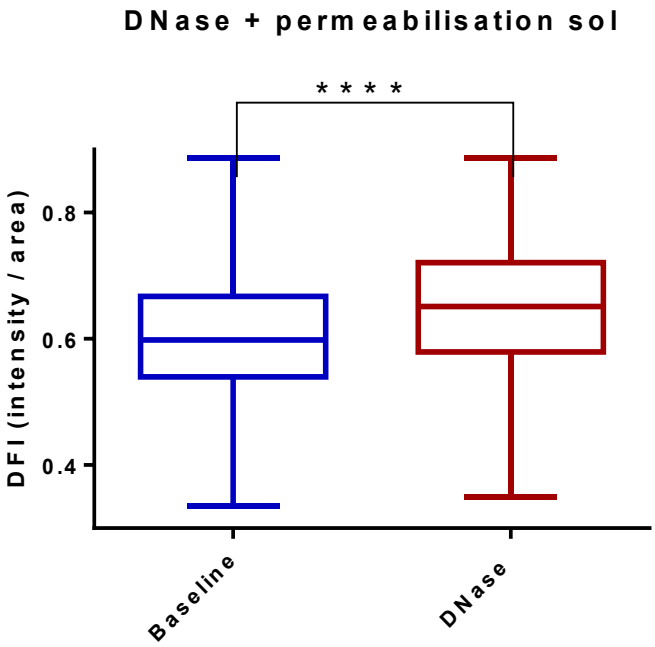

Figure 2.9 Effect of DNase on the DFI values of PBS-washed semen. The exposure to DNase diluted in permeabilisation solution (final concentration (3 U / ml) increased the DFI values of sperm cells from three donors (A, B, and E). Unpaired t-test with welch correction. Whisker gathered data from 2.5 to 97.5 percentile.

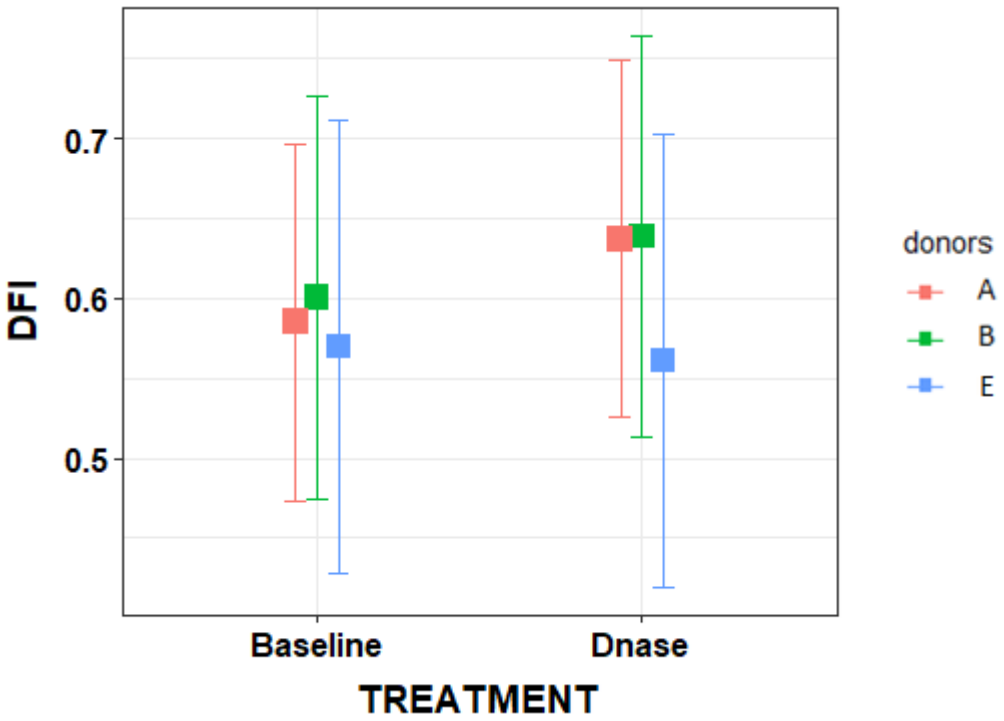

Figure 2.10 Inter-variability for DNase treatment. The Kruskal-Wallis test showed significant difference between the two groups ($p < 0.0001$). However, looking into more detail, according to Dunn's multiple comparison test donor A and B increased significantly the DFI values, while the difference on DFI values for donor E before and after the treatment was no statistically significant. This data corresponds to the ungrouped data from Figure 2.9.

c) Preliminary chromatin de-compaction by dithiothreitol

The effect of the chromatin relaxation prior AO protocol was studied. AO protocol was performed in samples immediately after their preparation (baseline), after 3 h immersion in PBS, after dithiothreitol **(**DTT) exposure (45 min), DTT followed by DNase treatment (1 h) with and without permeabilisation solution. According to Dunn's multiple comparison test, all the treatments including DTT itself significantly increased DFI values compared to the baseline slide (**Figure 2.11**).

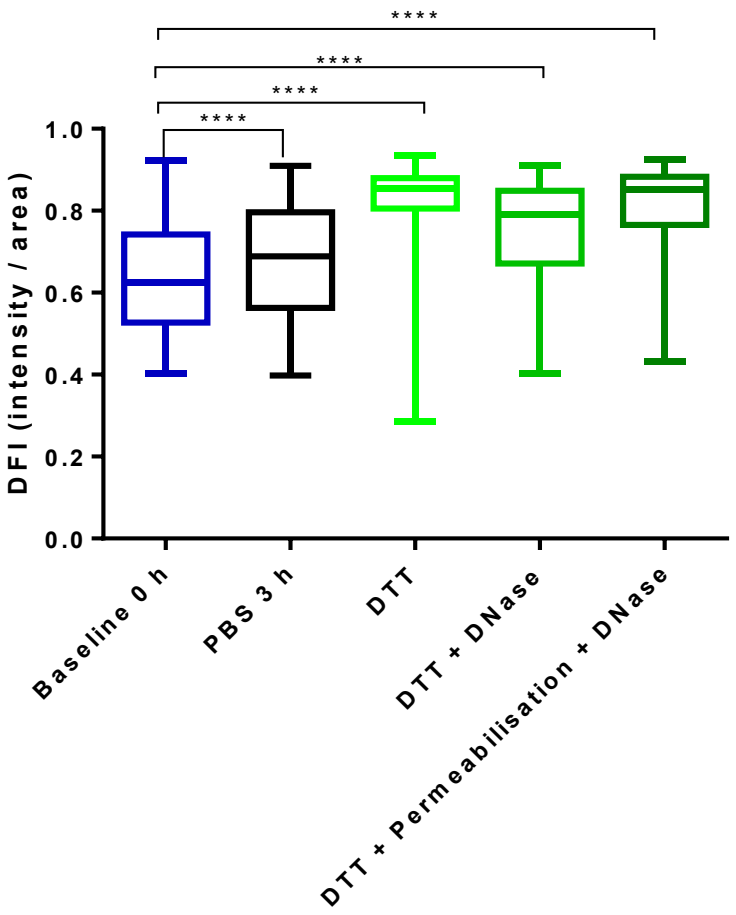

Figure 2.11 Effect of de-compaction by using DTT upon the DNA denaturation measured by AO with and without previous DNase treatment. The experiment was performed with three different donors (A, B, and E) in the same day. The immersion of the slides for 3 hours in PBS prior the AO assay increased the DFI values. However, the exposure of the slides to DTT for 45 min increased dramatically the DFI values. The later exposure to DNase with or without permeabilisation solution did not offer greater DFI values than the DTT treatment on its own.

2.4.2 AO scoring

2.4.2.1 AO visual scoring

A wide range of tonalities from green to red were observed under the microscope for the AO stained cells (**Figure 2.12**). An initial classification based on 4 colours (green, green-yellow, yellow-orange and orange-red) as described in 2.3.3.1 was performed to study in detail the light emission properties. The DNA damage score was based on the average of two counts for the proportion of yellow-orange and orange-red among 200 cells as explained in in the semen samples.

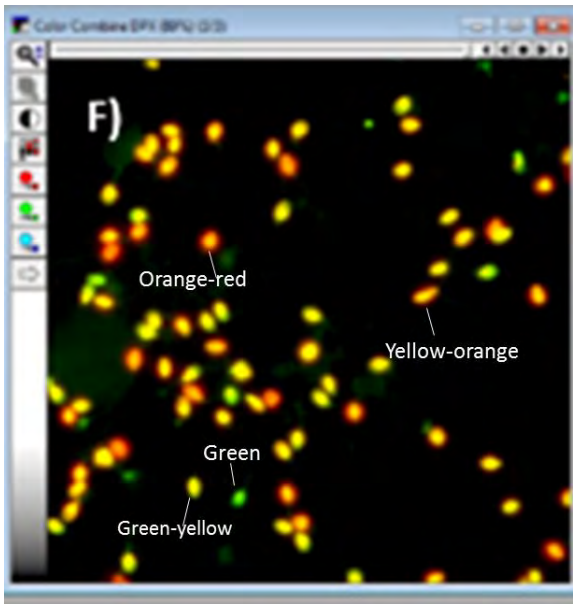

Figure 2.12 Colour image created by the addition of both planes, green and red. Both planes were individually acquired with the fluorescence microscope and filters described in methods

2.4.2.2 Semi-automatic AO scoring method based on acquired grey-scale images using correspondent filters for the red and green emission, Quantafrag

2.4.2.2.1 DFI as the best Quantafrag parameter to differentiate AO visual categories

Individual images were acquired with correspondent filters for the AO green and red emission. The values for both green and red emissions were extracted from every single ROI using the Metamorph® software (**Figure 2.2**) and the DFI as explained in 2.3.3.2

According to the green emission, two groups of cells were clearly differentiated (**Figure 2.13 A**); the green and green-yellow cells showed a higher average and range intensity compared to the yellow-orange and orange-red cells. According to the red emission **(Figure 2.13 B**), green cells exhibited much lower red emission when comparing to the other three groups. The orange-red cells had the higher average and intensity range for the red emission; however, it was not significantly different from the green-yellow cells. The DFI values increased across the visual categories, from the green cells to the orange-red cells (**Figure 2.13 C**).

Among the three parameters obtained from semi-automatic analysis of the grey-scales images (green and red average emissions, and DFI), DFI was the only one that consistently increased across the visual scale (from green cell to orange-red cells). Therefore, DFI could be used to transform the categorical values (colours) into a numerical scale and vice-versa. In this way, the scoring of the AO assay is automatically done, and it is free of subjectivity. The orange-red cells were considered

damaged while the yellow-orange partly damaged. The green and green-yellow cells were considered not damaged.

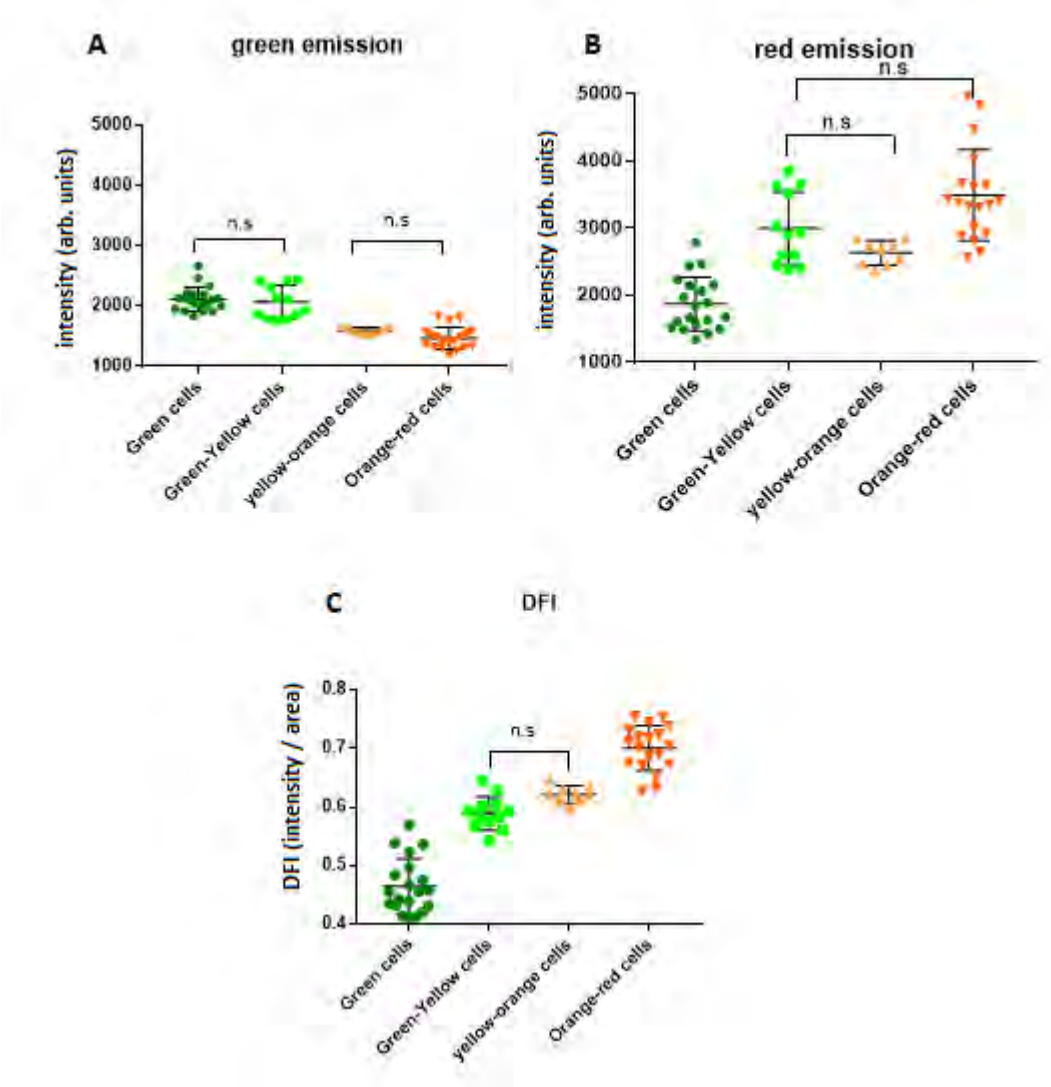

Figure 2.13 Distribution of the green intensity, red intensity and DFI single-cell data of visually different-coloured sperm. The intensity data for the green channel is shown in **A**, for the red in **B** and for the DFI in **C**. A better separation between the visual coloured sperm is obtained when using the DFI parameter among the green and red intensities. The data was obtained from the baseline slides created with the samples from donors A and B used in Figure 2.11. n. s: no significant according to the ANOVA with Dunnet's Post Hoc test.

Moreover, as explained in the methods section, the change of the excitation light, but keeping the ratio between the red and green channels (1.5) same results were obtained (**Figure 2.14**)

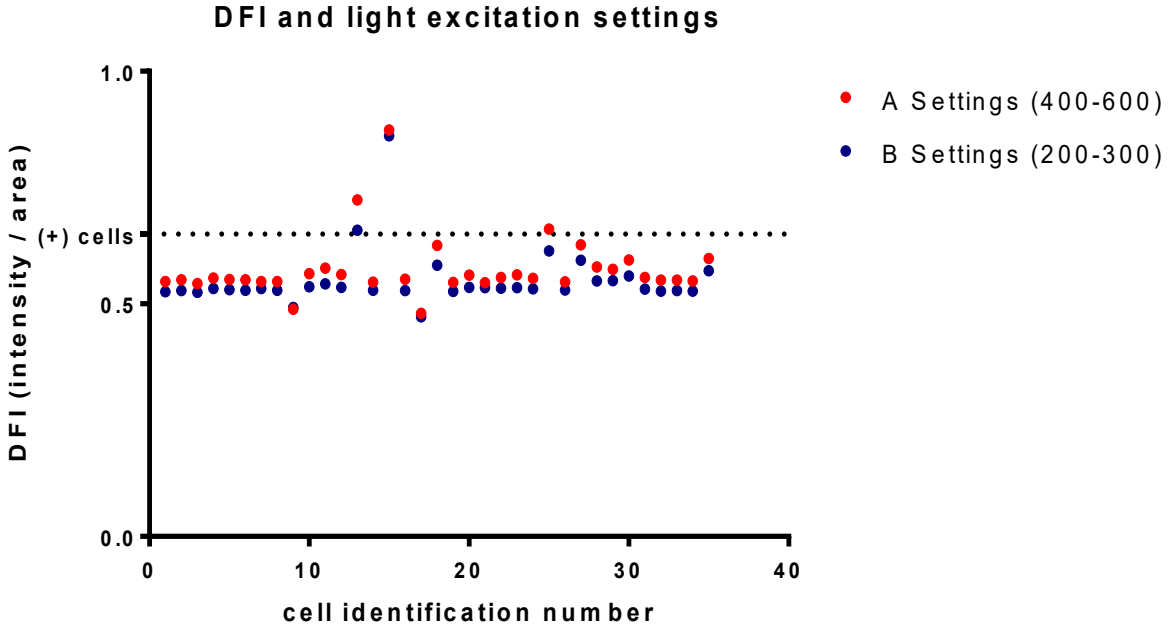

Figure 2.14 Single-cell DFI values for two sets of settings for the excitation light keeping the same ratio between channels. A total of 35 cells were imaged under 400 ms for the green channel and 600 ms for the red channel first. A second acquisition from the same cells was performed using lower excitation light, 200 ms for the green and 300 ms for the red channels. The DFI results obtained by both settings are very similar. One new baseline slide from donor A was used for this experiment.

2.4.2.2.2 Calibration of the DFI threshold of Quantafrag based on the traditional visual method

The yellow-orange and orange-red cells observed in the visual analysis and initially considered as damaged, obtained a DFI value ranging from 0.60 to 0.70 approximately

when the Quantafrag system was used (**Figure 2.13C**). Based on this finding, different cut-offs in the range of 0.6-0.7 were initially assessed to obtain the best correlation between the semi-automatic and the visual scoring methods for 118 patient samples (**Figure 2.15**). The strongest correlation according to the Pearson test was obtained when using a 0.66 cut-off (r=0.929, R^2=0.862) (in blue square in **Figure 2.15**)

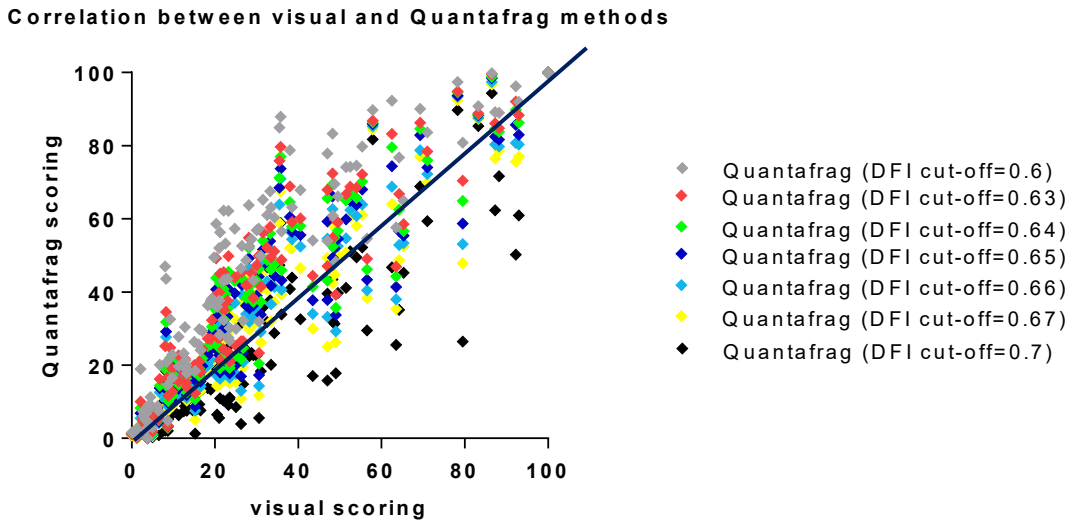

	Correlation between the Visual and the Quantafrag scoring methods						
DFI cut-off for Quantafrag	0.6	0.63	0.64	0.65	0.66	0.67	0.7
R	0.891	0.922	0.927	0.928	0.929	0.927	0.896
95% confidence interval	0.847 0.923	0.889 0.945	0.896 0.949	0.898 0.950	0.899 0.950	0.897 0.949	0.854 0.927
R square	0.794	0.849	0.859	0.862	0.862	0.86	0.803
Number of XY Pairs	118	118	118	118	118	118	118

Figure 2.15 Correlation between the visual scoring and the Quantafrag scoring when applying different DFI cut-offs (from 0.6 to 0.7). The dark line indicates the perfect correlation (R^2 = 1) between both methods. 118 patient samples were used in the analysis.

The agreement between the visual method and the semi-automatic when using a 0.66 cut-off was assessed by Bland-Altman analysis. The average of the differences was 2.33 (bias in **Figure 2.16**). Higher differences between both methods were obtained when the average fragmentation value was in between 30 to 80 while for smaller values the agreement between both methods was higher.

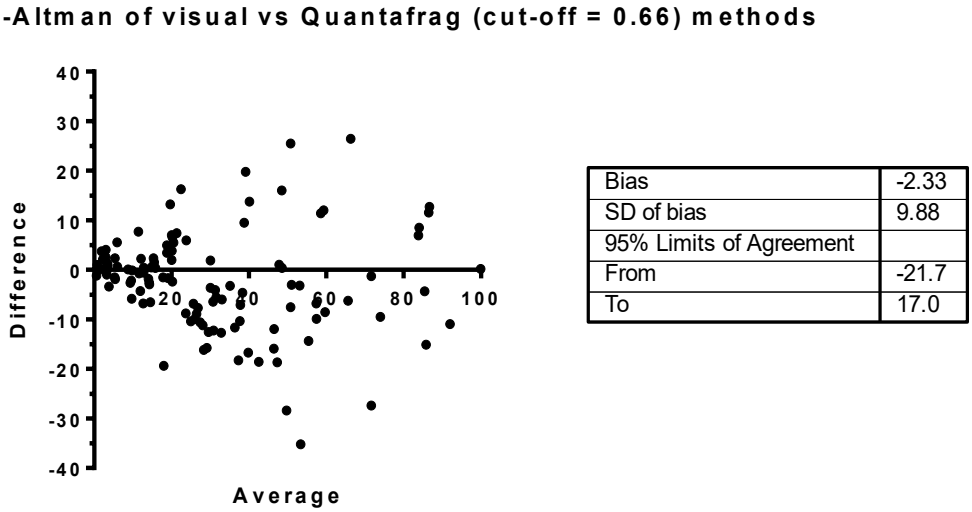

Figure 2.16 Bland-Altman for assessing the agreement between the visual and the Quantafrag system. Both methods showed a good agreement (bias of -2.33) when comparing results from the same 118 patients from Figure 2.15. However, the association was higher for samples with lower average of DFI % obtained by both methods.

Based on a hypothetical 30 % clinical threshold as suggested for natural conception and for a successful outcome for the assisted reproductive techniques (Bungum *et al.*, 2004, Larson-Cook *et al.*, 2003, Spano *et al.*, 2000) three patients were positive for the visual assessment but not for the semi-automatic Quantafrag (2.5 %) and 12 positive for the Quantafrag but not for the visual (8.5 %) out of the 118 analysed (**Figure 2.17**).

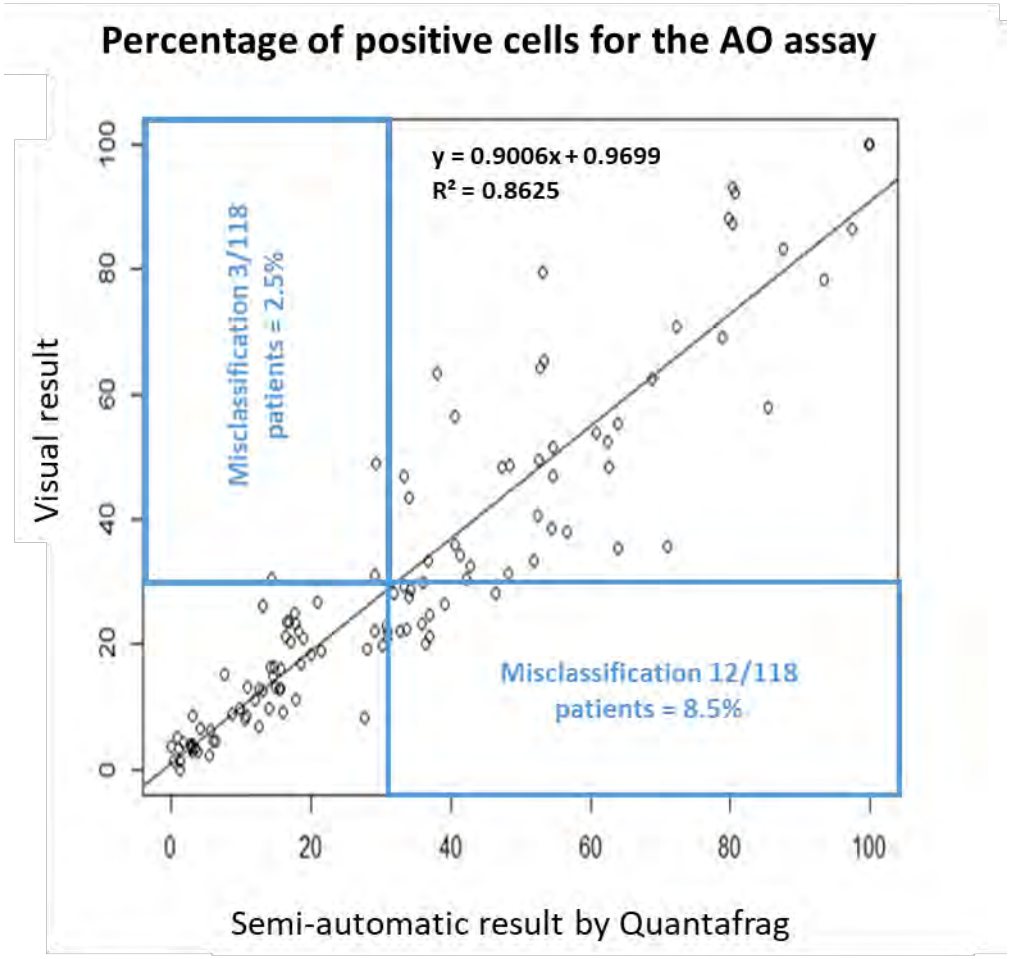

Figure 2.17 Clinical correlation between the visual and the Quantafrag methods for 118 patients. Considering 30 % of AO positive cells as a clinical threshold, 2.5 % or 8.5 % of the 118 patients do not agree in their clinical result and they could be misclassified as false positives or negatives.

2.4.2.3 Consistency of the AO assay: intra-variability for the AO visual and Quantafrag assessment

Patient samples previously prepared, frozen, stained and scored for AO by a collaborator laboratory in Leeds were sent to Birmingham so we could also perform our AO scoring employing the Quantafrag system to compare results and study the

inter-assay variability. Patterns of non-homogenous staining were repeated in many slides biasingthe scoring as it was difficult to differentiate between real staining and artifacts. Also many slides had very low concentrations that made obtaining a reliable % DFI difficult.

2.4.2.3.1 Intra-variability for the AO visual and Quantafrag assessment using duplicates

The visual assessment result for each replicate was based on the average of two independent scorings in order to check the acceptance of the replicate and to give a reliable percentage of damage for the sample. For the quantafrag method only one score was performed per replicate. After excluding the samples which replicates had a difference in DFI % not acceptable (look methods 2.3.3.1) shown in bold in **Table 2.4**, the CV % decreased from 9 to 6 for the Quantafrag assessment and from 12 to 8 for the visual assessment (shown in table as CV (*) (%) Average). The average for both replicates of donor B (in orange) was not acceptable (look methods 2.3.3.1) neither when doing the visual counting nor with Quantafrag suggesting lack of homogenous staining. The error of measurement obtained for the accepted samples by the Quantafrag was smaller than the visual assessment according to the CV (%) (6 *vs* 8.).

The same analysis for the error of measurements was performed with replicates of frozen-thawed samples from same donors (**Table 2.5**). The CV % decreased from 13 to 8 Quantafrag assessment (shown in table as CV (*) (%) Average). The difference between the visual scorings for the two replicates was in all donors inside the acceptance values and the CV (%) was 9. The error of measurement obtained for the

accepted samples by the Quantafrag was slightly smaller than with the visual assessment according to the CV (%) (8 *vs* 9).

Sample			*Baseline results*						
DONOR	**DATE**		**A1**	**A2**	**AVERAGE**	**ACCEPTED (WHO)?**	**|A1-A2|**	**SD**	**CV (%)**
Donor A	**29/07/2017**	**DFI**	**23.3**	**26.1**	**24.7**	**9**	**2.8**	**1.98**	**8**
		VISUAL	**22.3**	**27.3**	**24.8**	**9**	**5**	**3.54**	**14**
	23/06/2017	**DFI**	**44.4**	**43.6**	**44**	**10**	**0.8**	**0.58**	**1**
		VISUAL	**40**	**38.5**	**39.3**	**10**	**1.5**	**1.06**	**3**
Donor B	**23/06/2017**	**DFI**	**35.5**	**52.0**	**43.7**	**10**	**16.5**	**11.7**	**27**
		VISUAL	**23**	**33.8**	**28.3**	**9**	**10.8**	**7.59**	**27**
Donor E	**13/06/2017**	**DFI**	**11.4**	**11.9**	**11.7**	**7**	**0.6**	**0.40**	**3**
		VISUAL	**11.3**	**10.8**	**11**	**6**	**0.5**	**0.35**	**3**
	21/06/2017	**DFI**	**24.1**	**22.8**	**23.4**	**8**	**1.3**	**0.93**	**4**
		VISUAL	**19.5**	**16.8**	**18.1**	**8**	**2.8**	**1.94**	**11**
	23/06/2017	**DFI**	**15.5**	**18.6**	**17.1**	**8**	**3.1**	**2.18**	**13**
		VISUAL	**8.3**	**9.8**	**9**	**6**	**1.4**	**1.02**	**11**

	Error of measurements	
Quantafrag	**SD = 2.95**	**CV (%) Average = 9**
	SD (*) = 1.21	**CV (*) (%) Average = 6**
Eye	**SD = 2.58**	**CV (%) Average = 12**
	SD (*) = 1.58	**CV (*) (%) Average = 8**

Table 2.4 Intra-variability for the AO visual and Quantafrag assessment using duplicates of PBS-washed sperm samples. In bold are highlighted those duplicates which difference is not accepted according to WHO recommendations. Two duplicate slides from three donors (A, B, and E) were used for this experiment. SD: standard deviation, CV: coefficient of variance. (*) indicates SD and CV calculated only with the samples which replicates difference were accepted according the WHO criteria.

Sample			*Frozen-thawed results*						
DONOR	DATE		A1	A2	AVERAGE	ACCEPTED (WHO)	|A1-A2|	SD	CV (%)
	29/06/2017	DFI	63.4	61.2	62.5	10	1.8	1.29	2
		VISUAL	51	56.2	53.6	10	5.3	3.71	7
Donor	23/06/2017	DFI	62	55.4	58.7	10	6.6	4.67	8
A		VISUAL	49	44.8	46.9	10	4.3	3.01	6
	06/07/2017	DFI	53.0	58.9	56.1	10	6.0	4.21	8
		VISUAL	40.8	41.5	41.1	10	0.8	0.53	1
	13/06/2017	DFI	37.8	30.1	34.0	9	7.6	5.40	16
		VISUAL	27.3	25.7	26.5	9	1.5	1.05	4
Donor	15/06/2017	DFI	29.6	42.3	36.0	10	12.7	8.97	25
B		VISUAL	36.3	30.8	33.5	9	5.5	3.89	12
	23/06/2017	DFI	39.1	41.2	40.1	10	2.0	1.44	4
		VISUAL	35.5	36.3	35.9	10	0.8	0.53	2
	13/06/2017	DFI	13.8	10.6	12.2	7	3.1	2.21	18
		VISUAL	17	12.3	14.6	7	4.8	3.36	23
Donor	21/06/2017	DFI	26.0	26.4	26.2	9	0.4	0.26	1
E		VISUAL	23.8	21.5	22.63	8	2.3	1.59	7
	23/06/2017	DFI	14.4	24.2	19.3	8	9.8	6.90	36
		VISUAL	11.8	16.3	14	7	4.5	3.18	23

	Error Measurements	
Quantafrag	SD = 3.93	CV (%) Average = 13
	SD * = 2.78	CV (*) (%) Average = 8
Eye	SD = 2.31	CV (%) Average = 9

Table 2.5 Intra-variability for the AO visual and Quantafrag assessment using duplicates from frozen-thawed sperm samples. In orange are highlighted those duplicates which difference is not accepted according to WHO recommendations. The duplicates used in this experiment correspond to frozen-thawed aliquots from the same samples used in Table 2.4.

The correlation of % DFI assessed by Quantafrag and visually for replicates (two) of both, baseline and F-T donor samples was also assessed. The correlation (R^2) for the

duplicates scored by Quantafrag was 0.814 and 0.859 for the baseline and F-T samples, while for the visual assessment was 0.828 and 0.926 for the same sample (**Figure 2.18**)

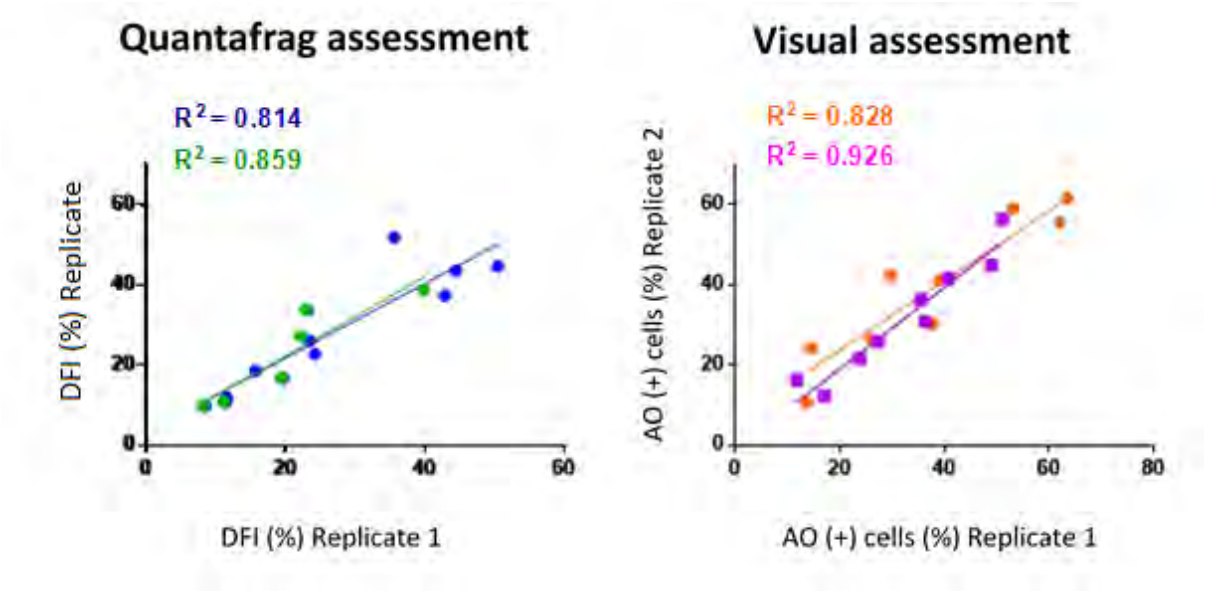

Figure 2.18 Correlation between the results for the AO assay. The correlation between duplicates of two donors was similar for both methods (Quantafrag and Visual assessment). The frozen-thawed (green and purple) duplicates had slightly higher correlation than the fresh duplicates. The replicates used in this experiment are the same as in Table 2.4 and 2.5

2.4.2.3.2 Study of the DFI ranges, histograms and number of AO positive cells (% DFI > 0.66) in donor replicates

In order to study the variability in DFI single-cell values and distribuiton, and DFI (%) five replicates (five different slides) from six donor samples were stained according to the AO protocol. The intensity values were extracted by the Quantafrag system and the DFI values for single cells were computed. The number of positive cells (%) was calculated as the number of cells with a DFI above the value of 0.66.

As suspected the median of the DFI values did not vary much across replicates (**Figure 2.19B**) or samples from different donors (**Figure 2.20A**). But the number of positive cells calculated as DFI (%) >0.66 was different across donors and ejaculates of different day (**Figure 2.20B**). Replicates of the same sample showed the same kind of distribution according to their histograms (**Figure 2.19C**). Interestingly, similar % of positive cells as in donor A (12.77 %) and donor D (12.32 %) had different DFI histogram distributions (**Figure 2.20C**)

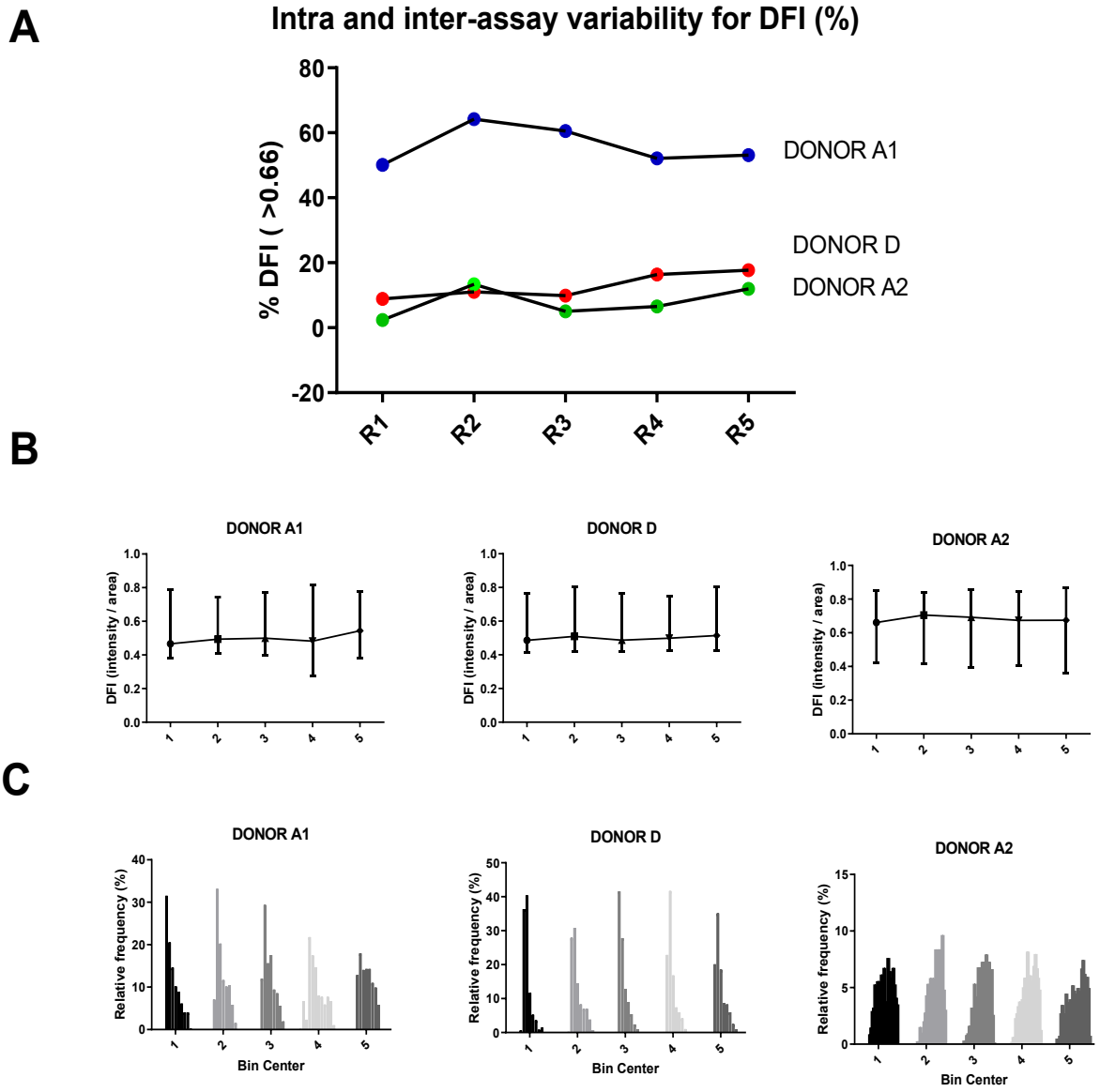

Figure 2.19 DFI (%), DFI ranges and histograms of five replicates performed with three PBS-washed donor samples. The DFI (%) was similar between the replicates of the same sample (**A**).Although different donors had different DFI (%) (**A**), the DFI range was similar in all the donors (from 0.4 to 0.85 approximately) and also the median apart from donor A2 which had higher values (**B**). The replicates from same donor sample had similar single-cell ITC intensity distribution according to their histograms (**C**). However, samples from same donor but different day (A1 and A2) had different DFI distributions. 5 replicates were made for each donor sample. In this xperiment, 2 of the donor samples correspond to donor A (from different day) and one to donor D.

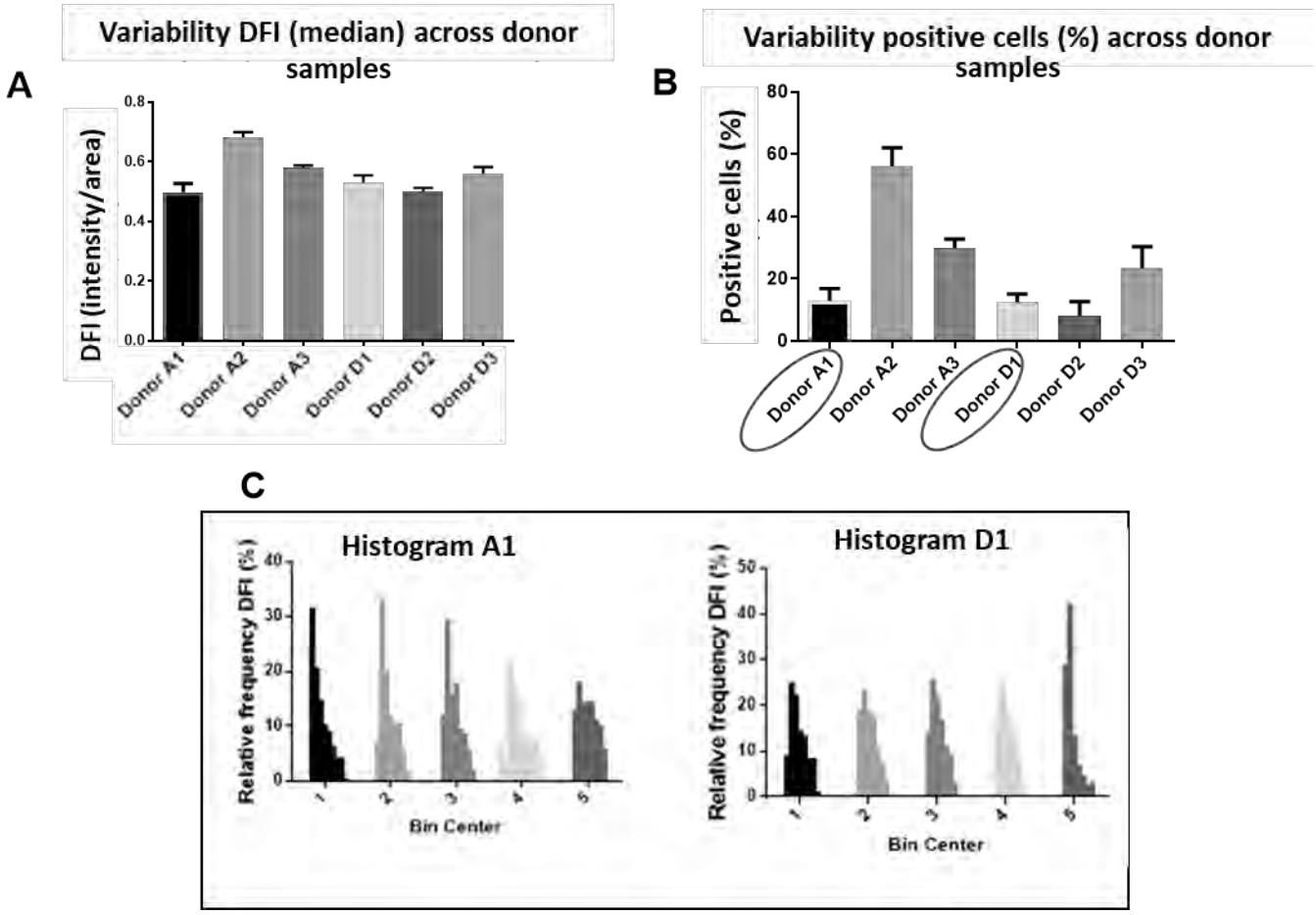

Figure 2.20 Variability in the DFI median and number of AO positive cells (% DFI) across 6 donor samples. Different DFI distribution patterns are obtained for samples with similar % DFI. There is not much difference in the median DFI of five replicates in six PBS-washed donor samples **(A).** However, the variability between the number of positive cells (% DFI > 0.66) averaged in the five replicates was quite different across the donor samples **(B)**. Samples with same DFI (%) as A1 and D1 (12 %) can exhibit different DFI distributions as shown **(C)**. The columns in A and B represent the mean value for the five replicates, and the bars the standard deviation.The data showed in this figure corresponds to the re-arrangement of the data from Figure 2.19 plus the replicates obtained from two new samples from donor D.

2.4.3 AO results for donor and patient samples

2.4.3.1 Relation between the AO assay and the basic semen parameters and the abstinence

The basic semen parameters were studied in fresh semen in 13 samples from four different donors (represented with different colour in **Figure 2.21**). No strong correlation was found between the percentage of positive cells according to % DFI (> 0.66) and any of the basic semen analysis parameters (concentration, total count, motility) or abstinence. The cut-off for DFI was set-up at 0.66 because it showed the best correlation with the visual assessment as explained above (**Figure 2.13**).

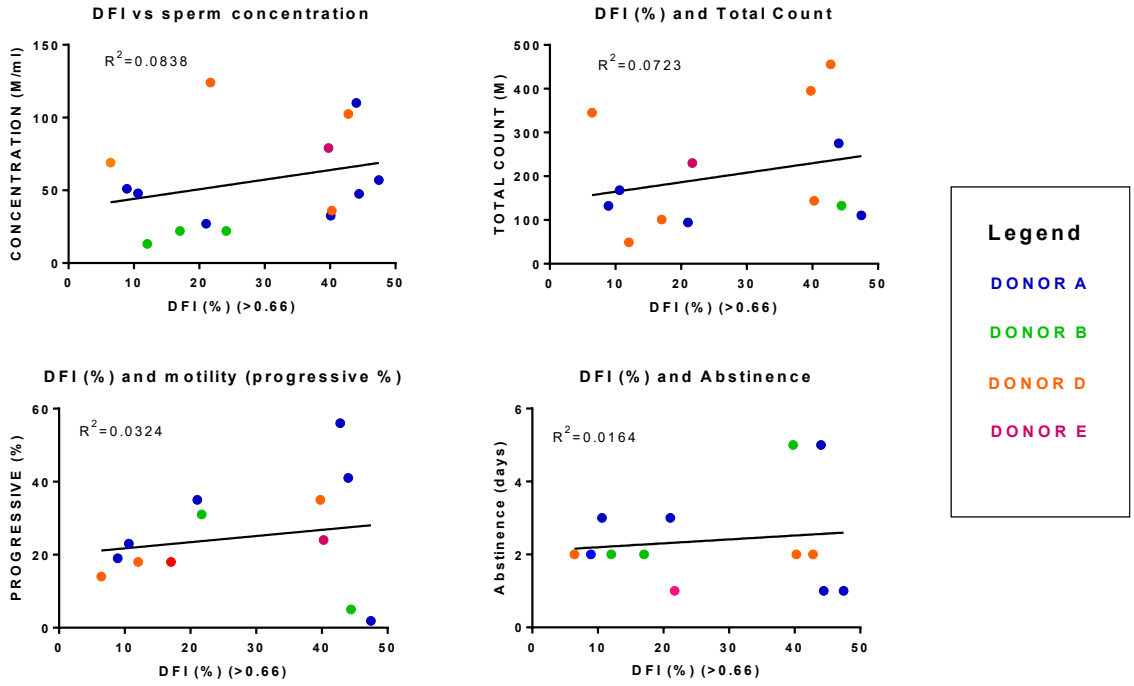

Figure 2.21 Analysis of correlation between the percentage of positive cells according to % DFI (>0.66) and the basic semen analysis parameters and abstinence. Five different donors were used in this experiment. The ejaculates collected from the same donor are shown with a same colour.

2.4.3.2 Evolution of DFI (%) across fresh donor samples

The DFI range for individual sperm cells (**Figure 2.22A**) and the percentage of cells with a DFI greater than 0.66 set for scoring positive cells (% DFI > 0.66) for the ejaculated (**Figure 2.22B**) were calculated in semen samples of three donors from different periods of time. Some donors experienced much larger fluctuations in DFI and DFI (%) (donor A) than other.

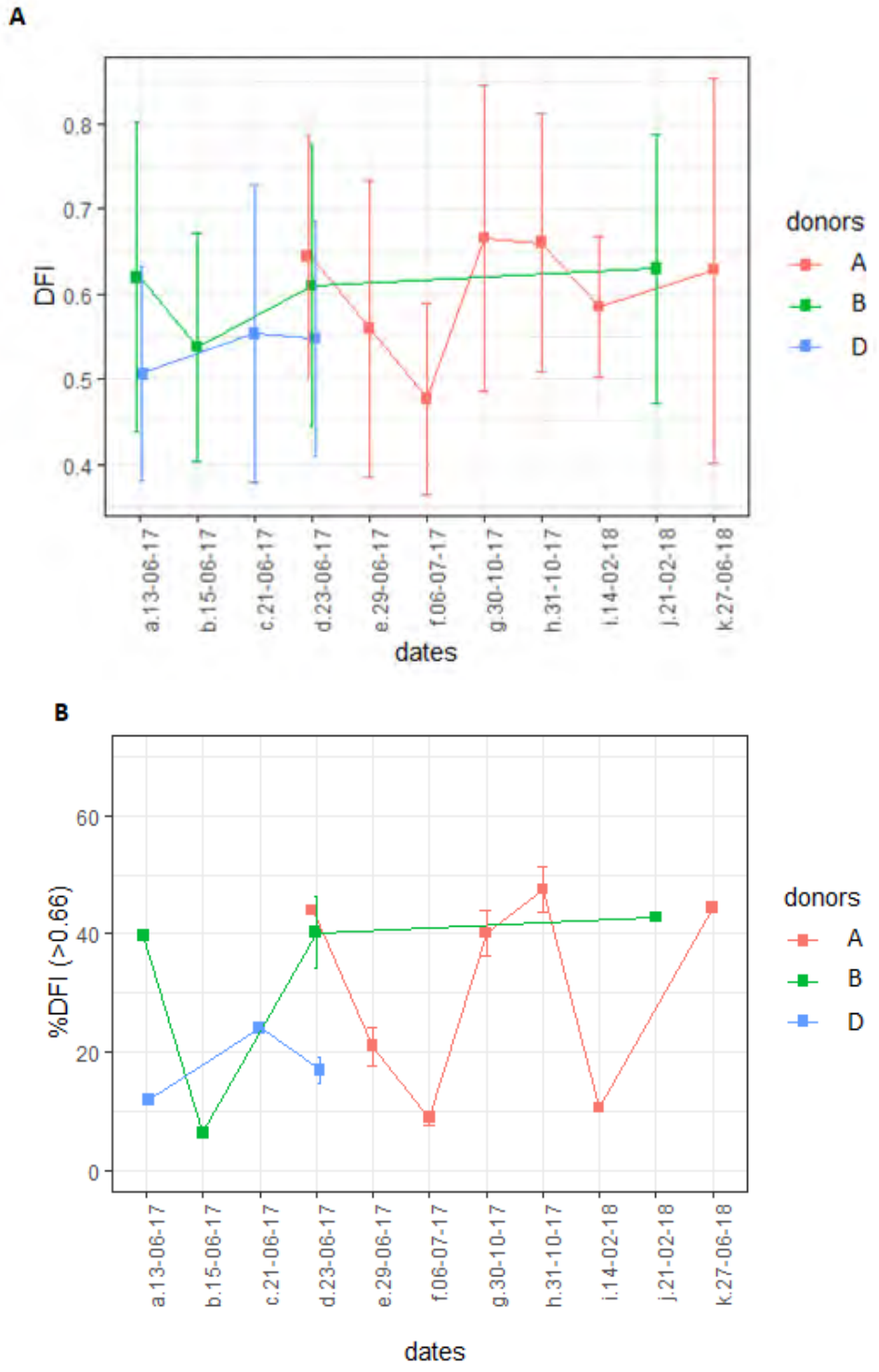

Figure 2.22 The DFI (ranges) and the number of AO positive cells (DFI (%)) was scored in 14 ejaculates from three donors across time. A total of 3 donors (A, B, and D) were used for this experiment. Two different smears (duplicates) were used for each sample. The DFI (ranges) (**A**) were calculated by applying the formula DFI = Red average intensity/ (Red +

Green) average intensities in the single-cell intensity data obtained from the semi-automatic acquisition system. The DNA Fragmentation Index DFI (%) was obtained by applying a 0.66 cut-off to the single-cell data (**B**). In **A**, the median and the whole range of DFI values is represenred by dots and whiskers.In B the dots represent the DFI average and the bars the standard deviation between the two duplicates.

2.4.3.3 Study of the induction of DNA damage in sperm freezing procedures

The % DFI (> 0.66) of three samples from three donors was evaluated before (baseline) and after the freezing-thawing protocol (**F-T in Figure 2.23**) specified in the methods section. Donors showed different susceptibility to the freezing-thawing protocol. Donor A experienced a large increased on the DFI after freezing-thawing while donor D didn't show differences after the treatment. Only one sample from donor B increased its DFI, the rest remained with similar value after the freezing-thawing. The data showed in this experiment corresponds to the data already showed in Table 2.4 and 2.5

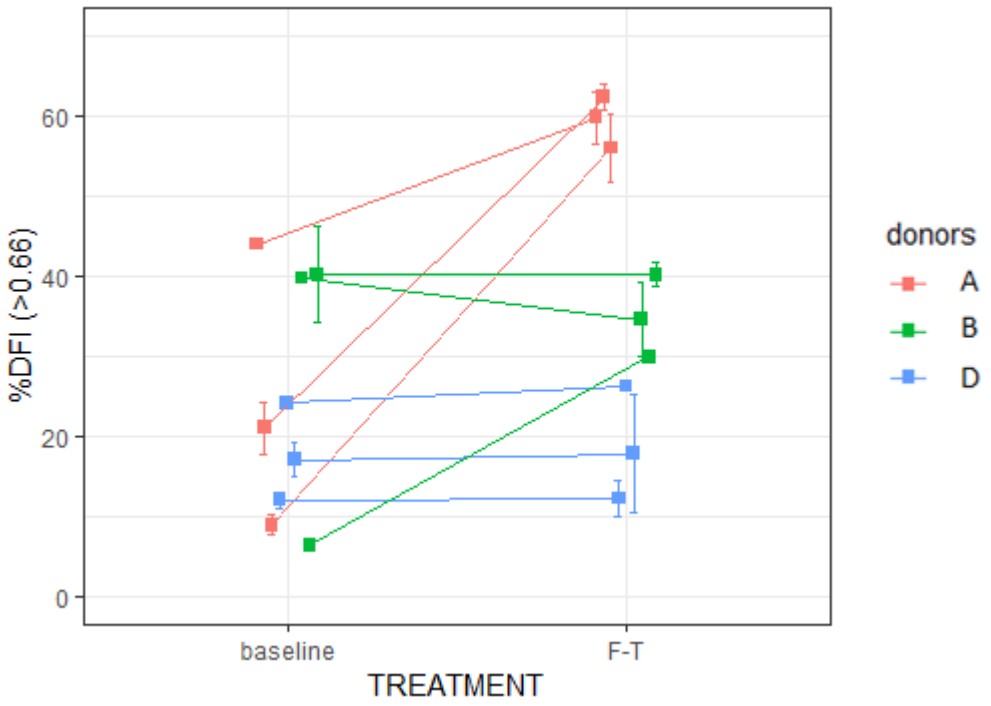

Figure 2.23 Levels of DNA Fragmentation Index (DFI (%) in 9 samples from 3 donors before and after freezing. The DFI (%) were scored with a semi-automatic acquisition and scoring system when using a 0.66 cut-off based on previous comparison with the visual assessment. For each ejaculate two smears (duplicates) were performed for each sample. The means and standard deviations between the two duplicates are represented by squares and bars. Two baseline samples of Donor B did not have a replicate. Significant changes were observed after freezing for Donor A.

2.4.3.4 DFI in donors and patients comparison

The DFI range for individual cells obtained in donor samples fresh and frozen, and frozen patient samples was 0.36 - 0.92, 0.35 - 0.88, 0.1 - 1 respectively, and medians of 0.58, 0.60 and 0.58 repectively (**Figure 2.24**). The % DFI (> 0.66) value varied from 4.3 to 64.6 in the fresh donor samples, 10.6 to 63.4 in frozen donor samples and from 0 to 100 in frozen patient samples with medians of 36.4, 38.5, and 21.4 respectively. The percentage of positive cells was 30.74, 38.67 and 43.68 for the fresh donor samples, frozen donor samples and frozen patient samples. The difference in % positive cells across the three groups was statistically significant according the Chi-square test ($p < 0.0001$). The histogram data was also compared between the groups.

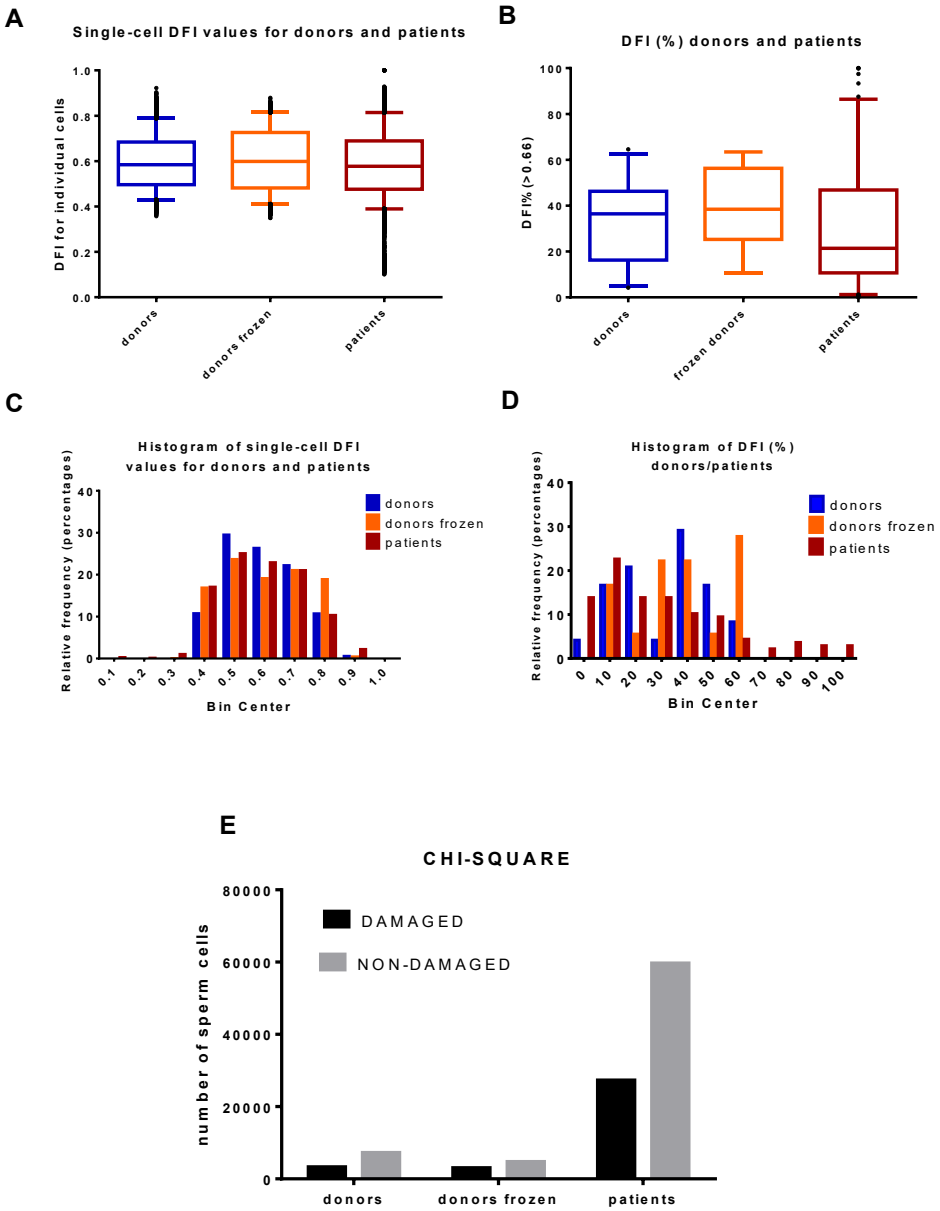

Figure 2.24 Comparison between the DFI ranges, % DFI (> 0.66) for fresh and frozen donor samples and frozen patient samples. The DFI values for individual cells and percentage of positive cells DFI (%) when applying a threshold of 0.66 in nine donor samples from different days (18 duplicates slides) were represented in 5-95 percentile box and plots (A and B) and histograms (C and D). Unlike donors, patient samples (118) had individual values lower than 0.2 DFI (A) but they also had higher % DFI (> 0.66) observed in the skewed population in the box plot (B) and also histogram where we can see that around 12 % of the patient samples had a % DFI (> 0.66) value greater than 60 %; values not seen in donor samples. The number of positive cells % DFI (> 0.66) was ranged from 0 to 60 % and 10-60

% in fresh and frozen donors respectively (D). However, in fresh donors the most represented values for % DFI (> 0.66) was 40 % and for frozen samples 60 %. The difference in % positive cells across the three groups was statistically significant according the Chi-square test ($p < 0.0001$) (E).

2.5 DISCUSSION

2.5.1 AO assay validation and optimisation

2.5.1.1 Mounting experiments

By studying the use of different mounting solutions we found that all were quite resistant to photobleaching but they exhibited very different red emission intensity depending on the chemical composition. From our data we conclude that all the aqueous-base mountants interfered with the red emission, and therefore they should never be used for the AOT as it will lead to false negative results. To our knowledge this is the first time that different mountants have been investigated in regards to the AO staining. We selected the DPX mountant for the rest of experiments with AOT as it was one of the most suitable regarding dynamic ranges.

2.5.1.2 AO assay validation with positive controls

H_2O_2 and DNase were employed to generate control high levels of damage due to their known ability to create DNA damage. H_2O_2 induces DNA oxidation which leads mostly to single strand breaks (Rueff *et al.*, 1993) while DNase catalyses double strand breaks (Kosower *et al.*, 1992). The effect of the DNase is known to vary depending upon the species due to differences on chromatin compaction (Villani *et al.*, 2010). We always

used a combination of permeabilisation solution containing Tris and Sodium Citrate to allow the enzyme to access the DNA. The exposure of the samples to DNase solution before the AO staining resulted in a significant increase on the DNA damage which validated our modified AO staining protocol and developed scoring system for detecting double strand breaks. Samples already exposed to HCl and permeabilised/fixed with Carnoy's solution did not increase the DFI when oxidised with H_2O_2, regardless the concentration and time of exposure to H_2O_2. However, the increase in DFI obtained when exposing washed sperm (without semen) before the HCl and fixation/ permeabilisation for 1 h to H_2O_2, suggests that single strand breaks created by oxisidation facilitate the DNA denaturation by the low pH of HCl and therefore increasing the DFI of the sample . Interestingly leaving the sample for 3 h in PBS previous AO staining also elevated the DFI in some extent suggesting that outside the human body the sperm cells increase their basal DNA damage and therefore the time for completing the assay is highly important, specially before fixing the cells. Same H_2O_2 concentration (2 mM) but for a longer period (3 h), resulted in a diminish on DFI, probably due to an excesive breakage of the damaged cells that facilitated their washing-out from the preparation after subsequents washing of the AO staining protocol. A total cell loss occurred when the smears were incubated at the stock solution concentration, 9.6 M for 3 h.

Most interesting was the effect of the DTT previous to the denaturation and staining protocol. When exposing the sperm to DTT before extracting the proteins of the chromatin by HCl and following with the fixation and staining steps, a very high denaturation corroborated with very high DFI was observed for almost all the cells in the preparation. Although combinations of DTT + DNase and DTT + DNase+

Permeabilisation were studied, the 45 min treatment with DTT iself was the most effective to cause and increase in DFI (%). Kosower *et al*. reached similar conclusions when he found that the sperm nuclei with DNA-associated protamines poor in disulfides emitted red fluorescence after acid treatment (Kosower *et al.*, 1992) in the same way that Zini *et al.* found a positive correlation between the DFI (%) assessed by SCSA and the sperm thiol content ($r = 0.53$, $p < 0.0001$) (Zini *et al.*, 2001). During the spermiogenesis the thiol groups of the protamines at specific cystidine residues are oxidized to form inter and intra-molecular disulfide bonds in order to strengthen and compact the nucleus of mature spermatozoa to resist mechanical and chemical disruptions (Bedford and Calvin, 1974, Huang *et al.*, 1984, Kosower *et al.*, 1992). By reducing the disulfides to thiols, DTT simmulates the scenario of immature cells that are poor in disulfides bonds and rich in thiols. By disrupting the inter and intra disulfide bonds, DTT relaxes the chromatin and seems to highly expose the DNA to the low-pH damage. We conclude that AO can identify immature sperm cells which have high thiol/disulfide content and compromised fertility potential.

2.5.2 AO scoring methods

2.5.2.1 Visual scoring method

The cells stained by AO when looking under the microscope with the correct filters mentioned in the material and methods section exhibited a range of colours from green to red. Due to this wide range of colours far from the single red or green cells, the classification in positive (damaged) or negative (non-damaged) was quite difficult in some cases.

Regarding the AO adsorption and lack of homogenous staining mentioned by Evenson (Evenson, 2016), although we found ocassionally slides with signs of lack of homogenous staining, specially next to the edges of the slide and coverslip, it was a rare event. We believe that the use of poly-lysine coated slides, the consistent image acquisition of the cells located in the centre of the slide, and the exclusion of clump of cells that sometimes exhibited a single red colour, probably can account for any lack of homogenous staining. The nature of the red emission of these clumps was unknown but we hypothesise that this could be due to a higher local exposure to reactive oxygen species (ROS) secreted by the sperm themselves (Fisher and Aitken, 1997, Sakkas *et al.*, 2003) it may also be that the cells originate from clumps of dead cells, which would be discarded and not scored in SCSA flow cytometry (due to exclusion by gating).

A scoring method based on the ratio between the red intensity and the total intensity of the AO emission at single-cell level, equivalent to the DFI (%) obtained with the SCSA assay, would be better than the traditional visual assessment in terms of consistency and objectivity. This semi-automatic scoring method would be also suitable for researchers presenting colour-blindness condition.

2.5.2.2 The development of a semi-automatic acquisition and scoring system based on grey-scale images

The AO staining method used in this chapter was similar but not identical to the AOT used by Tejada (Tejada *et al.*, 1984), the modified rigler-roschlau method (Erenpreiss *et al.*, 2001) or the SCSA (Evenson *et al.*, 1980). In our AO assay we used poly-L-lysine coated slides to cover irregularities of the slide surface and to minimise the AO adsorption phenomenon, and we included a preliminary step with HCl 0.1M to relax

the chromatin by extraction of the chromatin proteins as in the rigler-roschlau method. HCl acts similarly as the acid-detergent solution employed in the SCSA to permeabilise the nuclear membrane. The reaction with HCl was then stop by adding NaOH 0.1M. From this point, the protocol was same as developed by Tejada; the cells were fixed/denaturised with Carnoy and stained with AO. We also added a suitable mounting solution (previously tested), and coverslip in order to prevent photobleaching reported many times in Tejada method (Erenpreiss *et al.*, 2001).

DFI (%) obtained by the Quantafrag system was found to identify more effectively different AO coloured sperm observed by the visual assessment than the individual red or green emission intensities on their own. Moreover, we demonstrated that changing the ilumination settings, as long as the same ratio between the exposure time for both channels (green and red) is mantained, same single-cell DFI values are obtained, showing Quantafrag as a consistent and reproducible methods for the AO assessment. The best correlation between positive cells scored by the two methods, the visual assessment and the Quantafrag, was found when a cutoff of DFI = 0.66 was employed. According to the Bland-Altman analysis the average difference between the two methods was not very high (2.33). However, when looking into the clinical classification (in low and high SDD) based on the presence of more than 30 % positive cells (according to the majority of publications) identified as those with DFI > 0.66 for the Quantafrag, or those with orange and red colour for the visual assessments, the two methods disagreed in 11 % of the patients. We know both scoring methods, Quantafrag and visual, are comparable, and probably Quantafrag is more accurate and consistent scoring positive cells as it is not dependent of the visual acuity of the operator.

In the worst scenario, a patient could be misclassified into the low DNA damage group (false negative) and not measures would be recommended to reduce the sperm DNA damage or to personalise the fertility treatment for high sperm DNA damage men, IVF better than IUI, and ICSI better than IVF, according to the literature (2.1.2.5). On the other hand, men misclassified as high DNA damage (false positive) could be asked to adopt measures to decrese their ROS and advised to choose a more expensive ART, ICSI. In any case those measures would not be detrimental for the health of the man or future baby.

2.5.2.3 Consistency of the AO assay: intra-variability for the AO visual and Quantafrag assessments

A high SCSA repeatability due to the similarity between the cryptograms (Green vs Red emission) obtained from repeated measures of a single semen sample and the standard deviation (SD) between 2 aliquots from 1 single donor (SD = 0) was reported by Evenson (Evenson, 2013, Evenson, 2016). When using our Quantafrag system alongside the acceptance rule suggested by WHO for binomial assays (WHO, 2010a) we obtained a CV of 6 % and 8 % for fresh and frozen-thawed samples. When using the visual scoring method instead of the Quantafrag we obtained a slightly higher CV, 8 % and 9 % for fresh and frozen samples, respectively. In both cases, the CV obtained are in the same range of the CV obtained by SCSA in frozen samples by Erenpreiss *et al.* (intra-assay CV of 5 % to 7 %) (Erenpreiss *et al.*, 2006) and Apedaile *et al*. (intra-assay CV of 13 %).

In terms of correlation, we obtained high coefficients of correlation for fresh and frozen-thawed donor aliquots, 0.814 and 0.859 respectively, that were similar to the degree

of correlation in the range of 0.96 to 0.9886 reported by Evenson when assessing aliquots from the same samples in different laboratories (Evenson, 2017). In spite of this we also obtained a high correlation for the Quantafrag and the AO visual assessment for the same aliquots when one only trained person performed the assessements, however this relies on visual sensitivity to the wavelengths used and hence is very individual specific, and impossible for red-green colourblind researchers. The implementation of Quantafrag with common settings will entail the obtention of robust data free of subjectivity.

2.5.2.4 The single-cell distribution (histogram) can offer additional information to the DFI (%)

We demonstrated that the DFI (%) computed by the average of 5 replicates stained by AO and scored by the Quantafrag system was not necessarily related with the median of the DFI values in the replicate. The median was very similar in all the replicates and donor samples, while the DFI (%) was quite different between donors. We observed that the replicates for each donor seemed to have very similar single-cell distribution according to their histograms. However, donors with the same DFI (%) obtained different histograms. Therefore, the study of the single-cell distribution by histograms or parameters such as the skewness or kurtosis alongside the DFI (%) could add valuable information to the study of SDD.

2.5.3 AO in donor and patient samples

2.5.3.1 AO and semen parameters in fresh semen from donors. AO and abstinence

No strong relatinoship was observed in our study between the DFI (%) and any of the sperm parameters of concentration, total count or the percentage of progressive sperm in the ejaculate; R^2 was in all cases inferior than 0.1 in our studies. The majority of the studies only found a weak or moderate negative correlation from 0.1 to 0.5 approximately between SCSA results and the motility, morphology and vitality of the ejaculate (Evenson *et al.*, 1991, Evenson *et al.*, 1999, Giwercman *et al.*, 2003, Spano *et al.*, 1998, Stahl *et al.*, 2015). Although it has also been reported the lack of correlation between SDF assessed by the Sperm Chromatin Dispersion (SCD) assay and the sperm parameters when assessing fertile men in contrast when assessing subfertile and infertile men (Evgeni *et al.*, 2015) which could explain why we did not observe any correlation with healthy donor samples. In any case, these findings justify the importance of assessing DNA damage as an additional test, as it can work as an independent attribute of semen quality and potentially predict the fertility outcomes.

Regarding the abstinence, we did not find any correlation between days of abstinence (0 - 5) and SDF value by our AO and Quantafrag assay. Shorter periods of abstinence can improve the semen quaility sample in terms of motility especially progressive motility and velocity while declining the sperm concentration and the ejaculate volume (Ayad *et al.*, 2018). However, there is no enough data to support shorter abstinence with an improvement in DNA damage and pregnancy rates according to a recent

systematic review including literature published during the past few decades (Ayad *et al.*, 2018).

2.5.3.2 Evolution of the SDD studied by the variation of the % DFI (> 0.66) across time in donor samples

Evenson published an average within-donor CV of 10 % for the DFI (%) measured in 8 monthly samples provided by 45 men (Evenson *et al.*, 1991), although other authors with larger human samples observed a CV around 30 % (Erenpreiss *et al.*, 2006, Oleszczuk *et al.*, 2016).

We found large fluctuations of DFI (%) for two of the three donors analysed over time. We know that the maladjustment of the apoptotic process during the spermatogenesis (Rodriguez *et al.*, 1997), the deficient chromatin packaging during the spermiogenesis (Ni *et al.*, 2016) and also the exposure to ROS (Agarwal *et al.*, 2003, Gharagozloo and Aitken, 2011) might also lead to sperm DNA damage through different mechanisms Therefore different spermatogenesis cycles, and punctual periods of time involving sickness/infection or smoking that lead to an increase of ROS might influence the DNA damage result (Adewoyin *et al.*, 2017, Agarwal *et al.*, 2016, D'Agata *et al.*, 1990). Even the abstinence has been observed to influence the sperm DNA damage (Agarwal *et al.*, 2016). However, it is also entirely possible that some people are more resistant to DNA damage inductors than others based on chromatin compaction and physiological antioxidants levels. In men with high variability of SDF over time could be advisable to freeze the sample and to use an aliquot to test the SDF prior the fertility treatment.

2.5.3.3 Study of the effect of cryopreservation in the induction of DNA damage

The majority of the SCSA samples are shipped frozen in raw semen and analysed after being thawed. However, the effect of the freezing-thawing protocol on the DNA status is still in debate. The damage to the sperm membrane and a decreased in viability and motility has been reported after freezing-thawing procedures (Hammerstedt *et al.*, 1990) and it is likely these events lead to DNA damage. Different species show different resistence to the freezing-thawing protocol probably due to different level of chromatin compaction; for example mouse samples did not show difference in the DFI before and after freezing-thawing protocol (Evenson *et al.*, 1989), but ram did, specially with higher post-incubation times (Peris *et al.*, 2004). Sperm human samples showed higher damage after the freezing-thawing protocol according the TUNEL (Amor *et al.*, 2018) and SCSA assays (Riva *et al.*, 2018). However, the potential damage induced during this process depends on the cryopreservation method as observed in bull (Karabinus *et al.*, 1991), and human (Liu *et al.*, 2016, Riva *et al.*, 2018). Liu *et al*. obtained less damge induction by storing the neat samples at - 80 ºC while Riva *et al.* obtained better results when using ultra-rapid freezing with sucrose as cryoprotectant (Liu *et al.*, 2016, Riva *et al.*, 2018). In our experiments where the samples were frozen similarly as in the HABSelect clinical trial by diluting the prepared sperm cells with locally-employed ART media and cryoprotectant prior equilibration at room temperature (RT) for 10 min and immersion in LN_2. When we examined this protocol in our donor population we observed different DNA cryodamage across donors. Only 1 out of the 3 donors experienced a significative increase on the DNA damage after the freezing-thawing protocol. This could be due to lower chromatin quality as proposed before in boar (Fernandez-Gonzalez *et al.*, 2008), however higher

DNA cryodamage was not always correlated with higher pre-freezing DFI levels in our experiments. Nevertheless, it could be interesting to measure the compaction of the chromatin by other assays like CMA_3 in relation to the induction of the cryodamage. In any case, men with high cryodamage should be advised to perform the fertility treatment with fresh sample rather than frozen-thawed sperm. However, If freezing is necessary, the use of neat semen appears to be a better solution as discussed above. Perhaps metabolites or proteins present in neat semen protect sperm cells against cryodamage.

2.5.3.4 DFI comparison in donor and patient samples

The DFI (%) was significatly different for donors and patients; positive cells for fresh and frozen donor samples were 30.74 % and 38.67 % while for the patients was 43.68 % ($p < 0.0001$). However, our donor population was quite small and it would be recommendable to do more studies involving a higher population of men with proven fertility to be able to set up a clinical cut-off by using the AO assay and Quantafrag scoring system developed in this study.

2.5.4 Conclusion

We developed an economical, objective and consistent slide-base DNA damage assay by using the metachromatic properties of the AO, a staining protocol based on the AO test (AOT) published by Tejada (Tejada *et al.*, 1984), and a fluorescence microscope coupled to a high-resolution camera that allowed the semi-automatic quantification of

positive cells to determine the SDD, similarly as per flow cytometry when using the SCSA protocol. Although we found good correlation between the automatic scoring system and the traditional assessment performed by a well-trained operator, the use of the former when applying an standard protocol for the sample preparation and the staining as defined in this chapter, alongisde the use of an specific calibration for the relative exposure and gain for the light excitation of the green and red channel, would allow different laboratories with operators with different visual acuity and even colour blindness conditions to obtain the same result when using the same samples.

In future, clinical cut-offs to differentiate between fertile and infertile men and couples with successful or unsuccessful ART treatment when using the modified AOT described in this chapter alongside the semi-automatic scoring system Quantafrag should be investigated. Also, it could be interesting to study more in depth the nature and type of DNA damage presented in the red cells stained by AO; sperm cells could be sorted based on their DFI and evaluated by the number of breaks that present at single-cell level by different assays such as the TUNEL and Comet assays presented in chapter 1, or by using Single-Cell Pulsed-Field Gel Electrophoresis (Kaneko *et al.*, 2012) where the DNA of embedded sperm into agarose are lysed, deprotected from the binding proteins, and exposed to an electrophoretic field in order to visualised and score the DNA fragments by nucleic gel staining. Moreover, in light of our DTT experiments, the degree of compaction of the DNA could be related to the level of AO positivity in terms of red fluorescence emitted by the sperm cells. This should be studied in further investigations alongiside the HDS parameter that has been correlated to IVF fertilisation rates (Virro *et al.*, 2004), miscarriage (Lin, M. H. *et al.*, 2008) and

used in combination with the DFI (%) to predict natural pregnancy (Evenson *et al.*, 1999).

To summarise:

- The study of the mountant for AO staining is key in order to get reliable results. While aqueous mountants interfered with the red emission of the AO, non-aqueous-based mountants such DPX offered good results.
- H_2O_2, DNase and specially DTT can be used as inductors of SDD when used washed-sperm before the AO staining protocol.
- The freezing-thawing procedure can affect the AO results by increasing the DFI (%). Different levels of increase can be found in different samples.
- DFI (%) is an independent parameter from the basic semen analysis parameters (motility, concentration, and total count), and abstinence, that generally is lower in healthy donor than patient samples.
- The method developed in this chapter offers a robust and accurate measurement of AO-positive cells superior to the traditional AO visual assessment in terms of objectivity and reproducibility (low intra-variability) and more affordable than the SCSA flow cytometry assay when correctly calibrated and consistent excitation settings are used.

CHAPTER 3: The TUNEL assay as an indicator of human sperm DNA damage

3.1 INTRODUCTION

3.1.1 Principle of the TUNEL assay: a method to detect single and double strand breaks

Terminal Deoxynucleotidyl Transferase (TdT), a template-independent polymerase that catalyses the addition of nucleotides to the 3'-OH ends of the DNA molecules in combination with labelled nucleotides (Gavrieli *et al.*, 1992, Motea and Berdis, 2010), allows the quantification of single strand breaks (SSB) and double strand breaks (DSB). The labelling available methods include the use of radio-isotopes, fluorophores like FITC, or molecules such as digoxygenin and biotin (Li, X. *et al.*, 1995). When employed to quantify SSB and DSB in DNA the assay is known as the terminal deoxynucleotidyl Transferase dUTP Nick End Labelling (TUNEL) assay. TUNEL was developed as a modification of the *In Situ* Nick Translation (ISNT) assay which used DNase and DNA polymerase I (Pol I) to serve as a tracer or to detect rare homologous sequences by fluorescent *in situ* hybridization (FISH), re-association kinetic analysis and blotting techniques (Rigby *et al.*, 1977). Later, the ISNT assay, in the absence of DNase, was proposed for measuring pre-existing SSB and it was the origin for the TUNEL assay (Thiry, 2002, van Dierendonck, 2002) (**Figure 3.1**).

Unlike DNA Pol, which detects SSB, the TdT enzyme due to its template-independent mechanism can detect DSB and with less sensitivity SSB (Chen, J. *et al.*, 1997, Chen,

J. *et al.*, 1997, Yamadori *et al.*, 1998). Partial denaturation of the DNA prior to the assay was suggested to increase the sensitivity of the assay for the SSB detection (Honda *et al.*, 2004).

Initially, TUNEL assay was proposed as a method for detecting apoptosis (Gavrieli *et al.*, 1992, Wang, R. A. *et al.*, 1998). But later, it was found able to detect strand breaks produced during necrosis, and by cytostatic drugs and irradiation, but with less sensitivity than ISNT (Dmitrieva and Burg, 2007, Gold *et al.*, 1994). The explanation for this different sensitivity is due to the different fragments encountered in both cell death processes; TdT is more effective in the presence of 3'-overhang which arespecific to apoptosis and DNase I (Deng, G. and Wu, 1983, Didenko and Hornsby, 1996, Roychoudhury *et al.*, 1976).

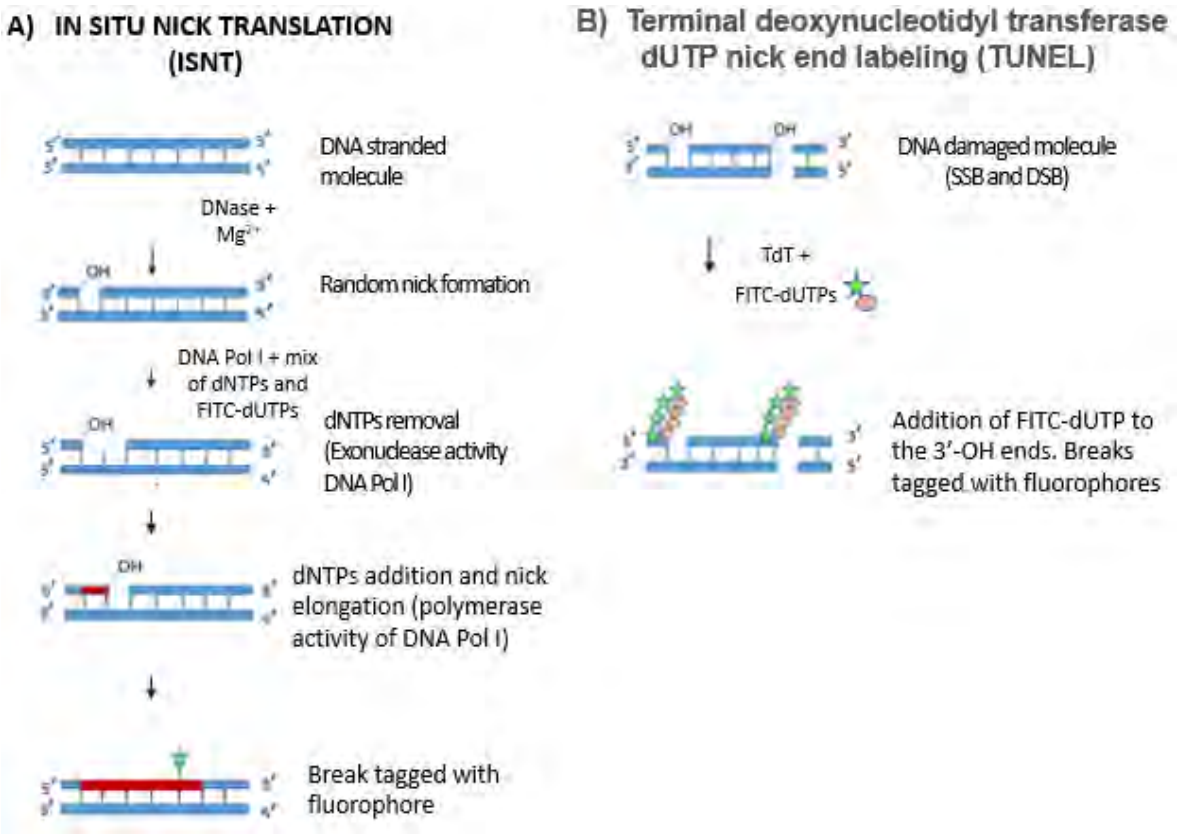

Figure 3.1 Simplified mechanisms of in situ nick translation (ISNT) (1A) and terminal deoxynucleotidyl transferase dUTP nick end labelling (TUNEL) assay (1B). The labelling method shown is fluorescence (dUTP-FITC), however other alternative labels are available as explained in the text. DNA Pol I and TdT need the existence of 3'-OH ends to add the dNTPs, however DNA Pol is template-dependent and adds the homologous nucleotides to the nicks (**1A**), while TdT is template-independent and adds labelled dUTPs (**1B**). (Source: personal collection)

3.1.2 TUNEL, laboratory outcomes and clinical utility

3.1.2.1 TUNEL and basic semen parameters

A link between the sperm DNA damage (SDD) measured by TUNEL and the semen basic parameters has been previously reported; for example, in a group of couples with male factor/unknown infertility the percentage of TUNEL-positive cells was higher in those men with abnormal basic semen analysis compared with those with normal semen parameters; 2.5 ± 2.5 *vs* 12.3 ± 12.2 (p = 0.000) (Di Santo *et al.*, 2016). A more in depth study performed with 1562 infertile patients found that the alteration of any single semen parameter (concentration, motility and morphology) was correlated with TUNEL (%); 29 % *vs* 47 % for the normozoospemic and oligozoospermic men ($p < 0.0001$), 25 % *vs* 50 % for the normal motility and asthenozoospermic groups ($p < 0.0001$), 25 % *vs* 43 % for the normal morphology and teratozoospermic groups ($p < 0.0001$), and 22 % vs 54 % for the normal semen analysis vs oligoasthenosteratozoospermic groups ($p<0.0001$) (Ganzer *et al.*, 2017). Another study with 150 men undergoing ICSI treatment found that the study of motility and morphology parameters (p = 0.002) but not sperm concentration in semen could predict the TUNEL (%) which was also correlated with the fertilisation rate (r = −0.23;

p = 0.0117) (Lopes, S. *et al.*, 1998). Interestingly, a small study of 19 men found that between 20-66.6% of the normal and motile sperm cells were TUNEL-positive in a small proportion of the sub fertile men (1 / 5) and in all of the infertile patients (10 / 10), but this event was not observed in the fertile men (Avendano *et al.*, 2009).

3.1.2.2 TUNEL and fecundability

It has been observed that a subgroup of infertile men generally has higher TUNEL (%). For example, a study comparing infertile men with men of proven fertility showed that the former group exhibited a higher mean level of TUNEL (%) (40.9 ± 14.3 % *vs* 13.1 ± 7.3 %, respectively; $p < 0.001$) (Sergerie *et al.*, 2005). When comparing with healthy donors, infertile men also exhibited a higher mean level of TUNEL (%) (29.5 ± 18.7 % *vs* 11.9 ± 6.8 % ($p < .001$)) (Sharma, R. K., Sabanegh *et al.*, 2010). However, a high heterogeneity in TUNEL results across infertile men has been observed; a study with 1633 patients referred for infertility investigation found that 40.9% patients had a TUNEL scoring between 0-20 %, 28.4 % had 20-30 %, 8.8 % had 20-30%, 17.5 % had 30-40 %, and 13.2 % had values > 40 % (Cohen-Bacrie *et al.*, 2009). This heterogeneity of results is to be expected, as sperm DNA damage, detected by TUNEL, would only ever be one of an array of causes of fertility problems and would not be expected to explain them all.

An approximate cut-off of 20% TUNEL-positive cells has been suggested for the diagnosis of sperm DNA damage relevant to male fertility based on publications. For example, Sharma *et al*. reached 100 % specificity when using a 19.5 % cut-off comparing 43 donors and 114 and infertile patients (Sharma, R. K. *et al.*, 2010). Sergerie *et al*. when employing a 20 % threshold reached 89.4 % specificity (95 %

confident interval (CI)), 96.9 % sensitivity (95 % CI), 92.8 % positive predictability (95 % CI) and 95.5 % negative predictability (95 % CI) (Sergerie *et al.*, 2005).

3.1.2.3 TUNEL and assisted reproductive techniques

IUI

Couples whose male partner had higher TUNEL (%) value are less likely to achieve a clinical pregnancy (CP) by Intra-Uterine Insemination (IUI) as demonstrated in several studies. For example, the TUNEL (%) values assessed in 119 patients who underwent 154 cycles of IUI were significantly lower in those patients who achieved a CP *vs* those who did not (7.3 ± 3.5 *vs* 13.9 ± 10.8, p = 0.044). Moreover, none of the pregnant couples scored more than 12 % in the TUNEL assay (Duran *et al.*, 2002). In a smaller study with 53 IUI cycles, the TUNEL (%) of pregnant couples was lower than in non-pregnant couples although it did not reach statistically significance (4.1 *vs* 7.3 %, p = 0.08) (Thomson *et al.*, 2009).

IVF and ICSI fertilisation rates

There is some disparity regarding data for fertilisation rates and the cut-offs used for low and high TUNEL. Some studies found no correlation between TUNEL (%) and the *In Vitro* Fertilisation (IVF) Rates (FR) in 147 cycles (Choi *et al.*, 2017) or found no significant difference in IVF FR between the low and high damaged groups when using cut-offs of 15 % (Benchaib *et al.*, 2007) and 35% for IVF (Frydman *et al.*, 2008). Others found that TUNEL (%) is negatively correlated with FR in IVF patients (Borini *et al.*, 2006, Host *et al.*, 2000) and that an increase in TUNEL values is associated with a

diminish in FR (Huang, C. C. *et al.*, 2005). After applying a 35 % cut-off based on ROC analysis Henkel *et al.* found a significant difference between the FR of low and high TUNEL (%) groups in 208 cycles (Henkel *et al.*, 2003). This discrepancy among different publications, could be due to the heterogeneity of the studies in terms of sample size and cut-off used for TUNEL which varied from 4 to 36.5 %. It seems that the presence of certain SDD calculated by TUNEL could have a negative impact on fertilisation

Regarding TUNEL studies in Intra-Cytoplasmic Sperm Injection (ICSI) patients, all studies generally find no correlation between TUNEL (%) and FR or not significant difference in the fertilisation rates between low and high TUNEL groups when using cut-offs that ranged from 4-36.5 % (Benchaib *et al.*, 2007, Borini *et al.*, 2006, Henkel *et al.*, 2003, Host *et al.*, 2000). However, in a study of 86 ICSI cycles, the patient group of TUNEL > 15 % had a significantly lower FR than the lower TUNEL groups (< 4 %, 4-10 %, and > 10 %) (Huang, C. C. *et al.*, 2005).

IVF and ICSI embryo development

In embryology data, the risk of developmental arrest was observed to be statistically significantly higher with the group of high TUNEL (%) in ICSI but not in IVF patients (Benchaib *et al.*, 2007). The good quality embryo rate diminished with the percentage of TUNEL-positive cells and were statistically significant for the groups of TUNEL > 10 % and TUNEL > 15 % compared to groups of lower damage (< 4 %, 4-10 %) in IVF patients (Huang, C. C. *et al.*, 2005). In ICSI patients the decrease in good quality embryos became significant for men with TUNEL > 15% (Huang, C. C. *et al.*, 2005).

However, other studies found no statistical difference between the good quality embryos obtained with men with high and low TUNEL when using a 35 % cut-off in 117 IVF cycles with female partners with adequate ovarian follicular status (Frydman *et al.*, 2008) or in oligozoospermic men when using a 4 % cut-off in 50 IVF cycles and 61 ICSI cycles (Host *et al.*, 2000).

IVF and ICSI clinical pregnancies

The implications of the SDD assessed by TUNEL in achieving CP by IVF or ICSI are not clear. A meta-analysis found a significant higher OR to achieve CP for patients conducting IVF but not ICSI when the TUNEL results were lower than 27 % (Zhang, Z. *et al.*, 2015). Similarly, Zhao *et al*. also found an association with TUNEL (%) and the IVF pregnancy rate but not with the ICSI pregnancy rate suggesting that DNA-damaged sperm can still fertilise the oocyte and set a pregnancy when selected by ICSI, which involves the selection of motile and normal sperm cells (Zhao *et al.*, 2014).

However, past studies found no significant difference in their IVF or ICSI pregnancy rates using a different range of TUNEL cut-offs from 4 to 35 % (Benchaib *et al.*, 2007, Henkel *et al.*, 2003, Host *et al.*, 2000, Huang, C. C. *et al.*, 2005). But, after applying a 36.5 % cut-off for TUNEL, the CP was significantly lower in IVF but not ICSI patients (Henkel *et al.*, 2003), On the contrary, another study found significant different CP rate in the high and low TUNEL groups in the ICSI patients but not in the IVF when applying a cut-off = 10 % (Borini *et al.*, 2006)

TUNEL has shown good discrimination between fertile controls and infertile patients, although it was not able to predict CP for 50 IVF and 61 ICSI patients (Garolla *et al.*, 2015). However, according to the large metanalysis performed by Cissen *et al.* TUNEL

was able to predict CP with reasonable sensitivity (0.84, 95% CI 0.75 to 0.90) and specificity (0.24, 95% CI 0.11 to 0.44) for both IVF and ICSI groups (Cissen *et al.*, 2016).

3.1.2.4 TUNEL and miscarriage

Miscarriage has also been related to the presence of higher TUNEL-positive sperm cells in the ejaculate (Robinson *et al.*, 2012), though this finding is controversial and not considered proven to diagnostic acceptability levels (Kirkman-Brown, J. C. and De Jonge, 2017).The hypothesis would be that some sperm with DNA damage are still capable of fertilising the oocyte, and in the event of the impossibility of the DNA repair by the oocyte, the most likely scenario is a miscarriage (Gonzalez-Marin *et al.*, 2012).

In a meta-analyses that included a total of 16 cohort studies (2969 couples) a strong association between the TUNEL assay (6 studies) and miscarriage was observed (RR = 3.94 (2.45, 6.32), $p < 0.00001$) (Robinson *et al.*, 2012). Moreover, couples with recurrent miscarriage have shown higher TUNEL values than donors with known fertility and males from the general population (Carrell *et al.*, 2003, Kamkar *et al.*, 2018, Sergerie *et al.*, 2005).

When considering IVF and ICSI separately, some publications found an association between TUNEL (%) and IVF miscarriage (Benchaib *et al.*, 2007, Choi *et al.*, 2017, Frydman *et al.*, 2008), and others found such association in ICSI but not IVF patients which is corroborated in the meta-analysis conducted by Zhao *et al*., (Borini *et al.*, 2006, Zhao *et al.*, 2014). Moreover, in the meta-analysis of Zhang *et al.,* when stratifying by DNA sperm assay no association between any of the damage assays

and miscarriage was found, for example the OR for TUNEL was OR (95%CI) = 0.349 (0.103–1.175), p = 0.089 (Zhang, Z. *et al.*, 2015).

3.1.2.5 Clinical utility TUNEL assay

In summary, high TUNEL (%) values seem to negatively impact the fertilisation rates, especially in IVF (Borini *et al.*, 2006, Host *et al.*, 1999, Huang, C. C. *et al.*, 2005). The effect elevated TUNEL on clinical pregnancy is less clear, however higher values of TUNEL (%) are associated with higher miscarriage rates in IVF and ICSI (Benchaib *et al.*, 2007, Borini *et al.*, 2006, Frydman *et al.*, 2008). Nevertheless, more studies with appropriate sample sizes should be conducted as many of the given citations in this chapter found a trend but no significance probably due to low number of patients; for example Esbert *et al.* found that patients with TUNEL > 36 % had a miscarriage rate higher than those patients with TUNEL< 36 % (3/26 (11.5 %) *vs* 2/4 (50 %), respectively) but it did not reach significance (Esbert *et al.*, 2011).

The value of the TUNEL or other SDD test that assess different aspects of the DNA integrity, lies in the fact that men diagnosed with high SDD, if concomitant with oxidative stress, can try to decrease their ROS levels by the intake of antioxidants (Lewis, S. E. *et al.*, 2013). Shorter abstinence periods which improve sperm motility have been proposed to decrease SDD, although the available data regarding the benefit of shorter abstinence on SDD and pregnancy is insufficient (Ayad *et al.*, 2018). ICSI seems to be more effective when comparing with the rest of ART in terms of achieving fertilisation and pregnancy according to the clinical results showed in this section, although there is still risk of miscarriage. Methods to select sperm with low DNA damage prior ICSI based on hyaluronic-acid binding, high-magnification

morphology based on the Motile Sperm Organellar Morphology Examination (MSOME) criteria, and density gradient combined with Zeta potential selection (based on negative surface electrical charge) have shown to select sperm with lower TUNEL (%) and increase the pregnancy rate (Mongkolchaipak and Vutyavanich, 2013, Nasr Esfahani *et al.*, 2016)

Study	IVF-FR	ICSI-FR	IVF-ED	ICSI-ED	IVF-CP	ICSI-CP	IVF-M	ICSI-M	IVF-LB	ICSI-LB
Benchaib 2007 88 IVF/234 ICSI cut-off=15%	NO	NO	nd	nd	NO	NO	YES (-)	YES (-)	nd	nd
Borini 2006 82 IVF/ 50 ICSI cut-off=10 -20%	YES (-)	NO	nd	nd	NO	YES (-)	NO	YES (-)	nd	nd
Frydman 2008 117 IVF cut-off=35%	NO	nd	NO	nd	YES (-)	nd	YES (-)	nd	YES (-)	nd
Henkel 2003 208 IVF/54 ICSI cut-off 36.5% for ICSI, 24.3% for IVF	NO	NO	nd	nd	YES (-)	NO	nd	nd	nd	nd
Huang 2005 217 IVF/ 86 ICSI cut-off from 4% to 15%	YES (-)	YES (-)	YES(-)	NO	NO	NO	nd	nd	nd	nd
Host 2000 175 IVF/ 61 ICSI cut-off=4%	YES (-)	NO	nd	nd	NO	NO	nd	nd	nd	nd

Table 3.1 Summary of the studies mentioned in the text that looked the association or correlation between TUNEL (%) levels and Fertilisation rate (FR, Embryo Development (ED), Clinical Pregnancy (CP), Miscarriage (M) and Live Birth (LB).

Associations/correlation are shown in green whilst no association/correlation are shown in red.

nd: no data available

3.1.3 Lack of standardised protocol for the TUNEL assay

TUNEL is considered a direct assay that identifies and quantifies actual SSB and DSB. However, major disadvantages of the TUNEL assay are the price of the reagents, and the time-consuming and non-standardised protocol. There are many published protocols using labelling, fixative and detection methods which offer different sensitivity and efficiency, there are a number of key factors which may alter assay results:

1. The accessibility of the TdT enzyme to the DNA is a key factor in the TUNEL assay. Due to the high compaction of the human sperm DNA, a preliminary incubation with dithiotreitol (DTT), a reducing agent which breaks the di-sulphide bridges in the chromatin, has been suggested to relax the DNA structure and facilitate the TdT access to the strand breaks (Mitchell *et al.*, 2011). However, not all the laboratories apply this preliminary step of chromatin relaxation and this might cause the underestimation of the SDD (Mitchell *et al.*, 2011).
2. The type and duration of the fixation method, which vary across protocols, can indirectly influence the accessibility of the TdT to the DNA (Davison *et al.*, 1995) and influence the TUNEL results.
3. The duration of storage of fixed samples prior the staining step or microscope visualization can also influence the TUNEL results (Muratori, Tamburrino, Tocci *et al.*, 2010).
4. Exposure to some fixatives, such as formaldehyde, has been demonstrated to cause SDD with an inter-subject variability response (Muratori, Tamburrino, Marchiani *et al.*, 2010). This inter-subject variability could be due to hypothetical variation in protamine content between patients (Muratori, Tamburrino,

Marchiani *et al.*, 2010). However, a paradoxical decrease of the DNA fragmentation levels in some patients was observed and explained as a loss of fragmented cells caused by the formaldehyde itself. In light of these findings, a shorter formaldehyde incubation (30 min) in the TUNEL assay has been suggested so the effect on cell fragmentation is minimised (Muratori, Tamburrino, Marchiani *et al.*, 2010) , although there are no published data confirming this suggestion.

Beyond the major factors outlined above, there are also other specifics that can alter TUNEL results, for example often DAPI is used to counterstain the cells. However, excitation with UV can result in the photoconversion of DAPI to a form which can then be excited with blue light and emit in the FITC/GFP (Fluorescein isothiocyanate/ Green fluorescent protein) channel leading to false-positive results if the main assay measure employs a green fluorescent conjugate (Jez *et al.*, 2013, Karg and Golic, 2018). The photoconversion phenomenon depends on the DAPI concentration, excitation duration, cell fixation method and the composition of the mounting medium (Jez *et al.*, 2013). To minimise DAPI photoconversion, lower DAPI concentrations should be used, the DAPI images should be acquired after all other higher wavelength images and a mountant that prevents the photoconversion should be chosen. However, different laboratories use different mountings, DAPI concentrations and mountings which lead to a further lack of consistency of the assay.

3.1.4 Analysis of the advantages and pitfalls of the detection method for TUNEL: fluorescence microscopy and flow cytometry

Another source of variability in the protocol is the use of different detection methods such as fluorescence microscopy or flow cytometry. The results obtained by both methods have demonstrated good correlation, however flow cytometry was observed to yield greater (Dominguez-Fandos *et al.*, 2007) but also lower (Cohen-Bacrie *et al.*, 2009) percentage of damage than the fluorescence microscopy when assessing the same semen samples. This difference could be easily explained by a poor calibration of the flow cytometry or by the gating procedure. Similarly as in fluorescence microscopy, in flow cytometry the excitation light can be individually modified for each channel so the emission light intensity and therefore TUNEL signal ultimately depends on the initial settings for the excitation light. In flow cytometry this is also dependent upon the photomultiplier gain set for detection. Therefore, it is very important for both methods to investigate and apply the light settings that offer better results in terms of sensitivity and dynamic range, as well as to choose a correct threshold intensity to quantify positive cells. Gating of flow cytometry results is a complex judgement where without visual confirmation decisions are being made on what may be cells and real results and what is debris, this therefore has the potential to radically skew data.

In a flow cytometry scenario, the TUNEL fluorescence is usually determined as a binary positive or negative for sperm cell, but in our study the single-cell fluorescence quantitation is theoretically possible. In previous microscopy studies the threshold that separates the negative and positive cells has been based on the person's eyes accuracy, which in turn will be dependent upon excitation strength, quality and magnification of the lenses employed, as well as the assessment of a negative control.

In flow cytometry it is usually based solely on a negative control sample. A negative control consists of a sample stained with the labelling solution (fluorophore) but without the TdT enzyme. A threshold that typically includes 95-99% of the cells from the negative control is set-up so when assessing patient samples those cells above the threshold are considered as TUNEL positive. This is the method designated as threshold-setting (TS) (Muratori, Tamburrino, Tocci *et al.*, 2010). Another way to analyse the intensity data is by subtracting the negative control histogram from the patient sample histogram, named as the subtraction of the blank method (SB) (Muratori, Tamburrino, Tocci *et al.*, 2010, Sergerie *et al.*, 2005, Sergerie *et al.*, 2005). The correlation between both methods was reported to be high for 32 samples (R = 0.6), however with the SB method the TUNEL-positive % was slightly higher than for the TS method which could lead to clinical misclassification if only one universal clinical threshold is considered (Muratori, Tamburrino, Tocci *et al.*, 2010).

Regarding amount of data, flow cytometry analyses the cell fluorescence according a threshold channel value on a relative intensity scale which allows the study of more cells in less time in a reproducible manner. On the other hand, fluorescence microscopy is cheaper and permits the simultaneous study of single-cell morphology and fluorescence.

The use of a combined TUNEL/Propidium Iodide (PI) assay coupled to a standardised bench top flow cytometer has been suggested as a reference protocol for the assessment of DNA fragmentation (Agarwal *et al.*, 2016, Sharma, R. *et al.*, 2016) and to improve the accuracy of the measures (Muratori, Marchiani *et al.*, 2008, Muratori, Forti *et al.*, 2008). The PI as other nuclear dyes can help to distinguish and exclude M540 bodies; M540 are membrane surrounded round bodies with similar size and

complexity to sperm that can be stained with the lipophilic compound merocyanine 540 (M540), but not with nuclear dyes like PI due to the lack of chromatin (Marchiani *et al.*, 2007, Muratori *et al.*, 2004, Muratori, Forti *et al.*, 2008, Muratori, Marchiani *et al.*, 2008).

Although TUNEL results are based on the proportion of positive and negative cells, the fluorescence emission of positive cells can be classified and quantified in a gradual scale that can be observed by simply plotting a histogram with the fluorescence intensity data. Such gradualism could indicate differences in the severity or amount of DNA damage within the TUNEL-positive population that could be clinically relevant.

Fluorescence microscopy with coupled sensitive monochrome camera and filters could offer similar results to flow cytometry; single-cell intensity for the TUNEL fluorophore could be recorded and applying an appropriate threshold cells would be identified as damaged. In this way, SDD as the percentage of damaged cells, could be easily and objectively calculated similarly as per flow cytometry while keeping the cost of the assay low and affordable for fertility patients.

3.2 AIM OF THE STUDY

The main aim of the study was to develop and optimise a method that allowed the direct quantification of the Sperm DNA Damage (SDD) in a reliable and reproducible manner using the TUNEL assay and fluorescence microscopy.

The study involved:

- The assessment of the effect of commercial mountants on FITC fluorescence emission.

- The use of fluorescence microscopy and high-resolution camera to acquire images and measure single-cell fluorescence intensity.
- The development and comparison of different methods for estimating the level of damage of the semen sample on a 0-100% scale by using the single-cell data acquired by the fluorescence microscope and high-resolution camera.
- The validation of the revised TUNEL assay by comparison with traditional visual assessment and by using negative and positive controls
- The analysis of the intra and inter-variability of the visual and semi-automatic assessment of TUNEL.
- The study of possible DNA induction damage by the freezing-thawing effect when storing sperm samples for later assessment.
- The comparison of TUNEL (%) levels in donors and patients of the clinical trial HABSelect.

3.3 MATERIAL AND METHODS

Unless otherwise stated all reagents were purchased from Sigma-Aldrich

3.3.1 Sperm preparation

3.3.1.1 Fresh donor samples

Control semen samples were acquired from five volunteer donors of the Birmingham Women's Hospital (HFEA centre 0119, Ethics Committee Reference Number 13/EM/0272). These donors were the same as per Chapter 2 (donors A, B, C, D, and

E). All ejaculates presented good concentration, motility and morphology results according to WHO criteria (WHO, 2010a)

The protocol followed was the same as in chapter 2 (2.3.1.1) but stained with the TUNEL protocol detailed below (3.3.2) instead of AO.

The number of donors, samples and replicates used in each experiment is detailed in the captions below the figures and tables in the results section (3.4)

3.3.1.2 Frozen donor samples

The same frozen samples from donors A, B and D as in Chapter 2 were used to test the effect of freezing-thawing on DNA damage. On the day of the experiment, the thawed samples were stained according the TUNEL protocol detailed below (3.3.2) instead of AO.

The induction of damage was studied by calculating the percentage of positive-TUNEL cells in aliquots before freezing and after the freezing and thawing procedure in eight donor samples.

3.3.1.3 HABSelect patient samples

A subset of 620 male patient samples from the HABSelect trial were used in this chapter. 16 assisted conception units licensed by the Human Fertilisation and Embryology Authority (HFEA) in the UK took part in the trial. HABSelect was approved by the National Research Ethics Service (approval number 13/YH/0162) and by the doctors of the assisted conception units. Patients eligible for HABSelect trial gave

consent for the donation of the residual semen samples for biomedical research to the Human Biomaterials Resource Centre (HBRC) Biobank, University of Birmingham. All patients were indicated for ICSI treatment and their age was comprised between 18-55 years old. The sperm preparation and fertility treatment were performed outside the University of Birmingham by the participating clinics as explained in chapter 2 (2.3.1.3). The samples arrived frozen in cryovial and then were thawed following same protocol described in 2.3.1.2, then they were stained with the TUNEL protocol (below, 3.3.2).

The percentage of TUNEL-positive cells obtained from the HABSelect patients was compared with those obtained from a normal population (15 fresh PBS-washed sperm samples from seven donors and nine frozen sperm samples from three donors).

3.3.2 TUNEL assay

The protocol was adapted from the methods published by Mitchell *et al*. using DTT decondensation to avoid underestimation of TUNEL signal (Mitchell *et al.*, 2011). Briefly, the smeared slides were immersed for 45 minutes in freshly prepared 2mM dithiothreitol (DTT) in PBS solution in order to reduce the disulphide bonds to thiols in the chromatin and allow the TdT to reach the strand breaks in the DNA. The DTT was removed from the samples by doing a 5 min PBS-wash with and the slides were then fixed in a fume hood for 15 min with 2 % Paraformaldehyde (PFA) in PBS solution previously cooled in ice (2-8 ºC). The PFA solution was prepared in advance by adding 4 g of PFA to 200 mls PBS, 400 µL NaOH (5 N) and stirring at 50 ºC to facilitate the

dissolution. Once all PFA was dissolved the pH was adjusted to 7.4 by dripping pure HCl. The 2 % PFA solution was aliquoted and kept at 4 ºC for a week or at -20 ºC for a month. The fixed slides were washed in PBS for 5 minutes 3 times and immersed for 2 min into permeabilisation solution freshly prepared with 0.1 % sodium citrate and 0.1 % Triton X-100 in distilled water and cooled in ice (2-8 ºC). The excess of permeabilisation solution was removed by two 5 min PBS-washes. The samples were labelled with the *In Situ* Cell Death Detection Kit with Fluorescein (11684795910, Roche). The reaction mixture was prepared by diluting 1:10 the enzyme solution in the labelled solution and kept on ice and protected from the light. The slides were placed in a humidifier chamber, pipetted with 25 µL of reaction mixture and covered with 25 x 25 coverslips to ensure the correct spreading of the labelled solution and they were kept at 37 ºC in the dark for 1 hour. Following incubation, the coverslips were carefully removed and the samples were washed three times in PBS for 5 min to remove all the labelled solution. The samples were counterstained for 3 min in the dark with 25 µL of 300 nM DAPI in PBS. The samples were then washed three times in PBS for 5 min to remove all the labelled solution and left to dry at room temperature (RT) before being mounted.

3.3.2.1 Study of the suitability of different commercial mounting solutions for use in combination of the TUNEL staining assay

The same procedure as per Chapter 2 was followed in order to test with donor samples the suitability of different mounting solutions for the TUNEL assessment. Subsequent to this study all samples stained with the TUNEL assay were mounted using Fluoroshield.

3.3.2.2 TUNEL assay validation with samples exposed to DNA-damage inductors (positive controls)

Negative controls for donors and patients were prepared by adding the labelling solution in the absence of the TdT enzyme in order to study non-specific fluorescence. In addition, the level of auto-fluorescence of the sperm cells was studied by omitting the addition of both TUNEL labelling solution and TdT enzyme but adding the DAPI dye.

Positive controls for donor and patient samples were prepared by pipetting 25 µl of 3 U/ml DNase prepared in10X DNase buffer and distilled water solution into the fixed samples. The samples were covered with coverslips and they were kept at 37ºC for 1 hour in a humidifier chamber. Following incubation, the coverslips were carefully removed and the samples were washed twice in PBS for 5 min before continuing with the TUNEL and DAPI labelling steps detailed in the TUNEL protocol (3.3.2).

The induction of SDD by H_2O_2 was studied in both, PBS-washed semen samples and fixed samples before proceeding with the TUNEL and DAPI labelling. Briefly, 25 µl of a range of H_2O_2 solutions from 50 µM to 10 M were pipetted into the slides. The samples were covered with coverslips and kept at 37 ºC in a humidifier chamber for different periods of time from 15 min to 3 h. Following incubation, the coverslips were carefully removed, and the samples were washed twice in PBS for 5 min before proceeding with the TUNEL and DAPI labelling protocol (3.3.2)

3.3.3 TUNEL scoring

The TUNEL-labelled slides were visualized on an Olympus fluorescence microscope (BX61) with LED light using 60x oil immersion objective, and excitation and emission

filters for FITC and DAPI. The characteristics of the excitation and emission filters used for the FITC fluorophore were 480±20nm and 525±36nm, and for DAPI 350±25nm and 455±25nm.

The exposure and gain used for the cell imaging were fixed to 150 and 50ms for FITC and 100 and 1ms for DAPI. These values demonstrated good signal/noise ratio, dynamic range and prevented the over-exposure (signal saturation) in our system.

3.3.3.1 TUNEL visual scoring

200 sperm cells were visualised by eye under the fluorescence microscope and classified into damaged (bright) and non-damaged (dim) according to the FITC intensity fluorescence observed and the % of damaged cells was calculated. A second count on the same slide but different fields to ensure the representability of the whole slide was performed and the % of damaged cells was also calculated. The average between both counts was performed to give a TUNEL (%) result that was accepted or rejected based on the WHO recommendations for binomial assays such as motility, vitality and acrosome reaction (WHO, 2010b) as detailed in 2.3.3.1

3.3.3.2 Semi-automatic TUNEL scoring method based on acquired grey-scale images using correspondent filters for the FITC and DAPI emission

FITC and DAPI emission lights were collected by using the emission filters detailed above. The images were automatically acquired by the motorized image capture microscope Olympus BX61 after predefining the slide area desired for imaging. The chosen area was always central to avoid any mounting irregularities and ensure the

full enzyme and DAPI solution coverage during the labelling protocol. Images were acquired using a QUANTUM: 512SC camera (Photometrics) and analysed using MetaMorph® Microscopy Automation and Image Analysis Software. The cells were identified by the DAPI mask and all the intensities for both DAPI and TUNEL were extracted and copied in an Excel spreadsheet alongside the size and shape factor values for individual cells. The whole procedure was summarised in a journal to facilitate to the user the image analysis task.

3.3.3.2.1 Acquisition settings

The exposure times for both channels were set up independently as the intensity range for the green fluorescence was lower compared to the blue. Good results were observed after applying greater exposure time and gain for the FITC channel. The exposure time was set-up at 150 milliseconds (ms) for the FITC channel and at 100 ms for the DAPI channel. The gain was set-up at 50 ms for FITC and at 1 ms for DAPI. The settings on a specific system ideally need to be consistent to allow the acquired intensities (in absolute numbers) to be comparable between experiments or samples.

3.3.3.2.2 Image analysis and data acquisition

Different fields of view were automatically imaged depending on the concentration of the sample. A minimum of 200 cells was suggested as baseline for the analysis, although a number between 500-1000 cells were usually reached.

For each field of view two greyscale images were acquired using the filters for DAPI and TUNEL. The Regions of Interest (ROI) were created around the sperm heads by automatic thresholding on the DAPI image. This thresholding was studied for each

sample and individually set-up as a specific number of pixels/area above the background intensity. The single-cell average intensity data regarding the DAPI and FITC was extracted from correspondent stacked planes using the binary mask containing the ROIs. The inclusion of debris and cell clumps into the data analysis was minimised by applying filters for area (between 18 pixels and 150 pixels), shape factor (0.7 to 1) and intensity above background for DAPI (400 intensity units). The image analysis process is summarised in **Figure 3.2.**

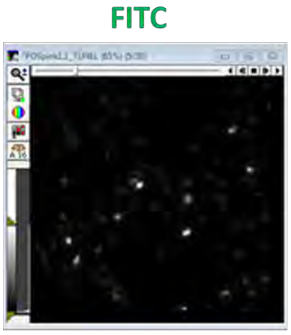

Grey-scaled images obtained for the DAPI (left) and FITC (right) channels

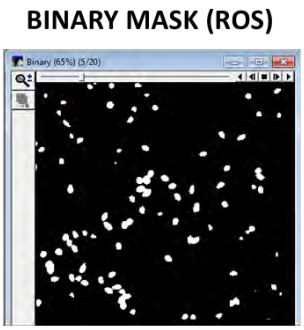

Creation of ROS by automatic thresholding on the DAPI image

Single-cell data extraction

Image Plane	Object	Area	Shape factor	DAPI Average intensity	DAPI Total intensity	FITC Average Intensity	FITC Total intensity
1	1	9.53	0.99	11710.08	1569151.00	1570.33	210424.00
1	2	9.18	1.00	8969.36	1157048.00	1665.70	214875.00
1	3	10.67	1.00	12631.90	1894785.00	1747.70	262155.00
1	5	11.59	1.00	12934.82	2108375.00	1674.65	272968.00
1	6	11.95	0.97	11947.89	2007246.00	1696.40	284995.00
1	7	11.02	1.00	12645.68	1960081.00	1683.56	260952.00
1	8	10.60	0.97	12109.05	1804248.00	1808.06	269401.00
1	9	14.65	1.00	17694.52	3645072.00	1871.84	385600.00
1	10	15.15	0.99	13032.32	2775884.00	1686.34	359190.00
2	2	11.17	0.99	11020.88	1730278.00	1854.51	291158.00

Figure 3.2 Process for image acquisition and single-cell data extraction. The grey-scaled images are obtained for the DAPI and TUNEL channels first. Then, Regions of Interest (ROIs) are created around sperm heads in the DAPI image by using the automatic thresholding tool in combination with filters for area, shape and background. This process is repeated for every plane (field of view acquired) and the single-cell intensity data is extracted for the DAPI and FITC intensities alongside the size and shape factor of the sperm heads. (Source: personal collection)

3.3.3.2.3 Data analysis for the single-cell intensity data

Graph-gating method

Initially, positive TUNEL cells were identified by applying manual gating similar as per flow cytometry. The single-cell intensity distribution was plotted for every patient in a scatter plot and then unique threshold for TUNEL-positive cells was decided based on intensity proximity to the baseline. The thresholds were individually decided for each sample.

Clustering method: mixed model

The TUNEL data distribution in donors with high and low levels of damage was studied with the package of fitdistrplus and the descdist function in R. As no positive results were obtained for single distribution, the TUNEL data was though as a combination of two distributions and the use of unsupervised learning clustering methods was investigated. We chose as a good approximation for the single-cell TUNEL data, a mixed model with two normal distributions to differentiate between the non-damaged and the damaged cells. Briefly, for every sample, two Gaussian equations with different mean of FITC intensity were mathematically calculated based on the FITC single-cell distribution data; the Gaussian with lower mean corresponded to the non-damage subpopulation and the Gaussian with higher mean to the damaged population. The cells were automatically associated to the first (non-damaged) or second (damaged) Gaussian according to their probability to belong to each of the Gaussians based on their FITC intensity levels. The proportion of damaged cells (TUNEL (%)) in the

ejaculate was calculate based on the number of cells associated to the Gaussian with lower mean and the total number of cells given in every sample.

3.3.4 Comparison between the different scoring methods: visual, gating and mixed model clustering method

The correlation and the agreement according the Bland Altman analysis for the visual and the gating, and for the gating and the mixed model clustering methods were assessed in 559 and 583 patient samples, respectively.

3.3.5 Consistency of the TUNEL semi-automatic scoring system: inter and intra-variability for the gating and mixed model methods

The intra-assay variability for the gating and the mixed-model methods was assessed by studying the % of coefficient of variation (CV (%)) of the TUNEL positive cells (TUNEL (%)) scored in duplicates of donor samples.

3.3.6 TUNEL optimisation

To test the homogeneity of the staining of the slides, images were acquired according to the protocol detailed above (3.3.3.2) until 600 cells were obtained in 4 different slides from different donors. The cells of each donor were divided in groups of 200 in order of acquisition, so they were relatively close to each other in the slide. The distributions

for each group of 200 cells were plotted using box plots and compared to each other. Then, the mean for the FITC intensity of the first Gaussian (non-damaged subpopulation) and the percentage of positive cells (TUNEL (%)) were calculated by the mixed model for each subgroup of 200 cells.

We also investigated if increasing the number of cells, the % of TUNEL positive cells (TUNEL (%)) varied in order to stablish the minimum number of cells required for the mixed model to obtain a reliable result. The TUNEL (%) was calculated with 200, 400 and 600 cells in 4 donors.

3.3.7 Statistics

The measurement error for the TUNEL assay was calculated within sperm donor sample replicates in different forms as Bland and Altman described (Bland and Altman, 1996):

CV (%) = SD/Average

The agreement between two methods was studied by the Bland-Altman test (average of the measurement for both methods against the difference between the measurements for both methods). And the bias compute by the SD was studied.

The correlation was calculated by the Pearson r and R square coefficients

To analyse if the difference of the number of TUNEL-positive cells (TUNEL (%)) between different groups was statistically significant the non-parametric test of Mann-Whitney was employed if only two groups were compared and the Kruskal-Wallis

alongside the post-hoc of Dunn’s multiple comparison test if more than two groups were compared.

To analyse if the damage inductors increased significantly the percentage of positive cells for TUNEL the Chi-squared 2-sided test was performed.

3.4 RESULTS

3.4.1 TUNEL assay

3.4.1.1 Mounting assessment

Clearium, DPX and Eukitt exhibited higher intensities for the negative controls, while Fluoromount, Permafluor and Fluoroshield were closer to background levels, Fluoroshield being the closest (**Fig 3.3.A**). The largest dynamic detection range for stained cells corresponded to those slides mounted with Fluoroshield (**Fig 3.3.B**).

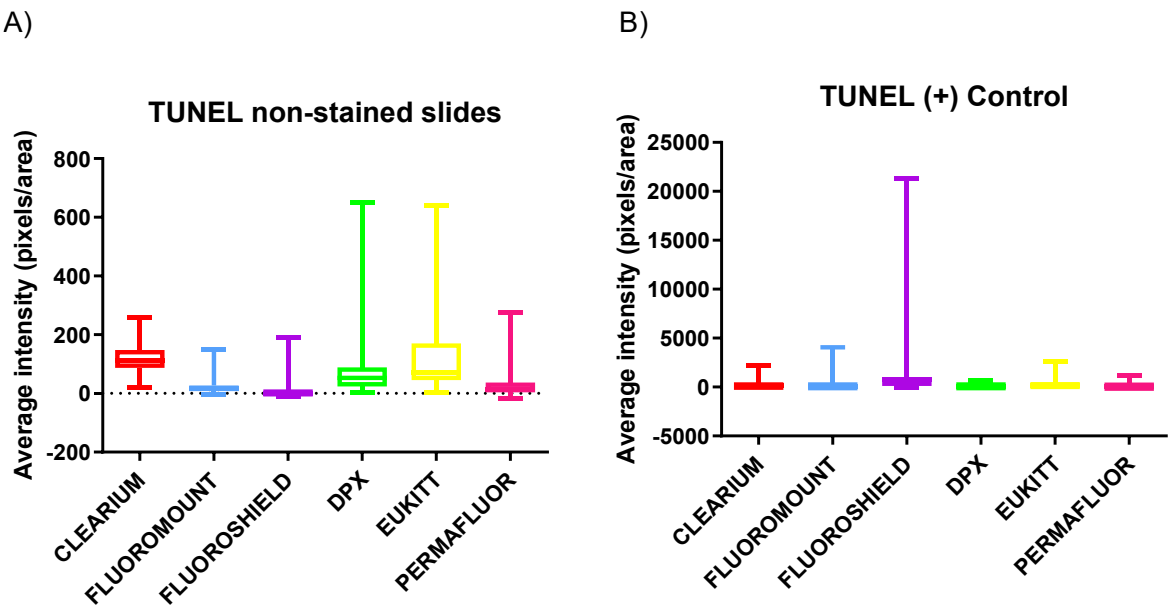

Figure 3.3 Intensity range for different mounting solutions. A. FITC Intensities for non-stained cells using the six different mountants. 1662 cells from three different donors were scored**. B.** FITC Intensities for 1909 cells treated with H_2O_2 from same donors.

In order to test the photoconversion between DAPI and FITC when using different mountants, the slides were stained with the TUNEL assay and the DAPI counterstain

were exposed for a period of 10 minutes to DAPI excitation light (350 ± 25nm) and switched to FITC excitation light (455 ± 25 nm) so an image of the FITC emission was taken every 10 seconds. The strongest photo-conversion occurred in Fluoromount slides; after exposing samples to 10 seconds of DAPI excitation (350 nm) wavelength, the FITC intensity increased almost 850 % with Fluoromount, 300 % with Eukitt and Clearium, 80 % with DPX, and 40 % with Fluoroshield (**Figure 3.4**). After 1 min the FITC intensity of the slides mounted with Fluoroshield was found to be stable when a 70 % -80 % increase was reached.

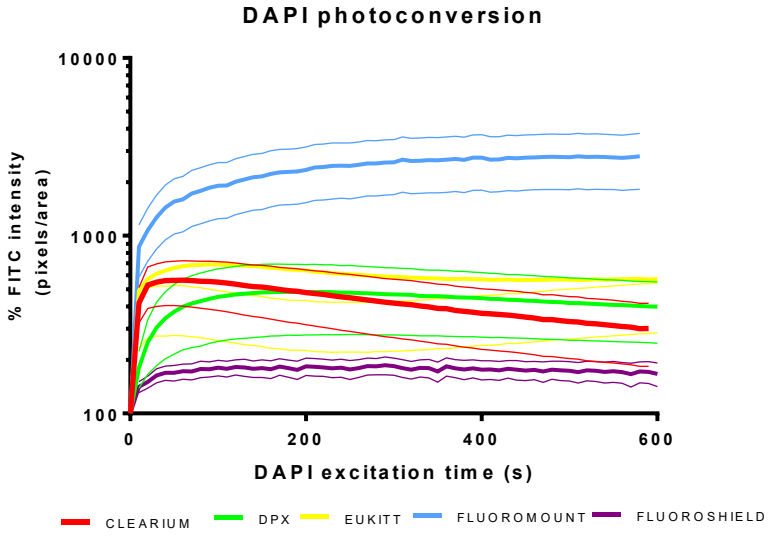

Figure 3.4 DAPI photoconversion curve for different mountants in the TUNEL assay.

In total 79 cells from three donors stained with DAPI and FITC and mounted with different solutions showed the greater photoconversion effect for Fluoromount and the lowest for Fluoroshield.

The magnitude of photobleaching was also tested with new smeared slides and also stained with the TUNEL assay and the DAPI counterstaining. After exposing the cells to FITC excitation wavelength the initial intensity was reduced in 15 - 25% after ten seconds exposure, and in more than 80 % irrespectively of the mountant used. Fluoroshield bleached the fastest and Clearium the slowest (**Figure 3.5**).

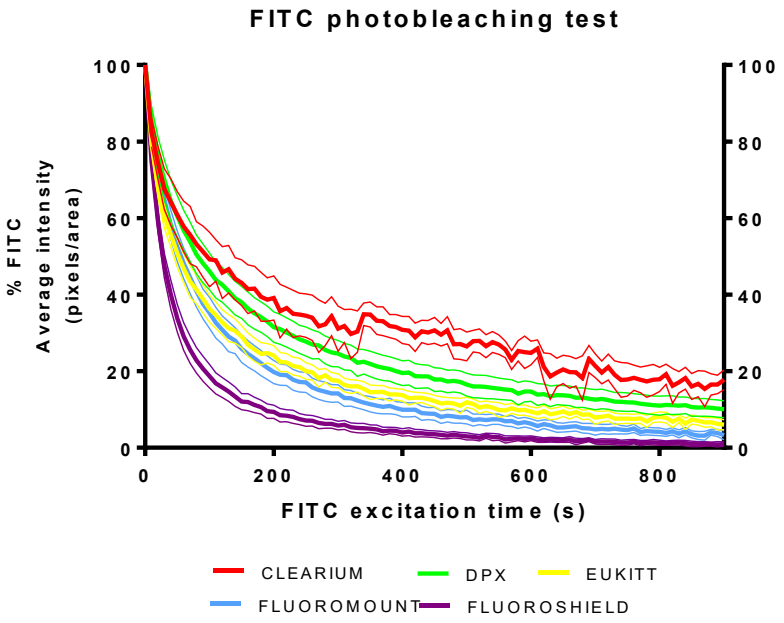

Figure 3.5 FITC photobleaching test. 78 cells from three different donors were continuously exposed to the FITC exaltation light (450 / 50) and FITC emission was tracked every ten seconds for ten minutes.

3.4.1.2 TUNEL assay validation with positive (samples exposed to DNA-damage inductors) and negative controls

Initially, negative and positive controls were performed using 3 donor samples and compared to their respective baseline levels (**Figure 3.6**). For positive controls DNase was used in 3 U / ml concentration during one hour and for negative controls only the label solution was used in absence of the enzyme in order to study non-specific fluorescence. In addition, the level of auto-fluorescence of the sperm cells was studied by omitting the addition of the TUNEL labelled solution and the TdT enzyme but adding the DAPI dye. The three donors had similar levels of auto-fluorescence and non-

specific fluorescence but different baseline damage and also different increase of damage by using DNase (**Table 3.2**).

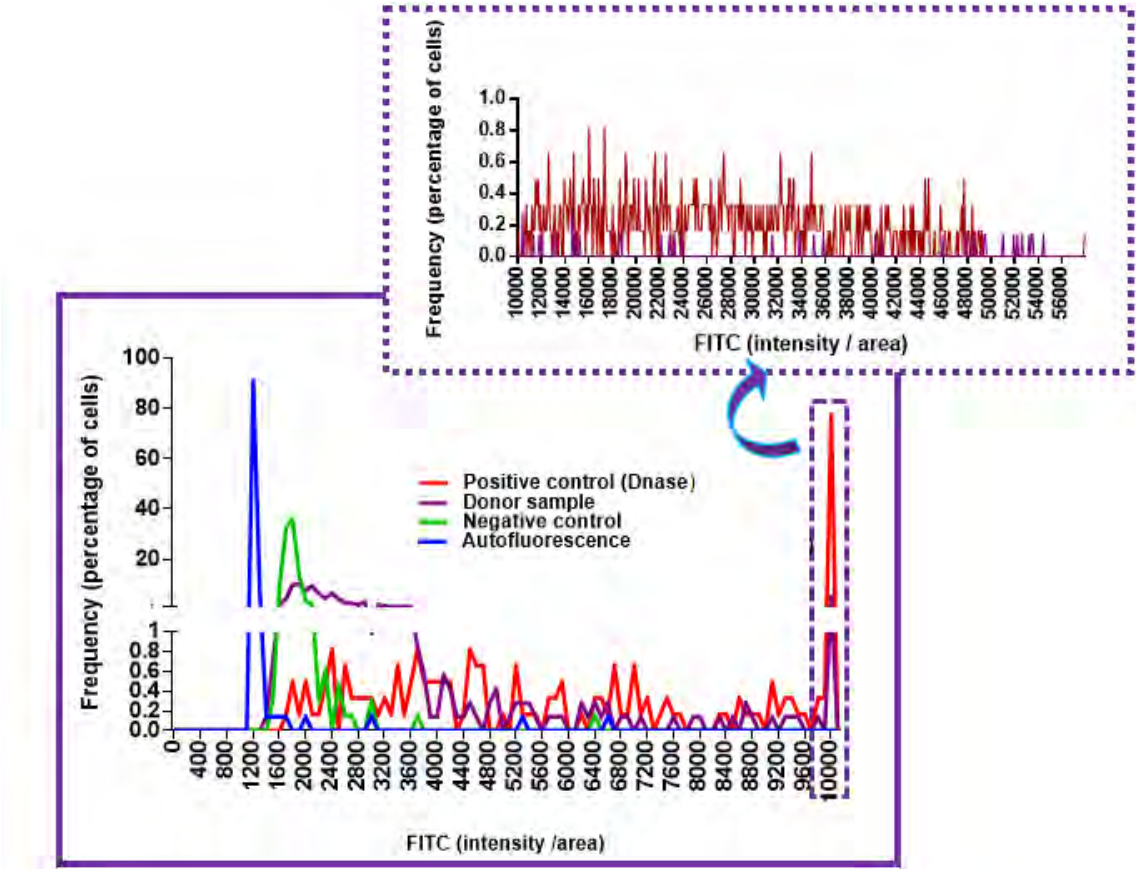

Figure 3.6 Histogram for single-cell FITC average intensities for auto-fluorescence, baseline, positive and negative controls from Donor A. 99 % of 700 cells single-stained cells with DAPI showed a FITC auto-fluorescence intensity between 1200 and 1300 (blue line). 95 % of 648 stained cells with DAPI and labelling solution in the absence of TdT enzyme showed an unspecific FITC fluorescence between 1600 and 2000 (green line). The cells stained with the normal TUNEL protocol and DAPI, showed a wide range of FITC intensities from 1200 to 50000 (purple line). The addition of DNase (3 U / ml) to sperm cells shifted the histogram to the right, as approximately 80 % of the cells showed a FITC average intensity greater than 10000 (red peak enclosed with the dotted line). The frequency of cells with FITC average intensity greater than 10000 is shown in the upper histogram enclosed with the dotted line. As in the rest of the chapter, the FITC intensities showed on the X-axis are the average of intensities (arb.units) per head area (µm).

DONOR	AUTO-FLUORESCENCE	NEGATIVE CONTROL	SAMPLE	POSITIVE CONTROLS
A	**1231 ± 269**	**1796 ± 246**	**4417 ± 7802**	**22221 ± 12895**
C	**1247 ± 75.04**	**1605 ± 231.5**	**3258 ± 2754**	**8675 ± 8562**
D	**1662 ± 128**	**1752 ± 333**	**5719 ± 7171**	**26111 ± 7747**

Table 3.2 Measurements of intensity for the auto-fluorescent, for the negative and positive controls and also baseline in donor samples. The intensity levels were measured by the average of intensity (arb. units) and the size of the sperm heads (μm). The results are expressed in average and standard deviation (average ± SD) for the whole sperm population.

3.4.2 TUNEL scorings

3.4.2.1 TUNEL visual scorings

The visualization under the microscope using the system and filters described in Material and Methods section (3.3.3) of sperm cells stained with the TUNEL protocol (3.3.2) resulted in bright green cells (TUNEL-positive cells) and dim green cells (TUNEL-negative cells) (**Figure 3.7**). However, it was difficult to classify some cells as positive or negative due to the broad spectrum of intensities which made the assay dependant on the operator personal judgment and vision acuity. On the other hand, all cells showed similar DAPI intensities (blue).

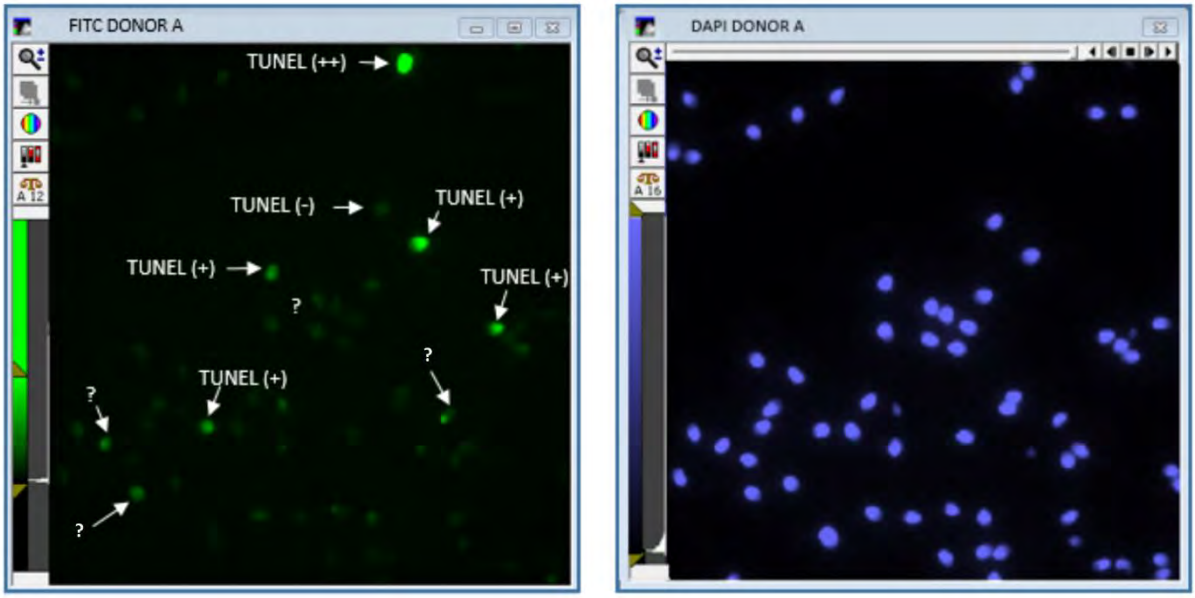

Figure 3.7 Intensity ranges for FITC and DAPI staining from the TUNEL assay with cells from Donor A. A very broad FITC intensities was obtained (left panel) while the DAPI intensity was similar between the cells (right panel). In some cases, the FITC intensity was very bright (TUNEL (++)), while in others was less bright (TUNEL (+)) or not bright at all (TUNEL (-)). There were also cells difficult to classify as TUNEL positive or negative (marked with question mark in the figure).

3.4.2.2 Quantitative intensity analysis method

Visual vs Semi-automatic acquisition combined with gating scoring methods

The traditional visual analysis (3.3.3.1) was compared with the manual gating method (3.3.3.2.3) based on the FITC intensity distribution extracted from the acquired grey-scale images. A total of 559 sample patients were assessed by both methods, the visual (A) and the gating (B) method, showing significant disparities for some of the samples when comparing the results distribution and correlation by both methods (**Figure 3.8**). An average bias of - 6.63 between the two methods was computed by the Bland-Altman analysis (**Figure 3.9)** and the detailed analysis of the graph showed that the percentages of damage obtained by the visual analysis were generally lower

than for the gating method, especially when average damage was between 0 % and 35% damage. The samples with greater difference of damage between the two methods generally had an average of damage greater than 25 % (**Figure 3.13**).

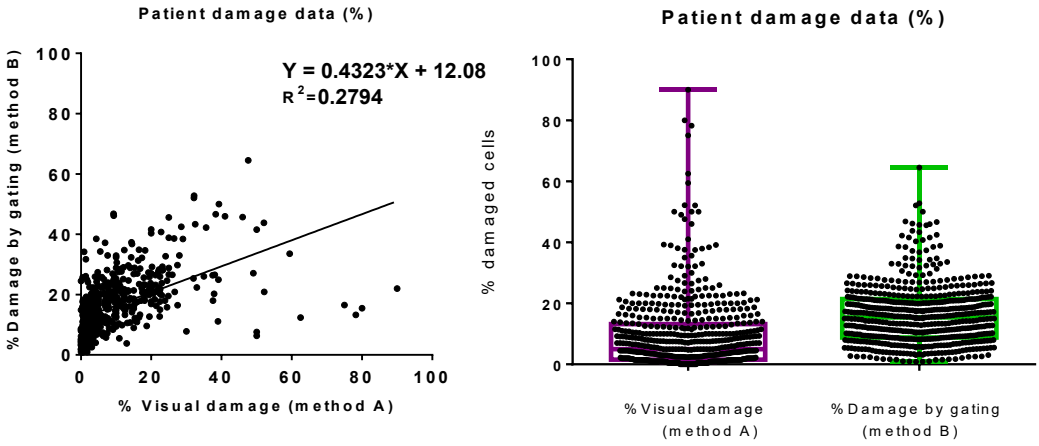

Figure 3.8 Correlation and distribution for the visual and gating scoring methods. The correlation between both methods was not very high (R^2 = 0.2794) (left graph) and the distribution for the same samples (559) was different for each method (right graph). Box plots show all the data points and the median.

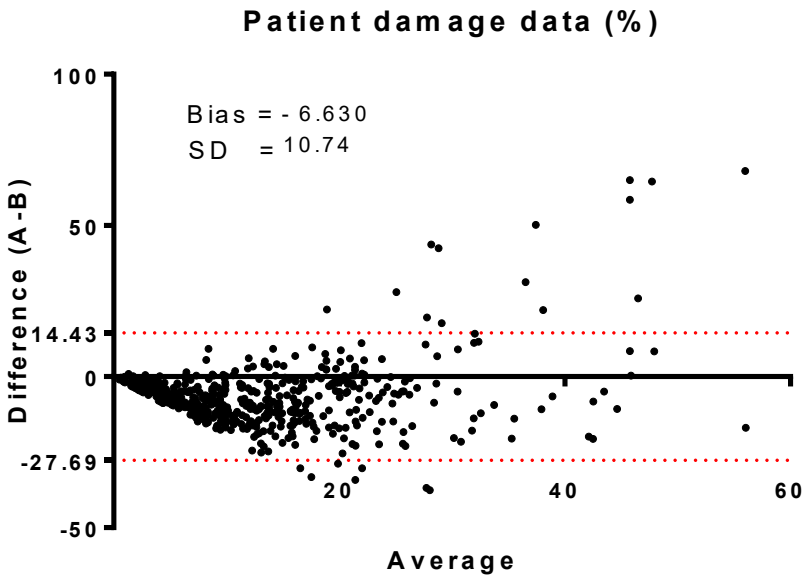

Figure 3.9 Bland-Altman analysis for the visual (A) and the gating scoring methods.

There was an average bias of - 6.63 between the two methods for 559 patient samples and the difference between both methods was between - 27.7 (%) and 14.4 (%) in 95 % of the observations. Generally, the samples which difference by the two methods was greater than the confidence interval (- 27.69 to 14.43) had an average percentage of damage superior to 25 %. 95 % interval confidence is shown in red dotted lines.

Mixed Gaussian model as an alternative for the gating method

The Cullen and Frey graph based on the skewness and kurtosis of the samples showed most likely a Beta distribution for both, low and high damage samples (**Figure 3.10)**. But, when looking into detail the Q-Q plots, the Beta distribution failed to fit correctly the centre (Q-Q plots in **Figure 3.11**) but also the right tails of the distribution (P-P plots in **Figure 3.11)** which is very important for determining the extension of the damage, especially for the low-damage sample. Therefore, a new strategy based on clustering with mixed distributions was studied. Two Gaussian equations were drawn based on the single-cell FICT intensity data using the Mclust package in the R software (**Figure 3.12**). The left Gaussian, with lower FITC intensity mean (blue line in **Figure**

3.12), was generated with the cells with lower FITC intensity (non-damaged cells) while the Gaussian with higher FITC intensity (red line in **Figure 3.12**) mean, was generated with the cells with higher FITC intensity (DNA-damaged cells). The percentage of TUNEL positive cells (TUNEL (%)) was computed by calculating the number of cells inside the right Gaussian corresponded to the damaged cells. The distance between the two Gaussians, indicates the degree of damage of the cells inside the right Gaussian. However, to simplify, we only calculated the percentage of positive cells (TUNEL (%)) in a sample, and not the degree of positivity of them in this chapter.

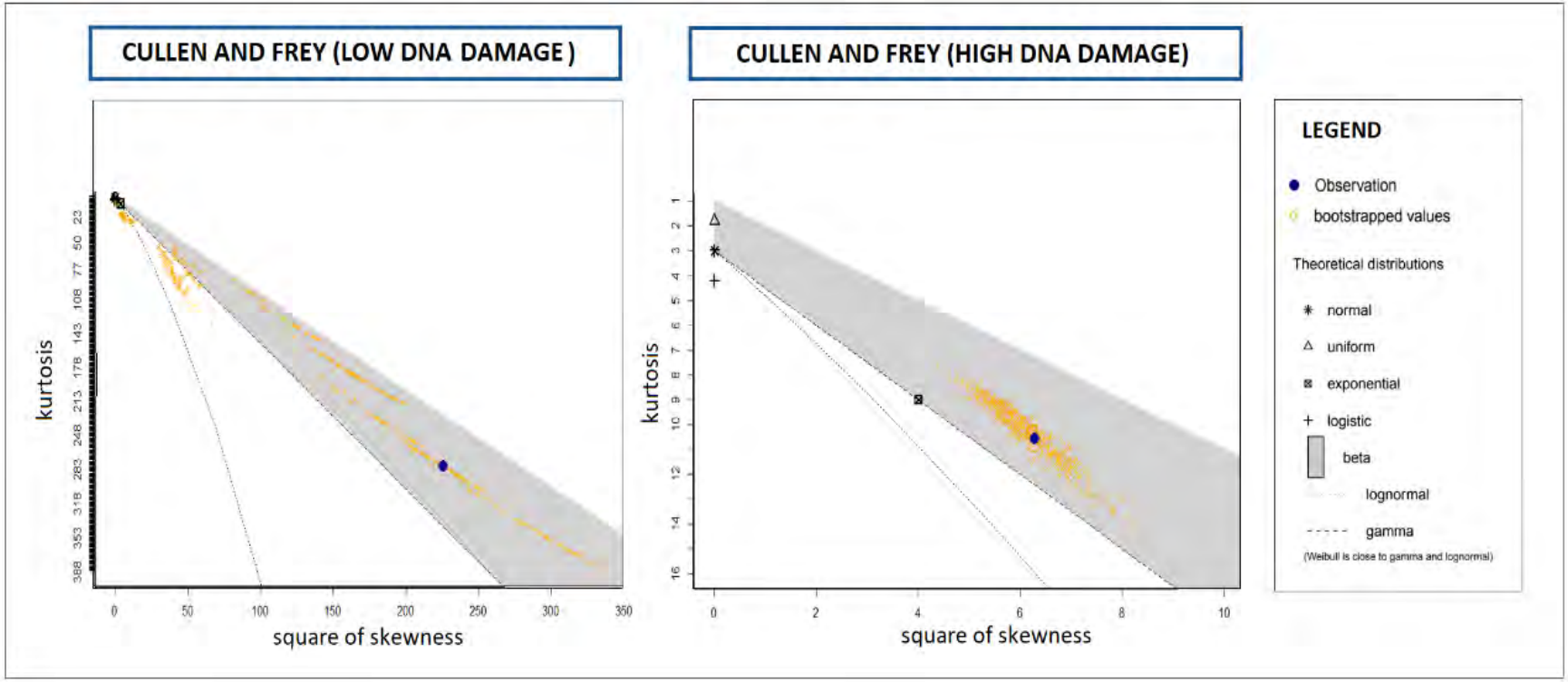

Figure 3.10 Cullen and Grey graph for the assessment of the goodness-of-fit for different types of distributions. The Beta distribution had the best fit for two low (left) and high (right) damage samples.

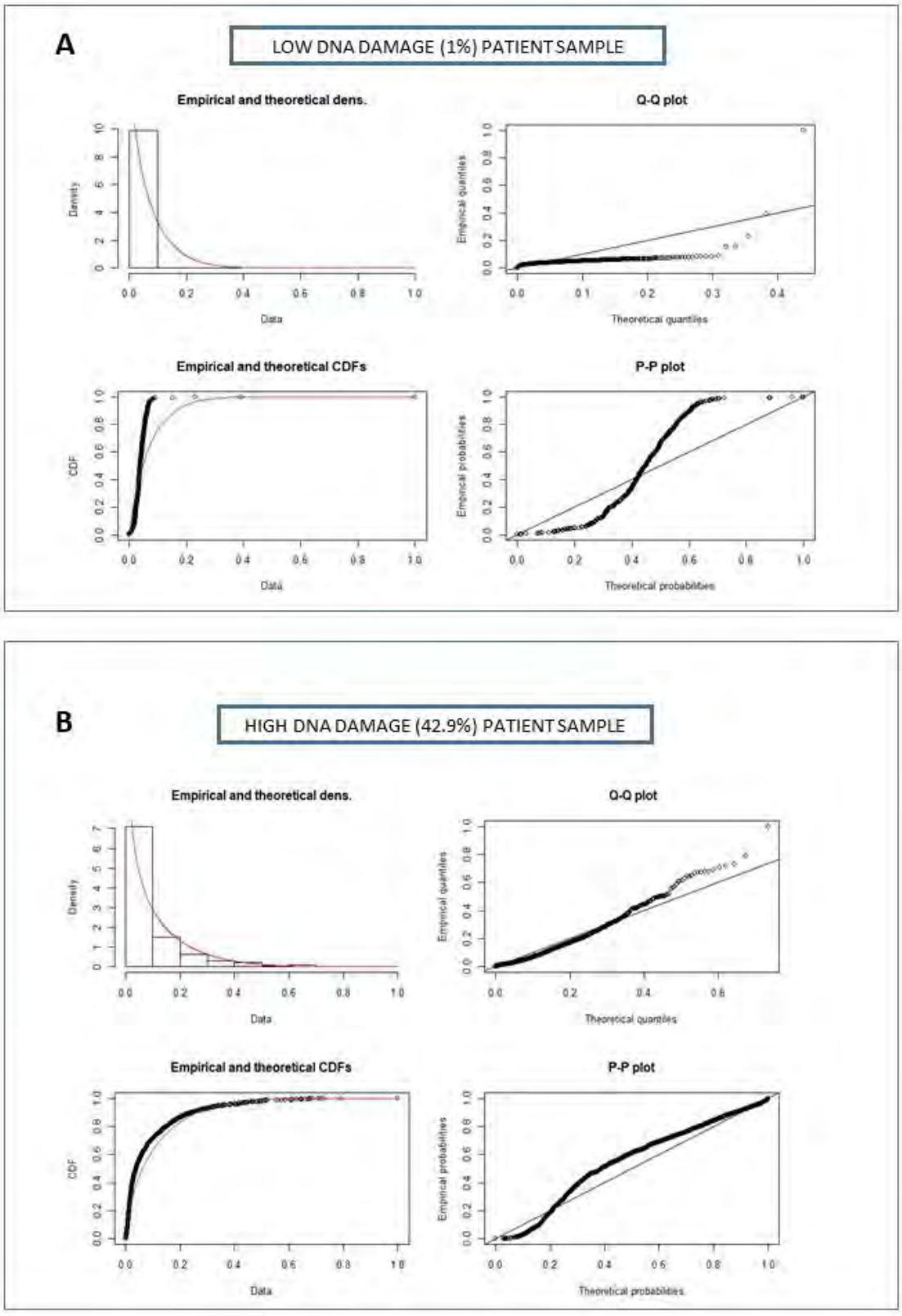

Figure 3.11 Study of the fit of a Beta distribution for our FITC single-cell intensity data when low and high DNA damage measured by (TUNEL (%). The basic goodness-of-fits plots such as the density, the CDF, the Q-Q and the P-P plots are shown for a low-damaged

(**A**) and high–damaged samples (**B**). There is a lack of fit at the tails (Q-Q plots) and at the centre of the distribution (P-P plots), specially for the low-damaged sample (**A**).

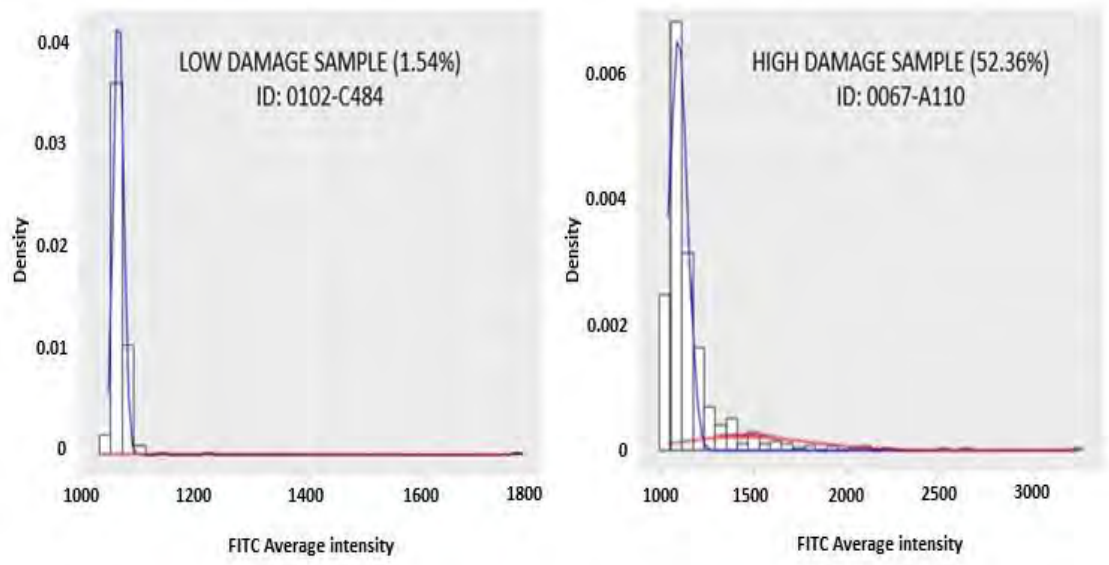

Figure 3.12 Gaussian mixed model for low and high DNA damage samples. The blue curve corresponds to the Gaussian with lower mean for the FITC Average Intensity (non-damaged subpopulation) and the red curve to the Gaussian with higher mean (damaged subpopulation). The samples with lower damage (A) have lower density of cells inside the red Gaussian, while higher damage samples (B) have more cells inside the red curve. Moreover, apart from calculating the percentage of damaged cells (percentage of cells inside the red Gaussian), the difference between the means of the two Gaussians indicates the degree of damage for the damaged cells; the more displaced to the right on the X-axis the more damage the cells present inside the red Gaussian.

3.4.2.3 Comparison between the gating and the Gaussian mixed model scoring methods

The comparison between the gating and the Gaussian methods using the data of 582 patients showed a good correlation and agreement (**Figure 3.13**). The coefficient of correlation was R^2 = 0.7305 and the bias for the agreement for both methods was -0.8398. However, if a clinical threshold of TUNEL (%) = 20 (based on publications) is applied for performing the clinical classification in low or high damage, 9 % or 4 % of the patients did not agree in the clinical classification giving by both methods.

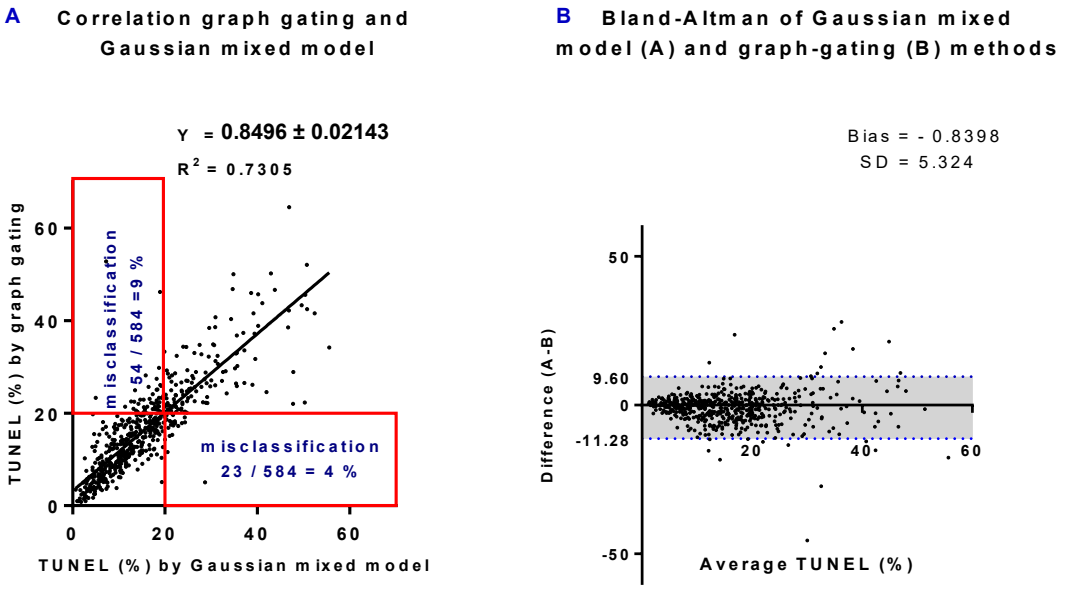

Figure 3.13 Correlation and Bland-Altman analysis for the TUNEL (%) obtained with the graph-gating and the Gaussian mixed model for 582 HABSelect patient samples.

There was a good correlation between both methods (R^2 = 0.7305) (**A**). The agreement with both methods was also good as the bias was - 0.8398 and the 95 % limits of agreement was quite narrow (from - 11.28 to 9.60) as shown by the grey shadowed area in the Bland-Atman plot (**B**). Considering 20 % of TUNEL positive cells as a clinical threshold for high or low damage, 9 % or 4 % of the patients did not agree in the clinical classification giving by both methods, they would be false positives or negatives (**A**).

3.4.3 Consistency of the TUNEL assay coupled to the semi-automatic acquisition system: intra-assay coefficient of variance

The TUNEL assay variability was studied by the Coefficient of Variance (CV (%)) for both the gating and the mixed model method with eight fresh (**Table 3.3)** and eight thawed semen samples (**Table 3.4**) from three donors (A, B and D). The mixed model exhibited similar coefficient of variance (CV (%)) for the gating and mixed model methods for the fresh (13 %), while for the frozen samples the mixed model exhibited higher CV (%) compared to the mixed model (23 % vs 13 %) (**Table 3.5**)

DONOR	*METHOD*	*BASELINE RESULTS*						
		A1	A2	AVERAGE	ACCEPTANCE (WHO)	|A1-A2|	SD	CV%
Donor A 230617	MM	14.99	25.79	20.39	8	10.8	7.63	37.44
	GATING	15.28	26.12	20.7	8	10.84	7.67	37.06
Donor A 290617	MM	15.93	10.88	13.4	7	5.05	3.57	26.63
	GATING	15.93	10.24	13.08	7	5.69	4.02	30.74
Donor A 060717	MM	11.10	8.77	9.93	6	2.33	1.64	16.55
	GATING	11.10	9.55	10.32	6	1.55	1.09	10.58
Donor B 130617	MM	12.27	9.35	10.81	6	2.92	2.06	19.08
	GATING	14.72	12.95	13.83	7	1.77	1.25	9.05
Donor B 150617	MM	8.80	8.94	8.87	6	0.14	0.1	1.12
	GATING	9.29	10.28	9.79	6	0.99	0.7	7.12
Donor B 230617	MM	16.48	8.8	12.64	7	7.68	5.43	42.95
	GATING	12.82	16.1	14.46	7	3.28	2.32	16.08
Donor D 210617	MM	5.72	5.72	5.72	5	0.00	0.00	0.06
	GATING	7.51	6.83	7.17	5	0.68	0.49	6.77
Donor D 230617	MM	16.26	4.25	10.25	6	12.01	8.49	82.85
	GATING	12.81	6.13	9.47	6	6.68	4.72	49.86

Table 3.3 Variability among replicates for fresh semen samples with the two TUNEL analysis methods, the mixed model (MM) and the gating model.

The A1, A2 and average columns are expressed in % of damage. Samples that exhibited a difference between duplicates not accepted according WHO (WHO, 2010a) are shown in orange

DONOR ID	*METHOD*	*F-T RESULTS*						
		A1	**A2**	**AVERAGE**	**ACCEPTANCE (WHO)**	**A1-A2**	**SD**	**CV%**
Donor A 230617	MM	10.68	10.18	10.43	6	0.5	0.35	3.39
	GATING	6.30	8.35	7.33	5	-2.05	1.45	19.74
Donor A 290617	MM	7.13	14.83	10.98	6	**-7.7**	5.45	49.63
	GATING	16.18	14.25	15.22	7	1.93	1.36	8.97
Donor A 060717	MM	12.02	10.93	11.48	6	1.09	0.77	6.73
	GATING	15.43	11.54	13.48	7	3.89	2.75	20.41
Donor B 130617	MM	11.98	12.14	12.06	7	-0.16	0.11	0.94
	GATING	12.77	12.32	12.55	7	0.45	0.32	2.55
Donor B 150617	MM	12.78	19.00	15.89	7	-6.22	4.39	27.65
	GATING	10.25	9.15	9.70	6	1.1	0.78	8.01
Donor D 130617	MM	8.91	7.90	8.41	6	1.01	0.71	8.48
	GATING	7.92	10.42	9.17	6	-2.5	1.76	19.25
Donor D 210617	MM	5.89	10.96	8.43	6	-4.98	3.59	42.58
	GATING	7.76	10.31	9.04	6	-2.55	1.80	19.90
Donor D 230617	MM	4.64	1.61	3.12	4	3.03	2.14	68.59
	GATING	4.86	10.29	7.57	5	**-5.43**	3.84	50.73

Table 3.4 Variability among replicates for frozen-thawed semen samples with the two TUNEL analysis methods, the mixed model (MM) and the gating model. The A1, A2 and average columns are expressed in % of damage. Samples that exhibited a difference between duplicates not accepted according WHO (WHO, 2010a) are shown in orange.

SUMMARY	*MIXED MODEL*	*GATING METHOD*
Average CV (%) fresh samples	28.34	20.90
Average CV (%) fresh samples *	12.68	13.39
Average CV (%) thawed samples	24.12	18.69
Average CV (%) thawed samples*	22.62	12.79

Table 3.5 Summary table for the CV (%) results for the Mixed Model (MM) and Gating methods. The gating method offered slightly less variability than the mixed model method for the fresh and frozen-thawed samples. The (*) symbol is for the CV (%) calculation after discarding those samples whose difference in TUNEL (%) in duplicates was not accepted according to WHO (WHO, 2010a).

3.4.4 TUNEL assay optimisation

3.4.4.1 Study of the staining homogeneity

We observed the occasional disruption of the baseline FITC intensity when analysing TUNEL data (**Figure 3.14)**. The degree of homogeneity for the staining was studied in four samples by making subgroups of 200 cells in the same order as they were initially acquired (**Figure 3.15**). The mean of the non-damage population and the percentage of damage after performing the clustering analysis with the mixed model were compared for each group. Two out of the four donors (donor A and donor D) showed different distribution between the different cell subgroups (0-200, 201-400 and 401-600) as it can be seen by the different boxes, however the median was very similar (**Figure 3.15 A**). After performing the clustering by the mixed model, the average intensity for the subpopulation non-damaged was very similar between cell groups (0 - 200, 201 - 400 and 401 - 600) for all the donors, including donor A and donor D (**Figure 3.15 B**), however the damaged cells had different weight in the different cell subgroups (0 - 200, 201 - 400 and 401 - 600), especially in donor A and D as it can be seen by the large error bars (**Figure 3.15 C)**

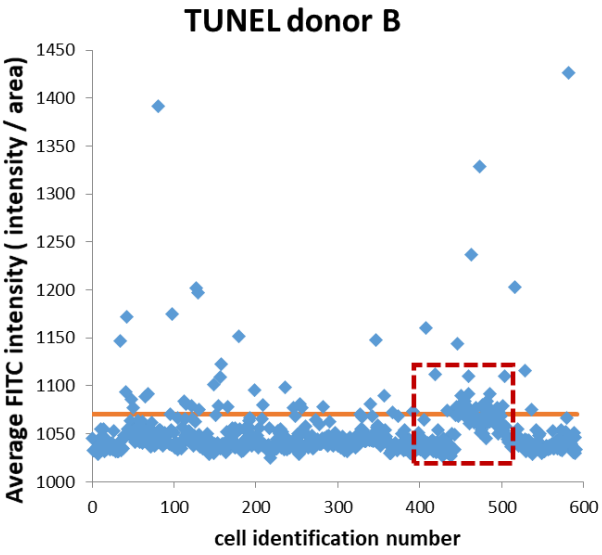

Figure 3.14. Non-homogenous staining found in the aliquot A2 of a donor sample. The cells of the graph are ordered in the X axis according to the field acquisition order. Closer cells in the x-axis belong to the same field or to the next field acquired, therefore the cells enclosed in the red-dotted line square belong to the same field that was most likely incorrectly stained.

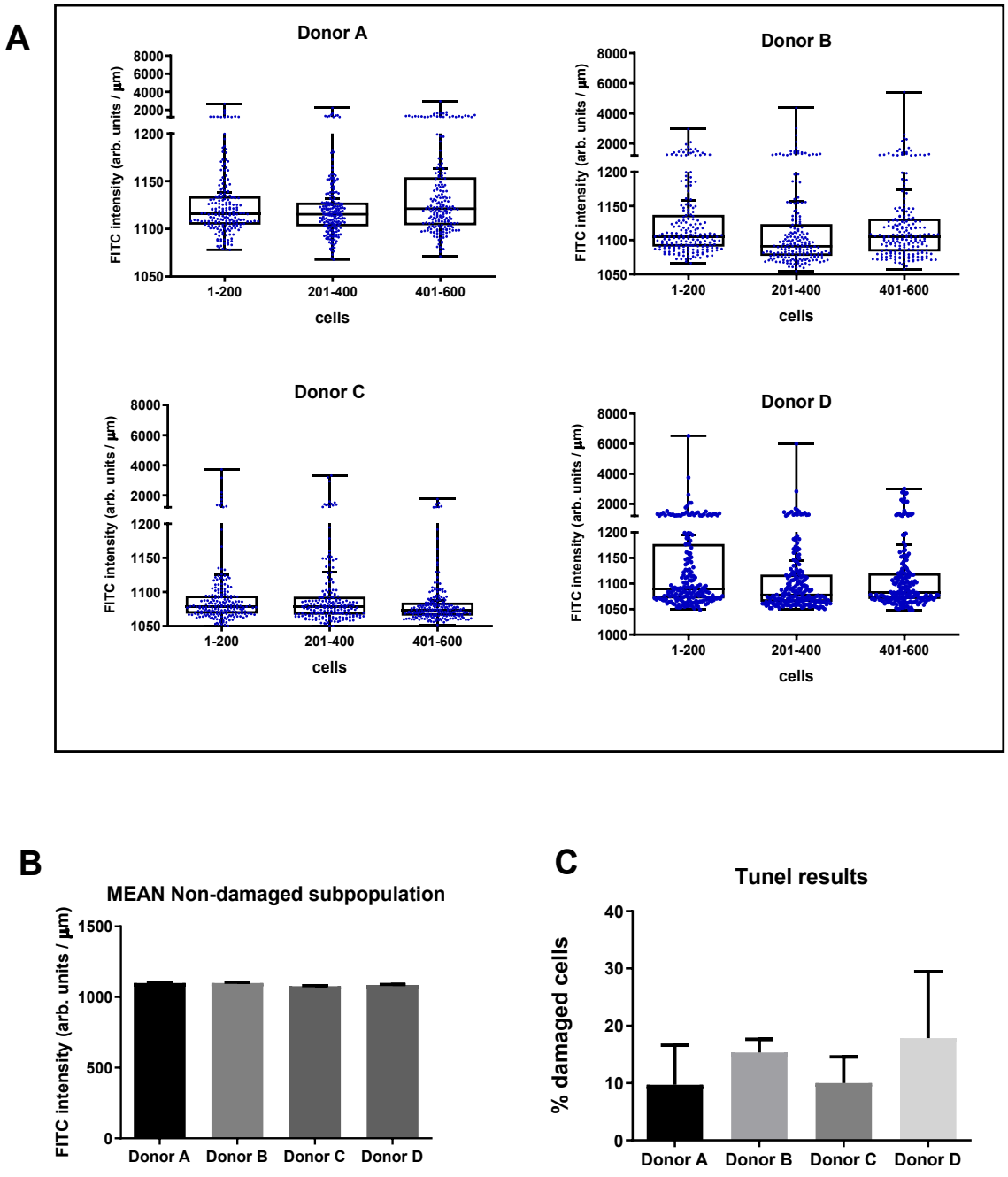

Figure 3.15 Study of the single-cell FITC intensity distribution, the mean of the non-damaged subpopulation and the percentage of positive TUNEL in groups of cells acquired subsequently and therefore close to each other in the slide. The distribution for each subgroup of 200 cells was similar for the four donors (A, B, C and D) **(A).** After doing the clustering analysis, the algorithm showed very similar mean for the non-damaged cells of the different cell subgroups of the 4 donors **(B).** However, the percentage of damaged cells was

very different between subgroups of cells for donor A and donor D as it is shown by the large error bars **(C)**.

3.4.4.2 Number of cells required for a reliable result

The percentage of damage was then calculated with 200, 400 and 600 cells for these same donors showing similar results for donors A, B and C, but different for donor D who decreased from 31 % to 16.5 % while for A, B and C the % of damage when increasing the number of cells analysed from 300 to 600 only changed in 3.3 %, 1.5 %, 3.1 % respectively (**Figure 3.16**).

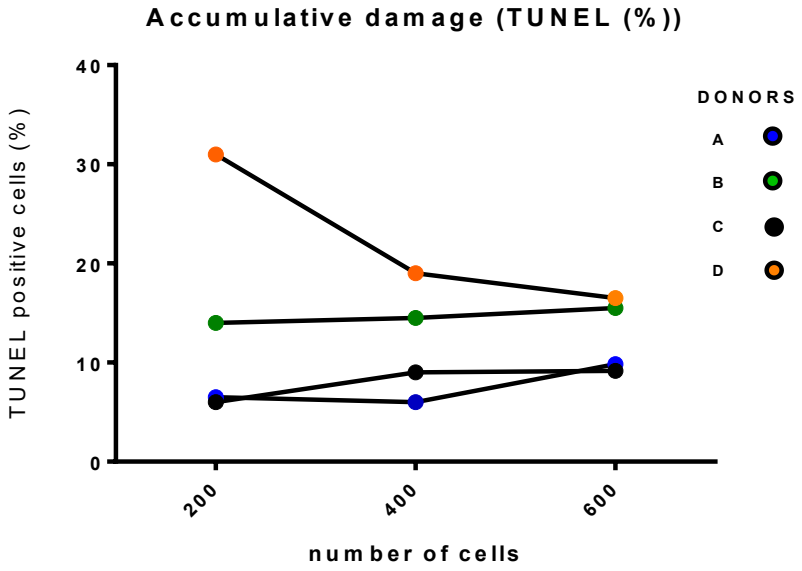

Figure 3.16 Effect of cell number in the quantification of damaged cells (%).

The TUNEL positive cells (%) in donors A, B and C did not experience important changes when accounting 200, 400 and 600 cells. However, donor D experienced a dramatically decreased in TUNEL positive cells (%) when accounting 400 cells instead of 200.

3.4.5 TUNEL results for donor and patient samples

3.4.5.1 Fresh donor semen and basic semen parameters

The basic semen parameters were studied in fresh semen in 4 donors. No strong correlation was found between the percentage of TUNEL positive cells (TUNEL (%)) scored by the semi-automatic acquisition system coupled to clustering methods based in a Gaussian mixed model algorithm (3.3.3.2) and the total count, and abstinence. But a small positive correlation was observed with the progressive motility (R^2 = 0.2459) and with the concentration (R^2 = 0.5102). The ejaculates collected from the same donor are shown with same colour (**Figure 3.17**).

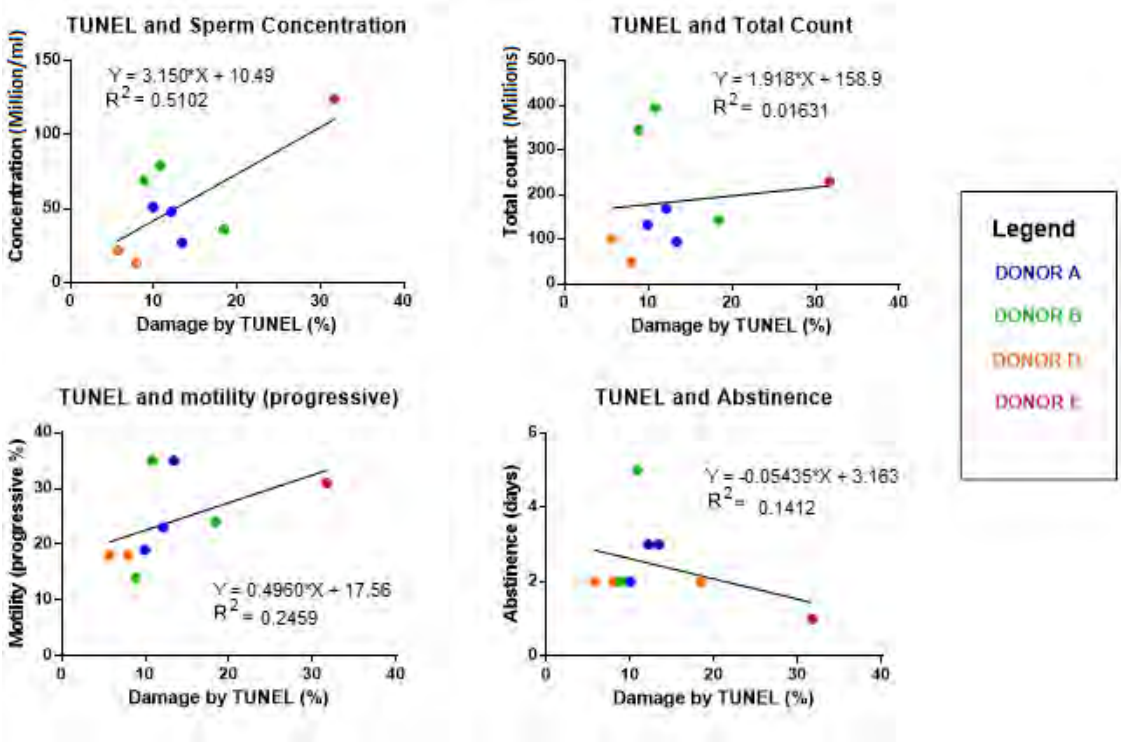

Figure 3.17 Correlation between the basic semen parameters in fresh semen and the TUNEL (%) in PBS-washed, fixed and stained with TUNEL sperm cells of nine samples of four donors. No correlation was observed between TUNEL (%) and the total count of cells (millions of cells) or with the days of abstinence. But small correlations were observed with the progressive motility (%) and the sperm concentration (millions of cells /ml).

The SDD according to the TUNEL assay was calculated with the semi-automatic acquisition system coupled to clustering methods based on Gaussian mixed model (3.3.3.2) in PBS - washed semen samples of five donors from different periods of time. The majority of the donors kept a constant level of damage (TUNEL (%)) across time with a difference lower than 6 % between ejaculates. Donor B (yellow in **Figure 3.18**) experienced the greatest variability between ejaculates in different periods of time (11 %, 9 % and 18 %), although such differences in the TUNEL (%) were always below a 10 % difference.

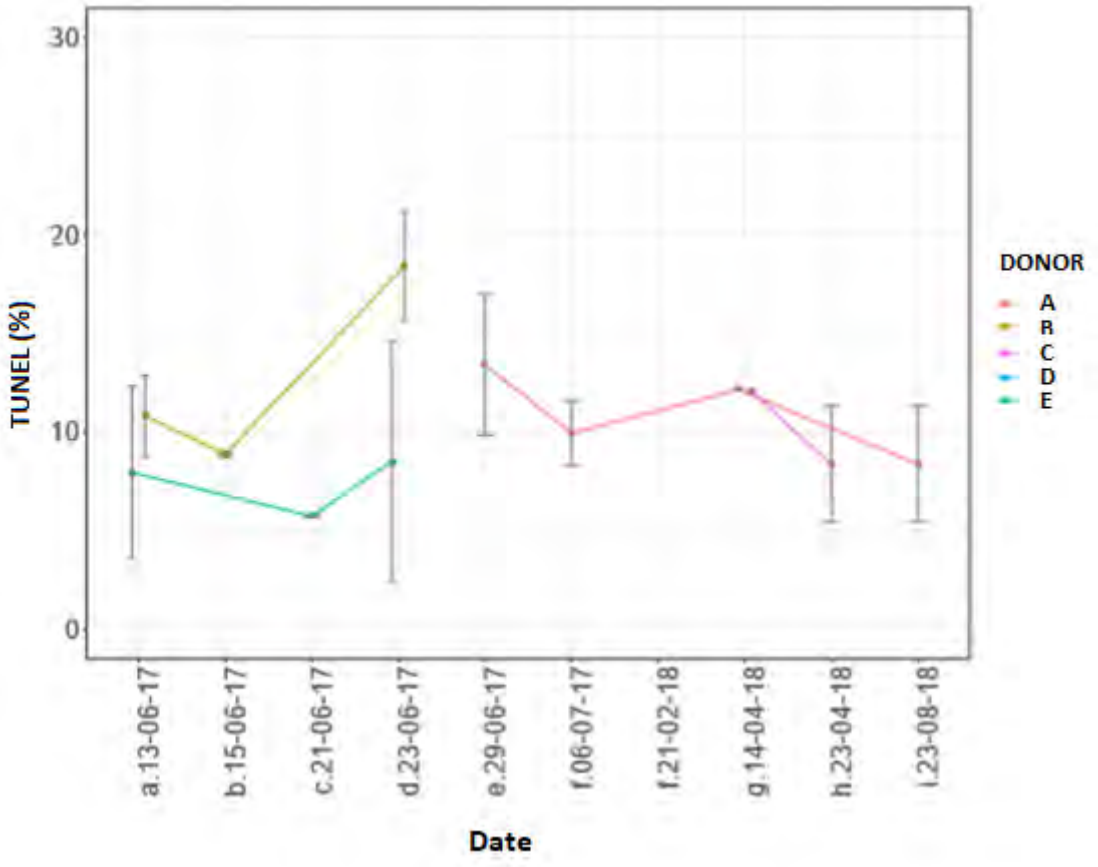

Figure 3.18 Levels of TUNEL positive cells (TUNEL (%)) in five donors across time.

The TUNEL (%) was scored with a semi-automatic acquisition system coupled to a clustering method based on Gaussian mixed models (3.3.3.2). For each ejaculate two smears (duplicates) were stained according the TUNEL protocol and scored with the system mention

and the clustering methods. The graph represents the means and standard deviation between the two duplicates.

3.4.5.2 Study of the induction of DNA damage by TUNEL in freezing sperm procedures

To investigate the possibility of damage induction by the freezing procedure in the patient samples from the HABSelect trial, we studied the levels of TUNEL (%) in PBS - washed fresh donor samples before and after the freezing procedure. Before freezing the samples, they were prepared by gradients and then frozen according to the protocol detailed in 3.3.1.2. However, the freezing procedure executed in the different clinics that participated in the HABSelect trial were based on internal protcols and small differences with our freezing protocol are expected. A total of eight samples from three different donors were investigated. The majority of the donors did not experience significative changes in the TUNEL (%) before and after the freezing procedure (**Figure 3.19**). One sample of donor B (green) experienced a greater increse in the TUNEL (%) after freezing (from 9 % to 16 % approximately) and one sample of donor A (red experienced a greater decrease after the freezing (from 14 % to 6 %), but the differences were in any case lower than 8 % (**Figure 3.19**).

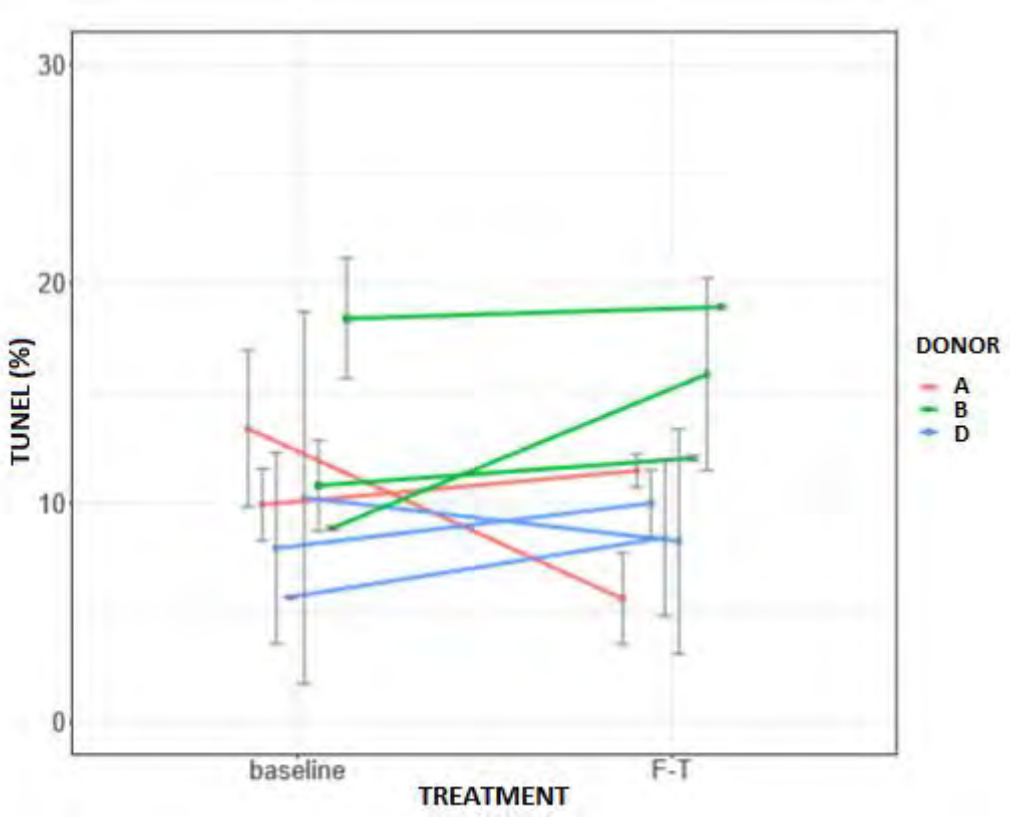

Figure 3.19 Levels of TUNEL positive cells (TUNEL (%)) in eight samples from three donors before and after freezing. The TUNEL (%) was scored with a semi-automatic acquisition system coupled to a clustering method based on Gaussian mixed models (3.3.3.2). For each ejaculate two smears (duplicates) were stained according the TUNEL protocol and scored with the system mention and the clustering methods. The graph represents the means and standard deviation between the two duplicates. There were no changes greater than 8 % after freezing.

3.4.5.3 TUNEL (%) in donors and patients comparison

The number of TUNEL positive cells (TUNEL (%)) was studied in15 donor samples, 616 HABSelect patients and six donor samples exposed to DNase.

The distribution of TUNEL (%) across donors, patients and donor exposed to DNase is shown in **Figure 3.20**. The HABSelect patients obtained a TUNEL (%) between zero and 50, with the majority of them (approximately 40 %) having a value between 10 and

15. On the other hand, donors did not have TUNEL (%) values greater than 20 %. DNase used as an inductor of DNA damage showed different efficiency in different donors as the TUNEL (%) values obtained varied from 35 to 100 damage.

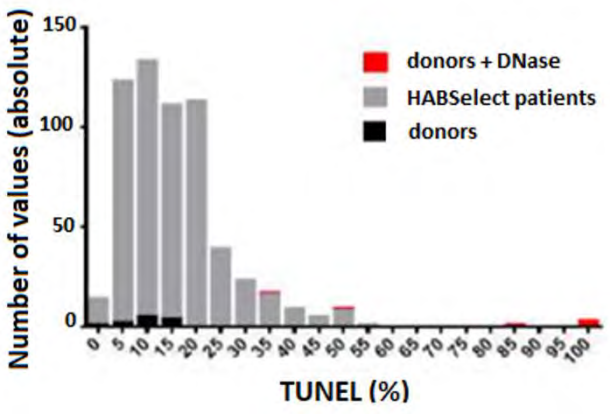

Figure 3.20 TUNEL (%) values across donors, patients from HABSelect and donors after being exposed to DNase treatment (3 U / mL for 1 h). 15 donor samples (black), 616 patients (grey) and six donor (red) samples exposed to DNase. The percentage of damage is represented against the absolute number of patients and donors

3.5 DISCUSSION

3.5.1 TUNEL assay

3.5.1.1 Mounting assessment

The validation of the mounting solution used is highly important as different mountants showed very different FITC intensity range and photo-conversion due to the DAPI dye which is often used as a counterstain with the TUNEL assay. Fluoroshield showed the best results but with the highest FITC photo-bleaching over a prolonged period of 15 min. However, during the first 10 seconds of exposure, which is reasonable time to focus and acquire a field, all the mountants showed a very similar decrease in the TUNEL intensity (between 15 % - 21 %). Nonetheless a possible alternative could be the use of different nuclear staining fluorophores such as Hoetch 33342. Hoetch 33342 showed some photo-conversion but in a lesser magnitude (Jez *et al.*, 2013). To our knowledge this is the first research done regarding mounting optimisation.

3.5.1.2 TUNEL assay validation with positive (samples exposed to DNA-damage inductors)

Samples exposed to DNase, which creates SSB and DSB, showed a high increase in their FITC intensity demonstrating the usefulness of the TUNEL assay for assessing DNA damage in the form of strand breaks. Not all sperm cells were damaged to the same extent, exhibiting different susceptibility across cells in the ejaculate and also across donors. The accessibility of chromatin is very important for the DNase action and therefore we used it dissolved in permeabilisation solution. Different species have shown different susceptibility to DNase treatment (Villani *et al.*, 2010). Similarly, it is

possible that human ejaculates contain sperm cells with different chromatin compaction that have different sensitivity to the DNAse effect. In the same way, the percentage of high and low compacted sperm cells can vary across males and therefore some people could be more resistant to the DNase effect than others.

3.5.2 TUNEL scorings

Different donors showed similar but different levels of sperm cell auto-fluorescence, baseline and negative control intensity. These small differences in the intensity levels between donors impair the use of an absolute threshold for counting positive cells as every sample should be independently analysed. On the other hand, the broad spectrum of FITC intensities encountered in the visual assessment of the TUNEL-stained sperm cells complicated the binary classification of the cells in TUNEL positive and negative. The new developed scoring method based on manual gating facilitated the binary classification of the cells but it had a relatively weak correlation with the visual assessment (R^2 = 0.2794). The TUNEL results obtained by the visual assessment were generally lower than the results obtained by the clustering method. In our opinion the human eye is not very efficient at discriminating between small differences in intensity levels or brightness and therefore it is likely the visual assessment underestimates the damage in comparison with the gating method.

However, this graph-gating method was still subjected to human decision based on the threshold to differentiate negative and positive cells which made the assessment both subjective and tedious. Therefore, scoring methods based on the relative intensity

distribution were studied. Because none of the single distributions (gamma, normal, lognormal, Beta) showed a good fit to the TUNEL intensity data we proposed the use of a mixed model to classify the cells in two subpopulations. The mixed distribution used was a mixed Gaussian distribution, although other combinations like Gaussian (for the non-damaged subpopulation) and Beta (for the damaged subpopulations) could also offer good results and therefore they should be studied and compared with the mixed Gaussian model in future. The Gaussian mixed model scoring method allowed the classification and quantification of DNA damaged cells in a reliable and consistent manner free from subjectivity and with a strong correlation (R^2 = 0.7305) and agreement (bias = -0.8398) with the graph-gating method. However, a clinical disagreement of 13 % of the patients was obtained after applying the most common clinical threshold found in the literature (20 %). This clinical threshold proposed in the literature was based on different staining sample preparation, staining protocols, and usually on flow cytometry analysis. Therefore, this clinical threshold should be revised in a reasonable number of patients and healthy donors using our new methodologies for staining and scoring before drawing final conclusions. In case of the clinical assignment to the wrong group of DNA damage (high or low), the first-line measures are addressed to reduce the levels ROS by enriching the diet in antioxidants or taking supplements (Lewis, S. E. *et al.*, 2013), neither of which could put at risk the health of the patient.

3.5.3 Consistency of the TUNEL assay coupled to the semi-automatic acquisition system: intra-assay coefficient of variance

After discarding those samples whose replicates had a difference in their TUNEL (%) not accepted according to WHO (WHO, 2010a), the CV (%) was very similar (approximately 13 (%) for both scoring methods; the mixed model and the graph-gating methods). For the frozen-thawed samples, the CV (%) was still 13 % when using the graph-gating method, but for the mixed model method the CV (%) was 23 %. However, for the accepted fresh and frozen-thawed samples, the differences between the TUNEL (%) obtained with the first replicate and with the average from the two replicates were in all the cases, and for the graph-gating and the mixed model, always below 5 %; Sharma *et al.* obtained a difference below 10 % in 90 % of the cases when comparing the first replicate TUNEL (%) result with the average result from the first and second replicates in 40 patients when using flow cytometry (Sharma, R. K., Sabanegh *et al.*, 2010).

3.5.4 TUNEL assay optimisation

The presence of FITC bright (damaged cells) and dim cells (non-damaged) should be uniformly distributed all over the slide if the TUNEL staining is correctly performed. However, in other staining and slide-based assays such as AO, glass imperfections on the surface of the slide have been described to provide different microenvironment conditions that affect the fluorescence emission of the dye (Evenson *et al.*, 1999). In our staining, the distribution of dim and bright cells looked homogenous under the microscope, although occasional clumps of cells or subareas of the slide looked

brighter under the microscope. These areas were not included into the TUNEL scoring as they were easily spotted in the single-cell intensity dot-plot. The evaluation of the homogeneity of the staining confirmed that occasionally some areas had a higher number of positive cells. The analysis of groups of 200 adjacent cells from different areas of the slide (3 areas in total) showed similar distribution in four donors. After applying the clustering method based on mixed models, the non-damaged population for different donors and areas of the slide was very similar, but the percentage of positive cells varied across donors and occasionally across areas of the slide for each donor confirming that the possibility of lack of homogeneity is possible. Therefore, the scoring should be performed within different areas of the slide and with a sufficient number of cells to minimise the lack of homogeneity and artefact fluorescence. 400 cells from two separated areas in the slide (200 + 200) are enough to give a reliable TUNEL (%) according to our results with four slides from different donor samples. The acceptance of the two counts should be assessed using the WHO recommendations for binomial assays (WHO, 2010a).

3.5.5 TUNEL results for donor and patient samples

3.5.5.1 Fresh donor semen and basic semen parameters

The influence of ejaculatory abstinence on semen quality, including DNA fragmentation, has been studied in the past with no conclusive results according to a recent literature review by Ayad *et al*. (Ayad *et al.*, 2018). If only the TUNEL assay is considered from the studies reviewed by Ayad *et al*., it seems there is actually a tendency among the studies to reach a negative correlation between abstinence and

SDD (Agarwal *et al.*, 2016, Sukprasert *et al.*, 2013). In our experiments we observed a very weak correlation between TUNEL (%) and the abstinence period (R^2 = 0.1412). However, all the donors with an abstinence period of 2 - 5 days had much lower TUNEL (%) than the donor who had only 24 h abstinence. In future, we should include more donors and study the effect of abstinence in periods longer than 48 h to ensure about the benefit of the ejaculatory abstinence in the decrease of the DNA fragmentation.

The correlation between SDD measured by the TUNEL and the basic semen parameters such as concentration and motility in neat semen vary across publications. In the case of the concentration, either no correlation (Lopes, S. *et al.*, 1998) or negative correlations (Ganzer *et al.*, 2017) have been observed in the literature, although the mechanisms leading to this decrease in sperm concentration are not clear. However, in our results we found a moderate correlation between TUNEL (%) and sperm concentration in the neat semen in donor samples (R^2= 0.5102). One of the possible causes for SDD is the maladjustment of the apoptosis; a defective apoptosis will lead to an increase in the number of sperm cells and defects in their DNA (McPherson, S. and Longo, 1993). Regarding motility, the lipid peroxidation caused by ROS such as H_2O_2 can lead to sperm motility impairment (Aitken, Gibb *et al.*, 2012, Jones *et al.*, 1979). However, we found a weak positive correlation between the TUNEL (%) and the sperm motility in neat semen from donors. Since we did not measure the amount of ROS in their semen it is possible that the SDD was not linked to ROS and actually was connected to apoptosis or deficient chromatin packing. The correlation of motility with apoptosis measured by assays such as Annexin V/PI (Ricci *et al.*, 2002) and chromatin compaction by assays such as Aniline Blue and CMA_3 (Kazerooni *et al.*,

2009, Lolis *et al.*, 1996, Nasr-Esfahani *et al.*, 2001) varies across publications and is not clear.

In any case, it has also been shown that a percentage of normal and motile sperm cells can be TUNEL positive (Avendano *et al.*, 2009).

Our study was carried out with the limited number of donors that were available in our hospital, and as the correlation was not very strong we recommend to repeat the study with a bigger sample set to ensure these results.

3.5.5.2 Evolution of the DNA damage scored by TUNEL across time in donors

All donors had similar values for the TUNEL assay in different periods with a difference no greater than 6 %. Only one donor, over the period of nine days, experienced differences in the TUNEL (%) up to 9 % in the different ejaculations. There is no published data regarding the variability or stability of TUNEL (%) across time. However, we know periods that coincide with infection that involve an increase in leukocytes that release ROS. Other external sources of ROS like tobacco, herbicides, radiotherapy and chemotherapy can increase SDD as explained in Chapter 1 (1.4.3.1) and therefore be reflected in a higher TUNEL (%).

3.5.5.3 Study of the induction of DNA damage by TUNEL in freezing sperm procedures

Sperm cryopreservation techniques are routinely used in ART, however they have shown to increase the sperm DNA damage (Zribi *et al.*, 2012).

Nevertheless, the protocols followed such as the cooling rates and cryoprotectants used varied across the clinicians. Recently, a new type of freezing kwons as vitrification has become more popular. Vitrification consists of the rapid cooling of water to a glassy state without intracellular ice crystalisation through an extreme elevation of its viscosity, with or without the use of non-permeable cryoprotectants (Aizpurua *et al.*, 2017). However, by using Spermfreeze as cryoprotectant, leaving the sample to equilibrate at RT for 10 min, and putting the sample into - 20 ºC prior its immersion in LN_2 we found no difference in the SDD measured by TUNEL (%) in donor samples before and after the cryopreservation. It should be noted these samples belonged to healthy donors and maybe different resistance to cryodamage is found in patients with altered semen parameters.

3.5.5.4 TUNEL in donors and patients comparison

Increasing evidence suggests that sperm DNA damage has a negative impact on male fertility potential as explained in chapter 1 (1.7). Infertile men tend to exhibit higher values of TUNEL (%) than healthy donors and men with proven fertility (Sergerie *et al.*, 2005, Sharma, R. K., Sabanegh *et al.*, 2010). In our research, donors exhibited lower TUNEL (%) than HABSelect patients; the TUNEL (%) values for donors were in the range of 0 and 19 %, while patients exhibited a wider range of values from 0 % to 54 %, although approximately 80 % of the patients had a value between 10 and 19%. These figures seems to be in agreement with the 20 % threshold set-up by most researchers to classify the damage in low and high (Sergerie *et al.*, 2005, Sharma, R. K. *et al.*, 2010, Sharma, R. K., Sabanegh *et al.*, 2010).

3.5.6 Conclusions

The SDD assessed by the TUNEL assay could provide an explanation for couples with unexplained infertility and serve as a guide towards a more personalised ART. Men with high values of TUNEL (%), if linked with high oxidative stress, should first be recommended to decrease their ROS levels; one possibility is the intake of antioxidants (Lewis, S. E. *et al.*, 2013). Based on current and previous research, ICSI has demonstrated to be able to by-pass the SDD and therefore it should be the elective treatment among IVF and IUI in case of high TUNEL values. However, there is still a risk of miscarriage according to publications which needs to be evaluated.

TUNEL and other SDD tests are not routine in the study of infertility mainly due to the lack of consistent protocols, reproducible results, clinical thresholds and expense. TUNEL has been demonstrated to effectively identify SDD, as shown by our positive controls, and to have a relatively low intra-assay variability (with a CV lower than 5 % between replicates) when using an optimal staining assay that includes a step for chromatin decompaction to allow the TdT enzyme to reach the DNA strand breaks in the nucleus and a suitable mounting solution that minimises the photobleaching and DAPI photoconversion. The count of 400 sperm cells from two different areas of a slide (200+200) in combination with a semi-automatic scoring system based on single-cell FITC intensity (or the fluorophore used in TUNEL assay kit) coupled with mathematical clustering methods ensures the reliability and reproducibility of the TUNEL results. Different laboratories would obtain same results when applying the same settings (gain and exposure for the illumination system) when analysing the SDD from the same slides (or ejaculates if same sample preparation protocol is followed).

The new modified developed method would not only allow the quantification of the positive or damaged cells in the ejaculate but also the degree of damage for each cell in a relative scale and the simultaneous study of the sperm morphology. The use of the new modified TUNEL staining slide-base protocol and the clustering scoring strategies described in this chapter seem a good method for the SDD evaluation in terms of consistency, objectivity and affordability

To summarise:

- The study of the mountant for TUNEL staining is key in order to get reliable results. Fluoroshield offered good results in terms of high dynamic range and prevention of DAPI photoconversion.
- DNase can be used as SDD inductor when used in washed and permeablised sperm cells prior TUNEL staining.
- TUNEL can be used in fresh and frozen-thawed samples with no increase in the SDD (%).
- TUNEL (%) is an independent parameter from the basic semen analysis parameters (motility and total count) and abstinence. But, it seems to moderately correlate with the concentration of healthy donor samples.
- Patient samples generally have higher TUNEL (%) than samples from healthy donors.
- The method developed in this chapter offers a robust and accurate measurement of TUNEL-positive cells superior to the traditional TUNEL visual

assessment in terms of objectivity and reproducibility (low intra-variability) when correctly calibrated and consistent excitation settings are used.

CHAPTER 4: Variability and inter-relationship between sperm DNA damage assays and analysis of the clinical relevance of sperm DNA damage

4.1 INTRODUCTION

This chapter investigates some of the main sources of variability that complicate the use of the TUNEL and SCSA/AO tests for DNA damage assessment in clinic. The relationship between the different SDD assays is also studied.

4.1.1 Sources of variability in DNA damage assay results

4.1.1.1 Types of DNA damage assay

Most authors consider DSB as the most deleterious type of damage for the future embryo as they are more difficult for the oocyte to repair (1.5.2). However, poorly compacted chromatin in mature sperm may break at many points during the journey to the oocyte overwhelming the DNA repair ability of the new embryo, especially if it is a low-quality oocyte. As such, the dual assessment of direct and indirect damage could increase the prediction of the clinical outcomes such as pregnancy, miscarriage and live birth.

As introduced in Chapter 1, SDD assays can detect both actual and potential DNA damage in mature sperm. The actual damage is detected and measured by direct SDD assays and the potential damage by indirect SDD assays.

DSB and SSB present in the mature sperm cells are considered as actual damage and they are measured by direct assays such as TUNEL and neutral Comet. Strand breaks usually originate during spermatogenesis or as a consequence of encountering high concentrations of Reactive Oxygen Species (ROS) during transit through the male reproductive tract (Chapter 1, 1.4.3). The TUNEL assay can identify and quantify SSB and DSB (Chen, J. *et al.*, 1997, Yamadori *et al.*, 1998) while the neutral Comet is thought to identify mostly DSB (Hughes *et al.*, 1997, Tarozzi *et al.*, 2007).

The acid labile sites in sperm DNA can turn into strand breaks during transit through the male and female reproductive tracts. Poorly compacted sperm chromatin can also experience breakage after exposure to ROS present in the reproductive tracts. This susceptibility to denaturation by pH changes and ROS can be measured by indirect assays such as AO. These breaks are usually SSB.

Results obtained by different DNA damage assays are therefore not equivalent and may be difficult to compare (Kirkman-Brown, J. C. and De Jonge, 2017, Lewis, S. E. *et al.*, 2013). Nevertheless, there are many other sources of variability when using a specific DNA damage test as explained below.

4.1.1.2 The nature of the sample: raw semen, prepared sperm or frozen semen

The recent meta-analysis published by Tan *et al*. (Tan *et al.*, 2018) on DNA damage and recurrent pregnancy loss can be used as evidence of sample preparation variability across laboratories. The meta-analysis includes TUNEL, SCSA, SCD and

comet assays. TUNEL assay publications variously used; washed and centrifuged sperm (Carlini *et al.*, 2017), washed sperm fixed in paraformaldehyde (Bareh *et al.*, 2016), sperm prepared by density centrifugation gradients (Coughlan *et al.*, 2015), frozen raw semen (Imam *et al.*, 2011) and frozen sperm previously fixed in acetic/methanol (Brahem *et al.*, 2011). SCSA was performed in three out of the fourteen studied included in Tan *et al.* meta-analysis; two used frozen raw semen (Carrell *et al.*, 2003, Kumar *et al.*, 2012) and one used frozen sperm previously diluted in TNE (Eisenberg *et al.*, 2017). Although the SCSA assay might have some variability across laboratories, it has a very well-defined protocol (Evenson, 2013b). Conversely, the TUNEL assay has many variations regarding the sample preparation as commented below and also regarding sample permeabilisation and the kit used for labelling the DNA as explained in Chapter 3.

4.1.1.2.1 Impact of sample freezing on DNA damage levels

The decrease in sperm motility and vitality seen after the freezing-thawing of raw semen and especially of prepared sperm by Percoll density centrifugation and swim-up has been linked to an increase in the amount of DNA damage as measured by alkaline comet (Donnelly *et al.*, 2001) and TUNEL (Thomson *et al.*, 2009, Zribi *et al.*, 2010). An increase in both oxidative stress measured by the 8-OHdG assay and sperm DNA damage after cryopreserving semen samples has been previously described (Thomson *et al.*, 2009, Zribi *et al.*, 2010). Therefore, the induction of oxidative stress rather than caspase activation and apoptosis has been suggested as the main cause of DNA damage induction during cryopreservation (Thomson *et al.*, 2009). It has been demonstrated that during the freezing procedure, the reduction of temperature during the process of semen cryopreservation can cause a significant increase in ROS

generation by sperm and leukocytes (Mazzilli *et al.*, 1995, Wang, A. W. *et al.*, 1997). The superoxide anion was identified as the major ROS produced by frozen-thawed stallion spermatozoa (Treulen *et al.*, 2019).

The amount of DNA damage induced also depends on the technique used for freezing and cryopreserving the sperm cells; for example, Riva *et a*l. found that an ultra-rapid freezing procedure combined with the addition of the cryoprotectant sucrose diminished the cryodamage calculated as % DFI by TUNEL when compared to a slow-freezing procedure (Riva *et al.*, 2018).

4.1.1.2.2 Impact of sperm selection by swim-up and density gradients centrifugation on DNA damage

Prior to IVF / ICSI treatment, semen samples are routinely prepared by swim-up and/or density gradients centrifugation (DGC). These procedures select sperm cells based on motility and morphology (Thijssen *et al.*, 2014) and when gentle centrifugation steps are used, they can also decrease the level of SDD (Younglai *et al.*, 2001). Jayaraman *et al.* showed that swim-up and / or DGC select sperm without DNA damage (Jayaraman *et al.*, 2012). Therefore, both the swim-up and DGC procedures improve the quality of the sample prior to fertility treatment.

Furthermore, the selection of sperm cells by techniques such as swim-up and Percoll gradients combined with the addition of substances to prevent oxidative stress have been suggested to diminish the cryodamage to the sperm sample (Donnelly *et al.*, 2001, Yang, C. *et al.*, 2019). Different laboratories use different procedures and antioxidants when freezing the sperm samples which contributes to the variability in

the sample preparation protocol and therefore to the results obtained by the DNA damage assays.

4.1.1.2.3 Flow cytometry *vs* fluorescence microscopy for the sperm DNA damage assessment

The AO / SCSA assays label all DNA with a fluorescent molecule (AO) whilst the TUNEL assay incorporates modified dUTPs at the DNA breaks; these modifications include fluorophores that can be directly detected by fluorescence or other haptens such as biotine or bromine that can be indirectly detected with streptavidin or antibodies respectively. However, the most common version of TUNEL uses nucleotides combined with a fluorophore which can be detected and quantified by either fluorescence microscopy or flow cytometry. Although generally a good correlation between fluorescence microscopy and flow cytometry results for the TUNEL assay is obtained, some differences can be found, especially if the calibration is not correctly performed, the gating is poor, or the presence of M540 or artefacts is confirmed (see chapter 3, (3.1.4)). In the case of the AO assay, the most popular protocol is the SCSA protocol published by Evenson which uses flow cytometry (Evenson, 2013b). This assay was first published in 1980 and has a robust and detailed protocol compared with other sperm DNA damage assays where there is far more variation in their protocols (Evenson, 2016). DNA stained with AO can also be visualised with fluorescence microscopy (Tejada *et al.*, 1984). Usually, visual counting has the disadvantage of being time-consuming, subjective and less reproducible. However, semi-automated scoring can be performed in a reliable and reproducible manner as demonstrated in Chapter 2. As evidence of the higher variability for the TUNEL in comparison with the AO assay, in the meta-analysis of Tan *et al*. five out of

six TUNEL studies were performed using fluorescence microscopy and different counterstain protocols in contrast with only one study using flow cytometry (Tan *et al.*, 2018). All three studies included for staining with AO were performed following the detailed SCSA protocol using flow cytometry (Tan *et al.*, 2018).

4.1.1.2.4 Thresholds used in the sperm DNA damage assessment

Cells can exhibit a very wide spectrum of damage, from damage-free to completely-damage. Single-cell fluorescence data acquired by fluorescence microscopy or flow cytometry is therefore very complex and not necessarily bimodal. However, this single-cell fluorescence data is usually transformed into categorical data by applying a threshold to classify the cells into damaged or non-damaged. In reality, both of these categories are formed by the numerical data that is dispersed over two wide ranges determined by the set-up threshold.

The way to establish the threshold is open to discussion, and different laboratories use different methods. For example, Muratori *et al.* published two different methods to analyse TUNEL data (see chapter 3 (3.1.4)), the threshold-setting method (TS) and the subtraction of the blank method (SB) (Muratori, Tamburrino, Tocci *et al.*, 2010). In flow cytometry, the categorical data is obtained by a gating process based on negative controls; the gating has a certain amount of subjectivity and different patient samples are often compared to a single control and an individual control for each patient is not necessarily performed. However, some patients might have different levels of auto fluorescence and therefore the negative controls might not be applicable across all of them. In the case of the visual analysis of fluorescence microscopy data, the cut-off

used to categorise the data into damaged or non-damaged is subjective based on the sight of the operator and the relative intensity observed between cells.

4.1.2 Clinical relevance of specific sperm DNA damage assays and inter-assay correlation

There are many papers showing a negative relationship between SDD assessed by individual assays such as AO and TUNEL and reproductive outcomes. According to a number of meta-analyses the TUNEL, comet and SCSA assays have the strongest correlation between DNA damage and miscarriage (Robinson *et al.*, 2012), poor IVF/ICSI outcomes (Zhao *et al.*, 2014), and recurrent pregnancy loss (Tan *et al.*, 2018). However, differences in inclusion and exclusion criteria, the different principles of the assays, and variability in the protocols and thresholds across the studies included in the meta-analyses makes it difficult to compare the results. Moreover, there are few studies where multiple SDD assays were performed on the same patients to assess the inter-relationship between the different DNA damage tests and their comparative clinical relevance.

Regarding the relationship between the different DNA damage assays, some authors found a strong correlation between SCSA and TUNEL ($r = 0.79$; $p < 0.001$) (Ribas-Maynou *et al.*, 2013), but, most do not find a strong correlation between SCSA and TUNEL. For example, Stahl *et al*. found a very weak Spearman's rank correlation coefficient ($r = 0.31$) between the percentage of damage obtained by SCSA and TUNEL, and only 40.6% (86 of 212) of the patients received the same classification (normal or abnormal) by both assays (Stahl *et al.*, 2015). Conversely, Henkel *et al.* found a high coefficient of correlation ($r = - 0.994$) between the SCSA DFI (%) and the

number of TUNEL negative cells (TUNEL-neg. %) in 79 patients. However, the Bland and Altman assessment, Passing–Bablok regression and concordance correlation results seemed to indicate that SCSA and TUNEL are not comparable methods (Henkel *et al.*, 2010)

4.1.3 DNA damage assessment in the HABSelect clinical trial

4.1.3.1 Selection of sperm cells with ability to bind hyaluronic acid

Hyaluronic acid (HA) is the compound which holds the cells of the cumulus oophorus; the cluster of cells that surround the oocyte inside the ovarian follicle and post-ovulation. HA receptors present on mature sperm allows them to bind the cumulus oophorus and digest the HA before fertilizing the oocyte (Parmegiani, Cognigni, Ciampaglia *et al.*, 2010). There is a link between the ability of the sperm to bind the HA and the completion of the plasma remodelling, cytoplasmic loss and nuclear maturation of sperm cells (Huszar *et al.*, 2007). Sati *et al.* previously showed a link between DNA damage measured by the TUNEL assay and cytoplasmic retention, which is a feature of immature cells, by using the Aniline blue assay (Sati *et al.*, 2008). Moreover, HA-bound sperm have been demonstrated to have normal nuclear morphology and compaction and fewer chromosomal anomalies and less DNA fragmentation according to the SCD assay (Jakab *et al.*, 2005, Parmegiani, Cognigni, Bernardi *et al.*, 2010).

The combination of the HA-binding assay with ICSI treatment, known as PICSI (physiological intracytoplasmic sperm injection), has been demonstrated to increase the number of grade 1 embryos for transfer and to improve the live birth rate (LBR) when compared to ICSI (Parmegiani, 2010). In PICSI the sperm cells are doubly

selected, first by their affinity for HA and secondly according to morphology and motility by the embryologist.

A larger clinical trial showed that the miscarriage rate decreased from 10 % to 4.3 % when using PICSI instead of ICSI (Worrilow *et al.*, 2013). When stratifying the patients according to their HA-binding score, the CP rate increased from 37.9 % to 50.8 % while the miscarriage rate decreased from 18.5 % to 0 % when PICSI was used instead of ICSI (Worrilow *et al.*, 2013). These results suggest that although PICSI is generally beneficial for all the patients, it is especially recommended for those patients with lower HA-binding score. This trial also suggested that the HA-binding assessment should be performed on prepared samples and not raw semen, as the sperm cells used in ICSI and PICSI were previously selected by swim-up or DGC as is usual in clinic. HABSelect is a very recent trial that tested the efficacy of PICSI *vs* ICSI for livebirth outcome. In this chapter we tested DNA damage in a subset of patients from the HABSelect trial with our optimised AO and TUNEL assays.

4.1.3.2 Patient population for the HABSelect trial and subsequent DNA damage assays

HABSelect was a blind randomised controlled trial to test the benefit of PICSI *vs* ICSI treatment for infertile patients. 16 IVF-licensed hospitals and clinics across the UK participated in the HABSelect clinical trial. The inclusion and exclusion criteria are summarised in **Figure 1**. Initially 6700 couples were randomised for the trial but after excluding those who did not meet the inclusion criteria such as not being able to produce a semen sample on the day of the ICSI/PICSI treatment, the final number of couples available for the primary clinical analysis was 2752 couples.

On the day of the ICSI/PICSI treatment the semen samples were washed and prepared by gradients (DGC) before performing the ICSI/PICSI treatment. The remaining fraction of the semen sample was frozen according to the local protocol and distributed to different basic science laboratories for DNA damage testing. A summary of the entire clinical trial is shown in **Figure 4.1**.

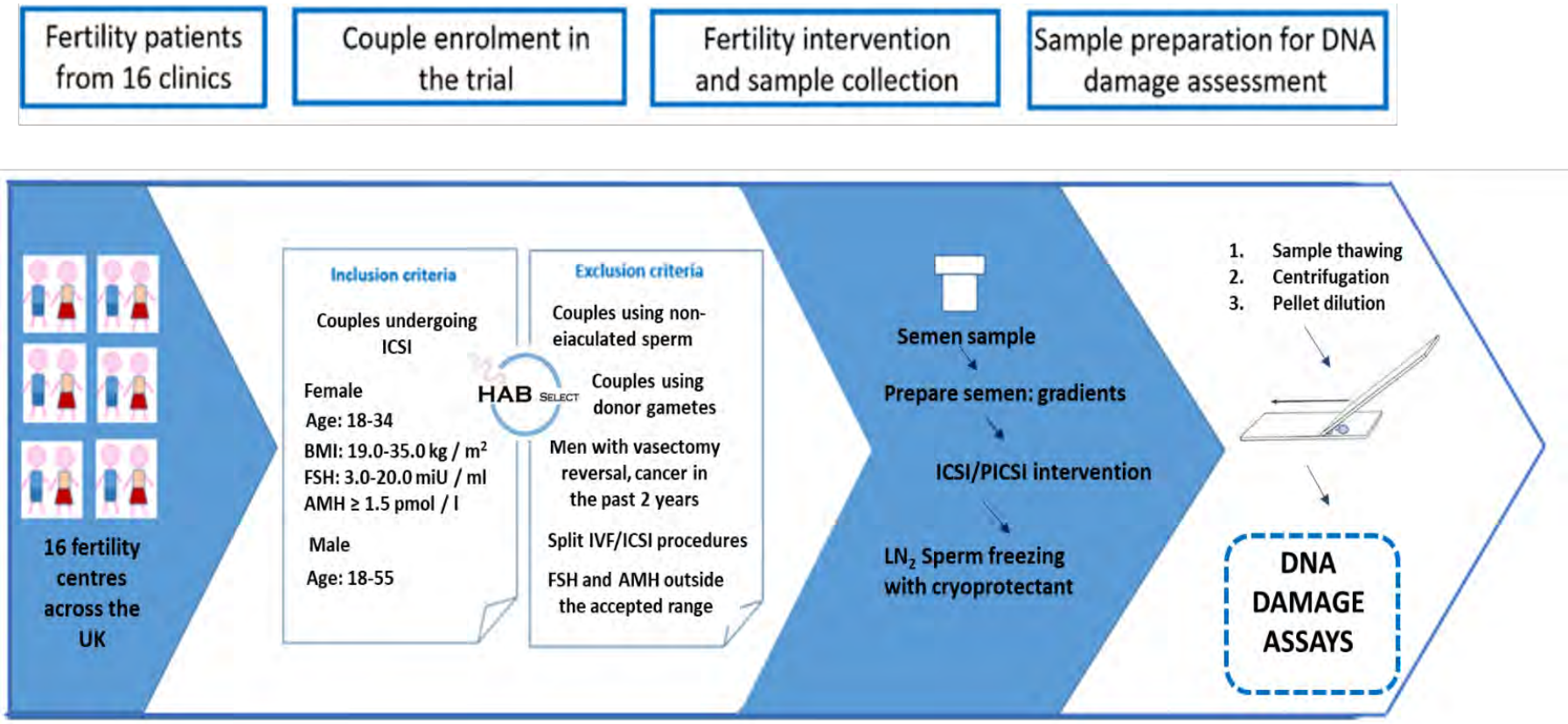

Figure 4.1 Summary of the inclusion and exclusion criteria and the procedure from the sample acquisition until the preparation of smears for the assessment of the DNA damage assessment.

4.2 AIM OF THE STUDY

In this chapter, multiple DNA integrity tests have been performed simultaneously with the same patient samples. The tests used were previously optimised in our laboratory for the assessment of TUNEL, AO, and CMA_3 (see Chapters 2 and 3). In this way, we can investigate the correlation between different assays and compare their relationship to in clinical pregnancy, miscarriage and live birth rates in an objective and reliable manner, free of the inter-subject and sample preparation variability.

The principal aim of the study was to apply our optimised TUNEL and AO assays with the semi-automatic scoring system and the robust and objective analysis in a subset of infertile patients from the HABSelect clinical trial.

The study involved:

- The thawing, smear preparation, staining and mounting of HABSelect frozen samples for the AO (136), TUNEL (583) and CMA_3 (91) assays.
- The AO and TUNEL scoring (%) according to the protocols and methods developed in chapter 2 and 3.
- The study of the inter-assay relationship.
- The study of the relationship of DNA damage measured by AO and TUNEL with the status of the chromatin compaction measured by the CMA_3 assay.
- The study of the correlation between the sperm DNA damage measured by AO and TUNEL and the clinical outcomes in the HABSelect trial.

4.3 MATERIALS AND METHODS

4.3.1 Sample preparation

Sample preparation was performed by the clinics participating in the HABSelect clinical trial. Briefly, the semen was previously prepared by the local protocol, generally by gradients (2.3.1.2) and used for the ICSI/PICSI treatment.

After the ICSI/PICSI treatment, the remaining sperm sample was centrifuged (500 g, 10 min) and frozen according the local protocol. The samples were thawed by immersing the cryovials in a water bath at 37 ºC and later transfer to a 15 ml Falcon tube (05-527-90, Fisher Scientific) and 1.75 ml of PBS was gently added to the samples. Samples were mixed by flicking the tube and centrifuge (500 g, 10 min), supernatant removed, the pellet re-suspended in 2 ml of PBS and centrifuged a second time (500 g, 10 min). Finally, the pellet was diluted in PBS and adjusted to a minimum concentration of 2.5 x 10^6 spermatozoa / ml. 10 µl of sperm were pipetted over the centre of poly-lysine pre-coated slides and spread manually by circular and gentle movements with the tip of the pipette in a small area of approximately 3 x 3 cm. The slides were allowed to dry for an hour at room temperature (RT). 136, 583 and 91 individual patient samples were used for the assessment of AO, TUNEL and CMA_3, respectively.Donor samples were used for making smears, staining and scoring the DFI (%) and TUNEL (%) in chapters 2 and 3, respectively. The results from donors A, B and D are used in this chapter for studying the intra-assay correlation in fresh and frozen samples and to compare with the intra-assay correlation obtained with the patient samples.

4.3.2 DNA damage assays

4.3.2.1 Acridine orange assay staining and scoring

The slides were stained following the protocol described in 2.3.2 and mounted with DPX as detailed in 2.3.3.

The slides were scored for AO positive cells (%) using the semi-automatic AO scoring method based on acquired grey-scale images (2.3.4.2) and using a 0.66 cut-off for the positive cells as described in chapter 2.

4.3.2.2 TUNEL assay labelling and scoring

The slides were stained following the protocol detailed in 3.2.2 and mounted with Fluoroshield as detailed in 2.3.3.

The slides were scored for TUNEL positive cells (%) using the visual assessment (3.3.3.1) and the semi-automatic scoring method based on acquired grey-scale images (3.3.3.2). The number of positive cells (%) was automatically calculated by the Mclust mixed model package in R as it demonstrated good correlation and to agree with the manual gating method (3.4.4).

4.3.3 Chromatin compaction assay staining and scoring

The staining protocol was adapted from the methods published by Bianchi *et al*. (Bianchi *et al.*, 1996). Carnoy's solution was prepared by mixing methanol 100 % (BDH-VWR) and acetic acid (100 %) (BDH Laboratory Supplies) in a ratio of 9:1 in a fume cupboard. McIlvane buffer (pH 7.0) was prepared with 200 mM Na_2HPO_4, 100mM citric acid and 10 mM $MgCl_2$. CMA_3 staining solution (0.25 mg/ml) was prepared by

diluting Chromomycin A_3 from Streptomyces griseus (Sigma-Aldrich, C2659) in McIlvane buffer. McIlvane buffer and CMA_3 staining solution were wrapped with foil to protect them from light exposure and stored at 4 ºC for up to one month.

The smears were first fixed with Carnoy's solution for 10 min at room temperature (RT) and allowed to air dry for 60 min before staining or stored for 24 h at 4º C before staining. 100µl of CMA_3 staining solution was pipetted onto the slides and left for 20 min protected from light. The slides immersed in approximately 350 ml of McIlvane buffer and a total of three washes were performed under gentle manual agitation for 5 min to ensure the elimination of the CMA_3 excess. The samples were allowed to dry for 60 min at RT before proceeding with the mounting with DPX (2.3.3).

The stained slides were visualized with an Olympus fluorescence microscope (BX61) with Xenon lamp using 60x oil immersion objective, and QUANTUM: 512SC camera (Photometrics) attached to a PC running Cairn Metamorph software. The excitation and emission filters were set up in a filter cube. The characteristics of the excitation and emission filters were 420 ± 20 nm and 465 long-pass (lp), respectively.

Grey-scaled images were obtained for every slide and the image analysis was performed similarly as per AO and TUNEL (2.3.4.2 and 3.3.3.2). The intensity was measured as average intensity and total intensity for each sperm cell. Positive-CMA_3 cells which exhibit bright yellow fluorescence are sperm with deficient protamination, while the negative-CMA_3 cells which are dimmer or not fluorescent correspond to the completely protaminated cells (Bianchi *et al.*, 1996, Talebi *et al.*, 2016). The intensity values were plotted and the positive subpopulation (CMA_3 (+) (%)) was scored by applying a general set-up threshold (2800 arb. units/ pixels) based on visual assessment of donor samples and negative controls.

4.3.4 Statistics

Statistical analysis was performed using Graphpad Prism software.

The distribution of the AO, TUNEL and CMA_3 patient results were studied by the normality tests of D'Agostino and Pearson (alpha = 0.05) and Shapiro-Wilk (alpha = 0.05) suggesting the use of non-parametric tests as the distribution found was not normal. Due to the non-normal distribution, the representation of the average values in the results section was performed using the medians rather than means.

The correlation between assays was tested by linear regression.

To calculate if the difference between the clinical outcomes obtained for low and high DNA fragmentation ("Damage > 20 %" and "Damage < 20 %" for TUNEL and ("Damage > 30 %" and "Damage < 30 %" for AO) was statistically significant, the Fisher's exact test (two-tailed P value) was performed.

The primary outcomes for this study were the SDD assessed by TUNEL and AO in a subset of HABSelect patients, pregnant and not pregnant, and miscarriage and no miscarriage. Previously, different publications shown a miscarriage rate (defined as the pregnancy loss during the first trimester) in women receiving ICSI treatment of 12.6 % (Buckett *et al.*, 2008) and 18.8 % (Bahceci and Ulug, 2005). Therefore, in order to observe a 5 % difference in the miscarriage rate between the two groups (low and high DNA damage), with an α-type error of 5 % and power (1-β) of 80%, a total of 1660 patients (830 patients with low and 830 with high sperm DNA damage) needed to enrol in the study. According to the 2008 UK national average for ICSI success (Human Fertilisation and Embryology Authority (HFEA), 2008) , the LBR at ≥ 37 weeks' gestation was estimated to be 24%. Therefore, in order to observe a 5 % difference in

the miscarriage rate between the two groups (low and high DNA damage), and with an α-type error of 5 % and power (1-β) of 80 %, a total of 2288 patients (1144 patients with low and 1144 with high sperm DNA damage) need to enrol the study.

4.4 RESULTS

4.4.1 Optimisation of the chromatin compaction assay (CMA_3) and its correlation with the sperm DNA damage

Sperm cells from donor ejaculates fixed in Carnoy's solution and stained with CMA_3 emitted fluorescence with different intensity (**Figure 4.2A**). Negative controls of different donors showed similar but not identical fluorescence intensities, indicating variable autofluorescence across donors (**Figure 4.2B**). All cells incorporated some CMA_3 dye as it can be seen when comparing a baseline sample against the individual negative control. The single-cell intensities for the negative control of donor A varied from 1000 to 1750 (arb. units / pixels) (**Figure 4.2B**), while the majority of the single-cell intensities for the baseline sample of same donor were slightly higher than in the negative control (**Figure 4.2C**). A general threshold for scoring positive cells was set-up according to the visual assessment; cells with an average intensity above 2800 (arb. units / pixels) were considered as positive (blue arrows in 2A).

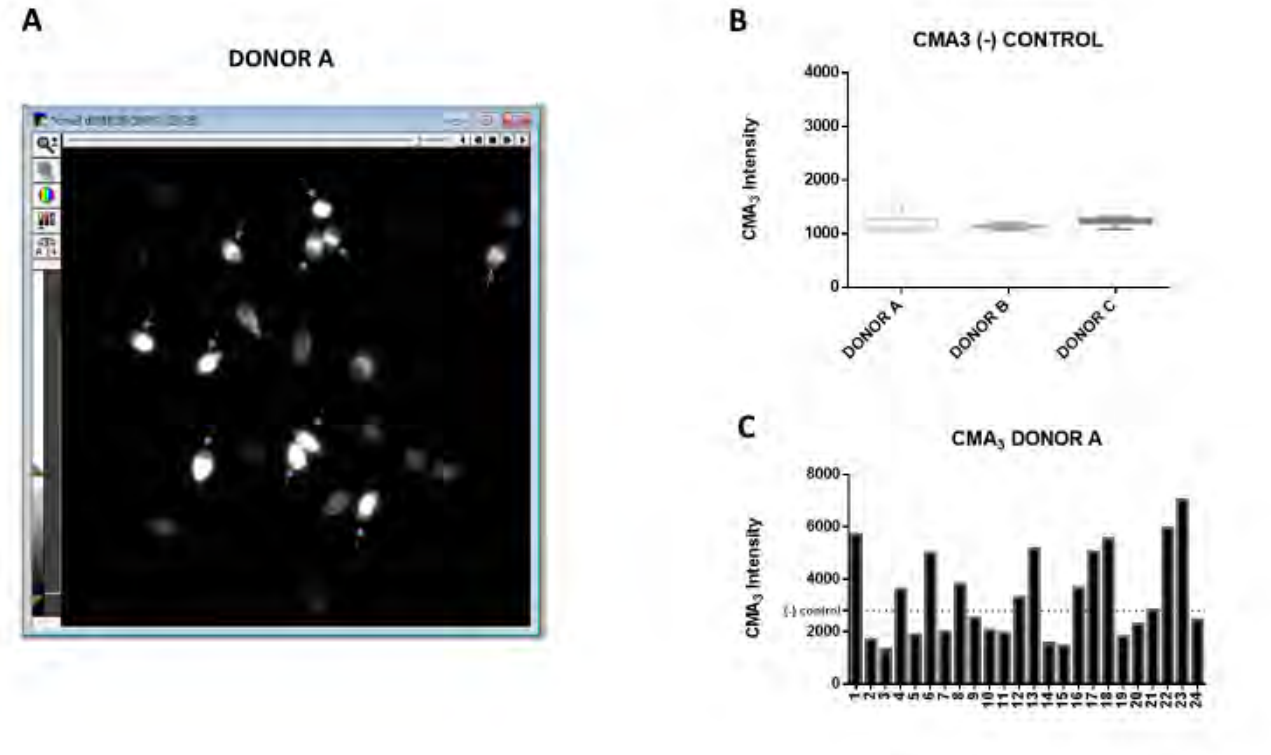

Figure 4.2 Fluorescence microscopy of sperm cells stained with CMA3 and set-up threshold for the semi-automatic scoring method. **A**. Grey-scale image of a field of CMA_3 stained sperm from donor A showing the heterogeneity of single-cell intensities. Positive cells are marked with blue arrows. **B**. Distribution of the negative controls for three different donors (median and extremes of range are represented). **C**. Bar graph showing the single-cell intensities for donor A (same field as in 1.A). All the bright cells in A had an average intensity greater than 2800. The dot line in C shows the set-up threshold based on the visual assessment (2800).

4.4.2 Patient distribution values for AO, TUNEL and CMA_3 assays and inter-assay relationship

Sperm cells were subjected to SDD assays (TUNEL and AO) and chromatin compaction assay (CMA_3). The percentage of damage was calculated according to 4.3.2 and the results are shown in **Figure 4.3** for a total of 615, 136 and 77 samples, for TUNEL, AO and CMA_3, respectively. For all the three assays, the distribution was right-skewed.

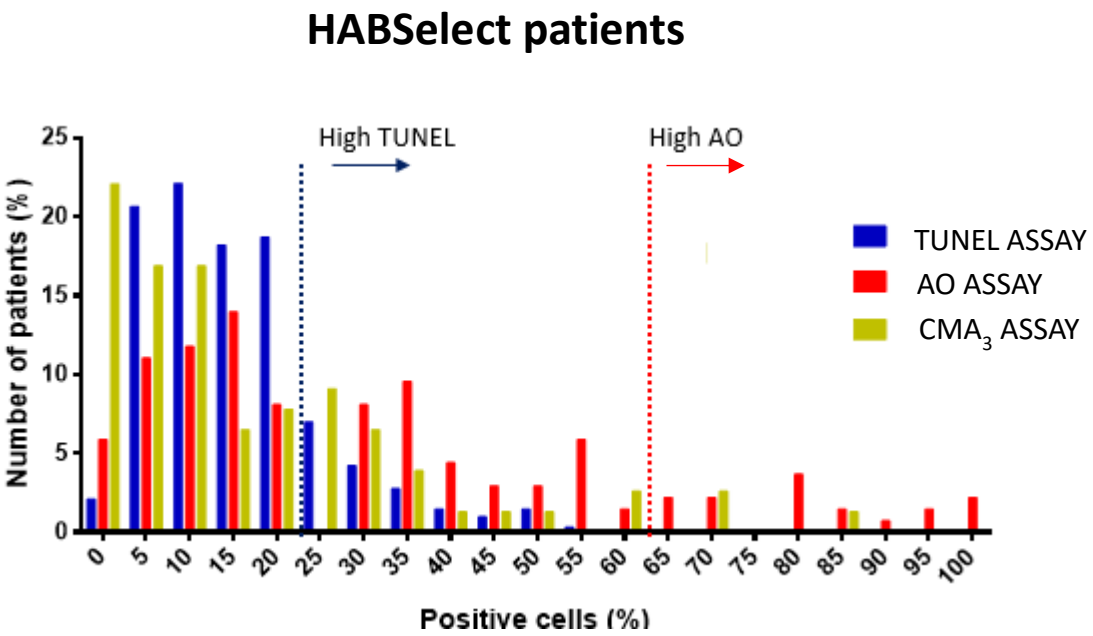

Figure 4.3 Percentage of positive cells for the different SDD and CMA3 assays for the HABSelect patients. TUNEL values for 615 patients (blue), AO values for 136 (red), and CMA_3 for 77 patients. The number of patients in the y-axis correspond to the percentage and not to the total number of patients. The dotted-lines in blue and red show the maximum values for TUNEL and AO obtained with frozen donor samples (see Chapters 2 and 3).

The percentage of damage for each SDD assay (TUNEL and AO) was measured in a cohort of the patient samples from the HABSelect clinical trial. The correlation between the two assays was investigated in a total of 85 patient samples. Cells were considered AO-positive when the DNA Fragmentation Index (DFI) was greater than 0.66 according to the grey-scales images acquired by the Quantafrag system developed in Chapter 2. TUNEL-positive cells were identified on the fluorescence single-cell data extracted from the grey-scale images acquired by fluorescence microscopy by using the

clustering method based on the mixed Gaussian model developed in Chapter 3. No correlation was found between the two assays (R^2 = 0.001032) (**Figure 4.4**)

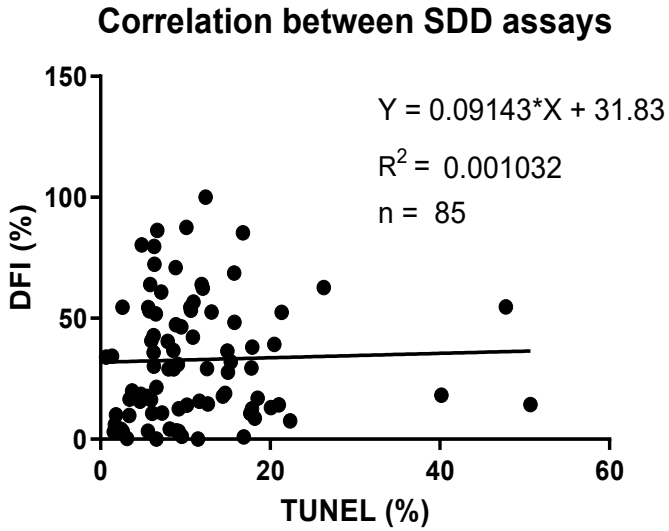

Figure 4.4 Correlation between the SDD of TUNEL and AO for 85 HABSelect patients. The y-axis DFI (%) corresponds to the percentage of AO-positive cells when applying a cut-off DFI = 0.66 for the ratio between the red fluorescence and total fluorescence obtained by the Quantafrag system in single-cells. The x-axis TUNEL (%) corresponds to the percentage of TUNEL-positive cells according to the clustering method based on Gaussian mixed model on single-cell data acquired by fluorescence microscopy.

The correlation between both assays was also studied in donor samples that were previously assessed for both AO and TUNEL assays in chapter 2 and 3. A moderate-strong intra-assay correlation (R^2 = 0.6787) was obtained when the donor samples used were fresh, while the correlation for the same samples when frozen-thawed was found to be 0 (**Figure 4.5**).

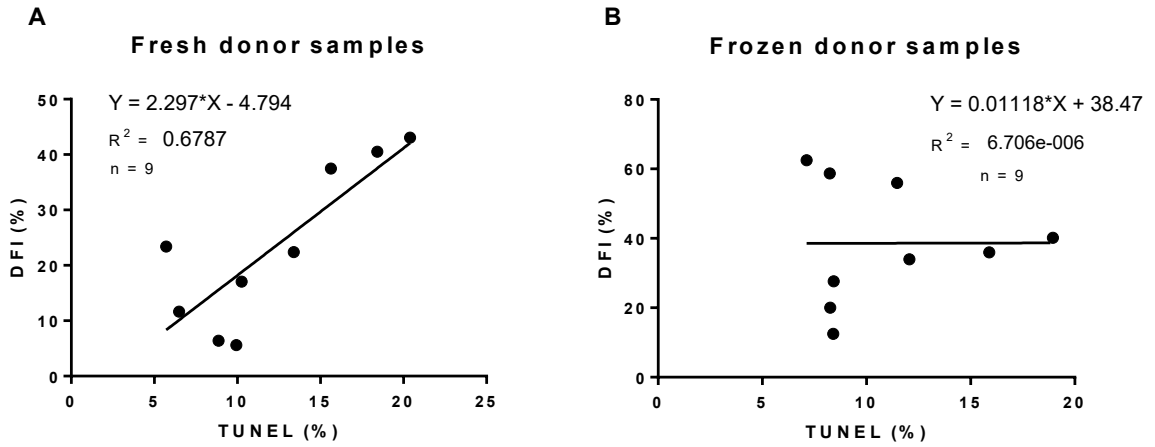

Figure 4.5. **Correlation between the TUNEL and AO results obtained for donor samples.** **A** shows the correlation for fresh donor samples while **B** shows the correlation for the same donor samples after being frozen and thawed. A total of 9 samples corresponding to 3 donors (A, B and D) were used in this experiment. The y-axis DFI (%) corresponds to the percentage of AO-positive cells when applying a cut-off DFI = 0.66 for the ratio between the red fluorescence and total fluorescence obtained by the Quantafrag system in single-cells. The x-axis TUNEL (%) corresponds to the percentage of TUNEL-positive cells according to the clustering method based on Gaussian mixed model on single-cell data acquired by fluorescence microscopy.

The percentage of damage obtained for each assay (TUNEL and AO) was compared with the level of compaction (CMA_3 (%)) in a cohort of HABSelect patients (**Figure 4.6**). The level of compaction for individual samples (CMA_3 (%) in **Figure 4.3** was measured by quantifying the percentage of cells with an average fluorescence intensity higher than the threshold determined by previous visual assessment (> 2800 arb. units/ pixels). The single-cell data for CMA_3 intensity was extracted from grey-scale images acquired in fluorescence microscopy similarly as per TUNEL and AO. No correlation was observed between CMA_3 and the AO or the TUNEL assay when assessed using 43 and 57 patient samples respectively. The percentage of damage for the AO and

TUNEL assays was not significantly different between samples with poorly and highly compacted chromatin according to the CMA_3 assay (> 40 %, and < 40 %, respectively) (**Figure 4.7**).

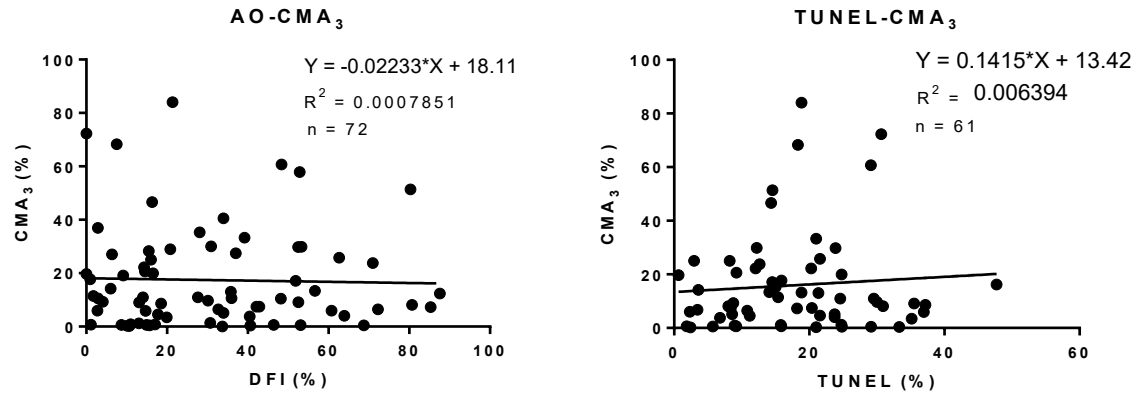

Figure 4.6 Correlations between percentages of DNA damage by AO and TUNEL and DNA compaction measured by CMA3 in HABSelect patients. DFI (%) indicates the percentage of AO-positive cells based on a 0.66 set-up threshold. TUNEL (%) indicates the percentage of TUNEL-positive cells according to the Gaussian mixed model for clustering positive cells. All the single-cell intensities were extracted from grey-scaled images obtained by fluorescence microscopy.

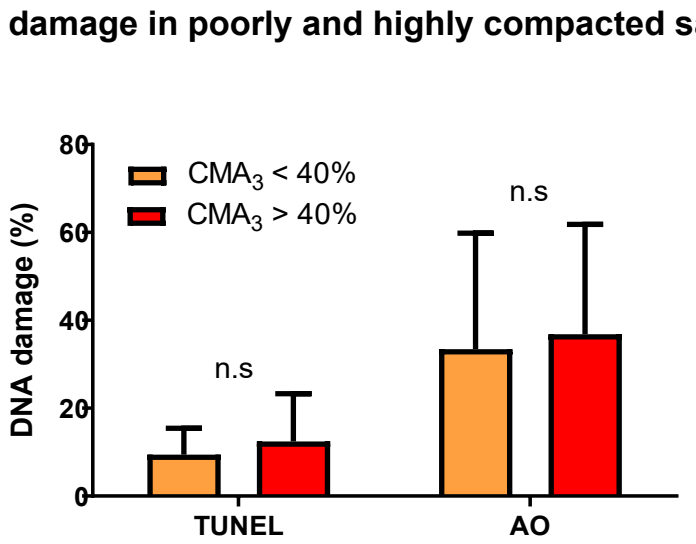

Figure 4.7 DNA damage (%) in HABSelect with low and high chromatin compaction. DNA damage (%) by AO and TUNEL was quantified for samples with poorly compacted (CMA_3 > 40 %) and highly compacted (CMA_3 < 40 %) chromatin. n. s: not statistically significant.

4.4.3 Study of TUNEL levels and clinical outcomes in a subgroup of patients from the HABSelect clinical trial

In order to test the correlation of high sperm DNA damage measured by TUNEL with the clinical outcomes of CP, miscarriage and LB, a cohort of patients from the HABSelect trial, whose main characteristics and demographics are summarised in **Table 4.1**, were used. After the staining and TUNEL (%) quantification, the patients were split into low and high DNA damage based on a 20 % threshold established from our TUNEL data from Chapter 3 and used in a number of previous publications (Sergerie *et al.*, 2005, Sharma, R. K., Sabanegh *et al.*, 2010) **(Table 4.2)**, and according to the treatment group (PICSI or ICSI) **(Table 4.3)**.

TREATMENT	F AGE (mean)	M AGE (mean)	COUNT (10^6/ML) (mean)	MOT (%) (mean)	HBA (%) (mean)	ETs (mean)	CP (%)	M (%)	LB/ET (%)
PICSI	**34**	**36**	**27**	**40**	**68**	**1.4**	**122/280 (43)**	**21/122 (17)**	**103/280 (36)**
ICSI	**34**	**36**	**25**	**41**	**70**	**1.5**	**116/267 (43)**	**33/116 (28)**	**83/267 (31)**

Table 4.1 Demographics, semen and HBA parameters of the HABSelect subset of patients used in this chapter for the investigation of the correlation between the TUNEL scores and the clinical outcomes. Percentages for clinical pregnancy (CP), miscarriage (M) and live birth per embryo transfer (LB/ET) are shown in brackets. F AGE: female age, M AGE: male age, MOT: motility, HBA: hyaluronan binding assay, ETs: embryo transfers.

VARIABLE	PATIENTS LOW TUNEL (<30%)	PATIENTS HIGH TUNEL (>30%)	P-VALUE
TOTAL	**432**	**151**	**-**
ET (%)	**410 / 432 (95)**	**143 / 151 (95)**	**p = 1**
CP (%)	**184 / 410 (45)**	**54 / 143 (38)**	**p = 0.1428**
M (%)	**50 / 184 (27)**	**4 / 54 (7)**	**p = 0.0016 ***
LB / ET	**136 / 410 (33)**	**50 / 143 (35)**	**p = 0.7579**

Table 4.2 Classification for the subset of HABselect patients according to TUNEL levels. P-value (two-tailed) calculated by the Fisher's exact test. * shows statistical significance. Percentages shown in brackets. ET: embryos transferred, CP: clinical pregnancy, M: miscarriage, LB/ET: live births per embryos transferred.

TREATMENT	VARIABLE	PATIENTS LOW TUNEL (< 20 %)	PATIENTS HIGH TUNEL (> 20 %)	P-VALUE
PICSI	**Total PICSI**	**225**	**77**	**-**
	ET	**214 / 225 (95)**	**72 / 77 (94)**	**0.5643**
	CP (%)	**98 / 214 (46)**	**24 / 72 (33)**	**0.0738**
	Miscarriage (%)	**18 / 98 (18)**	**3 / 24 (13)**	**0.7631**
	LB / ET (%)	**82 / 214 (39)**	**21 / 72 (29)**	**0.1391**
ICSI	**Total ICSI**	**207**	**74**	**-**
	ET	**196 / 207 (94)**	**71 / 74 (96)**	**1**
	CP (%)	**86 / 196 (44)**	**30 / 71 (42)**	**0.8891**
	Miscarriage (%)	**32 / 86 (37)**	**1 / 30 (3)**	**0.0003***
	LB / ET	**54 / 196 (28)**	**29 / 71 (41)**	**0.0512**

Table 4.3 Clinical outcomes for the subset of HABSelect patients studied in this chapter after being classified according to the level of DNA damage encountered by the optimised TUNEL assay developed in chapter 3 and by the treatment received as ICSI or PICSI. P-value (two-tailed) calculated by the Fisher's exact test at significant level of 0.05. * shows statistical significance. Percentages shown in brackets. ET: embryos transferred, CP: clinical pregnancy, M: miscarriage, LB/ET: live births per embryos transferred.

4.4.4 Study of AO levels and clinical outcomes in a subgroup of patients from the HABSelect clinical trial

The main characteristics and demographics of the subset of patients from the HABSelect trial used in our study are summarised in **Table 4.4**. After the staining and AO (%) quantification, the patients were split into low and high DNA damage based on a 30 % threshold established from our AO data from Chapter 2 and used in a number of previous publications (Bungum *et al*., 2007, Evenson et al., 1999, Virro *et al*., 2004) **(Table 4.5)**, and according to the treatment group (PICSI or ICSI) **(Table 4.6)**.

TREATMENT	F AGE (MEAN)	M AGE (MEAN)	COUNT (10^6/ML) (MEAN)	MOTILITY (MEAN)	HBA (%) (MEAN)	ETS (MEAN)	CP (%)	MISCARRIAGE (%)	LB/ET (%)
PICSI	**35**	**37**	**33**	**45**	**81**	**1.3**	**24/66 (36)**	**5/24 (21)**	**22/85 (26)**
ICSI	**34**	**36**	**47**	**48**	**75**	**1.4**	**32/68 (47)**	**14/32 (44)**	**23/97 (24)**

Table 4.4 Demographics, semen and HBA parameters of the HABSelect subset of patients used in this chapter for the investigation of the correlation between the AO scores and the clinical outcomes. Percentages for clinical pregnancy (CP), miscarriage (M) and live birth per embryo transfer (LB/ET) are shown in brackets. F AGE: female age, M AGE: male age, MOT: motility, HBA: hyaluronan binding assay, ETs: embryo transfers.

VARIABLE	PATIENTS LOW AO (<30%)	PATIENTS HIGH AO (>30%)	P-VALUE
TOTAL	**73**	**61**	**-**
ET	**67 / 73 (92)**	**56 / 61 (92)**	**1**
CP (%)	**30 / 100 (30)**	**26 / 68 (32)**	**0.3521**
M (%)	**7 / 30 (23)**	**12 / 26 (46)**	**0.0936**
LB/ET	**25 / 100 (25)**	**20 / 82 (24)**	**1**

Table 4.5 Classification for the subset of HABselect patients according to AO levels. P-value (two-tailed) calculated by the Fisher's exact test. Percentages shown in brackets. ET: embryos transferred, CP: clinical pregnancy, M: miscarriage, LB/ET: live births per embryos transferred.

	VARIABLE	PATIENTS LOW AO% (<30 %)	PATIENTS HIGH AO% (>30 %)	P-VALUE
PICSI	Total	**35**	**31**	**-**
	ETS	**33 / 36 (92)**	**28 / 31 (90)**	**0.6595**
	CP (%)	**15 / 48 (31)**	**9 / 37 (24)**	**0.3086**
	M (%)	**2 / 15 (13)**	**3 / 9 (33)**	**0.3256**
	LB/ET (%)	**15 / 48 (31)**	**7 / 37 (19)**	**0.2222**
ICSI	Total	**39**	**30**	**-**
	ETS	**35 / 39 (90)**	**28 / 30 (93)**	**0.6905**
	CP (%)	**15 / 54 (28)**	**17 / 45 (38)**	**0.3883**
	M (%)	**5 / 15 (33)**	**9 / 17 (53)**	**0.3075**
	LB/ET (%)	**10 / 54 (19)**	**13 / 45 (29)**	**0.2421**

Table 4.6 Clinical outcomes for the subset of HABSelect patients studied in this chapter after being classified according to the level of DNA damage encountered by the optimised AO assay developed in chapter 2 and by the treatment received as ICSI or PICSI. P-value (two-tailed) calculated by the Fisher's exact test at significant level of 0.05. Percentages shown in brackets. ET: embryos transferred, CP: clinical pregnancy, M: miscarriage, LB/ET: live births per embryos transferred.

4.5 DISCUSSION

4.5.1 Sources of variability in the sperm DNA damage assays

Different types of DNA damage would be expected to have relevance for different stages of the fertilisation process and embryo development. DSB are generally considered the most deleterious type of DNA damage, but, as previously mentioned, the severity of the impact of DNA damage depends on the quality of the oocyte and its

ability to repair SDD. Different SDD assays are usually considered equivalent in the literature while they measure different types of damage. The lack of methods for measuring oocyte repair ability complicates the risk assessment of SDD.

Moreover, the sample preparation is another source of variability for DNA damage assessment as we know that incubation times, centrifugation steps and temperature decrease during the freezing procedures might lead to an increase in DNA damage. Interestingly, frozen samples are commonly used for the SCSA assay, but while no difference in DFI was observed when using fresh *versus* frozen samples in mice (Evenson *et al.*, 1989), and ram (Peris *et al.*, 2004), human sperm samples showed higher % DFI after the freeze-thawing procedure according to our data in chapter 2. This difference in sensitivity to cryodamage suggests a possible link between the DNA cryodamage and variation in chromatin compaction inter-species. More studies should be addressed to investigate the effects of the freezing and cryopreservation methods on human sperm DNA when using the different SDD assays.

Meta-analyses studying SDD often do not provide details in the nature of the sample used, while results obtained with selected sperm by gradients or swim-up procedures might not be representative of the damage presented in the ejaculate.

It is very important to consider all these sources of variability to avoid misunderstandings and confusions when drawing conclusions.

4.5.2 Optimisation of the CMA_3 assay and its correlation with the sperm DNA damage

The chromomycin A_3 molecule used in the CMA_3 assay competes with the protamines for the protamine binding sites in the chromatin, hence lower-compacted chromatin

looks brighter than high-compacted chromatin after staining with CMA_3. Our CMA_3 stained samples showed two differentiated populations of sperm cells, one brighter and one dimmer, in the same ejaculate. Previous publications showed a correlation between the CMA_3 positivity (%) and the sperm DNA damage measured by SCD (Tavalaee *et al.*, 2009) , AO (Iranpour, 2014) and TUNEL (Tarozzi *et al.*, 2009). We did not find any strong correlation between the compaction measured as CMA_3 positive cells and the number of TUNEL positive (R^2 = 0.0064) or AO positive cells (R^2 = 0.0008). Tavalaee *et al.* observed an increase in the DNA fragmentation measured by Sperm Chromatin Dispersion (SCD) in samples with CMA_3 positivity higher than 40 % (Tavalaee *et al.*, 2009). We did not find any statistically significant increase in the TUNEL (%) or in the AO (%) in those samples with CMA_3 positivity higher than 40 %. Our findings do not necessarily contradict Tavalaee *et al*. results as we used different SDD assays than SCD. Different SDD assays might involve identification and quantification of a different type of DNA damage and therefore the correlation between compaction and SDD might be specific for the SCD assay. Moreover, according to Amor *et al.* SDD measured by TUNEL was negatively correlated with the P1:P2 ratio but not with CMA_3 (Amor *et al.*, 2019).

External regions of the chromatin could potentially be directly damaged by changes in pH or oxidant agents without the need for poorly compacted chromatin. Currently, it is difficult to know the specific regions of the chromatin or structural position of the damage targeted by the different SDD assays.

4.5.3 Patient distribution values for AO, TUNEL and CMA_3 assays and inter-assay relationship

We showed AO had the higher inter-subject variability ranging from 0 % to 100% while for the TUNEL and CMA_3, the SDD range across patient values was narrower, specially TUNEL (from 0 % to 50 %). In any case, the distribution obtained for all the assays was right-skewed, showing the majority of patients had lower values of SDD, suggesting that only those patients with higher values (more right-skewed) could have a clinically relevant level of SDD. According to our limited data from normal donor samples compiled in Chapters 2 and 3, a relevant percentage of damage for the AO is 60 % while for TUNEL is a 20 %. However, there is no guarantee that all the donors used in our experiments are completely free of SDD.

The lack of correlation between the DNA damage assays TUNEL and AO ($R^2 = 0.0168$) of 85 patient samples seems to support that different DNA damage assays measure different aspects of the DNA as observed previously with the SCSA and TUNEL assays (Henkel *et al.*, 2010, Stahl *et al.*, 2015). However, the moderate-strong correlation found in fresh donor samples suggests that the lack of correlation found in the patient samples could be due to the process of freezing-thawing. The loss of correlation found in the same donor samples when frozen-thawed seems to confirm this hypothesis. In chapters 2 and 3, AO demonstrated to be more vulnerable than TUNEL to the effect of freezing-thawing as the majority of the donor samples increased their DFI (%) after the freezing procedure, while for TUNEL no significant changes were found. However, the number of donor samples used for this purpose was quite limited and this experiment should be repeated in future with a greater data-set.

Interestingly, our CMA_3 data did not correlate with any of the sperm DNA damage data, neither with the AO (R^2 = 0.0044) nor with TUNEL (R^2 = 0.0170) while other authors found weak correlations between CMA_3, AO and the DNA fragmentation SCD assay (Iranpour, 2014, Tavalaee *et al.*, 2009).

4.5.4 Study of the TUNEL levels and clinical outcomes in a subgroup of patients from the HABSelect clinical trial

In our sub-analysis with the subset of patients from the HABSelect trial, PICSI and ICSI allocations had same CP (43 %) and similar LB/ET (36 % *vs* 31 %, respectively). In the original HABSelect trial the CP and LB are also similar in PICSI and ICSI groups; 35.2 % *vs* 35.7 %, p = 0.8 for CP, and 27.4 % *vs* 25.2 %, p = 0.22 for LB. The total of miscarriages (%) in the original HABSelect trial and in our subset of patients was similar (16 % *vs* 23 %). When studying the arm allocation as PICSI and ICSI separately, the miscarriage rate in our subset of patients was significantly lower in PICSI compared to ICSI (17% *vs* 28%, p = 0.0446) which is in line with the HABSelect clinical trial results (12.3 vs 19.6 %, PICSI vs ICSI, respectively; p = 0.0095). The percentage of patients in our subset of data with high SDD in the ejaculate was the same for both groups, PICSI and ICSI (26 %) which suggests that this decrease in miscarriage in the PICSI group could be due to the selection of sperm with healthy DNA through the HA-binding assay (Jakab *et al.*, 2005). However, when pooling all patients together (PICSI and ICSI) we found the opposite effect; surprisingly a lower miscarriage rate was found in the group of patients with high DNA damage (7 % *vs* 27 %). The association between SDD and miscarriage was also studied in the PICSI and ICSI patients separately as the selection of mature sperm cells with expressed HA receptors by the HA binding assay (prior PICSI) could potentially select those sperm

with better DNA quality and therefore ejaculates with high SDD will not be reflected in worst clinical outcomes. Then, PICSI could be masking the negative effect of the SDD in the ICSI clinical outcomes. However, miscarriage rate was not statistically different in low and high SDD groups when considering PICSI patients, and it was lower in ICSI patients with high SDD men. The analysis of the separate subgroups showed that PICSI patients with low SDD (< 20 % of TUNEL positive cells) had an increase in the clinical pregnancy rate compared to the high SDD group (> 20 % TUNEL positivity) (46 % *vs* 33 %), although this difference did not reach statistically significance (p = 0.0738). No significant differences were found between the PICSI and ICSI subgroups for the LB/ET and miscarriages rates; Live birth was 39 % *vs* 29 %, p = 0.1391 for PICSI and ICSI, respectively; and miscarriage rate was 13 % *vs* 18 %, p = 0.76310, for PICSI and ICSI, respectively. For the ICSI patients, both types of SDD showed no statistically significant differences in the CP (42 % *vs* 44%; p= 0.8891), but surprisingly the LB/ET was higher in the high SDD group (28 % *vs* 41 %; p = 0.0512), and the miscarriage rate was lower (37 % *vs* 3 %; p = 0.0003).

In light of the results, PICSI seems to help avoid miscarriage. However, it seems not to be related to SDD but with some other unknown mechanism. This is in accordance with the TUNEL mean values found in the pregnant and miscarried women in the HABSelect trial results, as there was no difference between the two groups 10.24 and 12.57 (Kirkman-Brown, J. *et al.*, 2019). In our data, the low SDD subgroup in both scenarios, pooled or separate PICSI and ICSI patient allocations, paradoxically exhibited lower miscarriage rates. These results need to be interpreted with caution as there was a large difference in the total number of patients with low and high SDD and therefore in pregnant patients in both groups; this might make difficult the comparison

of both groups. Moreover, the number of HABSelect patients included in this chapter for the analysis of the effects of SDD in pregnancy and miscarriage subset of patients from HABSelect was insufficiently powered to draw conclusions although we believe it can be useful to make a case for further investigations in the field.

We cannot find any explanation for the lower miscarriage found in patients with SDD higher apart from the possibility that patients with lower DNA damage had other causes of infertility different from DNA damage that are not as efficiently bypassed by ICSI. Damaged sperm can bypass the natural barriers and fertilise the oocyte when using ICSI, but if the damage exceeds the oocyte's repair ability it can lead to chromosomal abnormalities in the embryo and trigger the miscarriage mechanism or to lead to uncertain long-term consequences for the health of the new-born. It is important to note that there were several limitations in our study to find a link between SDD and clinical outcomes, for example the use of samples that were stored after cryopreservation processes were carried out. Cryopreservation might elevate the levels of DNA damage found in the original samples, although according to our initial experiments with donor samples, TUNEL (%) did not increase after the cryopreservation in the majority of the donors. Other important limitations are the sample preparation procedures, i.e. swim-up, as the sample can be enriched with higher quality cells free-from or with low DNA damage (Younglai *et al.*, 2001), or sperm with more attractive motility and morphology aspects, which may be linked to the quality of their DNA, selected by the embryologist for oocyte microinjection in ICSI/PICSI treatment (Di Santo *et al.*, 2016, Ganzer *et al.*, 2017, Lopes, S. *et al.*, 1998). Moreover, for the PICSI group, the cells were also selected according to their ability to bind to HA which was suggested to be linked to the DNA quality. This was in fact the hypothesis for the original HABSelect trial. Higher

correlations between sperm DNA damage and clinical outcomes were expected in the ICSI group than in the PICSI group. However, this was not the case for the miscarriage rate. We consider that these conclusions should be compared in a larger study with unprocessed and potentially fresh ejaculates for IVF rather than ICSI treatment.

4.5.5 Study of the AO levels and clinical outcomes in a subgroup of patients from the HABSelect clinical trial

As in the clinical trial HABSelect and our TUNEL sub analysis (4.5.4) the miscarriage rate was lower in PICSI patients than in ICSI patients (21 % vs 44 %) while the LB/ET rate was very similar (26 % *vs* 24 %). However, when looking at these patients screened for AO, the CP rate was higher in the ICSI patients than the PICSI (47 % *vs* 36 %), although this difference was found not statistically significant ($p = 0.2249$). The similar percentage of patients with high damage (>30% AO) obtained for both allocation arms (47 % *vs* 44 % for PICSI and ICSI, respectively) suggests that this decrease in miscarriage rate in the PICSI group could be due to a selection of sperm with low damage. This is also supported by the increase in the miscarriage rate observed in patients with high AO damage in comparison with patients with low AO damage (46 % *vs* 23 %). However, the miscarriage rates found in patients with high damage were 20 % higher in comparison with patients with low damage not only in the ICSI, but also in the PICSI group; the difference between groups was not statistically significant probably due to the low number of patients investigated. The sperm selection carried out by PICSI seems to be independent of the SDD. This is also in accordance with the HABSelect trial results as pregnant women and miscarried women had similar TUNEL values, and with our sub analysis for the TUNEL assay with a subset of patients from the HABSelect trial (4.5.4). The CP and LB/ET rates were

higher in PICSI patients with low damage in comparison with high damage (31 % *vs* 24 %, and 31 % *vs* 19 %, respectively), but these increases were not statistically significant. Conversely, CP and LB/ET rates were 10 % higher in the ICSI high damage group compared to low damage (38 % vs 28%, and 29 % vs 19 %), but again these differences were not statistically significant.

In light of these results we can conclude that a high percentage of AO-positive cells (>30 %) increases the chance of miscarriage (I), PICSI decreases the chance of miscarriage in comparison with ICSI by approximately 20 % (II), and that the decrease in miscarriage observed in the PICSI group is not related with a selection of sperm with low SDD but to other unknown mechanisms (III).

The number of patients used in this sub analysis was smaller than in the TUNEL sub analysis (134 *vs* 583) and therefore insufficiently powered to draw conclusions, although we consider it useful as a preliminary study. All the limitations explained in the TUNEL sub analysis (4.5.4) regarding treatment (ICSI / PICSI) and sample preparation (cryopreservation, gradients) also apply for our AO sub analysis. We consider that the conclusions obtained in this sub analysis should be interpreted with caution and therefore should be confirmed in a larger study with unprocessed and potentially fresh ejaculates for IVF rather than ICSI treatment.

4.5.6 Conclusion

Sperm DNA damage and its implication for fertility potential has been studied for several decades and an increase in sperm DNA damage has been observed in infertile men (Carrell *et al.*, 2003, Evenson *et al.*, 1999, Giwercman *et al.*, 2010, Spano *et al.*, 2000). SDD has also been correlated with miscarriage (Robinson *et al.*, 2012), although some authors found this correlation only in ICSI treatments and not IVF (Zhao *et al.*, 2014). Nevertheless, this evidence has not been considered sufficient for the inclusion of the sperm DNA damage assessment in the clinic as part of the routine investigation of infertility and miscarriage (Practice Committee of the American Society for Reproductive Medicine, 2013). We believe that the lack of consistent relationship between SDD and clinical outcomes, as well as the weak predictability for IVF and ICSI clinical pregnancies and miscarriage according to the American Society for Reproductive Medicine is mainly due to:

1. Studies with low number of subjects, lack of controls and validation of the thresholds used for the tests.
2. Lack of consensus regarding the most appropriate sample for the SDD assay (raw semen, prepared sperm by gradients or swim-up, frozen-thawed sperm)
3. Lack of standard protocols and cut-offs for the different SDD assays
4. Consideration of all the SDD assays as equivalent, while they give information about different aspects of the DNA integrity as we have demonstrated by the lack of correlation between AO, TUNEL and CMA_3.

The study performed in this chapter was insufficiently powered and had the limitations of using prepared and frozen-thawed sperm alongside the selection methods of ICSI and PICSI. I believe that assessing SDD with validated and objective protocols for

different SDD assays such as TUNEL, AO, SCSA, Comet, and CMA_3, as performed in this chapter, but in a larger number of fertile men and patients undergoing IVF and ICSI with no frozen sperm could help to find clinical thresholds for the individual SDD assays and to develop an algorithm to predict clinical outcomes based on the combination of information regarding DNA integrity obtained with the different assays.

To summarise:

- The distribution obtained for the AO and TUNEL results from the HABSelect patients was widely spread and skewed indicating the cause of infertility in some of the patients as high SDD.
- The correlation between AO and TUNEL appear to be moderate-strong when fresh samples are used, while this correlation disappears if frozen-thawed samples are used. According to our previous data in chapters 2 and 3, frozen samples increase their DFI (%) while they keep their TUNEL (%) with no significant changes.
- The sperm chromatin compaction tested by CMA_3 does not correlate with the TUNEL and AO assays in frozen samples from infertile patients. This experiment should be repeated with fresh samples for the reasons explained above.
- Patients with more than 30 % AO-positive cells have a greater chance of miscarriage when using ICSI or PICSI treatments.
- PICSI reduced the miscarriage rate in our patient data set, however this was not linked to the selection of lower-DNA damaged sperm. These results should be confirmed in fresh samples

CHAPTER 5: GENERAL DISCUSSION

5.1 Sperm DNA damage assessment, a controversial topic

Almost forty years have passed since the first Sperm DNA Damage (SDD) test was developed, SCSA (Evenson *et al.*, 1980a, Evenson *et al.*, 1980a, Evenson *et al.*, 1980b), there is still no agreement regarding which, if any test is best to use to diagnose male infertility and, or predict assisted reproduction outcomes. Over that time period IVF, ICSI and preimplantation genetic testing (PGT) have rapidly expanded the array of therapies available related to fertility but little has happened in terms of male diagnostic innovation.

Despite the accumulated evidence that indicates a link between SDD and male fertility and, or miscarriage, SDD has not been included as a routine test in the andrology laboratory (Practice Committee of the American Society for Reproductive Medicine, 2013). Conflicting results in meta-analysis are due to the inclusion and analysis of different SDD assays as if they measure same type of DNA damage, different sample preparation protocols, raw semen and frozen sperm, different methodology used to measure the signal as flow cytometry or fluorescence microscopy (see chapter 4). Special care should be taken when combining all these different variables in one single meta-analysis.

A key thing to note is that even though all the SDD tests are interrelated, they certainly measure different aspects of the DNA (Kirkman-Brown, J. C. and De Jonge, 2017, Lewis *et al.*, 2013), as corroborated by the lack of correlation found in our own research (see Chapter 4). Researchers are very busy trying to find the perfect test, when a better

approach could be the combination of several tests in order to have a better understanding of the SDD from the different information provided by the different assays. Equally certain tests may end up having no predictive value, but their constant use and adaptation whilst still being termed SDD confound understanding of an already complex dataset and clarity of what is happening.

Another important confounding factor in the study of the SDD, often neglected or not considered, is the ability of the oocyte to repair SDD; healthy young donors have higher quality oocytes that can repair SDD more efficiently that aged patients (Meseguer *et al.*, 2011) and therefore the age of the woman and the oocyte quality should be considered when assessing clinical outcomes from patients with SDD. The kind and extent of damage that can be repaired by the oocyte is not very well understood. We know SSB are more likely to be repaired by the oocyte than DSB (see Chapter 1). However, research would be advanced if the effects of different levels and types of damage induced by mechanisms such as radiation, oxidation and nuclease enzymatic reaction, were studied in relation to pregnancy and miscarriage (Ahmadi and Ng, 1999, Perez-Crespo *et al.*, 2008). Different types of damage, such as SSB or DSB could be quantified in human sperm, for example by using neutral and alkali comet, to study the effects of the type and extent of damage on the clinical outcomes in healthy oocyte donors and patients.

5.2 Value of the sperm DNA damage assessment

SDD testing is a promising and potentially powerful tool that has an additional value to the current sperm assessment based on morphology, concentration and motility.

Swimming sperm with normal morphology may still have their DNA or chromatin damaged and therefore SDD testing opens-up new therapies to improve sperm quality and the selection of sperm cells with high DNA integrity for use in ART.

The genetic details of what happens during SDD are not fully known. It would be interesting to study if the DNA damage occurs randomly in all the DNA or if there are specific regions of the genome that are more prone or vulnerable to suffer DNA damage. There is evidence regarding MAR regions enriched in histones and toroid linkers being more likely to suffer SDD as they are more accessible to nuclease and ROS (Ward, 2010). DNA linked to retained histones which form 15 % of the mammalian chromatin could be more susceptible to SDD. The promotor regions have been suggested as regions enriched in retained histones (Arpanahi *et al.*, 2009). Moreover, defects in the exchange between histones and protamines during the chromatin packing occurred during the spermiogenesis could lead to the presence of nicks in the DNA. If the sequences of DNA linked to protamines are conserved, specific genes proximal to protamines could be affected as a result of the deficient chromatin packing. It is also notable that the way chromosomes pack into a sperm follows a very specific organisational pattern (Ioannou *et al.*, 2011, Zalensky and Zalenskaya, 2007) meaning that certain areas of the genome are always more likely to be near the surface of the nucleus, whereas others may be deeper and more protected.

It could be argued the importance of assessing SDD as only 1.5 % of the genome consists in regions that code proteins, therefore, if there is any breakage, it is most likely to affect non-coding regions of the DNA based on the proportions of both types of DNA and probability. However, the functions of the remaining 98.5 % genome are unknown, and they should not be undervalued. These unknown regions could have structural functions or play important roles in regulation of gene expression and epigenetics (Allegrucci *et al.*, 2005, Dada *et al.*, 2012, Shapiro, 2005). Indeed many types of small non-coding RNAs, including microRNAs among others have been found in mammalian and human male germ cells and to play important regulatory roles in spermatogenesis (Chen *et al.*, 2016, Chu *et al.*, 2017) and some of them have been proposed as prognostic biomarkers for evaluating sperm quality for IVF (Hua *et al.*, 2019). Moreover, sperm RNA can be delivered into the oocyte and directly impact the phenotype of the future offspring via epigenetic inheritance (Bohacek and Rassoulzadegan, 2019).

Nevertheless, data showing a decrease in embryo quality and pregnancy, and an increase in miscarriage with ART (see chapter 1, 1.7.2), seem to confirm the clinical relevance of SDD and therefore its assessment. SDD can give explanation to many couples suffering from unexplained infertility but its use to change treatment modality may also increase the chances of successful pregnancy and live birth in patients with high SDD. The data currently support that ICSI can by-pass some levels of SDD (Lewis, 2015). The reasons why ICSI is more efficient that IVF in achieving pregnancy could be due to several reasons. Sperm cells used in ICSI are directly injected into the ooplasm within a few hours of ejaculation whilst in IVF they are exposed to a prolonged culture which is not their natural environment. A good proportion of infertile patients

have high levels of ROS and low antioxidant content (Aitken *et al.*, 2012), hence the long coculture with oocytes during IVF might increase the amount of ROS released by defective sperm and affect the oocytes diminishing their DNA repair ability (Lewis, 2015).

When the origin of the SDD is due to high levels of ROS, lifestyle changes and a diet rich in antioxidants could be advised to normalise the balance between oxidants and antioxidants in order to decrease SDD and boost the natural conception and the outcome of ART (Majzoub *et al.*, 2017, Showell *et al.*, 2014). However, according to a recent meta-analysis (Smits *et al.*, 2019), there is no enough evidence that antioxidant therapy increases LB or decreases miscarriage in subfertile men. The meta-analysis found an increase in CP in subfertile men treated with antioxidants compared to the placebo or no treatment groups, however, this evidence was based on 105 clinical pregnancies from 786 couples in 11 small studies and therefore low-quality (Smits *et al.*, 2019). Many of the publications studied for inclusion in the meta-analysis had poor reporting of methods of randomisation, failed to report live birth and clinical pregnancy rates, and were quite small in sample size (Smits *et al.*, 2019). Hence, further well-designed and larger placebo-controlled trials with CP, live birth and miscarriage as main outcomes are required to assess the benefits of antioxidant therapy in infertile and subfertile men.

Another approach consists in selecting those sperm cells with low or no damage for ART. Different techniques have been developed to physiologically select sperm cells with low damage based on electronegativity (electrophoresis and Z-potential techniques), apoptosis (selection of non-apoptotic sperm by MACS columns), and ultra-morphology (Intracytoplasmic Morphological Sperm Injection (IMSI)) (Yetunde

and Vasiliki, 2013). Placebo-controlled studies should be performed to investigate the benefits of using these selecting methods prior to ART as they could offer great improvements in the clinical outcomes whilst being cost-effective.

Sperm testicular retrieval has also been proposed to select sperm cells that have not been exposed to ROS during the epididymal transit in men with high SDD (Kovac and Lipshultz, 2016). Despite the need for further confirmatory research, with high-quality and larger sample, the current evidence corroborates the benefits and safety of sperm testicular retrieval for ICSI in non-azoospermic men with high SDD in semen to increase the CP rates (Lopes and Esteves, 2019).

Sperm can also be selected by the hyaluronan binding assay (HBA) based on membrane maturity as this has been correlated to normal nuclear morphology and compaction, fewer chromosomal anomalies and less DNA fragmentation (Jakab *et al.*, 2005, Parmegiani *et al.*, 2010). In the HABSelect trial explained in detail in Chapter 4, all the DNA damage assays correlated with the HA-binding assay, TUNEL assay being the most strongly correlated (Kirkman-Brown, J. *et al.*, 2019). Although no differences were found for the CP, preterm live birth rate (before 37 weeks' gestational age) or LB rates, a significant decrease in miscarriage was found in the experimental group. A further analysis of the miscarriages showed that this decrease in miscarriage corresponded to women over 37 years whilst women under 37 had similar miscarriage rate in both groups. This finding supports the idea that older women had lower quality oocytes and therefore are more likely to fail to repair sperm DNA and experience miscarriage. Therefore, couples formed between men with SDD and older women undergoing ART could benefit from using PICSI by reducing their miscarriage rate.

In Chapter 4 we tested the effects in clinical outcome of high SDD assessed by TUNEL in prepared sperm in a subset of patients of HABSelect. No statistical difference was found between patients with low and high TUNEL in regards to CP or LB/ET. ICSI patients with low TUNEL exhibited higher miscarriage rate compared to the high TUNEL group. However this might be due to the reduced sample size for that specific group (30 pregnancies and 1 miscarriage). Despite the study being performed with optimised SDD assays and scoring methods, the percentage of damage was calculated in the whole prepared sperm and not in the picked sperm by the embryologist which is more likely to have higher quality than the rest of sperm. Moreover, the sperm samples for SDD assessment were shipped frozen which could affect the integrity of the DNA, increasing and biasing the original SDD. For these reasons, this study should be repeated in raw semen and prepared sperm, in a larger number of patients undertaking IVF and ICSI treatment.

5.3 Sperm DNA damage can be an affordable, objective and reproducible tool for personalised reproductive medicine

I believe my research has contributed to develop and optimise slide-based tests for the assessment of SDD. These slide-based tests combined with consistent and reproducible scoring systems validated in this thesis allow the user the quick, objective, affordable and user-friendly assessment of the SDD of thousands of cells by using fluorescence microscopy. This methodology does not need the use of expensive flow cytometry, which is one of the main factors holding back SDD assessment of being

broadly available to researchers and patients. The baseline methods and findings presented, such as on mountants, provide key groundwork for any future studies.

It would be interesting to compare results using our methodology and flow cytometry. An association or correlation should be expected between both scorings when both methodologies have been properly calibrated in terms of equivalence between the photomultiplier gains of the flow cytometry and time exposure and gain of the fluorescence microscopy. The gating method used in flow cytometry should also be compared with the size and shape factor filters applied for the single-cell data extraction in fluorescence microscopy.

In summary, in light of the results from the validation tests with positive controls and intra-assay variability, I believe the methodology developed for the staining and scoring of damaged cells by using fluorescence microscopy as described in this thesis offers a cheaper and more reproducible version of the AO and TUNEL assays and could help towards the implementation of the SDD assessment in the routine for the diagnosis of infertility and miscarriage. The number of available donors was very limited and there is no guarantee that they were free of SDD, therefore the clinical thresholds suggested in this thesis should only be considered as a guidance. Further research should include the assessment of SDD by the standardised and developed tests included in this thesis in a reasonable number of controls, IVF and ICSI patients in order to correlate the SDD to clinical pregnancy and miscarriage and obtain clinical thresholds to predict the success of the different assisted reproductive treatments.

By assessing the SDD in a subset of 583 patients from HABSelect we could not find any correlation between TUNEL (%) and CP or miscarriage. However, as commented

above ICSI has been suggested to by-pass DNA damage. HABSelect did demonstrate a strong and significant reduction in miscarriage after PICSI was performed. We hypothesise that the cause of this difference is likely to be due to selection against SDD-laden cells, but this was not detected as we are only examining prepared sperm cells.

5.4 Final conclusions

SDD testing still needs further improvements, such as the validation of clinical thresholds for the different patient conditions like infertility and miscarriage, and agreement in the best sample preparation and methodology to visualise and quantify the damage. Whilst we are close to finding all the unknowns, there is no doubt that SDD is a promising and valuable parameter, and that with further effort and perseverance could become a primary tool in infertility.

REFERENCES

Adewoyin M, Ibrahim M, Roszaman R, Isa MLM, Alewi NAM, Rafa AAA, Anuar MNN. Male Infertility: The Effect of Natural Antioxidants and Phytocompounds on Seminal Oxidative Stress. *Diseases* 2017;**5**:10.3390/diseases5010009.

Afanas'eva KS, Zazhitskaia MO, Sivolob AV. Mechanisms of DNA exit during neutral and alkaline comet assay. *Tsitol Genet* 2009;**43**:3-7.

Agarwal A, Sharma R. Spermatogenesis: An Overview. Agarwal A. and Zini A (eds). Sperm Chromatin: Biological and Clinical Applications in Male Infertility and Assisted Reproduction2011. Springer, New York, pp. 31.

Agarwal A, Gupta S, Du Plessis S, Sharma R, Esteves SC, Cirenza C, Eliwa J, Al-Najjar W, Kumaresan D, Haroun N *et al.* Abstinence Time and Its Impact on Basic and Advanced Semen Parameters. *Urology* 2016;**94**:102-110.

Agarwal A, Saleh RA, Bedaiwy MA. Role of reactive oxygen species in the pathophysiology of human reproduction. *Fertil Steril* 2003;**79**:829-843.

Agarwal A, Sekhon LH. Oxidative stress and antioxidants for idiopathic oligoasthenoteratospermia: Is it justified? *Indian J Urol* 2011;**27**:74-85.

Ahmadi A, Ng SC. Fertilizing ability of DNA-damaged spermatozoa. *J Exp Zool* 1999;**284**:696-704.

Aitken RJ. The capacitation-apoptosis highway: oxysterols and mammalian sperm function. *Biol Reprod* 2011;**85**:9-12.

Aitken RJ, Baker MA. Causes and consequences of apoptosis in spermatozoa; contributions to infertility and impacts on development. *Int J Dev Biol* 2013;**57**:265-272.

Aitken RJ, Buckingham D, Harkiss D. Use of a xanthine oxidase free radical generating system to investigate the cytotoxic effects of reactive oxygen species on human spermatozoa. *J Reprod Fertil* 1993;**97**:441-450.

Aitken RJ, Curry BJ. Redox regulation of human sperm function: from the physiological control of sperm capacitation to the etiology of infertility and DNA damage in the germ line. *Antioxid Redox Signal* 2011;**14**:367-381.

Aitken RJ, De Iuliis GN. On the possible origins of DNA damage in human spermatozoa. *Mol Hum Reprod* 2010;**16**:3-13.

Aitken RJ, De Iuliis GN, McLachlan RI. Biological and clinical significance of DNA damage in the male germ line. *Int J Androl* 2009;**32**:46-56.

Aitken RJ, Fisher HM, Fulton N, Gomez E, Knox W, Lewis B, Irvine S. Reactive oxygen species generation by human spermatozoa is induced by exogenous NADPH and inhibited by the flavoprotein inhibitors diphenylene iodonium and quinacrine. *Mol Reprod Dev* 1997;**47**:468-482.

Aitken RJ, Gibb Z, Mitchell LA, Lambourne SR, Connaughton HS, De Iuliis GN. Sperm motility is lost in vitro as a consequence of mitochondrial free radical production and the generation of electrophilic aldehydes but can be significantly rescued by the presence of nucleophilic thiols. *Biol Reprod* 2012;**87**:110.

Aitken RJ, Jones KT, Robertson SA. Reactive oxygen species and sperm function--in sickness and in health. *J Androl* 2012;**33**:1096-1106.

Aitken RJ, Paterson M, Fisher H, Buckingham DW, van Duin M. Redox regulation of tyrosine phosphorylation in human spermatozoa and its role in the control of human sperm function. *J Cell Sci* 1995;**108 (Pt 5)**:2017-2025.

Aitken RJ, Smith TB, Jobling MS, Baker MA, De Iuliis GN. Oxidative stress and male reproductive health. *Asian J Androl* 2014;**16**:31-38.

Aizpurua J, Medrano L, Enciso M, Sarasa J, Romero A, Fernandez MA, Gomez-Torres MJ. New permeable cryoprotectant-free vitrification method for native human sperm. *Hum Reprod* 2017;**32**:2007-2015.

Allegrucci C, Thurston A, Lucas E, Young L. Epigenetics and the germline. *Reproduction* 2005;**129**:137-149.

Almeida C, Sousa M, Barros A. Phosphatidylserine translocation in human spermatozoa from impaired spermatogenesis. *Reprod Biomed Online* 2009;**19**:770-777.

Amor H, Shelko N, Hamad MF, Zeyad A, Hammadeh ME. An additional marker for sperm DNA quality evaluation in spermatozoa of male partners of couples undergoing assisted reproduction technique (IVF/ICSI): Protamine ratio. *Andrologia* 2019;:e13400.

Amor H, Zeyad A, Alkhaled Y, Laqqan M, Saad A, Ben Ali H, Hammadeh ME. Relationship between nuclear DNA fragmentation, mitochondrial DNA damage and standard sperm parameters in spermatozoa of fertile and sub-fertile men before and after freeze-thawing procedure. *Andrologia* 2018;**50**:e12998.

Ankem MK, Mayer E, Ward WS, Cummings KB, Barone JG. Novel assay for determining DNA organization in human spermatozoa: implications for male factor infertility. *Urology* 2002;**59**:575-578.

Aoki VW, Liu L, Carrell DT. Identification and evaluation of a novel sperm protamine abnormality in a population of infertile males. *Hum Reprod* 2005;**20**:1298-1306.

Arpanahi A, Brinkworth M, Iles D, Krawetz SA, Paradowska A, Platts AE, Saida M, Steger K, Tedder P, Miller D. Endonuclease-sensitive regions of human spermatozoal chromatin are highly enriched in promoter and CTCF binding sequences. *Genome Res* 2009;**19**:1338-1349.

Audebert M, Salles B, Calsou P. Involvement of poly(ADP-ribose) polymerase-1 and XRCC1/DNA ligase III in an alternative route for DNA double-strand breaks rejoining. *J Biol Chem* 2004;**279**:55117-55126.

Avendano C, Franchi A, Taylor S, Morshedi M, Bocca S, Oehninger S. Fragmentation of DNA in morphologically normal human spermatozoa. *Fertil Steril* 2009;**91**:1077-1084.

Ayad BM, Horst GV, Plessis SSD. Revisiting The Relationship between The Ejaculatory Abstinence Period and Semen Characteristics. *Int J Fertil Steril* 2018;**11**:238-246.

Aydos OS, Yukselten Y, Kaplan F, Sunguroglu A, Aydos K. Analysis of the correlation between sperm DNA integrity and conventional semen parameters in infertile men. *Turk J Urol* 2015;**41**:191-197.

Bahceci M, Ulug U. Does underlying infertility aetiology impact on first trimester miscarriage rate following ICSI? A preliminary report from 1244 singleton gestations. *Hum Reprod* 2005;**20**:717-721.

Bareh GM, Jacoby E, Binkley P, Chang TC, Schenken RS, Robinson RD. Sperm deoxyribonucleic acid fragmentation assessment in normozoospermic male partners of couples with unexplained recurrent pregnancy loss: a prospective study. *Fertil Steril* 2016;**105**:329-36.e1.

Barratt CL, Aitken RJ, Bjorndahl L, Carrell DT, de Boer P, Kvist U, Lewis SE, Perreault SD, Perry MJ, Ramos L *et al.* Sperm DNA: organization, protection and vulnerability: from basic science to clinical applications--a position report. *Hum Reprod* 2010;**25**:824-838.

Barratt CL, Bjorndahl L, Menkveld R, Mortimer D. ESHRE special interest group for andrology basic semen analysis course: a continued focus on accuracy, quality, efficiency and clinical relevance. *Hum Reprod* 2011;**26**:3207-3212.

Barros C, Gonzalez J, Herrera E, Bustos-Obregon E. Human sperm penetration into zona-free hamster oocytes as a test to evaluate the sperm fertilizing ability. *Andrologia* 1979;**11**:197-210.

Bedford JM. The status and the state of the human epididymis. *Hum Reprod* 1994;**9**:2187-2199.

Bedford JM, Calvin HI. The occurrence and possible functional significance of -S-S- crosslinks in sperm heads, with particular reference to eutherian mammals. *J Exp Zool* 1974;**188**:137-155.

Burkman LJ, Coddington CC, Franken DR, Krugen TF, Rosenwaks Z, Hogen GD. The hemizona assay (HZA): development of a diagnostic test for the binding of human spermatozoa to the human hemizona pellucida to predict fertilization potential. *Fertil Steril* 1988;**49**:688-697.

Benchaib M, Lornage J, Mazoyer C, Lejeune H, Salle B, Francois Guerin J. Sperm deoxyribonucleic acid fragmentation as a prognostic indicator of assisted reproductive technology outcome. *Fertil Steril* 2007;**87**:93-100.

Bianchi PG, Manicardi GC, Urner F, Campana A, Sakkas D. Chromatin packaging and morphology in ejaculated human spermatozoa: evidence of hidden anomalies in normal spermatozoa. *Mol Hum Reprod* 1996;**2**:139-144.

Bland JM, Altman DG. Measurement error. *BMJ* 1996;**313**:744.

Boe-Hansen GB, Fedder J, Ersboll AK, Christensen P. The sperm chromatin structure assay as a diagnostic tool in the human fertility clinic. *Hum Reprod* 2006;**21**:1576-1582.

Boerke A, Brouwers JF, Olkkonen VM, van de Lest CH, Sostaric E, Schoevers EJ, Helms JB, Gadella BM. Involvement of bicarbonate-induced radical signaling in oxysterol formation and sterol depletion of capacitating mammalian sperm during in vitro fertilization. *Biol Reprod* 2013;**88**:21.

Bohacek J, Rassoulzadegan M. Sperm RNA: Quo vadis? *Semin Cell Dev Biol* 2019;.

Borini A, Tarozzi N, Bizzaro D, Bonu MA, Fava L, Flamigni C, Coticchio G. Sperm DNA fragmentation: paternal effect on early post-implantation embryo development in ART. *Hum Reprod* 2006;**21**:2876-2881.

Brahem S, Mehdi M, Landolsi H, Mougou S, Elghezal H, Saad A. Semen parameters and sperm DNA fragmentation as causes of recurrent pregnancy loss. *Urology* 2011;**78**:792-796.

Brown J, Brown T, Fox KR. Affinity of mismatch-binding protein MutS for heteroduplexes containing different mismatches. *Biochem J* 2001;**354**:627-633.

Buckett WM, Chian RC, Dean NL, Sylvestre C, Holzer HE, Tan SL. Pregnancy loss in pregnancies conceived after in vitro oocyte maturation, conventional in vitro fertilization, and intracytoplasmic sperm injection. *Fertil Steril* 2008;**90**:546-550.

Bungum M, Bungum L, Giwercman A. Sperm chromatin structure assay (SCSA): a tool in diagnosis and treatment of infertility. *Asian J Androl* 2011a;**13**:69-75.

Bungum M, Bungum L, Giwercman A. Sperm chromatin structure assay (SCSA): a tool in diagnosis and treatment of infertility. *Asian J Androl* 2011b;**13**:69-75.

Bungum M, Humaidan P, Axmon A, Spano M, Bungum L, Erenpreiss J, Giwercman A. Sperm DNA integrity assessment in prediction of assisted reproduction technology outcome. *Hum Reprod* 2007;**22**:174-179.

Bungum M, Humaidan P, Spano M, Jepson K, Bungum L, Giwercman A. The predictive value of sperm chromatin structure assay (SCSA) parameters for the outcome of intrauterine insemination, IVF and ICSI. *Hum Reprod* 2004;**19**:1401-1408.

Carlini T, Paoli D, Pelloni M, Faja F, Dal Lago A, Lombardo F, Lenzi A, Gandini L. Sperm DNA fragmentation in Italian couples with recurrent pregnancy loss. *Reprod Biomed Online* 2017;**34**:58-65.

Carrell DT, Liu L, Peterson CM, Jones KP, Hatasaka HH, Erickson L, Campbell B. Sperm DNA fragmentation is increased in couples with unexplained recurrent pregnancy loss. *Arch Androl* 2003;**49**:49-55.

Cates W, Farley TM, Rowe PJ. Worldwide patterns of infertility: is Africa different? *Lancet* 1985;**2**:596-598.

Check JH, Graziano V, Cohen R, Krotec J, Check ML. Effect of an abnormal sperm chromatin structural assay (SCSA) on pregnancy outcome following (IVF) with ICSI in previous IVF failures. *Arch Androl* 2005;**51**:121-124.

Chen J, Jin K, Chen M, Pei W, Kawaguchi K, Greenberg DA, Simon RP. Early detection of DNA strand breaks in the brain after transient focal ischemia: implications for the role of DNA damage in apoptosis and neuronal cell death. *J Neurochem* 1997;**69**:232-245.

Chen Q, Yan W, Duan E. Epigenetic inheritance of acquired traits through sperm RNAs and sperm RNA modifications. *Nat Rev Genet* 2016;**17**:733-743.

Chi HJ, Kim SG, Kim YY, Park JY, Yoo CS, Park IH, Sun HG, Kim JW, Lee KH, Park HD. ICSI significantly improved the pregnancy rate of patients with a high sperm DNA fragmentation index. *Clin Exp Reprod Med* 2017;**44**:132-140.

Cho CL, Agarwal A. Role of sperm DNA fragmentation in male factor infertility: A systematic review. *Arab J Urol* 2017;**16**:21-34.

Choi HY, Kim SK, Kim SH, Choi YM, Jee BC. Impact of sperm DNA fragmentation on clinical in vitro fertilization outcomes. *Clin Exp Reprod Med* 2017;**44**:224-231.

Christova Y, James PS, Jones R. Lipid diffusion in sperm plasma membranes exposed to peroxidative injury from oxygen free radicals. *Mol Reprod Dev* 2004;**68**:365-372.

Chu C, Yu L, Wu B, Ma L, Gou LT, He M, Guo Y, Li ZT, Gao W, Shi H *et al.* A sequence of 28S rRNA-derived small RNAs is enriched in mature sperm and various somatic tissues and possibly associates with inflammation. *J Mol Cell Biol* 2017;**9**:256-259.

Cissen M, Wely MV, Scholten I, Mansell S, Bruin JP, Mol BW, Braat D, Repping S, Hamer G. Measuring Sperm DNA Fragmentation and Clinical Outcomes of Medically Assisted Reproduction: A Systematic Review and Meta-Analysis. *PLoS One* 2016;**11**:e0165125.

Clermont Y. Spermatogenesis in man. A study of the spermatogonial population. *Fertil Steril* 1966;**17**:705-721.

Cohen-Bacrie P, Belloc S, Menezo YJ, Clement P, Hamidi J, Benkhalifa M. Correlation between DNA damage and sperm parameters: a prospective study of 1,633 patients. *Fertil Steril* 2009;**91**:1801-1805.

Collins JA, Barnhart KT, Schlegel PN. Do sperm DNA integrity tests predict pregnancy with in vitro fertilization? *Fertil Steril* 2008;**89**:823-831.

Comar VA, Petersen CG, Mauri AL, Mattila M, Vagnini LD, Renzi A, Petersen B, Nicoletti A, Dieamant F, Oliveira JBA *et al.* Influence of the abstinence period on human sperm quality: analysis of 2,458 semen samples. *JBRA Assist Reprod* 2017;**21**:306-312.

Cook PR, Brazell IA. Spectrofluorometric measurement of the binding of ethidium to superhelical DNA from cell nuclei. *Eur J Biochem* 1978;**84**:465-477.

Corzett M, Mazrimas J, Balhorn R. Protamine 1: protamine 2 stoichiometry in the sperm of eutherian mammals. *Mol Reprod Dev* 2002;**61**:519-527.

Coughlan C, Clarke H, Cutting R, Saxton J, Waite S, Ledger W, Li T, Pacey AA. Sperm DNA fragmentation, recurrent implantation failure and recurrent miscarriage. *Asian J Androl* 2015;**17**:681-685.

Dada R, Kumar M, Jesudasan R, Fernandez JL, Gosalvez J, Agarwal A. Epigenetics and its role in male infertility. *J Assist Reprod Genet* 2012;**29**:213-223.

D'Agata R, Vicari E, Moncada ML, Sidoti G, Calogero AE, Fornito MC, Minacapilli G, Mongioi A, Polosa P. Generation of reactive oxygen species in subgroups of infertile men. *Int J Androl* 1990;**13**:344-351.

Darzynkiewicz Z, Traganos F, Sharpless T, Melamed MR. Thermal denaturation of DNA in situ as studied by acridine orange staining and automated cytofluorometry. *Exp Cell Res* 1975a;**90**:411-428.

Darzynkiewicz Z, Traganos F, Sharpless T, Melamed MR. Thermal denaturation of DNA in situ as studied by acridine orange staining and automated cytofluorometry. *Exp Cell Res* 1975b;**90**:411-428.

Das UB, Mallick M, Debnath JM, Ghosh D. Protective effect of ascorbic acid on cyclophosphamide- induced testicular gametogenic and androgenic disorders in male rats. *Asian J Androl* 2002;**4**:201-207.

Davison FD, Groves M, Scaravilli F. The effects of formalin fixation on the detection of apoptosis in human brain by in situ end-labelling of DNA. *Histochem J* 1995;**27**:983-988.

De Iuliis GN, Newey RJ, King BV, Aitken RJ. Mobile phone radiation induces reactive oxygen species production and DNA damage in human spermatozoa in vitro. *PLoS One* 2009;**4**:e6446.

De Iuliis GN, Thomson LK, Mitchell LA, Finnie JM, Koppers AJ, Hedges A, Nixon B, Aitken RJ. DNA damage in human spermatozoa is highly correlated with the efficiency of chromatin remodeling and the formation of 8-hydroxy-2'-deoxyguanosine, a marker of oxidative stress. *Biol Reprod* 2009;**81**:517-524.

de Lamirande E, O'Flaherty C. Sperm activation: role of reactive oxygen species and kinases. *Biochim Biophys Acta* 2008;**1784**:106-115.

Deng C, Li T, Xie Y, Guo Y, Yang QY, Liang X, Deng CH, Liu GH. Sperm DNA fragmentation index influences assisted reproductive technology outcome: A systematic review and meta-analysis combined with a retrospective cohort study. *Andrologia* 2019;**51**:e13263.

Deng G, Wu R. Terminal transferase: use of the tailing of DNA and for in vitro mutagenesis. *Methods Enzymol* 1983;**100**:96-116.

Derijck A, van der Heijden G, Giele M, Philippens M, de Boer P. DNA double-strand break repair in parental chromatin of mouse zygotes, the first cell cycle as an origin of de novo mutation. *Hum Mol Genet* 2008;**17**:1922-1937.

Devroey P, Van Steirteghem A. A review of ten years experience of ICSI. *Hum Reprod Update* 2004;**10**:19-28.

Di Santo M, Tarozzi N, Nadalini M, Borini A. Analysis of Sperm DNA Fragmentation and Aneuploidy in 109 Infertile Patients. Are the Two Parameters Correlated? *Gynecol Obstet Case Rep* 2016;**2:2**.

Didenko VV, Hornsby PJ. Presence of double-strand breaks with single-base 3' overhangs in cells undergoing apoptosis but not necrosis. *J Cell Biol* 1996;**135**:1369-1376.

Dmitrieva N, Burg M. Osmotic stress and DNA damage. Häussinger D and Sies H (eds). 2007. Elsevier, San Diego, California, pp. 241-253.

Dominguez-Fandos D, Camejo MI, Ballesca JL, Oliva R. Human sperm DNA fragmentation: correlation of TUNEL results as assessed by flow cytometry and optical microscopy. *Cytometry A* 2007;**71**:1011-1018.

Donnelly ET, McClure N, Lewis SE. Cryopreservation of human semen and prepared sperm: effects on motility parameters and DNA integrity. *Fertil Steril* 2001;**76**:892-900.

Duran EH, Morshedi M, Taylor S, Oehninger S. Sperm DNA quality predicts intrauterine insemination outcome: a prospective cohort study. *Hum Reprod* 2002;**17**:3122-3128.

Eisenberg ML, Sapra KJ, Kim SD, Chen Z, Buck Louis GM. Semen quality and pregnancy loss in a contemporary cohort of couples recruited before conception: data from the Longitudinal Investigation of Fertility and the Environment (LIFE) Study. *Fertil Steril* 2017;**108**:613-619.

Encyclopaedia Britannica. www.britannica.com/science/human-reproductive-system#/media/1/498625/101919. 2012;**Accessed: 16 September 2019**.

Erel O. A new automated colorimetric method for measuring total oxidant status. *Clin Biochem* 2005;**38**:1103-1111.

Erenpreiss J, Bars J, Lipatnikova V, Erenpreisa J, Zalkalns J. Comparative study of cytochemical tests for sperm chromatin integrity. *J Androl* 2001;**22**:45-53.

Erenpreiss J, Bungum M, Spano M, Elzanaty S, Orbidans J, Giwercman A. Intra-individual variation in sperm chromatin structure assay parameters in men from infertile couples: clinical implications. *Hum Reprod* 2006;**21**:2061-2064.

Esbert M, Pacheco A, Vidal F, Florensa M, Riqueros M, Ballesteros A, Garrido N, Calderon G. Impact of sperm DNA fragmentation on the outcome of IVF with own or donated oocytes. *Reprod Biomed Online* 2011;**23**:704-710.

Evenson DP. Chapter 4. Sperm Chromatin Structure Assay (SCSA (R)). Evolution from origin to clinical utility. Agarwal A and Zini A (eds). A Clinician's Guide to Sperm DNA and Chromatin Damage2018. Springer, Switzerland, pp. 65.

Evenson DP. Sperm Chromatin Structure Assay (SCSA®): 30 Years of Experience with the SCSA®. Zini A and Agarwal A (eds). Sperm Chromatin2011. Springer, New York, NY.

Evenson DP. Evaluation of sperm chromatin structure and DNA strand breaks is an important part of clinical male fertility assessment. *Transl Androl Urol* 2017;**6**:S495-S500.

Evenson DP. The Sperm Chromatin Structure Assay (SCSA((R))) and other sperm DNA fragmentation tests for evaluation of sperm nuclear DNA integrity as related to fertility. *Anim Reprod Sci* 2016;**169**:56-75.

Evenson DP. Sperm chromatin structure assay (SCSA(R)). *Methods Mol Biol* 2013a;**927**:147-164.

Evenson DP. Sperm chromatin structure assay (SCSA(R)). *Methods Mol Biol* 2013b;**927**:147-164.

Evenson DP, Baer RK, Jost LK. Long-term effects of triethylenemelamine exposure on mouse testis cells and sperm chromatin structure assayed by flow cytometry. *Environ Mol Mutagen* 1989;**14**:79-89.

Evenson DP, Darzynkiewicz Z, Melamed MR. Comparison of human and mouse sperm chromatin structure by flow cytometry. *Chromosoma* 1980a;**78**:225-238.

Evenson DP, Darzynkiewicz Z, Melamed MR. Relation of mammalian sperm chromatin heterogeneity to fertility. *Science* 1980b;**210**:1131-1133.

Evenson DP, Jost LK, Baer RK, Turner TW, Schrader SM. Individuality of DNA denaturation patterns in human sperm as measured by the sperm chromatin structure assay. *Reprod Toxicol* 1991;**5**:115-125.

Evenson DP, Jost LK, Marshall D, Zinaman MJ, Clegg E, Purvis K, de Angelis P, Claussen OP. Utility of the sperm chromatin structure assay as a diagnostic and prognostic tool in the human fertility clinic. *Hum Reprod* 1999;**14**:1039-1049.

Evenson DP, Larson KL, Jost LK. Sperm chromatin structure assay: its clinical use for detecting sperm DNA fragmentation in male infertility and comparisons with other techniques. *J Androl* 2002;**23**:25-43.

Evenson DP, Thompson L, Jost L. Flow cytometric evaluation of boar semen by the sperm chromatin structure assay as related to cryopreservation and fertility. *Theriogenology* 1994;**41**:637-651.

Evgeni E, Lymberopoulos G, Gazouli M, Asimakopoulos B. Conventional semen parameters and DNA fragmentation in relation to fertility status in a Greek population. *Eur J Obstet Gynecol Reprod Biol* 2015;**188**:17-23.

Fagbemi AF, Orelli B, Scharer OD. Regulation of endonuclease activity in human nucleotide excision repair. *DNA Repair (Amst)* 2011;**10**:722-729.

Fawcett DW. The mammalian spermatozoon. *Dev Biol* 1975;**44**:394-436.

Fawcett DW, Ito S, Slautterback D. The occurrence of intercellular bridges in groups of cells exhibiting synchronous differentiation. *J Biophys Biochem Cytol* 1959;**5**:453-460.

Fawcett DW, Phillips DM. The fine structure and development of the neck region of the mammalian spermatozoon. *Anat Rec* 1969;**165**:153-164.

Fernandez JL, Muriel L, Rivero MT, Goyanes V, Vazquez R, Alvarez JG. The sperm chromatin dispersion test: a simple method for the determination of sperm DNA fragmentation. *J Androl* 2003;**24**:59-66.

Fernandez-Gonzalez R, Moreira PN, Perez-Crespo M, Sanchez-Martin M, Ramirez MA, Pericuesta E, Bilbao A, Bermejo-Alvarez P, de Dios Hourcade J, de Fonseca FR *et al.* Long-term effects of mouse intracytoplasmic sperm injection with DNA-fragmented sperm on health and behavior of adult offspring. *Biol Reprod* 2008;**78**:761-772.

Finch JT, Klug A. Solenoidal model for superstructure in chromatin. *Proc Natl Acad Sci U S A* 1976;**73**:1897-1901.

Fisher HM, Aitken RJ. Comparative analysis of the ability of precursor germ cells and epididymal spermatozoa to generate reactive oxygen metabolites. *J Exp Zool* 1997;**277**:390-400.

Fishman EL, Jo K, Nguyen QPH, Kong D, Royfman R, Cekic AR, Khanal S, Miller AL, Simerly C, Schatten G *et al.* A novel atypical sperm centriole is functional during human fertilization. *Nat Commun* 2018;**9**:2210-018-04678-8.

Ford WC. Regulation of sperm function by reactive oxygen species. *Hum Reprod Update* 2004;**10**:387-399.

Forti G, Krausz C. Clinical review 100: Evaluation and treatment of the infertile couple. *J Clin Endocrinol Metab* 1998;**83**:4177-4188.

Franken DR, Bastiaan HS, Oehninger SC. Physiological induction of the acrosome reaction in human sperm: validation of a microassay using minimal volumes of solubilized, homologous zona pellucida. *J Assist Reprod Genet* 2000;**17**:374-378.

Frydman N, Prisant N, Hesters L, Frydman R, Tachdjian G, Cohen-Bacrie P, Fanchin R. Adequate ovarian follicular status does not prevent the decrease in pregnancy rates associated with high sperm DNA fragmentation. *Fertil Steril* 2008;**89**:92-97.

Ganzer L, Sad Larcher J, Avramovich V, Tissera A, Estofan G. Relationship between semen parameters and sperm DNA fragmentation. *Fertil Steril* 2017;**108**:e137.

Garolla A, Cosci I, Bertoldo A, Sartini B, Boudjema E, Foresta C. DNA double strand breaks in human spermatozoa can be predictive for assisted reproductive outcome. *Reprod Biomed Online* 2015;**31**:100-107.

Gatewood JM, Cook GR, Balhorn R, Schmid CW, Bradbury EM. Isolation of four core histones from human sperm chromatin representing a minor subset of somatic histones. *J Biol Chem* 1990;**265**:20662-20666.

Gavrieli Y, Sherman Y, Ben-Sasson SA. Identification of programmed cell death in situ via specific labeling of nuclear DNA fragmentation. *J Cell Biol* 1992;**119**:493-501.

Gawecka JE, Marh J, Ortega M, Yamauchi Y, Ward MA, Ward WS. Mouse zygotes respond to severe sperm DNA damage by delaying paternal DNA replication and embryonic development. *PLoS One* 2013;**8**:e56385.

Gervasi MG, Visconti PE. Molecular changes and signaling events occurring in spermatozoa during epididymal maturation. *Andrology* 2017;**5**:204-218.

Gharagozloo P, Aitken RJ. The role of sperm oxidative stress in male infertility and the significance of oral antioxidant therapy. *Hum Reprod* 2011;**26**:1628-1640.

Ghosh D, Das UB, Misro M. Protective role of alpha-tocopherol-succinate (provitamin-E) in cyclophosphamide induced testicular gametogenic and steroidogenic disorders: a correlative approach to oxidative stress. *Free Radic Res* 2002;**36**:1209-1218.

Giwercman A, Lindstedt L, Larsson M, Bungum M, Spano M, Levine RJ, Rylander L. Sperm chromatin structure assay as an independent predictor of fertility in vivo: a case-control study. *Int J Androl* 2010;**33**:e221-7.

Giwercman A, Richthoff J, Hjollund H, Bonde JP, Jepson K, Frohm B, Spano M. Correlation between sperm motility and sperm chromatin structure assay parameters. *Fertil Steril* 2003;**80**:1404-1412.

Gold R, Schmied M, Giegerich G, Breitschopf H, Hartung HP, Toyka KV, Lassmann H. Differentiation between cellular apoptosis and necrosis by the combined use of in situ tailing and nick translation techniques. *Lab Invest* 1994;**71**:219-225.

Gonzalez-Marin C, Gosalvez J, Roy R. Types, causes, detection and repair of DNA fragmentation in animal and human sperm cells. *Int J Mol Sci* 2012;**13**:14026-14052.

Govin J, Caron C, Escoffier E, Ferro M, Kuhn L, Rousseaux S, Eddy EM, Garin J, Khochbin S. Post-meiotic shifts in HSPA2/HSP70.2 chaperone activity during mouse spermatogenesis. *J Biol Chem* 2006;**281**:37888-37892.

Gunes S, Al-Sadaan M, Agarwal A. Spermatogenesis, DNA damage and DNA repair mechanisms in male infertility. *Reprod Biomed Online* 2015;**31**:309-319.

Guzick DS, Overstreet JW, Factor-Litvak P, Brazil CK, Nakajima ST, Coutifaris C, Carson SA, Cisneros P, Steinkampf MP, Hill JA *et al.* Sperm morphology, motility, and concentration in fertile and infertile men. *N Engl J Med* 2001;**345**:1388-1393.

Hammerstedt RH, Graham JK, Nolan JP. Cryopreservation of mammalian sperm: what we ask them to survive. *J Androl* 1990;**11**:73-88.

Heller CH, Clermont Y. Kinetics of the Germinal Epithelium in Man. *Recent Prog Horm Res* 1964;**20**:545-575.

Hengstler JG, Bolm-Audorff U, Faldum A, Janssen K, Reifenrath M, Gotte W, Jung D, Mayer-Popken O, Fuchs J, Gebhard S *et al.* Occupational exposure to heavy metals:

DNA damage induction and DNA repair inhibition prove co-exposures to cadmium, cobalt and lead as more dangerous than hitherto expected. *Carcinogenesis* 2003;**24**:63-73.

Henkel R, Hoogendijk CF, Bouic PJ, Kruger TF. TUNEL assay and SCSA determine different aspects of sperm DNA damage. *Andrologia* 2010;**42**:305-313.

Henkel R, Kierspel E, Hajimohammad M, Stalf T, Hoogendijk C, Mehnert C, Menkveld R, Schill WB, Kruger TF. DNA fragmentation of spermatozoa and assisted reproduction technology. *Reprod Biomed Online* 2003;**7**:477-484.

Holstein AF, Schulze W, Davidoff M. Understanding spermatogenesis is a prerequisite for treatment. *Reprod Biol Endocrinol* 2003;**1**:107-7827-1-107.

Homa ST, Vessey W, Perez-Miranda A, Riyait T, Agarwal A. Reactive Oxygen Species (ROS) in human semen: determination of a reference range. *J Assist Reprod Genet* 2015;**32**:757-764.

Honda S, Sugita I, Miki K, Saito I. The semi-quantitative comparison of oxidative stress mediated DNA single and double strand breaks using terminal deoxynucleotidyl transferase mediated end labeling combined with a slot blot technique. *Free Radic Res* 2004;**38**:481-485.

Hoskins DD, Brandt H, Acott TS. Initiation of sperm motility in the mammalian epididymis. *Fed Proc* 1978;**37**:2534-2542.

Hossain F, Ali O, D'Souza UJ, Naing DK. Effects of pesticide use on semen quality among farmers in rural areas of Sabah, Malaysia. *J Occup Health* 2010;**52**:353-360.

Host E, Lindenberg S, Ernst E, Christensen F. DNA strand breaks in human spermatozoa: a possible factor, to be considered in couples suffering from unexplained infertility. *Acta Obstet Gynecol Scand* 1999;**78**:622-625.

Host E, Lindenberg S, Smidt-Jensen S. The role of DNA strand breaks in human spermatozoa used for IVF and ICSI. *Acta Obstet Gynecol Scand* 2000;**79**:559-563.

Hourcade JD, Perez-Crespo M, Fernandez-Gonzalez R, Pintado B, Gutierrez-Adan A. Selection against spermatozoa with fragmented DNA after postovulatory mating depends on the type of damage. *Reprod Biol Endocrinol* 2010;**8**:9-7827-8-9.

Hua M, Liu W, Chen Y, Zhang F, Xu B, Liu S, Chen G, Shi H, Wu L. Identification of small non-coding RNAs as sperm quality biomarkers for in vitro fertilization. *Cell Discov* 2019;**5**:20-019-0087-9. eCollection 2019.

Huang CC, Lin DP, Tsao HM, Cheng TC, Liu CH, Lee MS. Sperm DNA fragmentation negatively correlates with velocity and fertilization rates but might not affect pregnancy rates. *Fertil Steril* 2005;**84**:130-140.

Huang TT, Kosower NS, Yanagimachi R. Localization of thiol and disulfide groups in guinea pig spermatozoa during maturation and capacitation using bimane fluorescent labels. *Biol Reprod* 1984;**31**:797-809.

Hud NV, Allen MJ, Downing KH, Lee J, Balhorn R. Identification of the elemental packing unit of DNA in mammalian sperm cells by atomic force microscopy. *Biochem Biophys Res Commun* 1993;**193**:1347-1354.

Hughes CM, Lewis SE, McKelvey-Martin VJ, Thompson W. Reproducibility of human sperm DNA measurements using the alkaline single cell gel electrophoresis assay. *Mutat Res* 1997;**374**:261-268.

Hughes CM, Lewis SE, McKelvey-Martin VJ, Thompson W. A comparison of baseline and induced DNA damage in human spermatozoa from fertile and infertile men, using a modified comet assay. *Mol Hum Reprod* 1996;**2**:613-619.

Human Fertilisation and Embryology Authority (HFEA). A Long Term Analysis of the HFEA Register Data 1991–2006. *HFEA* 2008;.

Huszar G, Jakab A, Sakkas D, Ozenci CC, Cayli S, Delpiano E, Ozkavukcu S. Fertility testing and ICSI sperm selection by hyaluronic acid binding: clinical and genetic aspects. *Reprod Biomed Online* 2007;**14**:650-663.

Huszar G, Ozkavukcu S, Jakab A, Celik-Ozenci C, Sati GL, Cayli S. Hyaluronic acid binding ability of human sperm reflects cellular maturity and fertilizing potential: selection of sperm for intracytoplasmic sperm injection. *Curr Opin Obstet Gynecol* 2006;**18**:260-267.

Ichimura S, Zama M, Fujita H. Quantitative determination of single-stranded sections in DNA using the fluorescent probe acridine orange. *Biochim Biophys Acta* 1971;**240**:485-495.

Imam SN, Shamsi MB, Kumar K, Deka D, Dada R. Idiopathic recurrent pregnancy loss: role of paternal factors; a pilot study. *J Reprod Infertil* 2011;**12**:267-276.

Ioannou D, Meershoek EJ, Christopikou D, Ellis M, Thornhill AR, Griffin DK. Nuclear organisation of sperm remains remarkably unaffected in the presence of defective spermatogenesis. *Chromosome Res* 2011;**19**:741-753.

Iranpour FG. Impact of sperm chromatin evaluation on fertilization rate in intracytoplasmic sperm injection. *Adv Biomed Res* 2014;**3**:229-9175.145719. eCollection 2014.

Iyama T, Wilson DM,3rd. DNA repair mechanisms in dividing and non-dividing cells. *DNA Repair (Amst)* 2013;**12**:620-636.

Jakab A, Sakkas D, Delpiano E, Cayli S, Kovanci E, Ward D, Revelli A, Huszar G. Intracytoplasmic sperm injection: a novel selection method for sperm with normal frequency of chromosomal aneuploidies. *Fertil Steril* 2005;**84**:1665-1673.

Jaroudi S, Kakourou G, Cawood S, Doshi A, Ranieri DM, Serhal P, Harper JC, SenGupta SB. Expression profiling of DNA repair genes in human oocytes and blastocysts using microarrays. *Hum Reprod* 2009;**24**:2649-2655.

Jayaraman V, Upadhya D, Narayan PK, Adiga SK. Sperm processing by swim-up and density gradient is effective in elimination of sperm with DNA damage. *J Assist Reprod Genet* 2012;**29**:557-563.

Jerre E, Bungum M, Evenson D, Giwercman A. Sperm chromatin structure assay high DNA stainability sperm as a marker of early miscarriage after intracytoplasmic sperm injection. *Fertil Steril* 2019;**112**:46-53.e2.

Jez M, Bas T, Veber M, Kosir A, Dominko T, Page R, Rozman P. The hazards of DAPI photoconversion: effects of dye, mounting media and fixative, and how to minimize the problem. *Histochem Cell Biol* 2013;**139**:195-204.

Jiricny J. The multifaceted mismatch-repair system. *Nat Rev Mol Cell Biol* 2006;**7**:335-346.

Jones R, Mann T, Sherins R. Peroxidative breakdown of phospholipids in human spermatozoa, spermicidal properties of fatty acid peroxides, and protective action of seminal plasma. *Fertil Steril* 1979;**31**:531-537.

Jones R, Mann T, Sherins RJ. Adverse effects of peroxidized lipid on human spermatozoa. *Proc R Soc Lond B Biol Sci* 1978;**201**:413-417.

Jose-Miller AB, Boyden JW, Frey KA. Infertility. *Am Fam Physician* 2007;**75**:849-856.

Jun SH, Kim TG, Ban C. DNA mismatch repair system. Classical and fresh roles. *FEBS J* 2006;**273**:1609-1619.

Kamkar N, Ramezanali F, Sabbaghian M. The relationship between sperm DNA fragmentation, free radicals and antioxidant capacity with idiopathic repeated pregnancy loss. *Reprod Biol* 2018;**18**:330-335.

Kaneko S, Yoshida J, Ishikawa H, Takamatsu K. Single-cell pulsed-field gel electrophoresis to detect the early stage of DNA fragmentation in human sperm nuclei. *PLoS One* 2012;**7**:e42257.

Kapuscinski J, Darzynkiewicz Z, Melamed MR. Luminescence of the solid complexes of acridine orange with RNA. *Cytometry* 1982;**2**:201-211.

Karabinus DS, Evenson DP, Kaproth MT. Effects of egg yolk-citrate and milk extenders on chromatin structure and viability of cryopreserved bull sperm. *J Dairy Sci* 1991;**74**:3836-3848.

Karg TJ, Golic KG. Photoconversion of DAPI and Hoechst dyes to green and red-emitting forms after exposure to UV excitation. *Chromosoma* 2018;**127**:235-245.

Kazerooni T, Asadi N, Jadid L, Kazerooni M, Ghanadi A, Ghaffarpasand F, Kazerooni Y, Zolghadr J. Evaluation of sperm's chromatin quality with acridine orange test, chromomycin A3 and aniline blue staining in couples with unexplained recurrent abortion. *J Assist Reprod Genet* 2009;**26**:591-596.

Kirkman-Brown J, Pavitt S, Khalaf Y, Lewis S, Hooper R, Bhattacharya S, Coomarasamy A, Sharma V, Brison D, Forbes G *et al.* 2019;.

Kirkman-Brown JC, De Jonge C. Sperm DNA fragmentation in miscarriage - a promising diagnostic, or a test too far? *Reprod Biomed Online* 2017;**34**:3-4.

Koppers AJ, De Iuliis GN, Finnie JM, McLaughlin EA, Aitken RJ. Significance of mitochondrial reactive oxygen species in the generation of oxidative stress in spermatozoa. *J Clin Endocrinol Metab* 2008;**93**:3199-3207.

Kosower NS, Katayose H, Yanagimachi R. Thiol-disulfide status and acridine orange fluorescence of mammalian sperm nuclei. *J Androl* 1992;**13**:342-348.

Kothari S, Thompson A, Agarwal A, du Plessis SS. Free radicals: their beneficial and detrimental effects on sperm function. *Indian J Exp Biol* 2010;**48**:425-435.

Kovac JR, Lipshultz LI. Use of testicular sperm to combat the negative effects of DNA fragmentation. *Asian J Androl* 2016;**18**:434-682X.179158.

Kumar K, Deka D, Singh A, Mitra DK, Vanitha BR, Dada R. Predictive value of DNA integrity analysis in idiopathic recurrent pregnancy loss following spontaneous conception. *J Assist Reprod Genet* 2012;**29**:861-867.

Larson KL, Brannian JD, Singh NP, Burbach JA, Jost LK, Hansen KP, Kreger DO, Evenson DP. Chromatin structure in globozoospermia: a case report. *J Androl* 2001;**22**:424-431.

Larson-Cook KL, Brannian JD, Hansen KA, Kasperson KM, Aamold ET, Evenson DP. Relationship between the outcomes of assisted reproductive techniques and sperm DNA fragmentation as measured by the sperm chromatin structure assay. *Fertil Steril* 2003;**80**:895-902.

Leach M, Aitken RJ, Sacks G. Sperm DNA fragmentation abnormalities in men from couples with a history of recurrent miscarriage. *Aust N Z J Obstet Gynaecol* 2015;**55**:379-383.

Lejeune H, Skalli M, Chatelain PG, Avallet O, Saez JM. The paracrine role of Sertoli cells on Leydig cell function. *Cell Biol Toxicol* 1992;**8**:73-83.

Lerman LS. The structure of the DNA-acridine complex. *Proc Natl Acad Sci U S A* 1963;**49**:94-102.

Levron J, Aviram-Goldring A, Madgar I, Raviv G, Barkai G, Dor J. Sperm chromosome abnormalities in men with severe male factor infertility who are undergoing in vitro fertilization with intracytoplasmic sperm injection. *Fertil Steril* 2001;**76**:479-484.

Lewis B, Aitken RJ. A redox-regulated tyrosine phosphorylation cascade in rat spermatozoa. *J Androl* 2001;**22**:611-622.

Lewis SE. Should sperm DNA fragmentation testing be included in the male infertility work-up? *Reprod Biomed Online* 2015;**31**:134-137.

Lewis SE, Agbaje I, Alvarez J. Sperm DNA tests as useful adjuncts to semen analysis. *Syst Biol Reprod Med* 2008;**54**:111-125.

Lewis SE, John Aitken R, Conner SJ, Iuliis GD, Evenson DP, Henkel R, Giwercman A, Gharagozloo P. The impact of sperm DNA damage in assisted conception and beyond: recent advances in diagnosis and treatment. *Reprod Biomed Online* 2013;**27**:325-337.

Li X, Traganos F, Melamed MR, Darzynkiewicz Z. Single-step procedure for labeling DNA strand breaks with fluorescein- or BODIPY-conjugated deoxynucleotides: detection of apoptosis and bromodeoxyuridine incorporation. *Cytometry* 1995;**20**:172-180.

Lin MH, Kuo-Kuang Lee R, Li SH, Lu CH, Sun FJ, Hwu YM. Sperm chromatin structure assay parameters are not related to fertilization rates, embryo quality, and pregnancy rates in in vitro fertilization and intracytoplasmic sperm injection, but might be related to spontaneous abortion rates. *Fertil Steril* 2008;**90**:352-359.

Lin WW, Lamb DJ, Wheeler TM, Abrams J, Lipshultz LI, Kim ED. Apoptotic frequency is increased in spermatogenic maturation arrest and hypospermatogenic states. *J Urol* 1997;**158**:1791-1793.

Linck RW, Chemes H, Albertini DF. The axoneme: the propulsive engine of spermatozoa and cilia and associated ciliopathies leading to infertility. *J Assist Reprod Genet* 2016;**33**:141-156.

Lindahl T. Instability and decay of the primary structure of DNA. *Nature* 1993;**362**:709-715.

Liu T, Gao J, Zhou N, Mo M, Wang X, Zhang X, Yang H, Chen Q, Ao L, Liu J *et al.* The effect of two cryopreservation methods on human sperm DNA damage. *Cryobiology* 2016;**72**:210-215.

Liu DY, Lopata A, Johnston WI, Baker HW. A human sperm-zona pellucida binding test using oocytes that failed to fertilize in vitro. *Fertil Steril* 1988;**50**:782-788.

Lolis D, Georgiou I, Syrrou M, Zikopoulos K, Konstantelli M, Messinis I. Chromomycin A3-staining as an indicator of protamine deficiency and fertilization. *Int J Androl* 1996;**19**:23-27.

Lopes LS, Esteves SC. Testicular sperm for intracytoplasmic sperm injection in non-azoospermic men: a paradigm shift. *Panminerva Med* 2019;**61**:178-186.

Lopes S, Sun JG, Jurisicova A, Meriano J, Casper RF. Sperm deoxyribonucleic acid fragmentation is increased in poor-quality semen samples and correlates with failed fertilization in intracytoplasmic sperm injection. *Fertil Steril* 1998;**69**:528-532.

MacMillan RA, Baker HW. Comparison of latex and polyacrylamide beads for detecting sperm antibodies. *Clin Reprod Fertil* 1987;**5**:203-209.

Majzoub A, Agarwal A, Esteves SC. Antioxidants for elevated sperm DNA fragmentation: a mini review. *Transl Androl Urol* 2017;**6**:S649-S653.

Manandhar G, Simerly C, Schatten G. Highly degenerated distal centrioles in rhesus and human spermatozoa. *Hum Reprod* 2000;**15**:256-263.

Manicardi GC, Bianchi PG, Pantano S, Azzoni P, Bizzaro D, Bianchi U, Sakkas D. Presence of endogenous nicks in DNA of ejaculated human spermatozoa and its relationship to chromomycin A3 accessibility. *Biol Reprod* 1995;**52**:864-867.

Marchiani S, Tamburrino L, Maoggi A, Vannelli GB, Forti G, Baldi E, Muratori M. Characterization of M540 bodies in human semen: evidence that they are apoptotic bodies. *Mol Hum Reprod* 2007;**13**:621-631.

Martins RP, Krawetz SA. Nuclear organization of the protamine locus. *Soc Reprod Fertil Suppl* 2007;**64**:1-12.

Matsuda Y, Tobari I, Maemori M, Seki N. Mechanism of chromosome aberration induction in the mouse egg fertilized with sperm recovered from postmeiotic germ cells treated with methyl methanesulfonate. *Mutat Res* 1989;**214**:165-180.

Mazzilli F, Rossi T, Sabatini L, Pulcinelli FM, Rapone S, Dondero F, Gazzaniga PP. Human sperm cryopreservation and reactive oxygen species (ROS) production. *Acta Eur Fertil* 1995;**26**:145-148.

McAuliffe ME, Williams PL, Korrick SA, Dadd R, Marchetti F, Martenies SE, Perry MJ. Human sperm sex chromosome disomy and sperm DNA damage assessed by the neutral comet assay. *Hum Reprod* 2014;**29**:2148-2155.

McKay DJ, Renaux BS, Dixon GH. Human sperm protamines. Amino-acid sequences of two forms of protamine P2. *Eur J Biochem* 1986;**156**:5-8.

McLachlan RI, de Kretser DM. Male infertility: the case for continued research. *Med J Aust* 2001;**174**:116-117.

McPherson S, Longo FJ. Chromatin structure-function alterations during mammalian spermatogenesis: DNA nicking and repair in elongating spermatids. *Eur J Histochem* 1993;**37**:109-128.

McPherson SM, Longo FJ. Nicking of rat spermatid and spermatozoa DNA: possible involvement of DNA topoisomerase II. *Dev Biol* 1993;**158**:122-130.

McPherson SM, Longo FJ. Localization of DNase I-hypersensitive regions during rat spermatogenesis: stage-dependent patterns and unique sensitivity of elongating spermatids. *Mol Reprod Dev* 1992;**31**:268-279.

McQueen DB, Zhang J, Robins JC. Sperm DNA fragmentation and recurrent pregnancy loss: a systematic review and meta-analysis. *Fertil Steril* 2019;**112**:54-60.e3.

Mehta A, Nangia AK, Dupree JM, Smith JF. Limitations and barriers in access to care for male factor infertility. *Fertil Steril* 2016;**105**:1128-1137.

Men NT, Kikuchi K, Furusawa T, Dang-Nguyen TQ, Nakai M, Fukuda A, Noguchi J, Kaneko H, Viet Linh N, Xuan Nguyen B *et al.* Expression of DNA repair genes in porcine oocytes before and after fertilization by ICSI using freeze-dried sperm. *Anim Sci J* 2016;**87**:1325-1333.

Meseguer M, Santiso R, Garrido N, Garcia-Herrero S, Remohi J, Fernandez JL. Effect of sperm DNA fragmentation on pregnancy outcome depends on oocyte quality. *Fertil Steril* 2011;**95**:124-128.

Mitchell LA, De Iuliis GN, Aitken RJ. The TUNEL assay consistently underestimates DNA damage in human spermatozoa and is influenced by DNA compaction and cell vitality: development of an improved methodology. *Int J Androl* 2011;**34**:2-13.

Mongkolchaipak S, Vutyavanich T. No difference in high-magnification morphology and hyaluronic acid binding in the selection of euploid spermatozoa with intact DNA. *Asian J Androl* 2013;**15**:421-424.

Morris ID, Ilott S, Dixon L, Brison DR. The spectrum of DNA damage in human sperm assessed by single cell gel electrophoresis (Comet assay) and its relationship to fertilization and embryo development. *Hum Reprod* 2002;**17**:990-998.

Motea EA, Berdis AJ. Terminal deoxynucleotidyl transferase: the story of a misguided DNA polymerase. *Biochim Biophys Acta* 2010;**1804**:1151-1166.

Muratori M, Forti G, Baldi E. Comparing flow cytometry and fluorescence microscopy for analyzing human sperm DNA fragmentation by TUNEL labeling. *Cytometry A* 2008;**73**:785-787.

Muratori M, Marchiani S, Tamburrino L, Tocci V, Failli P, Forti G, Baldi E. Nuclear staining identifies two populations of human sperm with different DNA fragmentation extent and relationship with semen parameters. *Hum Reprod* 2008;**23**:1035-1043.

Muratori M, Porazzi I, Luconi M, Marchiani S, Forti G, Baldi E. AnnexinV binding and merocyanine staining fail to detect human sperm capacitation. *J Androl* 2004;**25**:797-810.

Muratori M, Tamburrino L, Marchiani S, Guido C, Forti G, Baldi E. Critical aspects of detection of sperm DNA fragmentation by TUNEL/flow cytometry. *Syst Biol Reprod Med* 2010;**56**:277-285.

Muratori M, Tamburrino L, Tocci V, Costantino A, Marchiani S, Giachini C, Laface I, Krausz C, Meriggiola MC, Forti G *et al.* Small variations in crucial steps of TUNEL assay coupled to flow cytometry greatly affect measures of sperm DNA fragmentation. *J Androl* 2010;**31**:336-345.

Muriel L, Goyanes V, Segrelles E, Gosalvez J, Alvarez JG, Fernandez JL. Increased aneuploidy rate in sperm with fragmented DNA as determined by the sperm chromatin dispersion (SCD) test and FISH analysis. *J Androl* 2007;**28**:38-49.

Muriel L, Meseguer M, Fernandez JL, Alvarez J, Remohi J, Pellicer A, Garrido N. Value of the sperm chromatin dispersion test in predicting pregnancy outcome in intrauterine insemination: a blind prospective study. *Hum Reprod* 2006;**21**:738-744.

Musset B, Clark RA, DeCoursey TE, Petheo GL, Geiszt M, Chen Y, Cornell JE, Eddy CA, Brzyski RG, El Jamali A. NOX5 in human spermatozoa: expression, function, and regulation. *J Biol Chem* 2012;**287**:9376-9388.

Nadel B, de Lara J, Finkernagel SW, Ward WS. Cell-specific organization of the 5S ribosomal RNA gene cluster DNA loop domains in spermatozoa and somatic cells. *Biol Reprod* 1995;**53**:1222-1228.

Nash D, Plaut W. On the Denaturation of Chromosomal Dna in Situ. *Proc Natl Acad Sci U S A* 1964;**51**:731-735.

Nasr Esfahani MH, Deemeh MR, Tavalaee M, Sekhavati MH, Gourabi H. Zeta Sperm Selection Improves Pregnancy Rate and Alters Sex Ratio in Male Factor Infertility Patients: A Double-Blind, Randomized Clinical Trial. *Int J Fertil Steril* 2016;**10**:253-260.

Nasr-Esfahani MH, Razavi S, Mardani M. Relation between different human sperm nuclear maturity tests and in vitro fertilization. *J Assist Reprod Genet* 2001;**18**:219-225.

NHS. Miscarriage symptoms. 2018. https://www.nhs.uk/conditions/miscarriage/symptoms/

NHS. Prevalence of infertility. 2020. https://www.nhs.uk/conditions/Infertility/

Ni K, Spiess AN, Schuppe HC, Steger K. The impact of sperm protamine deficiency and sperm DNA damage on human male fertility: a systematic review and meta-analysis. *Andrology* 2016;.

Nick McElhinny SA, Kissling GE, Kunkel TA. Differential correction of lagging-strand replication errors made by DNA polymerases {alpha} and {delta}. *Proc Natl Acad Sci U S A* 2010;**107**:21070-21075.

O'Donnell L. Mechanisms of spermiogenesis and spermiation and how they are disturbed. *Spermatogenesis* 2015;**4**:e979623.

O'Donovan A, Davies AA, Moggs JG, West SC, Wood RD. XPG endonuclease makes the 3' incision in human DNA nucleotide excision repair. *Nature* 1994;**371**:432-435.

O'Flaherty C, Vaisheva F, Hales BF, Chan P, Robaire B. Characterization of sperm chromatin quality in testicular cancer and Hodgkin's lymphoma patients prior to chemotherapy. *Hum Reprod* 2008;**23**:1044-1052.

Ohashi Y, Miharu N, Honda H, Samura O, Ohama K. High frequency of XY disomy in spermatozoa of severe oligozoospermic men. *Hum Reprod* 2001;**16**:703-708.

Oleszczuk K, Giwercman A, Bungum M. Sperm chromatin structure assay in prediction of in vitro fertilization outcome. *Andrology* 2016;**4**:290-296.

Olsen AK, Lindeman B, Wiger R, Duale N, Brunborg G. How do male germ cells handle DNA damage? *Toxicol Appl Pharmacol* 2005;**207**:521-531.

Osman A, Alsomait H, Seshadri S, El-Toukhy T, Khalaf Y. The effect of sperm DNA fragmentation on live birth rate after IVF or ICSI: a systematic review and meta-analysis. *Reprod Biomed Online* 2015;**30**:120-127.

Ostling O, Johanson KJ. Microelectrophoretic study of radiation-induced DNA damages in individual mammalian cells. *Biochem Biophys Res Commun* 1984;**123**:291-298.

Parmegiani L, Cognigni GE, Bernardi S, Troilo E, Ciampaglia W, Filicori M. "Physiologic ICSI": hyaluronic acid (HA) favors selection of spermatozoa without DNA fragmentation and with normal nucleus, resulting in improvement of embryo quality. *Fertil Steril* 2010;**93**:598-604.

Parmegiani L, Cognigni GE, Ciampaglia W, Pocognoli P, Marchi F, Filicori M. Efficiency of hyaluronic acid (HA) sperm selection. *J Assist Reprod Genet* 2010;**27**:13-16.

Perez-Crespo M, Moreira P, Pintado B, Gutierrez-Adan A. Factors from damaged sperm affect its DNA integrity and its ability to promote embryo implantation in mice. *J Androl* 2008;**29**:47-54.

Peris SI, Morrier A, Dufour M, Bailey JL. Cryopreservation of ram semen facilitates sperm DNA damage: relationship between sperm andrological parameters and the sperm chromatin structure assay. *J Androl* 2004;**25**:224-233.

Pienta KJ, Coffey DS. A structural analysis of the role of the nuclear matrix and DNA loops in the organization of the nucleus and chromosome. *J Cell Sci Suppl* 1984;**1**:123-135.

Pillarisetty LS, Gupta N. Recurrent Pregnancy Loss. Anonymous StatPearls2020. StatPearls Publishing LLC, Treasure Island (FL).

Plante M, de Lamirande E, Gagnon C. Reactive oxygen species released by activated neutrophils, but not by deficient spermatozoa, are sufficient to affect normal sperm motility. *Fertil Steril* 1994;**62**:387-393.

Plemel JR, Caprariello AV, Keough MB, Henry TJ, Tsutsui S, Chu TH, Schenk GJ, Klaver R, Yong VW, Stys PK. Unique spectral signatures of the nucleic acid dye acridine orange can distinguish cell death by apoptosis and necroptosis. *J Cell Biol* 2017;**216**:1163-1181.

Pluciennik A, Dzantiev L, Iyer RR, Constantin N, Kadyrov FA, Modrich P. PCNA function in the activation and strand direction of MutLalpha endonuclease in mismatch repair. *Proc Natl Acad Sci U S A* 2010;**107**:16066-16071.

Poccia D. Remodeling of nucleoproteins during gametogenesis, fertilization, and early development. *Int Rev Cytol* 1986;**105**:1-65.

Pons I, Cercas R, Villas C, Brana C, Fernandez-Shaw S. One abstinence day decreases sperm DNA fragmentation in 90 % of selected patients. *J Assist Reprod Genet* 2013;**30**:1211-1218.

Poppe K, Velkeniers B. Thyroid and infertility. *Verh K Acad Geneeskd Belg* 2002;**64**:389-99; discussion 400-2.

Practice Committee of the American Society for Reproductive Medicine. The clinical utility of sperm DNA integrity testing: a guideline. *Fertil Steril* 2013;**99**:673-677.

Prinosilova P, Kruger T, Sati L, Ozkavukcu S, Vigue L, Kovanci E, Huszar G. Selectivity of hyaluronic acid binding for spermatozoa with normal Tygerberg strict morphology. *Reprod Biomed Online* 2009;**18**:177-183.

Pujianto DA, Curry BJ, Aitken RJ. Prolactin exerts a prosurvival effect on human spermatozoa via mechanisms that involve the stimulation of Akt phosphorylation and suppression of caspase activation and capacitation. *Endocrinology* 2010;**151**:1269-1279.

Puppo V, Puppo G. Comprehensive review of the anatomy and physiology of male ejaculation: Premature ejaculation is not a disease. *Clin Anat* 2016;**29**:111-119.

Ribas-Maynou J, Garcia-Peiro A, Fernandez-Encinas A, Abad C, Amengual MJ, Prada E, Navarro J, Benet J. Comprehensive analysis of sperm DNA fragmentation by five different assays: TUNEL assay, SCSA, SCD test and alkaline and neutral Comet assay. *Andrology* 2013;**1**:715-722.

Ricci G, Perticarari S, Fragonas E, Giolo E, Canova S, Pozzobon C, Guaschino S, Presani G. Apoptosis in human sperm: its correlation with semen quality and the presence of leukocytes. *Hum Reprod* 2002;**17**:2665-2672.

Rigby PW, Dieckmann M, Rhodes C, Berg P. Labeling deoxyribonucleic acid to high specific activity in vitro by nick translation with DNA polymerase I. *J Mol Biol* 1977;**113**:237-251.

Riva NS, Ruhlmann C, Iaizzo RS, Marcial Lopez CA, Martinez AG. Comparative analysis between slow freezing and ultra-rapid freezing for human sperm cryopreservation. *JBRA Assist Reprod* 2018;**22**:331-337.

Robinson L, Gallos ID, Conner SJ, Rajkhowa M, Miller D, Lewis S, Kirkman-Brown J, Coomarasamy A. The effect of sperm DNA fragmentation on miscarriage rates: a systematic review and meta-analysis. *Hum Reprod* 2012;**27**:2908-2917.

Rodriguez I, Ody C, Araki K, Garcia I, Vassalli P. An early and massive wave of germinal cell apoptosis is required for the development of functional spermatogenesis. *EMBO J* 1997;**16**:2262-2270.

Rogers BJ, Van Campen H, Ueno M, Lambert H, Bronson R, Hale R. Analysis of human spermatozoal fertilizing ability using zona-free ova. *Fertil Steril* 1979;**32**:664-670.

Roosen-Runge EC, Holstein AF. The human rete testis. *Cell Tissue Res* 1978;**189**:409-433.

Ross J, Tang MS. Differentiation of apurinic/apyrimidinic sites and single-strand breaks in DNA by formamide- and alkaline-sucrose gradient sedimentation. *Anal Biochem* 1985;**144**:212-217.

Rothkamm K, Kruger I, Thompson LH, Lobrich M. Pathways of DNA double-strand break repair during the mammalian cell cycle. *Mol Cell Biol* 2003;**23**:5706-5715.

Rousseaux S, Reynoird N, Escoffier E, Thevenon J, Caron C, Khochbin S. Epigenetic reprogramming of the male genome during gametogenesis and in the zygote. *Reprod Biomed Online* 2008;**16**:492-503.

Royal College of Obstetricians and Gynaecologists. The investigation and treatment of couples with recurrent first-trimester and second-trimester miscarriage. 2011;.

Roychoudhury R, Jay E, Wu R. Terminal labeling and addition of homopolymer tracts to duplex DNA fragments by terminal deoxynucleotidyl transferase. *Nucleic Acids Res* 1976;**3**:863-877.

Rube CE, Zhang S, Miebach N, Fricke A, Rube C. Protecting the heritable genome: DNA damage response mechanisms in spermatogonial stem cells. *DNA Repair (Amst)* 2011;**10**:159-168.

Rueff J, Bras A, Cristovao L, Mexia J, Sa da Costa M, Pires V. DNA strand breaks and chromosomal aberrations induced by H2O2 and 60Co gamma-radiation. *Mutat Res* 1993;**289**:197-204.

Said TM, Paasch U, Glander HJ, Agarwal A. Role of caspases in male infertility. *Hum Reprod Update* 2004;**10**:39-51.

Sailer BL, Jost LK, Evenson DP. Mammalian sperm DNA susceptibility to in situ denaturation associated with the presence of DNA strand breaks as measured by the terminal deoxynucleotidyl transferase assay. *J Androl* 1995;**16**:80-87.

Sakkas D, Seli E, Bizzaro D, Tarozzi N, Manicardi GC. Abnormal spermatozoa in the ejaculate: abortive apoptosis and faulty nuclear remodelling during spermatogenesis. *Reprod Biomed Online* 2003;**7**:428-432.

Samplaski MK, Agarwal A, Sharma R, Sabanegh E. New generation of diagnostic tests for infertility: review of specialized semen tests. *Int J Urol* 2010;**17**:839-847.

Sanchez-Martin P, Sanchez-Martin F, Gonzalez-Martinez M, Gosalvez J. Increased pregnancy after reduced male abstinence. *Syst Biol Reprod Med* 2013;**59**:256-260.

Sanocka D, Kurpisz M. Reactive oxygen species and sperm cells. *Reprod Biol Endocrinol* 2004;**2**:12-7827-2-12.

Sati L, Ovari L, Bennett D, Simon SD, Demir R, Huszar G. Double probing of human spermatozoa for persistent histones, surplus cytoplasm, apoptosis and DNA fragmentation. *Reprod Biomed Online* 2008;**16**:570-579.

Schlegel PN, Paduch DA. Yet another test of sperm chromatin structure. *Fertil Steril* 2005;**84**:854-859.

Sergerie M, Laforest G, Bujan L, Bissonnette F, Bleau G. Sperm DNA fragmentation: threshold value in male fertility. *Hum Reprod* 2005;**20**:3446-3451.

Shapiro JA. A 21st century view of evolution: genome system architecture, repetitive DNA, and natural genetic engineering. *Gene* 2005;**345**:91-100.

Sharma R, Ahmad G, Esteves SC, Agarwal A. Terminal deoxynucleotidyl transferase dUTP nick end labeling (TUNEL) assay using bench top flow cytometer for evaluation

of sperm DNA fragmentation in fertility laboratories: protocol, reference values, and quality control. *J Assist Reprod Genet* 2016;**33**:291-300.

Sharma RK, Agarwal A. Role of reactive oxygen species in male infertility. *Urology* 1996;**48**:835-850.

Sharma RK, Gupta S, Thiyagarajan A, Sabanegh E, Agarwal A. Testing sperm DNA damage by tunel assay in specific cases of male infertility. 2010;**94**:S146.

Sharma RK, Sabanegh E, Mahfouz R, Gupta S, Thiyagarajan A, Agarwal A. TUNEL as a test for sperm DNA damage in the evaluation of male infertility. *Urology* 2010;**76**:1380-1386.

Shimura T, Inoue M, Taga M, Shiraishi K, Uematsu N, Takei N, Yuan ZM, Shinohara T, Niwa O. p53-dependent S-phase damage checkpoint and pronuclear cross talk in mouse zygotes with X-irradiated sperm. *Mol Cell Biol* 2002;**22**:2220-2228.

Showell MG, Mackenzie-Proctor R, Brown J, Yazdani A, Stankiewicz MT, Hart RJ. Antioxidants for male subfertility. *Cochrane Database Syst Rev* 2014;**12**:CD007411.

Silvestroni L, Frajese G, Fabrizio M. Histones instead of protamines in terminal germ cells of infertile, oligospermic men. *Fertil Steril* 1976;**27**:1428-1437.

Simon L, Liu L, Murphy K, Ge S, Hotaling J, Aston KI, Emery B, Carrell DT. Comparative analysis of three sperm DNA damage assays and sperm nuclear protein content in couples undergoing assisted reproduction treatment. *Hum Reprod* 2014;**29**:904-917.

Singh NP, McCoy MT, Tice RR, Schneider EL. A simple technique for quantitation of low levels of DNA damage in individual cells. *Exp Cell Res* 1988;**175**:184-191.

Smith TB, Dun MD, Smith ND, Curry BJ, Connaughton HS, Aitken RJ. The presence of a truncated base excision repair pathway in human spermatozoa that is mediated by OGG1. *J Cell Sci* 2013;**126**:1488-1497.

Smits RM, Mackenzie-Proctor R, Yazdani A, Stankiewicz MT, Jordan V, Showell MG. Antioxidants for male subfertility. *Cochrane Database Syst Rev* 2019;**3**:CD007411.

Sotolongo B, Lino E, Ward WS. Ability of hamster spermatozoa to digest their own DNA. *Biol Reprod* 2003;**69**:2029-2035.

Sotomayor RE, Sega GA. Unscheduled DNA synthesis assay in mammalian spermatogenic cells: an update. *Environ Mol Mutagen* 2000;**36**:255-265.

Spano M, Bonde JP, Hjollund HI, Kolstad HA, Cordelli E, Leter G. Sperm chromatin damage impairs human fertility. The Danish First Pregnancy Planner Study Team. *Fertil Steril* 2000;**73**:43-50.

Spano M, Kolstad AH, Larsen SB, Cordelli E, Leter G, Giwercman A, Bonde JP. The applicability of the flow cytometric sperm chromatin structure assay in epidemiological studies. Asclepios. *Hum Reprod* 1998;**13**:2495-2505.

Stahl PJ, Cogan C, Mehta A, Bolyakov A, Paduch DA, Goldstein M. Concordance among sperm deoxyribonucleic acid integrity assays and semen parameters. *Fertil Steril* 2015;**104**:56-61.e1.

Steger K, Cavalcanti MC, Schuppe HC. Prognostic markers for competent human spermatozoa: fertilizing capacity and contribution to the embryo. *Int J Androl* 2011;**34**:513-527.

Sukprasert M, Wongkularb A, Rattanasiri S, Choktanasiri W, Satirapod C. The effects of short abstinence time on sperm motility, morphology and DNA mDamage. *Andrology* 2013;**2(1)**.

Talebi AR, Fesahat F, Mangoli E, Ghasemzadeh J, Nayeri M, Sadeghian-Nodoshan F. Relationship between sperm protamine deficiency and apoptosis in couples with unexplained repeated spontaneous abortions. *Int J Reprod Biomed (Yazd)* 2016;**14**:199-204.

Tan J, Taskin O, Albert A, Bedaiwy MA. Association between sperm DNA fragmentation and idiopathic recurrent pregnancy loss: a systematic review and meta-analysis. *Reprod Biomed Online* 2018;.

Tanphaichitr N, Sobhon P, Taluppeth N, Chalermisarachai P. Basic nuclear proteins in testicular cells and ejaculated spermatozoa in man. *Exp Cell Res* 1978;**117**:347-356.

Tarozzi N, Bizzaro D, Flamigni C, Borini A. Clinical relevance of sperm DNA damage in assisted reproduction. *Reprod Biomed Online* 2007;**14**:746-757.

Tarozzi N, Nadalini M, Stronati A, Bizzaro D, Dal Prato L, Coticchio G, Borini A. Anomalies in sperm chromatin packaging: implications for assisted reproduction techniques. *Reprod Biomed Online* 2009;**18**:486-495.

Tavalaee M, Razavi S, Nasr-Esfahani MH. Influence of sperm chromatin anomalies on assisted reproductive technology outcome. *Fertil Steril* 2009;**91**:1119-1126.

Tavilani H, Goodarzi MT, Doosti M, Vaisi-Raygani A, Hassanzadeh T, Salimi S, Joshaghani HR. Relationship between seminal antioxidant enzymes and the phospholipid and fatty acid composition of spermatozoa. *Reprod Biomed Online* 2008;**16**:649-656.

Tejada RI, Mitchell JC, Norman A, Marik JJ, Friedman S. A test for the practical evaluation of male fertility by acridine orange (AO) fluorescence. *Fertil Steril* 1984;**42**:87-91.

Tesarik J, Greco E, Mendoza C. Late, but not early, paternal effect on human embryo development is related to sperm DNA fragmentation. *Hum Reprod* 2004;**19**:611-615.

Thijssen A, Klerkx E, Huyser C, Bosmans E, Campo R, Ombelet W. Influence of temperature and sperm preparation on the quality of spermatozoa. *Reprod Biomed Online* 2014;**28**:436-442.

Thiry M. In situ nick translation at the electron microscopic level. *Methods Mol Biol* 2002;**203**:121-130.

Thome MP, Filippi-Chiela EC, Villodre ES, Migliavaca CB, Onzi GR, Felipe KB, Lenz G. Ratiometric analysis of Acridine Orange staining in the study of acidic organelles and autophagy. *J Cell Sci* 2016;**129**:4622-4632.

Thomson LK, Fleming SD, Aitken RJ, De Iuliis GN, Zieschang JA, Clark AM. Cryopreservation-induced human sperm DNA damage is predominantly mediated by oxidative stress rather than apoptosis. *Hum Reprod* 2009;**24**:2061-2070.

Tommy's National Centre for Miscarriage Research. Pregnancy loss statistics. 2020;.

Treulen F, Aguila L, Arias ME, Jofre I, Felmer R. Impact of post-thaw supplementation of semen extender with antioxidants on the quality and function variables of stallion spermatozoa. *Anim Reprod Sci* 2019;**201**:71-83.

Trisini AT, Singh NP, Duty SM, Hauser R. Relationship between human semen parameters and deoxyribonucleic acid damage assessed by the neutral comet assay. *Fertil Steril* 2004;**82**:1623-1632.

Turner TT. On the epididymis and its role in the development of the fertile ejaculate. *J Androl* 1995;**16**:292-298.

Twigg JP, Irvine DS, Aitken RJ. Oxidative damage to DNA in human spermatozoa does not preclude pronucleus formation at intracytoplasmic sperm injection. *Hum Reprod* 1998;**13**:1864-1871.

Valavanidis A, Vlachogianni T, Fiotakis C. 8-hydroxy-2' -deoxyguanosine (8-OHdG): A critical biomarker of oxidative stress and carcinogenesis. *J Environ Sci Health C Environ Carcinog Ecotoxicol Rev* 2009;**27**:120-139.

van der Steeg JW, Steures P, Eijkemans MJ, F Habbema JD, Hompes PG, Kremer JA, van der Leeuw-Harmsen L, Bossuyt PM, Repping S, Silber SJ *et al.* Role of semen analysis in subfertile couples. *Fertil Steril* 2011;**95**:1013-1019.

van Dierendonck JH. DNA damage detection using DNA polymerase I or its Klenow fragment. Applicability, specificity, limitations. *Methods Mol Biol* 2002;**203**:81-108.

Vazquez-Gundin F, Gosalvez J, de la Torre J, Fernandez JL. DNA breakage detection-fish (DBD-FISH): effect of unwinding time. *Mutat Res* 2000;**453**:83-88.

Villani P, Eleuteri P, Grollino MG, Rescia M, Altavista P, Spano M, Pacchierotti F, Cordelli E. Sperm DNA fragmentation induced by DNAse I and hydrogen peroxide: an in vitro comparative study among different mammalian species. *Reproduction* 2010;**140**:445-452.

Virant-Klun I, Tomazevic T, Meden-Vrtovec H. Sperm single-stranded DNA, detected by acridine orange staining, reduces fertilization and quality of ICSI-derived embryos. *J Assist Reprod Genet* 2002;**19**:319-328.

Virro MR, Larson-Cook KL, Evenson DP. Sperm chromatin structure assay (SCSA) parameters are related to fertilization, blastocyst development, and ongoing pregnancy in in vitro fertilization and intracytoplasmic sperm injection cycles. *Fertil Steril* 2004;**81**:1289-1295.

Walczak-Jedrzejowska R, Wolski JK, Slowikowska-Hilczer J. The role of oxidative stress and antioxidants in male fertility. *Cent European J Urol* 2013;**66**:60-67.

Wang AW, Zhang H, Ikemoto I, Anderson DJ, Loughlin KR. Reactive oxygen species generation by seminal cells during cryopreservation. *Urology* 1997;**49**:921-925.

Wang RA, Nakane PK, Koji T. Autonomous cell death of mouse male germ cells during fetal and postnatal period. *Biol Reprod* 1998;**58**:1250-1256.

Ward WS. Function of sperm chromatin structural elements in fertilization and development. *Mol Hum Reprod* 2010;**16**:30-36.

WHO. 2. Standard procedures. Trevor C, Aitken J, Auger J, Baker G, Barratt C, Behre H, Björndahl L, Brazil C, De Jonge C, Doncel G *et al.* (eds). WHO laboratory manual for the Examination and processing of human semenfifth edn, 2010a. World Health Organisation, Switzerland, pp. 25.

WHO. WHO laboratory manual for the examination and processing human semen. 5th edn, 2010b. WHO, Switzerland.

WHO. World Health Organization. Report of the Meeting on the Prevention of Infertility at the Primary Health Care Level. WHO. 1984;

Whorton D, Milby TH, Krauss RM, Stubbs HA. Testicular function in DBCP exposed pesticide workers. *J Occup Med* 1979;**21**:161-166.

Worrilow KC, Eid S, Woodhouse D, Perloe M, Smith S, Witmyer J, Ivani K, Khoury C, Ball GD, Elliot T *et al.* Use of hyaluronan in the selection of sperm for intracytoplasmic sperm injection (ICSI): significant improvement in clinical outcomes--multicenter, double-blinded and randomized controlled trial. *Hum Reprod* 2013;**28**:306-314.

Wouters-Tyrou D, Martinage A, Chevaillier P, Sautiere P. Nuclear basic proteins in spermiogenesis. *Biochimie* 1998;**80**:117-128.

Yamadori I, Yoshino T, Kondo E, Cao L, Akagi T, Matsuo Y, Minowada J. Comparison of two methods of staining apoptotic cells of leukemia cell lines. Terminal deoxynucleotidyl transferase and DNA polymerase I reactions. *J Histochem Cytochem* 1998;**46**:85-90.

Yang C, Xu L, Cui Y, Wu B, Liao Z. Potent humanin analogue (HNG) protects human sperm from freeze-thaw-induced damage. *Cryobiology* 2019;**88**:47-53.

Yang K, Adham IM, Meinhardt A, Hoyer-Fender S. Ultra-structure of the sperm head-to-tail linkage complex in the absence of the spermatid-specific LINC component SPAG4. *Histochem Cell Biol* 2018;**150**:49-59.

Yetunde I, Vasiliki M. Effects of advanced selection methods on sperm quality and ART outcome. *Minerva Ginecol* 2013;**65**:487-496.

Yogev L, Kleiman SE, Hauser R, Botchan A, Lehavi O, Paz G, Yavetz H. Assessing the predictive value of hyaluronan binding ability for the freezability potential of human sperm. *Fertil Steril* 2010;**93**:154-158.

Younglai EV, Holt D, Brown P, Jurisicova A, Casper RF. Sperm swim-up techniques and DNA fragmentation. *Hum Reprod* 2001;**16**:1950-1953.

Zalensky A, Zalenskaya I. Organization of chromosomes in spermatozoa: an additional layer of epigenetic information? *Biochem Soc Trans* 2007;**35**:609-611.

Zegers-Hochschild F, Adamson GD, de Mouzon J, Ishihara O, Mansour R, Nygren K, Sullivan E, van der Poel S, International Committee for Monitoring Assisted Reproductive Technology, World Health Organization. The International Committee for Monitoring Assisted Reproductive Technology (ICMART) and the World Health Organization (WHO) Revised Glossary on ART Terminology, 2009. *Hum Reprod* 2009;**24**:2683-2687.

Zenzes MT, Puy LA, Bielecki R, Reed TE. Detection of benzo[a]pyrene diol epoxide-DNA adducts in embryos from smoking couples: evidence for transmission by spermatozoa. *Mol Hum Reprod* 1999;**5**:125-131.

Zhang X, San Gabriel M, Zini A. Sperm nuclear histone to protamine ratio in fertile and infertile men: evidence of heterogeneous subpopulations of spermatozoa in the ejaculate. *J Androl* 2006;**27**:414-420.

Zhang Y, Zhong L, Xu B, Yang Y, Ban R, Zhu J, Cooke HJ, Hao Q, Shi Q. SpermatogenesisOnline 1.0: a resource for spermatogenesis based on manual literature curation and genome-wide data mining. *Nucleic Acids Res* 2013;**41**:D1055-62.

Zhang Z, Zhu L, Jiang H, Chen H, Chen Y, Dai Y. Sperm DNA fragmentation index and pregnancy outcome after IVF or ICSI: a meta-analysis. *J Assist Reprod Genet* 2015;**32**:17-26.

Zhao J, Zhang Q, Wang Y, Li Y. Whether sperm deoxyribonucleic acid fragmentation has an effect on pregnancy and miscarriage after in vitro fertilization/intracytoplasmic sperm injection: a systematic review and meta-analysis. *Fertil Steril* 2014;**102**:998-1005.e8.

Zini A. Are sperm chromatin and DNA defects relevant in the clinic? *Syst Biol Reprod Med* 2011;**57**:78-85.

Zini A, Boman JM, Belzile E, Ciampi A. Sperm DNA damage is associated with an increased risk of pregnancy loss after IVF and ICSI: systematic review and meta-analysis. *Hum Reprod* 2008;**23**:2663-2668.

Zini A, Jamal W, Cowan L, Al-Hathal N. Is sperm DNA damage associated with IVF embryo quality? A systematic review. *J Assist Reprod Genet* 2011;**28**:391-397.

Zini A, Kamal KM, Phang D. Free thiols in human spermatozoa: correlation with sperm DNA integrity. *Urology* 2001;**58**:80-84.

Zribi N, Chakroun NF, Ben Abdallah F, Elleuch H, Sellami A, Gargouri J, Rebai T, Fakhfakh F, Keskes LA. Effect of freezing-thawing process and quercetin on human sperm survival and DNA integrity. *Cryobiology* 2012;**65**:326-331.

Zribi N, Feki Chakroun N, El Euch H, Gargouri J, Bahloul A, Ammar Keskes L. Effects of cryopreservation on human sperm deoxyribonucleic acid integrity. *Fertil Steril* 2010;**93**:159-166.